Cellulose Esters and Cellulose Ether Esters for Oral Drug Delivery Systems

Hale Cigdem Arca

Dissertation submitted to the faculty of the Virginia Polytechnic Institute and State University in partial fulfillment of the requirements for the degree of

Doctor of Philosophy

In

Macromolecular Science and Engineering

Kevin J. Edgar, Chair

S. Richard Turner

Nammalwar Sriranganathan

Richey M. Davis

Lynne S. Taylor

Sept. 7th, 2016

Blacksburg, VA

Keywords: Amorphous solid dispersions, cellulose ether ester, cellulose ester, structure-property relationship, anti-HIV, rifampicin, quercetin, ritonavir, efavirnez, etravirine, solubility enhancement

Cellulose Esters and Cellulose Ether Esters for Oral Drug Delivery Systems

Hale Cigdem Arca

Abstract

Amorphous solid dispersion (ASD) is a popular method to increase drug solubility and consequently poor drug bioavailability. Cellulose ω-carboxyesters were designed and synthesized specifically for ASD preparations in Edgar lab that can meet the ASD expectations such as high T_g, recrystallization prevention and pH-triggered release due to the free -COOH groups. Rifampicin (Rif), Ritonavir (Rit), Efavirenz (Efa), Etravirine (Etra) and Quercetin (Que) cellulose ester ASDs were investigated in order to increase drug solubility, prevent release at low pH and controlled release of the drug at small intestine pH that can improve drug bioavailability, decrease needed drug content and medication price to make it affordable in third world countries, and extent pill efficiency period to improve patient quality of life and adherence to the treatment schedule. The studies were compared with cellulose based commercial polymers to prove the impact of the investigation and potential for the application. Furthermore, the *in vitro* results obtained were further supported by *in vivo* studies to prove the significant increase in bioavailability and show the extended release.

The need of new cellulose derivatives for ASD applications extended the research area, the design and synthesis of a new class of polymers, alkyl cellulose ω-carboxyesters for ASD formulations investigated and the efficiency of the polymers were summarized to show that they have the anticipated properties. The polymers were synthesized by the reaction of commercial cellulose alkyl ethers with benzyl ester protected, monofunctional hydrocarbon chain acid chlorides, followed by removal of protecting group using palladium hydroxide catalyzed hydrogenolysis to form the alkyl cellulose w-carboxyalkanoate. Having been tested for ASD preparation, it was proven that the polymers were efficient in maintaining the drug in amorphous solid state, release the drug at neutral pH and prevent the recrystallization for hours, as predicted.

Dedication

For the love of education….

I dedicated my thesis to my beloved family; my parents (Huseyin Oktay Arca and Fatma Nurcan Arca) and my sisters Seyma Ozlem Dogruoz and Betul Cagla Ilarslan.

Acknowledgements

I am very thankful to Dr. Judy Riffle, whom was the reason why I dedicated my Ph.D. thesis for "the love of education" and who was the one supporting me when I felt lost in dark. Without her guidance, I could never complete my Ph.D. and I'll be always be thankful to her for believing in me in times even when I did not believe in myself.

I am very thankful to my advisor, Dr. Kevin Edgar, for his patience, support and for everything he taught me. Without his understanding and support, I could never complete my degree because, as everyone knows, he is a very good scientist and an excellent manager, who knows how to approach a student. I am also very thankful that he always supported me to follow my dreams and guided me for the best. He was the best thing happened to me in my graduate career.

I would like to thank to my committee members, Dr. Sriranganathan, Dr. Davis, Dr. Taylor and Dr. Turner, for guiding my research and helping me to improve my knowledge.

Special thanks to my family, close friends and lab mates: Huseyin Oktay Arca, Fatma Nurcan Arca, Seyma Ozlem Dogruoz, Betul Cagla Ilarslan, Seda Arat, Dagmar Wabel, Junia Pereira, Pinar Gurdal, Selen Olgun, Sevil Baytekin, Gaurav Jain, Sonal Mazumder, Shravanan Balasubramaniam, Jameison Rolle, Joyann Marks, Xiangtao Meng, Xueyan Zheng, Ruoran Zhang, Sidd Pawar, Yifan Dong, Ami Jo, Brittany Nichols, Shu Liu and Haoyu Liu. I love you all and thanks for bearing with me.

Abbreviations

ASD Amorphous solid dispersions

CABSeb Cellulose acetate butyrate sebacate

CASub Cellulose acetate suberate

CAPAd Cellulose Acetate Adipate propionate

CCAB 6-Carboxycellulose acetate butyrate

CMCAB Carboxymethyl cellulose acetate butyrate

DSC Differential scanning calorimetry

EC Ethyl cellulose

Efa Efavirenz

Etra Etravirine

HPC Hydroxypropyl cellulose

HPLC High-Performance liquid chromatography

HPMC Hydroxypropyl methyl cellulose

HPMCAS Hydroxypropyl Methyl Cellulose Acetate Succinate

MC Methyl cellulose

NaCMC Sodium carboxymethyl cellulose

PVP Polyvinylpyrrolidone

Rif Rifampicin

Rit Ritonavir

SEM Scanning electron microscopy

SP Solubility Parameter

TPGS Tocopherol polyethylene glycol 1000 succinate

Q Quercetin

XRD X-ray diffraction

Table of Contents

List of Figures

List of Tables

Chapter 1. Dissertation Overview

Poor drug solubility and accordingly low bioavailability are important issues that have been addressed by many previous investigations. In order to solve these problems, ASDs have emerged as a very efficient method for enhancing drug solution concentration. To date however, studies of polymeric carrier design and effect on ASD performances have been limited. In the view of the attractive characteristics of ASDs, we investigated a range of amphiphilic cellulose derivatives with carboxylic acid groups that will provide pH triggered release to oral drug delivery systems. In addition, having hydrophobic functional groups will enhance miscibility of the polymer with the hydrophobic drugs and moderate the release rate. Investigating types of cellulose ester or cellulose ether ester with different length of hydrocarbon chain and degree of substitution will define the impact of polymer hydrophobicity and help researchers choose suitable polymers for each drug to achieve the desired release properties.

My doctoral research thesis describes investigations of cellulose ester ASDs for oral drug delivery of a tuberculosis antibiotic rifampicin (Rif); anti-HIV drug combination of ritonavir (Rit), etravirine (Etra) and efavirenz (Efa); quercetin, a flavonoid used in the treatment of cardiovascular disease, obesity, and oxidative stress; and synthesis of a new family of cellulose ether esters with a range of solubility parameters that have potential for ASD drug delivery systems. Detailed spectroscopic structure property analyses, solid-state characterization of ASDs, *in vitro* dissolution studies and *in vivo* animal studies are presented.

An outline of the dissertation is as follows: **Chapter 2** is an introduction to cellulose ethers and ether esters that is a very brief summary of their synthesis, pharmaceutical applications, and structure property relationships. **Chapter 3** describes the investigation of Rif ASDs with a range of cellulose esters that have been tested for their solid-state properties and dissolution profiles in acidic conditions that mimic the stomach, and in neutral pH of small intestine environments *in vitro*. **Chapter 4** presents an *in vivo* Rif oral drug delivery study performed with mice that showed a significant increase in Rif bioavailability and extending the drug release time. **Chapter 5** describes anti-HIV three-drug combination ASDs of Rit, Etra and Efa, investigating effects of component drugs on

each other's solubility, as well as the cellulose ester ASD performance of three drug combinations. **Chapter 6** covers synthesis from commercial cellulose ethers and characterization of a range of amphiphilic alkyl cellulose ω-carboxyesters as ASD matrices, and their potential for ASD. **Chapter 7** discusses the complex process of Que ASD studies to enhance the solubility of the drug and prevent its recrystallization that have been tested with a range of cellulose esters and their blends with PVP *in vitro*. **Chapter 8** summarizes the results of the dissertation and suggests future work to be pursued.

Chapter 2. Literature Review: Pharmaceutical Applications of Cellulose Ethers and Cellulose Ether Esters

Adapted from "Arca HC.; Bi V.; Xu D., Edgar KJ. Biomacromolecules 2016 Submitted"

2.1 Abstract

Cellulose ethers have proven to be highly useful natural-based polymers, finding applications in food, personal care products, oil field chemicals, construction, paper, adhesives, and textiles. They have particular value in pharmaceutical applications due their many beneficial characteristics, including high glass transition temperatures (T_g), excellent chemical and photochemical stability, solubility, limited crystallinity, hydrogen bonding capability, and availability in a range of molecular weights. With regard to safety, they have limited ability to permeate through enterocytes, and some are already in formulations approved by the US Food and Drug Administration (FDA). We review pharmaceutical applications of these valuable polymers from a structure-property-function perspective, discussing each important commercial cellulose ether class; carboxymethyl cellulose (CMC), methyl cellulose (MC), hydroxypropylcellulose (HPC), hydroxypropyl methylcellulose (HPMC), and ethylcellulose (EC), and cellulose ether esters including hydroxypropyl methyl cellulose acetate succinate (HPMCAS) and carboxymethylcellulose acetate butyrate (CMCAB). We also summarize their syntheses, basic material properties, and key pharmaceutical applications.

2.2 Introduction

2.2.1 Cellulose and processing: Cellulose is an abundant naturally occurring biopolymer, with a linear polymer chain composed entirely of glucopyranose units (anhydroglucose units, or AGU, chemical repeating unit) linked by equatorial 1,4-glycosidic bonds without any branching (repeat unit →4)-b-D-Glc*p*-(1→); these rather rigid chains have the ability to hydrogen bond to one another, and can pack tightly into a crystal lattice. Cellulose has good mechanical properties (Young's modulus as high as 15 GPa)[1], biocompatibility with many tissues including those of the gastrointestinal (GI) tract, and biodegradability. Cellulose finds versatile applications in the food, wood,

paper, textile, cosmetic and pharmaceutical industries, to name just a few examples. In nature, about 1.5 X 10^{12} tons of cellulose has been estimated to be present in all plants and algae [2], with approximately 10^{10}-10^{11} tons of new cellulose biosynthesized each year[3], and in addition it can be also produced by other species including bacteria and tunicates [4]. Although entirely biodegradable (mineralized to CO_2 and water), cellulose cannot be metabolized by humans and is poorly absorbed from the GI tract [5]. Its renewable nature, low toxicity, and high strength make cellulose an important biomaterial. Due to its hydrophilic nature and crystalline structure, cellulose is insoluble in water or single organic solvents, and cannot be melt-processed because it decomposes before melting [6]. No glass transition temperature can be observed prior to cellulose decomposition. Due to its infusibility and insolubility, chemists have addressed these poor processing issues by synthesizing cellulose derivatives, utilizing the hydroxyl groups at the 2, 3 and 6 positions for appending substituents, creating derivatives which have much different physical properties than crystalline cellulose [7]. Etherification and esterification are the most common methods used to make processable and useful derivatives. After derivatization, solubility properties of the new polymers are frequently improved vs. cellulose, creating the potential for processing into various forms such as fibers, coatings or particles, opening up the potential for a variety of applications. Cellulose esters are frequently hydrophobically modified and because of how they are most often manufactured (peracylation followed by hydrolysis to the desired DS), tend to have high DS substituent, good organic solvent (but not water) solubility, and thermoplasticity; cellulose ester properties and applications have been summarized previously[8]. Cellulose ethers are manufactured in different fashion, by direct etherification to the desired DS, and therefore are often more water-soluble than commercial cellulose esters. As a result, they have different commercial applications; in particular, they are important materials for pharmaceutical applications where water affinity can be a great advantage. Cellulose ethers, and especially their pharmaceutical applications, have not been the topic of comprehensive recent scientific review[9–13]. Therefore we focus herein on pharmaceutical applications and structure-property-function relationships of cellulose ethers and ether esters.

2.2.2 Cellulose ether chemistry: Cellulose ethers are polymers prepared by nucleophilic reaction of cellulose hydroxyl groups with electrophiles such as alkyl halides or epoxides. They find use in a wide range of applications including as thickeners, binders, lubricants, emulsifiers, rheology modifiers, and film formers in many industries including food, pharmaceuticals and personal care products, oil field chemicals, construction, paper, adhesives, and textiles [11,14–17]. Cellulose ether mixtures are used in industrial adhesive mortar applications in order to provide the required properties from wet paste to the hardened structure [18]. Among commercial cellulose ethers, carboxymethylcellulose (CMC) is most heavily used worldwide (over half of the total cellulose ether consumption). Methyl cellulose (MC) and its derivatives have the second largest consumption by volume[19]. We will discuss the general characteristics of cellulose ethers, their preparation chemistry, and how these afford properties that influence pharmaceutical applications in particular.

Theoretically, all three hydroxyl groups of cellulose per anhydroglucose unit (AGU) can be fully etherified, resulting in a degree of substitution (DS) slightly in excess of 3.00 (considering that the end group hydroxyls at C1 and C4 can also be reacted), but frequently complete substitution is not achieved, either because it is not desirable due to the properties being targeted, and/or due to insufficient reactivity of cellulose hydroxyl groups. As noted above, the partially substituted cellulose ethers of commerce are obtained not by full substitution to DS ca. 3.0, followed by "back-hydrolysis" to the target DS, as is frequently the case for cellulose ester manufacture (this would be difficult or impossible due to the greater hydrolytic stability of cellulose ethers), but are reacted directly to the desired DS. This has implications with regard to variability of DS along the chain of ethers vs. esters. Because of the heterogeneous nature of commercial cellulose etherification reactions (generally a slurry of cellulose in aqueous sodium hydroxide, sometimes with an alcohol diluent, along with the desired electrophile), reaction with the electrophile tends to proceed faster in regions of the cellulose chain that were relatively amorphous, and more slowly in crystalline regions[20]. For this reason cellulose ethers, especially those with relatively low DS values, are believed to have relatively blocky structures, with highly substituted and nearly unsubstituted regions

existing on the same cellulose chain[2]. This has been shown with methyl cellulose by observing cellulose crystallinity (which must arise from unsubstituted regions[4]) even at DS(Me) of 1.0. In addition Mischnick and her co-workers have demonstrated blocky substitution in some cases, by partial hydrolysis of cellulose ethers (trifluoroacetic acid (TFA)/water) to oligosaccharides, and comparison of the monosaccharide distribution vs. those expected from modeling of hydrolysis of random, blocky, and other idealized structures[21]. These functionalization patterns along the cellulose chain have been investigated for various etherification reactions, since they impact polymer physical properties including solubility or gelation. Ether substituents may prevent crystallization or induce water solubility to different extents depending on whether they are randomly distributed or are concentrated in blocks. Cellulose ether gelation may be induced by "junction zones" existing in the blocky co-polymer, which have no substituents or very low DS of ether substituents, and so are able to hydrogen bond to one another to form a stable network[5]. Therefore distribution of ether substituents is influential upon polymer properties and is important, though somewhat challenging, to study. Besides heterogeneity along the polymer chain or between polymer chains, the possibility also exists for heterogeneity with regard to position of substitution within the AGU [22]. The three cellulose hydroxyl groups at positions 2, 3, and 6 are chemically non-equivalent to one another, as shown in **Figure 2.1**.

For the ideal case, it is assumed that the rates of reaction of all hydroxyl groups with the electrophile are equal, and remain so throughout the reaction in spite of changes in local environment with partial substitution, so that each hydroxyl group has the same potential to react without any influence by the other groups; this is known as the Spurlin model [23]. The monosaccharide content of a particular cellulose ether can usually be quantified, since complete TFA/water hydrolysis affords monosaccharides which may be analyzed by chromatographic techniques, and identified by comparison with authentic standards or by methods like mass spectrometry[24]. While esterification and subsequent hydrolysis reactions of cellulose are reversible, and thus the monosaccharide composition of a cellulose ester is the result of a number of competing processes, etherification is essentially irreversible. Therefore the monosaccharide composition of a cellulose ether directly and specifically reflects the results of a competition between the three hydroxyl

groups for a particular type and amount of electrophile. Detailed investigations of the monosaccharide compositions of various cellulose ethers prepared under different reaction conditions have shown that the cellulose hydroxyl groups do not possess equal reactivity towards electrophiles, resulting in deviations from the Spurlin model. Generally speaking the 2-OH is most reactive followed by the 6-OH; the order of these two may differ in some cases, but they are always more reactive than the 3-OH[6]. The observed order of reactivity is attributed to the fact that the 2-OH is more acidic (due to proximity to C1, the most electropositive carbon of the AGU) and the 6-OH is least sterically encumbered (wider available approach angles). Therefore more modification is typically seen at the 2-OH and 6-OH than at the 3-OH, with general reactivity order O2 > O6 >> O3[25]. Conventional cellulose etherification reactions usually provide products with at best only modestly regioselective substitution; protection and deprotection reactions, generally impractical in manufacturing processes, are required to obtain highly regioselectively substituted cellulose ethers[26]. This is significant since product properties can vary greatly depending upon regioselectivity of modification[27]. The extent of an etherification reaction can be controlled by varying the temperature, catalyst, solvent system and the mole ratio of electrophile to AGU. Cellulose ethers are relatively stable under the required alkaline reaction conditions (although some loss in degree of polymerization (DP) occurs due to so-called alkaline peeling, in which one monosaccharide at a time is lost in a base-catalyzed reaction from the reducing end of the chain[7]). Molecular weight, DS (and molar substitution, MS, where appropriate (*vide infra*)), and position and pattern of etherification determine the properties of the product cellulose ether[28]. Often molecular weight has a greater effect on mechanical properties, while physical properties (e.g. solubility and water absorption) depend more upon the type of substituent and its DS [18].

2.2.3 General properties: Cellulose ethers possess certain characteristic features that contribute to their value in pharmaceutical and other applications. Most commercial cellulose ethers are water-soluble, the exceptions being ethyl cellulose polymers with rather high DS(ethyl), and all have high affinity for water. Even those cellulose ethers that have hydrophobic substituents (e.g. methyl or ethyl) at low DS are water-soluble, since the substituents contribute to structural irregularity, impede hydrogen bonding, and

thereby limit crystallinity, which is the main source of poor solubility for cellulose. Therefore these water-soluble ethers can be used to modify the rheology of aqueous solutions (e.g., the shear-thinning properties of hydroxyethyl cellulose aqueous solutions contributing to the quality of latex paints)[8]. Cellulose ethers tend to have high molecular weights and possess many hydrogen bond acceptors and donors, therefore violating at least three of Lipinski's rules for ready permeation through the gastrointestinal (GI) epithelium [9]. As a result cellulose ethers typically remain within the GI tract and are unlikely to permeate into the bloodstream. Cellulose ethers are also even more stable to ultraviolet radiation than are cellulose esters (already rather stable to UV), since they do not even possess ester chromophores[14]. Finally commercial cellulose ethers typically possess some degree of amphiphilicity, due to the combination of hydrophilic OH groups and the hydrophobic backbone (and in some cases, substituents). Each individual cellulose ether has other important properties that influence pharmaceutical usage, as will be discussed for individual cases below.

2.2.4 Types of pharmaceutical application: Drug delivery systems have gained importance in medicine since the early 1970s, and polymers have played crucial roles in these systems, with cellulose derivatives being of special importance. Much of the attention early on was focused on oral controlled release systems, which aim to deliver drugs at controlled rate and duration while maintaining the plasma concentrations at therapeutic levels. Controlled release systems may enable reduction in dosage frequency, thereby improving patient adherence to dosage regimes[29]. In controlled release systems, the polymer may influence drug release rate by the rate of polymeric erosion/degradation, and/or by diffusion rate through the polymeric material, or through gels formed by contact of the material with water[30]. After drug release, polymeric delivery systems may also protect the drug from degradation or prevent drug crystallization. Drug delivery polymers must be biocompatible (defined as the ability of the material to invoke a tolerable host response upon application[31]) with the biological systems with which they come into contact; e.g. the GI enterocytes in the case of oral drug delivery. In addition, drug delivery follows the rule that "what goes in must come out"; polymers used in pharmaceutics must be cleared from the body, without the formation of toxic by-

products, by degradation of the polymer into non-toxic and readily cleared materials, or by clearance intact from the body[32]. Cellulose ethers, as semi-synthetic biocompatible polymers prepared from the natural polysaccharide cellulose, are usually suitable for oral[5,33–36], transdermal[37–39] or transmucosal[39,40] drug delivery systems but not for intravenous (IV) or inhalation application since humans do not possess cellulase enzymes in circulation, and so cellulose ethers in the bloodstream could not be broken down at an acceptable rate into fragments small enough to be cleared or metabolized.

2.2.5 Cellulose Ethers in ASDs: Drugs with low solubility (BCS Classes II and IV) present a great challenge to formulation scientists, since they often have poor and/or variable oral bioavailability[41]. Cellulose ethers and cellulose ether esters may be useful in ASD applications. We describe herein how ASDs can enhance solution concentration dramatically, especially for highly crystalline drugs, by eliminating drug crystallinity and stabilizing the amorphous drug against recrystallization both in the solid dispersion and after dissolution.

In ASDs, the drug is trapped in a thermodynamically unstable amorphous form, and accordingly tends towards recrystallization to reach the lower energy crystalline state. This tendency may lead to stability problems[42]. Crystallization can occur either in the solid state during transport and storage of formulations, accelerated by to exposure to high ambient moisture and/or temperature, or from solution after dissolution in the GI tract. In order to stabilize against crystallization, strong drug-polymer interactions are key, to overcome attractive forces between drug molecules and make crystallization less favorable[43]. Therefore in this review, we emphasize the ability of cellulose ethers to impart stability against drug crystallization. In addition to chemical interactions, high polymer T_g can also increase the stability of the formulations in the solid state by limiting drug mobility, thus retarding recrystallization[44]. Therefore, it is essential to have a formulation T_g higher than ambient temperature even in highly humid conditions; this is promoted by high polymer T_g. Cellulose ether physical properties are thoroughly described in the synthesis sections; these properties will strongly influence the type and extent of interaction with drug molecules. Moreover, the polymer should prevent recrystallization after the release of the drug in the GI tract for the best efficacy[45].

Accordingly, it is desirable to have partial solubility of the polymer in aqueous media to permit stabilization against crystallization from solution.

In this review we discuss individually the important commercial cellulose ether classes; CMC, MC, hydroxypropyl cellulose (HPC), hydroxypropyl methyl cellulose (HPMC), and ethyl cellulose (EC). We also discuss cellulose ether esters including hydroxypropyl methyl cellulose acetate succinate (HPMCAS) and carboxymethyl cellulose acetate butyrate (CMCAB), which are of growing interest for applications involving enhancement of solution concentrations of otherwise poorly water-soluble drugs.

2.3 Common types of cellulose ethers and their synthesis

2.3.1 Sodium carboxymethyl cellulose (NaCMC)

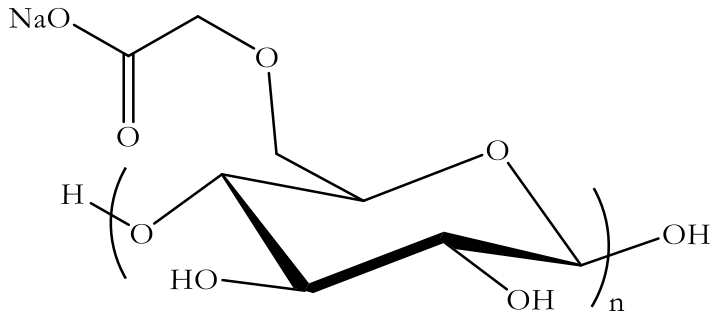

Figure 2.1: The chemical structure of NaCMC. This structure and others in this review are not meant to indicate regioselective substitution; depictions of substituent location are merely for convenience and clarity of depiction.

2.3.1.1 NaCMC synthesis and general polymer properties

NaCMC is a commercial, physiologically inert, low-cost, water-soluble, polyanionic derivative of cellulose, known as cellulose gum, sodium cellulose glycolate, or carboxymethyl cellulose. NaCMC has high water binding capacity and even though it has poor solubility in organic solvents, it can be dissolved in water-solvent mixtures (e.g. water-ethanol). If NaCMC is predissolved in water, it can tolerate addition of some proportion of water-miscible solvents to the solution without precipitation.

Cellulose, treated with sodium hydroxide, is reacted with chloroacetic acid in order to

synthesize sodium carboxymethyl cellulose. NaCl is a co-product of this reaction and glycolic acid is a by-product. The method used has a great impact on the functionalization pattern, highest achievable DS, and solubility, where a relatively low DS of this polar substituent is enough to make the polymer water-soluble[13]. Heinze et al. have shown that even DS(CMC) 0.45 was sufficient to make NaCMC water soluble, much less than is required for non-ionizable substituents[46]. Production of this commercial polymer is carried out by the slurry method, where cellulose is dispersed into a water, NaOH and alcohol system and then the solvent distributes the dissolved base to the hydroxyl groups of cellulose, disturbs the crystalline structure of cellulose by breaking hydrogen bonds, and thus activates hydroxyl groups towards etherification. Alternatively, a dry process can be used where alkali cellulose is prepared first, followed by the addition of monochloroacetate in the solid state. NaCMC can be also synthesized in homogeneous solution. Cellulose can for example be dissolved in DMAc/LiCl[11,47,48], then reacted with powdered NaOH and chloroacetic acid to afford a product that contains a significantly higher amount of tricarboxymethylated and unsubstituted monomers than by the slurry method[49]. In another study, Heinze et al. presented a fully homogeneous carboxylation method in one phase, where cellulose was dissolved in Ni(tren) and HPLC analysis after depolymerization showed that the distribution of the functional groups along the chain has a pattern similar to that of NaCMC prepared by the conventional slurry method, C-6 $\geq$ C-2 > C-3[46]. This implies that these homogeneous conditions surprisingly did not significantly impact the regioselectivity of CMC synthesis; heterogeneous activation of cellulose by mercerization and complete dissolution provide similar accessibility, and there appears to be no particular advantage of the latter method in the case of CMC. On the other hand, Bhandari et al. proposed a new method for synthesis of NaCMC, reactive extrusion, where the process takes less than 2 min and reduces solvent usage[50]. This process is continuous, convenient, and very fast. As an alternative to the use of a cellulose solvent, a homogeneous method can be developed by starting from solutions of cellulose esters (which tend to have good organic solubility), then using alkali both to remove the ester groups and deprotonate the cellulose hydroxyls thereby exposed. The resulting product has high DS NaCMC ($DS_{(Na\ CMC)}$ = 2.2) and shows a different substitution distribution, O-6 > O-3 > O-2. This NaCMC contains higher amounts of

trisubstituted and unsubstituted units than NaCMC prepared by the slurry method[51].

2.3.1.2 NaCMC Pharmaceutical applications

NaCMC has been used in pharmaceutical formulations as a thickener[52], stabilizer[53], disintegration agent (Wan, L.S.C.; Prasad, K.P.P.; Int. J. Pharm. 1989, 55, 115-121), bioadhesive material[54] and film-former[55,56].

NaCMC has been used as co-excipient in many pharmaceutical dosage forms to enhance the release rate while creating osmotic pressure, since the carboxylic acids are ionized at neutral small intestine pH. NaCMC has been used in matrix controlled drug release in combination with other cellulose ethers such as EC or HPMC. Diclofenac potassium in EC-NaCMC wet granulated tablets exhibited higher *in vitro* release rates in over 4-6 hours than from an ethyl cellulose – diclofenac potassium formulation (without NaCMC), which released the drug over 24h [57]. In another study, NaCMC osmotically controlled release tablets were formulated for the sustained release of glipizide by hot melt granulation, and in dissolution studies a zero order release profile was observed over 16h [58]. "Zero order" release rate refers to zero order kinetically with respect to time; that is, release rate is constant over time until the drug is virtually exhausted in the dosage form. Zero order release can often provide near-constant blood levels over prolonged time periods, which is conducive to once-daily oral dosing; this can help to promote patient adherence to dosage regime[59]. NaCMC has been also investigated for use in oral controlled delivery tablets, e.g. of losartan[60], metoprolol[61] and ibuprofen[62].

NaCMC has excellent film forming ability due in part to its high molecular weight. NaCMC films were used for oral thin film preparation for probiotic delivery purposes and probiotic viability was maintained for 150 days [56]. In another study, NaCMC films were used for transdermal delivery of acetylsalicylic acid and stratifin for wound healing (post burn scar treatment) purposes. Samples were found to be nontoxic towards human keratinocytes and fibroblasts[63]. NaCMC has been also used in preparation of film blends. Starch based films are odorless, semi-permeable to CO_2, and resistant to oxygen passage. On the other hand, starch films have poor mechanical properties. In order to improve the properties of starch films and coatings through blending, starch-NaCMC solvent-cast

films were prepared. It was shown that the blended edible films have higher mechanical strength but lower moisture absorption and lower solubility than starch films [64]. Badwaik, et al. showed that antimicrobial and antioxidant materials can be loaded to edible alginate/starch/NaCMC films, which were uniform and had good thermal stability for coating purposes[55]. In addition, the polyanionic nature of NaCMC can be exploited for preparation of polyelectrolyte multilayer (PEM) films by layer-by-layer assembly. Microparticles loaded with drugs (such as ibuprofen) can be embedded into the PEM[65].

A number of polyanionic polymers have been found to possess bioadhesive properties, which may have value in a number of drug delivery applications. Bioadhesion is defined as attachment onto a biological substrate that can be beneficial to prolong the contact time of the drug delivery system for both systemic and topical applications. Anionic NaCMC can form stronger bioadhesive attachment than most of the nonionic cellulose derivatives when applied to some biological surfaces, thus it is an attractive biomaterial for transmucosal and transdermal applications. For example, NaCMC tablets were designed for oral delivery of a water soluble drug, sotalol HCl. The tablets were evaluated *in vitro*, releasing drug for 14 hours, and showing good bioadhesive attachment to rabbit stomach or small intestinal tissue[66]. NaCMC adheres to the mucosal surface better than non-ionic MC and HPMC, as investigated by coating the polymers containing acetyl salicylic acid onto glass beads, and testing adhesion of the obtained microparticles to gastric and intestinal mucosa[67]. Increasing NaCMC concentration in the dosage form enhances mucosal adhesion. Delivery from a NaCMC matrix has been studied for various water soluble drugs such as ciprofloxacin[68] in order to lengthen the stay of the drug in the absorptive portion of the GI tract. For oral mucosal delivery, bucco-adhesive tablets have been prepared with NaCMC with poorly water-soluble drugs[54,69] including glipizide [70], and pindolol [71], and water-soluble drugs [72,73, 74] such as lignocaine HCl [75], miconazole nitrate [76] and triamcinolone acetonide [77], where the bioadhesive properties of NaCMC have been exploited for buccal delivery[78]. Nifedipine bucco-adhesive tablets showed zero-order drug release kinetics, and the adhesive force was affected by NaCMC percentage in the tablet, which adhered to the upper gums of the human volunteers for over 8 hours and released almost 100% of the nifedipine content[54]. According to the Food and Drug Administration (FDA), a formulation can contain up to 242 mg NaCMC for

oral applications, up to 10.95 mg for buccal applications and up to 0.5% for ophthalmic solutions[79].

In addition to oral drug delivery systems, NaCMC has been also used as lubricant and thickener for ophthalmic applications. Aqueous (aq.) NaCMC is a clear lubricant with cytoprotective properties and does not cause eye irritation. Therefore it has been used in artificial tears and lens lubricant rewetting products, usually at a concentration of 0.5%[80]. NaCMC can bind to corneal epithelial cells, increase corneal wound healing[39], and due to the high viscosity of aqueous NaCMC solutions, they can achieve prolonged residence time on the eye surface. There are multiple NaCMC-containing commercial products for ophthalmic applications.

Vaginal mucosal applications of NaCMC were developed for genitourinary tract infection treatment, since its bioadhesive property may enhance vaginal residence time. For mixed infections, clotrimazole and metronidazole bioadhesive tablets were formulated with NaCMC; stronger antimicrobial effects relative to the commercial products, Infa-V ™, Candid-V ™ and Canesten 1 ™, were shown in *in vitro* studies [81]. In another study, vaginal clotrimazole tablets were designed for daily application, where the bioadhesive strength of the tablets was tested on porcine vaginal mucosal membranes; they were shown to have strong attachment and good stability[82]. NaCMC was also used for acyclovir[83] and ketoconazole[84] vaginal bioadhesive tablet preparations. Although these studies are quite promising, they require further *in vivo* studies since the high rate of drug elimination is a key limitation on vaginal mucosal applications.

2.3.2 Methyl cellulose (MC)

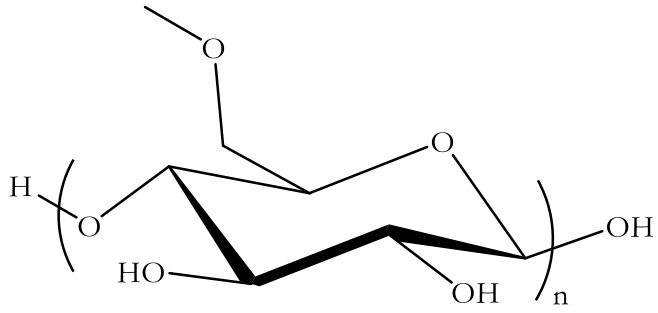

Figure 2.2: The chemical structure of MC.

2.3.2.1 Synthesis and General Polymer Properties

Denham et al., synthesized methyl cellulose for the first time in 1913 from cotton cloth and ordinary cotton wool via a base catalyzed reaction with dimethyl sulfate. The reaction had to be repeated 5 times to achieve DS(Me) 1.2, and the polymer was only partly water soluble[85]. Hauser et al.[86] carried out a similar synthesis, but separated the water soluble portion from the water insoluble one. The water soluble part was investigated and shown to have DS(Me) 1.74-2.00[87]. Houghton et al. improved the manufacture of MC with the application of ≥ 40% NaOH and mechanical disruption of cellulose. The reactions were carried out at temperatures of 40-85 °C with dimethyl sulphate electrophile[88]. Commercially, MC is synthesized by the etherification of alkali cellulose (cellulose treated with sodium hydroxide) with methyl chloride[89]. Like CMC, manufacture of MC can be performed via the so-called dry process or the slurry process. Diluents such as dimethyl ether, ethylene glycol dimethyl ether, or toluene are generally utilized for the slurry process.

The water solubility of the polymer is related to the methyl ether content (DS (Me)). For commercially prepared methyl cellulose products, when DS (Me) is between 0.1-1.1 the polymer swells, becoming water soluble between DS (Me) 1.4-2.0, but losing water solubility at DS (Me) ≥ 2.1[90]. MC with DS of 1.5 has very good solubility in cold water[87] and also at high temperatures (> 60 °C); it can be dissolved in pyridine, DMI, DMAc, or DMF. It is not soluble in lower polarity solvents such as THF, acetone or alcohols, which limits available formulation methods for drug delivery systems. MC solutions are stable

across a wide range of pH values (2-12) without apparent changes in viscosity. Commercial MC is available with viscosity 4-3500 cP (measured at 20 °C with 2-4 mg/ml solutions by capillary viscometry), which corresponds to a molecular weight range between approximately 46,000 and 300,000[89].

Aqueous MC solutions have the interesting property of thermo-reversible gelation; they gel upon heating, and then redissolve upon cooling. The current theory is that gelation of MC solutions is primarily caused by hydrophobic interaction between methyl groups. At low temperatures, molecules are hydrated and water forms an ice-like structure around the hydrophobic methoxy groups, which makes the polymer soluble. As the temperature is increased, water mobility increases and it partly departs from close association with the methoxyl groups, due to decreased relative viscosity and increased entropy of the solution. As the temperature continues to rise, hydrophobic groups interact by van der Waals forces, a network forms between hydrophobic polymer sites before the complete dehydration, relative viscosity increases sharply, and a gel forms. Gels go back into solution upon cooling with a hysteresis loop, and this cycle can be repeated multiple times[91,92]. Gel formation and gelation temperature are dependent on variables including DS (Me), solution concentration and salt content, and polymer molecular weight. Polymers with higher DS (Me) and higher molecular weight can form firmer gels[93] in an entropy driven process. MC fine structure (blockiness vs. randomness), resulting from the synthesis method, also has a great impact on gelation. For example, MC prepared under homogenous conditions does not gel due to the more even distribution of the substituents[94].

2.3.2.2 MC Pharmaceutical applications

MC is classified as a Generally Recognized As Safe (GRAS) by FDA, who approved its use in formulations with the following limits; up to 183 mg for oral applications, up to 4 mg for buccal applications, up to 102 mg for vaginal applications, and up to 0.5 % (v/v) for ophthalmic applications[79]. In addition, MC is non-allergic, vegetarian, metabolically inert, non-digestible, viscous and soluble in cold water. For these reasons, MC has been widely used in the pharmaceutical industry, including as a thickener[95], binder[96], stabilizer[97] and film former[98].

MC has been used in controlled release formulations as a polymer carrier, where its amphiphilicity and ability to dissolve to create viscous aqueous solutions are valuable. It has been shown that MC mixtures can be good carriers for ibuprofen, where controlled release tablets were prepared by direct compression of MC, HPMC and microcrystalline cellulose in order to extend the drug release time period; these formulations displayed linear release profiles, lasting over 12-16 hours. In addition, mixtures of MC and ι-carrageenan afforded zero order release. Water insoluble microcrystalline cellulose and HPMC helped prevent tablet matrix disintegration but swelled upon contact with water. On the other hand, water soluble MC increases water absorption and water penetration rate, promoting polymer swelling[99].

MC has been tested as a nanoparticle stabilizer[97], for example where gold nanoparticles are generated in the presence of MC by reduction of $HAuCl_4.4H_2O$ (H_2, 85°C). Gold nanoparticle size was determined to be stable at 30-50 nm by X-ray photoelectron spectroscopy (XPS) and energy dispersive X-ray spectroscopy. Control samples, gold nanoparticles without MC, agglomerated during the formulation preparation, illustrating the ability of MC to stabilize nanoparticles, presumably by hydrophobic interactions as well as by increasing viscosity. These nanoparticles have potential for diagnostic and therapeutic applications.

MC can be cast into water-soluble films; the hydrophilic films have low permeability for non-polar gases such as oxygen and carbon dioxide. These have potential to be used as film dosage forms, or for coating other delivery systems for various purposes, e.g. taste masking[100]. Stand-alone MC films have poor mechanical properties and processing characteristics, so are commonly plasticized. Solvent-cast edible films of MC were prepared with, e.g., the polymeric plasticizer polyethylene glycol (PEG) 400, where it was observed that water absorption by the films increases with increasing concentration of the hydrophilic PEG. Addition of plasticizer decreases film T_g in predictable fashion[101]. PEG addition also increases the rate of water, oxygen and aroma permeation. If the concentration of PEG is less than 30% in the film, the film remains transparent[102]. MC has also been blended with starch in order to form flexible and transparent edible films with moderate mechanical strength. Starch alone does not form films with adequate

mechanical properties and good moisture barrier performance. MC is a good candidate material to prepare blends with water-soluble starch via various methods such as hot extrusion, or hot pressing. Although a single T_g value was observed for the starch/MC/plasticizer (45/45/10) blend by thermal analysis (DSC-2nd heating), it is difficult to conclude on this basis whether there is phase separation[103]; according to Olabisi, it is not possible to distinguish a phase separated system from a miscible one if the T_g values of individual components are separated by less than 20°C[104]. Starch itself does not have an observable glass transition (most native polysaccharides do not). It appears unlikely that MC and starch are truly miscible.

2.3.3 Hydroxypropyl methyl cellulose (HPMC)

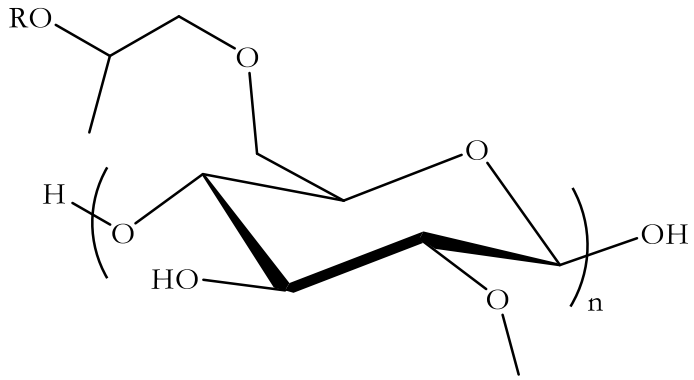

Figure 2.3: The chemical structure of HPMC (R= –H or $–CH_2CH(OH)CH_3$).

2.3.3.1 HPMC Synthesis and general polymer properties

Hydroxypropyl methyl cellulose (HPMC or hypromellose) is a cellulose ether formed by base catalyzed heterogeneous reaction of cellulose with methyl chloride and propylene oxide, [89,105,106]. The reaction with methyl chloride is a simple Williamson ether reaction, resulting in formation of methyl ethers as described for MC. Reaction with propylene oxide is however more complicated. Reaction of the cellulose alkoxide with propylene oxide results in predominant addition to the less hindered end of the epoxide, affording a 2-oxypropyl substituent whose 2-hydroxyl group is deprotonated and bears the same countercation as originally associated with the cellulose alkoxide. One complication is that the reaction is selective for addition to the less hindered end of the epoxide but not

exclusively so; thus some addition to the 2-carbon of propylene oxide occurs, resulting in a primary alkoxy anion. More importantly, either product contains an alkoxide that is now spaced apart from the cellulose main chain and thus enjoys wider approach angles than the original cellulose alkoxide. Thus, addition to a second molecule of propylene oxide can occur, creating an oligo(propylene oxide) side chain of DP 2. As a result, the final product HPMC contains more than 5 substituent types (H-, Me-, 2-hydroxy-1-propyl (major isomer), 1-hydroxy-2-propyl (minor isomer), as well as HP oligomers, and methyl-terminated HP oligomers), so that it is a remarkably complex copolymer. It can be readily appreciated that synthesis of this complex sequence of monomers is difficult to control, and difficult to analyze in detail. It has been determined that the oligomeric side chains stop at rather low DP value (2-3); this is at first surprising since one might assume that higher DP would further increase steric freedom and thus reactivity of the extended-length alkoxide[107]. Researchers have hypothesized that this is due to redistribution of the terminal cation from the growing oligohydroxypropyl chain due to hydrophobic interactions, while there is also the possibility that the growing polyether chain may coordinate the terminal cation and thus reduce the reactivity of the terminal anion.

The hydroxypropyl substituent is relatively hydrophilic and contributes to the rate of hydration, while the methyl substituent is relatively hydrophobic, making HPMC an amphiphilic polymer. Therefore the levels of methyl and hydroxypropyl substitution impact the hydration rate, and would likely have impact on the performance of the drug delivery system. HPMC can form thermoreversible gels upon heating, by a mechanism similar to that described for MC. Highly methylated HPMC chains can form crosslinks due to van der Waals interactions between the hydrophobic methoxy groups upon heating, but hydroxypropyl and oligomeric groups can inhibit crosslinking and gelation[91,108]. Therefore MC can form firmer films at lower gelation temperature than can HPMC, even if the particular HPMC has similar-molecular weight and DS (Me) to the MC of interest. As DS (Me) content of HPMC is reduced, gelation temperature increases. This odorless and tasteless polymer is soluble in water or water/solvent mixtures, e.g. ethanol/water and i-propyl alcohol/water. In addition, HPMC (DS (Me) 1.8-2.0, DS (HP) 0.2-0.34) can be dissolved in non-aqueous solvents such as mixtures of methylene

chloride and methyl, ethyl or isopropyl alcohols, pyridine, *N*-methyl pyrrolidone, mixtures of chloroform and methanol or ethanol, formic acid, glacial acetic acid, dimethyl formamide, or dimethyl sulfoxide[109], permitting fabrication of HPMC formulations by various methods such as solvent casting, spray drying and hot melt extrusion.

In addition to its complex, amphiphilic structure, HPMC is hygroscopic, further complicating analysis, e.g. of thermal properties. Therefore the HPMC glass transition is quite broad and difficult to measure by conventional DSC; often modulated DSC is required to observe the T_g. HPMC powder T_g has been measured as ca. 180 °C [110,111], but in the case of solvent cast films HPMC (DS (Me) 1.8-2.0, DS (HP) 0.2-0.34, viscosity 5 000 cP) has a T_g of 157 °C [111]. Adventitious water has the plasticization effect on the hydrophobic polymer and decreases the T_g.

2.3.3.2 HPMC Pharmaceutical applications

HPMC is used in the pharmaceutical industry as a film-coating agent[112], thickener[113], hydrophilic matrix material[114], tablet binder, and as an amorphous solid dispersion carrier. In addition, it has bioadhesive properties[115] and resists microbial attack. For this reason, strong water-soluble HPMC films provided antimicrobial protection e.g. against *Salmonella Montevideo*[16].

HPMC is recognized as a GRAS material by the FDA to be used in food based materials based on toxicology studies using oral and intraperitoneal routes of administration[116]. The suitability of dosage forms containing up to 20 mg/kg HPMC was confirmed by the lack of toxic effects to mice, rats, dogs and cynomolgus monkeys[117]. FDA approved drug products can contain HPMC at levels up to 670 mg in oral formulations, up to 54 mg for vaginal formulations, up to 24 mg for buccal formulations, and up to 2.25% for ophthalmic solutions[79]. In addition, pharmacokinetics and potential metabolism of this cellulose ether were investigated in rats and humans, leading to the conclusion that approximately 97% of orally dosed HPMC was recovered from the feces[116]. Therefore pharmaceutical grade HPMC can be used as an excipient, and it is listed in the European, United States (USP) and Japanese Pharmacopeias as hypromellose. In the National

Formulary (USP30-NF25,) HPMC is recognized as an excipient to be used as a coating agent, suspending or viscosity increasing agent, and as a tablet binder[118,119]. Benecel™, Methocel™ and Metolose™ are the trade names for products of Ashland Chemical, Dow Chemical, and Shin-Etsu Chemical Companies, respectively. HPMC is available in a wide range of molecular weights, presented on the basis of the viscosities of 2 % w/w aqueous solutions in a range from 3 to 200,000 cps[120,121] that represent 8 – 200 X 10^3 Dalton (degree of polymerization (DP) 40-1000)[122], making it possible for the formulation scientist to pick the required viscosity. In the USP nomenclature, four digit numbers represent the DS of each substituent group, where the first two digits refer to the methyl group and last two digits refer to the hydroxypropyl group; HPMC commercial product properties are summarized on **Table 2.1**. In controlled release applications, the E type (HPMC 2910) and K type (HPMC 2208) are the most commonly used products.

Table 2.1: Methyl and hydroxypropyl group (%) contents of HPMC commercial products[123–125]

Substitution Type (USP and EP)	Methoxy Group Content (%)	Hydroxypropyl Group Content (%)	DS of Methoxy group	DS of Hydroxypropyl group	Type (Dow, Ashland or Shin-Etsu)
HPMC 2910	28-30	7-12	1.8-2.0	0.2-0.34	E or 60SH
HPMC 2906	27-30	4-7.5	1.7-2.0	0.1-0.2	F or 65SH
HPMC 2208	19-24	7-12	1.15-1.6	0.18-0.33	K or 90SH

Alderman, et al. suggested that the amounts of substituents can affect the rate of polymer hydration, which follows HPMC K 4M > HPMC E 4M > MC A4M > HPMC F 4M (4000 cp) [9]. This idea was challenged by Mitchell et al., who found that there was no difference in the rate of hydration in different HPMC grades at the same viscosity (4000 cP). Viriden et al., supported this idea and claimed that DS of functional groups does not

have an effect on the rate of hydration, but the substituent pattern of the functional groups throughout the polymer chain does. The effect of heterogeneity of distribution of the functional groups of commercial polymers was investigated in order to understand how sensitive the polymer is to copolymer composition alterations. Blocky polymers, in which more- and less-substituted sequences may alternate, have lower solubility than do more homogenously substituted cellulose ethers, even at similar degrees of substitution[126]. Substituted segments have a tendency to associate and form gel-like components, increasing viscosity; as temperature increases, these gel-like components grow in size. Functional group substituent pattern along the polymer chain has an effect on polymer dissolution from the dosage form, where the homogenously substituted HPMC polymer chains have higher solubility, leading to greater tablet erosion[126,127], and consequently faster drug release. On the other hand, the more blocky samples have lower solubility, and thus show slower release profiles for hydrophobic drugs[128], whose release is erosion controlled while water-soluble drug release is often diffusion controlled. The more heterogeneous the polymer, the slower the erosion and the slower the release of hydrophobic drugs, e.g. carbamazepine, but such heterogeneity has no effect on release rate of diffusion controlled soluble drugs, e.g. theophylline[128]. As a result, erosion controlled drug release is very sensitive to alterations in HPMC chemical composition.

The effect of polymer viscosity on drug release rates has also been investigated. For water-soluble drugs such as aminophylline[129], promethazine HCl[130], and others[131,132], it was shown that there is no release rate dependence on HPMC viscosity[114]. On the other hand, HPMC solution viscosity, which depends upon molecular weight, plays an important role in the formulation of poorly water soluble drugs such as indomethacin where higher molecular weight of the polymer leads to slower release of the drug; a wet granulated formulation with 15,000 mPa. Viscosity polymer (2% K type HPMC in water at 20°C) releasing up to 90 % of the drug payload within 12 h, while a 4000 mPa.s viscosity polymer under otherwise equivalent conditions reached 90% release within 8 h[133]. It was found that drug release rate decreases as polymer viscosity and polymer content in the formulation increase, resulting in extended release profiles.

HPMC has been found to be useful as a hydrophilic carrier in drug delivery systems. By absorption of water, it creates osmotic pressure, which leads to rupture of the polymer

matrix and thus enhances drug release [62] either by diffusion or by erosion of the gel layer. Swellability and surface activity are key parameters that impact drug release rate. When HPMC contacts water or other biological fluids, it becomes hydrated, leading to polymer chain relaxation and volume expansion. In addition, cellulose ethers with methyl and/or hydroxypropyl groups can be adsorbed onto hydrophobic drug surfaces[134,135]. The adsorbed layers produce a steric stabilizing effect. The thickness of the adsorbed layer determines the magnitude of stabilization[136]. For these reasons, HPMC has been applied in solid dispersions as a rate controlling and stabilizing polymer.

High viscosity grades of HPMC were cited as preferable for use in matrices for hydrophilic drugs[114]. A high molecular weight HPMC 2208 (apparent viscosity 2 % w/w in water at 20°C 80,000 – 120,000 cp) was used for the extended release of metformin hydrochloride, a very hydrophilic drug with a variable but short half-life (1.5 – 4 h). Solid dispersions were prepared by solvent casting or co-grinding methods; dispersions prepared at 1:4 drug to HPMC ratio by either method were capable of prolonging the release of metformin for 10 h in *in vitro* dissolution studies [137]. Direct compression of tablets [138] and gel formation for hydrophilic matrix tablets [139,140] are other methods used to prepare HPMC rate-controlling formulations. Tablets from high molecular weight HPMC are harder, less plastic and less likely to deform by compression than those from lower molecular weight HPMC[141]. Besides direct compression, HPMC has been also used for wet granulation. Case studies of wet granulation of acetaminophen, ibuprofen, and ascorbic acid using low viscosity HPMC and MC were published by Ashland[142]; HPMC wet granulated tablets are less fragile than MC tablets. In addition, drug release from HPMC formulations was faster than from MC formulations. Although wet granulated HPMC tablets have good potential, the preparation method is costly and direct compression of controlled-release formulations has traditionally been a challenge due to poor compressibility and low final product content uniformity.

Low viscosity grades of HPMC are predominantly used for film coating of tablets[112,114], since they permit higher solids coatings solutions. HPMC is the most widely used cellulose derivative in pharmaceutical film coating, probably because it has better solvent solubility than most other commercial cellulose ethers while retaining high water affinity,

and because its flexible substituents can dissipate energy, thereby reducing friability.[143] In some formulations, film coating properties (e.g. moisture permeability, mechanical properties, ductility) were improved by addition of plasticizers (e.g. low MW polyethylene glycol[144,145], propylene glycol[145], or glycerol[112]). In addition, HPMC has been used for vegetarian capsule formation[119] as a replacement for gelatin. Gelatin capsules have major drawbacks including cross-linking, drug incompatibility, and their animal source, leading to concerns about contamination. HPMC is proposed as an alternative material for encapsulation since it is stable, and suitable for encapsulation of oxidatively labile and hygroscopic drugs as a result of the low oxygen permeability and greater hydrophobicity of HPMC than MC. HPMC films have also been investigated as tablet coatings for colon specific delivery in combination with pectin and chitosan at a ratio of 1:3:1, and have been administered to human volunteers. In all cases, tablets passed through the stomach and small intestine intact, and then films swelled and became degradable by pectinolytic enzymes in the colon[146,147] where the role of HPMC is to extend drug release time since it is not quickly degraded by colonic bacteria. Therefore the authors expect that pectin/chitosan/HPMC formulations may have significant potential for colon-targeted drug delivery.

Due to the reasonable solvent solubility of HPMC and its thermoplastic nature, respectively, HPMC based pharmaceuticals can be also prepared by spray drying[148–150] and melt-extrusion formulation[151,152]. Spray drying polymer and drug from a common solvent can be an efficient method to prepare ASDs of poorly soluble crystalline drugs such as naproxen[148,150] or indomethacin[150], or water-soluble drugs such as sodium pantoprazole[149] or acetaminophen[153]; all grades of HPMC are applicable for spray drying. On the other hand, only some specific grades of HPMC can be melt-extruded. HPMC E50 2910 (viscosity 5 mPa) extrusion led to an increase in back pressure and the melt-extrusion process was troubled, while HPMC 100 is readily extrudable at temperatures as low as 150°C and as high as 205°C with minimal color change even at the higher temperatures. T_g values of HPMC 100 and HPMC E50 are 110°C and 174°C respectively; the lower T_g of HPMC 100 provides a wider temperature window for melt

extrusion. Hot melt-extruded HPMC formulations have been prepared with lidocaine [154] and itraconazole[151].

HPMC is used as a crystallization inhibitor to prepare supersaturated solid dispersion systems, which may increase drug bioavailability. Paclitaxel showed minimal precipitation and improved pharmacokinetics after oral dosing of solid dispersions to rats. HPMC has been used to prevent or retard precipitation of various other poorly soluble drugs including tacrolimus [155,156,34].

Due to the bioadhesive property of HPMC, it has been used in numerous mucosal drug delivery formulations. Delivery systems prepared with HPMC have good buccal retention and controlled release characteristics. Therefore buccal adhesive tablets were prepared with various drugs[157,158,159] including chlorhexidine hydrochloride[160] and insulin[161]. After hydration, HPMC can adhere to oral mucosa and can withstand tongue movements, salivation and swallowing for a significant period of time. Taylan et al. showed that an HPMC and polycarbophil (8:2) formulation fulfills the criteria for buccal sustained release since it has a smooth plasma level profile and long duration effect; however it has no significant advantage over the commercial product, Dideral®[29]. In order to prevent sexually transmitted infections such as those caused by the human immunodeficiency virus (HIV), human simplex virus (HSV), or human papillomavirus (HPV), vaginal drug delivery systems have been developed. It has been shown that HPMC films can adhere to porcine vaginal tissue for 6 hours and can release 70% of the drug load (sodium dodecyl sulfate)[162]. In another study, acyclovir vaginal tablets were prepared with MC, NaCMC, HPMC or HPC by direct compression and wet granulation. HPMC stayed physically attached to cow vagina for 6 hours but the other tablets swelled rapidly, thus leading to disintegration[163]. The charged nature of NaCMC and the greater hydrophilicities of the other ethers enhance their water affinity. Directly compressed tablets of clotrimazole/HPMC combined with polyanionic NaCMC showed higher mucoadhesive strength and more controlled vaginal drug release than HPMC tablets with neutral guar gum[164]. Furthermore, vaginal thermosensitive gels were prepared with HPMC 2208 and cyclodextrin, providing slow release of the anticancer drug 5-fluorouracil (5-FU) over 90 hours *in vitro*; a human cervical carcinoma cancer (HeLa cells) study showed anticancer efficacy for these gels at a much lower 5-FU dose, with controlled and prolonged 5-FU

release[165]. Unlike tablets, the *in situ* gelling systems in the vaginal cavity offer the advantage of reduced outflow from the vagina. Although there are promising approaches for HPMC based vaginal delivery, the usefulness of the approach is still limited by the short vaginal residence time of the dosage forms, which necessitates frequent application.

Ophthalmic mucoadhesive systems also have been developed with HPMC due to the clear nature of its aqueous solutions, as well as its high solution viscosity and bioadhesive nature that lead to longer retention in the eye and low tendency to cause eye irritation. Opthalmic delivery faces the challenge that ocular formulations are typically eliminated from the eye within the first 5-20 min after administration, and the therapeutic dose must penetrate the cornea within this short time frame. Liu et al. showed that HPMC/alginate formulations of gatifloxacin, an antibacterial agent, were retained the drug in the eye for a longer time period *in vitro* and *in vivo* without causing any irritation, resulting also in increased gatifloxacin bioavailability[113] due to HPMC's *in situ* gel forming property that limits pre-corneal elimination. *In vitro* studies showed drug release sustained over 8 hours, while *in vivo* the half-life of the formulation is limited to 44 min; still significantly longer than with conventional systems. HPMC has also been used for the preparation of commercial artificial tear products for dry eyes.

Table 2.2: Examples of HPMC Containing Commercial Pharmaceutical Products.

Product name	Active ingredient name	Company	Application
Desogan	Desogestrel and ethinyl estradiol	Prasco laboratories	Oral contraceptives
Factive	Gemifloxacin mesylate	Oscient Pharmaceuticals, Inc	Oral antibiotic
Flumadine	Rimantadine hydrochloride	Forest Pharmaceuticals, Inc.	Oral antiviral
Flurbiprofen	Flurbiprofen	Caraco Pharmaceuticals	Oral non-steroidal anti-inflammatory drug (NSAID)
Isosorbide Dinitrate Extended Release	Isosorbide dinitrate	Inwood Laboratories	Oral vasodilator
Lopressor	Metoprolol tartrate	Caraco Pharmaceuticals, Inc	Oral antihypertensive
Oxycontin	Oxycodone hydrochloride	Endo Pharmaceuticals, Inc	Oral narcotic pain reliever
Rantidine or Zantac	Ranitidine hydrochloride	Genpharm Inc. and Glaxo Welcome	Oral nonsteroidal anti-inflammatory drugs (NSAIDs)
Trovan	Trovafloxacin	Pfizer Pharmaceuticals Group	Oral antibiotic
Ambien	Zolpidem tartrate	InvaGen Pharmaceuticals Inc.	Oral sedative-hypnotics

2.3.4 Ethyl cellulose (EC)

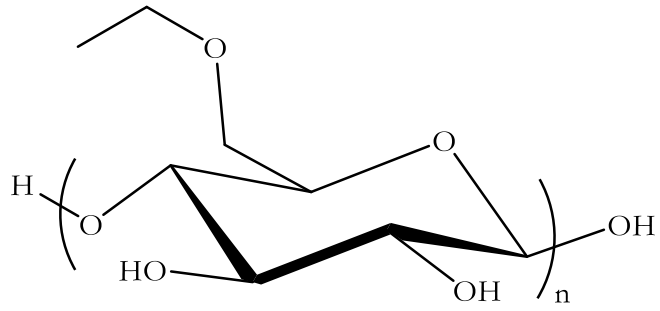

Figure 2.4: The chemical structure of EC.

2.3.4.1 EC synthesis and general polymer properties

Cotton linters or wood pulp can be used for the synthesis of ethyl cellulose (EC). In one of the earliest reported methods, cellulose was solubilized with trimethylbenzyl ammonium hydroxide and then reacted with diethyl sulfate [87]. Lilienfeld patented processes where the cellulose was pretreated by xanthation, or with cuprammonium, or by heating in 30-50% NaOH [166]. Cellulose was then reacted with an alkylating agent (diethyl sulfate) and heated. If a low-boiling alkylating agent was used, (ethyl chloride or ethyl bromide) the reaction had to be carried out in an autoclave or another pressure vessel, whereas if higher boiling alkylating agents were used, (ethyl iodide or diethyl sulfates) the reaction could be performed with a reflux condenser.[166] Compared with methylation of cellulose, ethyl cellulose production is less efficient under heterogeneous conditions due to the higher molar volume and hydrophobicity of ethyl halide, which can retard the diffusion-controlled reaction. Generally speaking, synthesis of ethyl cellulose requires more harsh conditions than those required for methyl cellulose, including higher alkalinity, higher reaction temperature, and longer reaction time. In commercial methods, ≥ 50% sodium hydroxide is used for alkalization, and then the alkali cellulose is reacted with ethyl chloride at < 50 °C for 10-20 hours [167,110]. The resulting EC has almost equal partial DS(Et) at C-2 and C-6, with lower DS(Et) at C-3[168].

Table 2.3: EC Physical Properties.

DS(Et)	2.2-2.8
T_g	140 °C (DS(Et) 2.3)
T_m	140-160 °C
Viscosity (5% solution at 25 °C in an Ubbelohde viscometer) [169]	4-350 cP
Solubility	Soluble in esters, aromatic hydrocarbons, alcohols, ketones and aromatic solvents but not water soluble
Color	White or light grey
Stability	Light stable (visible or UV), stable in alkali conditions but not acidic

The effect of increasing DS(Et) is quite dramatic; at low DS EC is water-soluble due to disruption of H-bonding and structural regularity by the ethyl groups, while at very high DS, solubility even in solvents as non-polar as aromatic hydrocarbons is observed. EC solubility parameters thus decrease with increasing DS(Et). In general, commercial EC grades are soluble in a variety of solvents such as esters, aromatic hydrocarbons, alcohols, ketones, and aromatic solvents, but insoluble in water. The physiologically inert bio-based material is thermoplastic, melting in a temperature range of 140-160 °C [170], and with T_g (DS(Et) 2.55, 48.5% ethyl content) 140 °C [110]. EC is a tasteless, and odorless powder that takes up very little water, due to the high DS(Et) and resulting relative hydrophobicity, is light stable (visible or ultraviolet) due to its lack of chromophores, and can form tough, flexible films. EC is generally non-toxic, non-irritant, biocompatible[12,171], and no significant biodegradation was recorded when exposed to *Aureobacterium saperdae* or *Pseudomonas lemoignei* for 30 days[172]. EC physical properties are summarized in **Table 2.3**.

2.3.4.2 EC pharmaceutical applications

EC has been used in many controlled drug delivery systems as a binder[173,174], film forming agent,[175] or coating material[176]. It is also used to mask the bitter taste of drugs to increase patient compliance[177]. EC is available in different viscosities as a granular (standard) particle size or as fine particles, which are produced specifically to be used as controlled release excipients in order to improve performance of the standard EC[178]. According to FDA, the EC daily maximum allowable dose is 308 mg for oral applications, 80 mg for transdermal applications, and 50 mg for vaginal applications[79]. It can be processed by hot melt extrusion[170,179–181], spray drying[182], co-precipitation,[173] or emulsification/solvent evaporation[177] for microparticles, and for tablet formation via either direct compression[183] or wet granulation[184]. NaCMC[62,185], HPMC[62,174], Eudragit copolymers (e.g. ethyl acrylate, methyl methacrylate and trimethylammonioethyl methacrylate copolymer with a ratio of 1:2:0.2) [173,186,187], and starch[62,185] are the hydrophilic co-excipients most commonly used in combination with EC in oral dosage forms in order to increase drug release rates.

Prominent recent studies of EC matrix systems are summarized to illuminate the increasing interest in this polymer. EC was proposed for use as an excipient for didanosine tablets, a drug substance used in the treatment of acquired immunodeficiency syndrome (AIDS) [186,187]. In this study, the directly compressed polymeric tablets (ethyl acrylate, methyl methacrylate and trimethylammonioethyl methacrylate copolymer–EC mixtures) allowed the sustained release of 60-70% of the drug *in vitro* over 6 hours. A study was performed for didanosine/EC tablets to optimize compression force, polymer particle size, and drug content variables to obtain the best formulation conditions. Drug load had the most significant effect on increasing dissolution efficiency, and drug release was inversely proportional to EC particle size[186]. Tablets of EC with another active pharmaceutical ingredient, diclofenac potassium, were prepared and subjected to *in vitro* dissolution studies, showing that EC significantly decreased diclofenac release rate, and that zero order release was observed[57]. Zero order drug release is desirable in controlled drug delivery systems since it is by definition constant drug release rate (independent of time) without any burst effect, frequently leading to near-constant blood concentration of

the drug, which is particularly favorable for drugs with narrow therapeutic indices. Such long-term constant release rates can also enable less frequent (ideally once daily) dosing, thereby increasing patient compliance. In another study, ibuprofen EC tablets were prepared for controlled release, where the influence of the different variables such as particle size, polymer molecular weight, drug to polymer ratio, and tablet preparation method were investigated[62,174]. For directly compressed formulations, the polymer molecular weight does not have a significant effect upon drug release. On the other hand, when a wet granulation method was used, drug release rate increased with lower molecular weight polymers. Nevertheless, drug content had greater impact upon drug release rate (the higher the drug content the higher the release rate) than that of polymer molecular weight[174]. In addition, controlled release from fine particle EC formulations was investigated for different drugs [183,188,189] such as naproxen[190]. Fine particles of EC were compared with standard EC, showing that fine particle EC releases drug with more extended release profiles of active pharmaceutical ingredients such as ibuprofen[174,185] and ofloxacin [184].

In EC dosage forms, increasing the ratio of the high T_g, thermoplastic, compressible polymer to drug caused tablet porosity decrease, and increasing tablet hardness. The increased proportion of relatively hydrophobic polymer reduced tablet wettability, while also reducing drug release rate. As the amount of hydrophobic EC increased, it became harder to absorb water and drug diffusion was also impeded[174,189]. Therefore, a relatively more hydrophilic co-excipient added to the formulation may provide increased release rate.

EC has been used in oral drug delivery systems as a carrier in order to improve the bioavailability of drugs[191,192]. For example, the anti-ulcer drug ranitidine hydrochloride was formulated in EC-based porous microparticles of 350-750 mm diameter, with encapsulation efficiencies up to 96% when prepared by an oil in oil method; paraffin and Span 60 comprised the dispersion medium for the drug and polymer mixture. These EC solvent evaporated microparticles were orally dosed to New Zealand rabbits, resulting in extended drug release (more than 12 hours), achieving drug plasma concentration around 15 mg/mL, and increasing drug bioavailability 2.4-fold relative to the pure drug[193]. In

another study, tramadol EC microcapsules were prepared by spray drying, and the effects of EC viscosity, solvent system, and plasticizer addition were investigated. Dichloromethane and ethyl acetate solvent systems led to regular particle morphology. Addition of the hydrophobic diethyl phthalate as plasticizer decreased drug release rate with low viscosity EC; on the other hand, it did not have an effect on release rate from medium viscosity EC [182].

The film forming ability of EC has enabled encapsulation of various drugs. EC films do not dissolve in water or in the GI tract, and can be used to provide oxygen barrier and/or taste masking. EC films can also regulate drug diffusion rate. Granules of theophylline, cellulose, and lactose coated with EC were investigated and zero order theophylline release from the coated granules was reported[194]. Moreover, 5-aminosalicylic acid was formulated in ethyl cellulose – amylose coated pellets for colon specific drug delivery, mediated by colonic bacterial degradation of the amylose component. The EC portion of the coating was more efficient in controlling swelling and accordingly drug release relative to other coatings (EC/amylose aqueous dispersion, and (ethyl acrylate/methyl methacrylate/trimethylammonioethyl methacrylate) copolymer-amylose coating)[195]. EC was used as a matrix with amidated pectin and calcium pectinate for ropivacaine delivery to the colon[196]. Pectin has been used for colon specific drug delivery systems since it is susceptible to enzymatic degradation by the enzymes of the gram-negative bacteria inhabiting the colon. The role of the EC in the formulation is to increase tablet strength and decrease dissolution rate.

Thermal extrusion of drug and polymer blends can lead to increased drug aqueous solubility by formation of drug/polymer ASDs. EC thermoplasticity is useful in this respect, making it a good candidate for ASD preparation by extrusion. The ability to make ASDs by co-extrusion of drug and polymer is valuable, since it eliminates the possibility of residual solvent in the ASD that exists with spray-dried formulations. EC is often co-extruded with a hydrophilic material, employed to provide the release mechanism, where the ratio of hydrophilic to hydrophobic polymers strongly influences the drug release rate. EC melt extrusion was studied with HPMC, dibutyl sebacate (matrix former and plasticizer) and xanthan gum for metoprolol tartrate[197] and ibuprofen

drug delivery systems. Optimum extrusion temperature depends on drug thermal properties and drug/polymer ratio, and was in the range 110-140°C[197] for metoprolol tartrate systems. In other studies, the optimum extrusion temperature for blends of 30% ibuprofen in EC formulations was 82°C; on the other hand, 60% ibuprofen-EC formulations gave smooth extrudates at 60-62°C[198–200]. Extrusion temperatures were far below the T_g of the EC used (133°C). This behavior was explained by the assumption that the drug acted as a plasticizer for EC, leading to a decrease in blend T_g[200].

Apart from oral drug delivery systems, ethyl cellulose has also been used to prepare spray-on transdermal delivery films, due to its excellent film forming properties[175], forming blends with ethyl acrylate/methyl methacrylate/trimethylammonioethyl methacrylate copolymer (at a ratio of 1:2:0.2) and fluconazole. Tests with healthy human volunteers showed that the films displayed good dermal adhesion and flexibility, while water washability was only moderate. The films improved fluconazole permeation through shed snakeskin over 13 h.

2.3.5 Hydroxypropyl Cellulose (HPC)

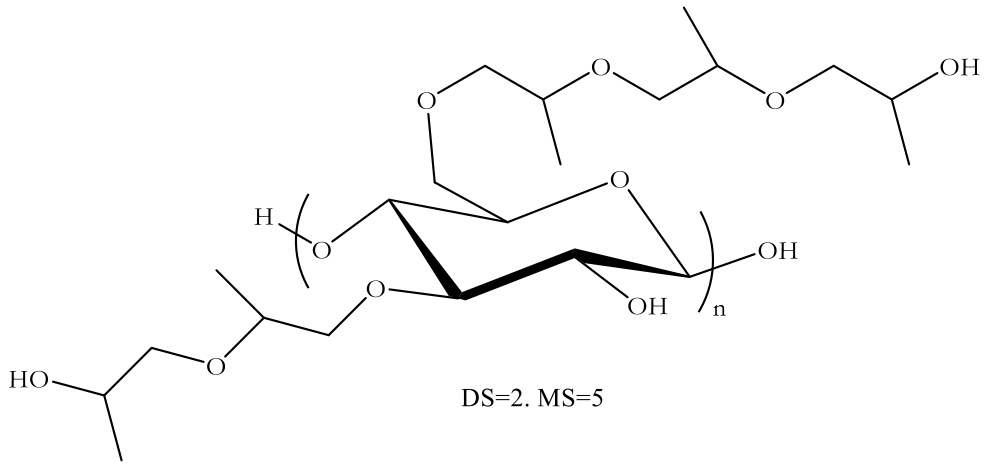

Figure 2.5: The chemical structure of HPC.

2.3.5.1 HPC synthesis and general polymer properties

HPC is manufactured by reacting alkali cellulose with propylene oxide at elevated temperatures and pressures. Propylene oxide can react with alkali cellulose by nucleophilic ring opening, predominantly though not exclusively at the less hindered end (carbon 1) of the epoxide, forming an ether linkage. Reaction can occur at any of the three reactive hydroxyls present on each anhydroglucose monosaccharide unit of the cellulose chain. Ring opening at the less hindered end of the epoxide affords hydroxypropyl substituents that contain almost entirely alkali salts of secondary hydroxyl groups. The alkali salt of the secondary hydroxyl present in a side chain is available for further reaction with propylene oxide, and in fact has available to it much wider approach angles than do the hydroxyls of the cellulose main chain. Therefore the alkoxyl of the side chain is prone to reaction with further molecules of propylene oxide, extending the oligo(propylene oxide) side chain. This results in formation of side chains containing more than one mole of combined propylene oxide. It is probable that most of the primary hydroxyls on the cellulose have been substituted and that the reactive groups remaining are secondary hydroxyls[201]. An idealized structure for a portion of a HPC molecule with a hydroxypropyl molar substitution (MS) of 5 is given in **Figure 5**. While DS is the average number of hydroxyl positions substituted per AGU, MS is the average number of substituents per AGU; note that DS is limited to a maximum of ca. 3 for cellulose, while MS can exceed 3 for adducts of cellulose with epoxides (like HPC) because of the possibility of forming oligo(hydroxyalkyl) substituent chains. Both DS and MS are important factors determining the properties of HPC.

HPC is a non-ionic water-soluble cellulose ether with a different range of properties than some other cellulose ethers, due to its relatively hydrophobic side chains. As a result, it is soluble in both aqueous and polar organic solvents. Those same somewhat hydrophobic substituents impart thermoplasticity[202] (unlike the more polar HEC), and some degree of surface activity. At the same time, HPC modifies rheological properties of aqueous solutions in ways similar to other water-soluble cellulose ethers, imparting thickening and stabilizing properties to those solutions.

Commercial HPC (MS 3.0-4.0)[203] is soluble in many polar organic solvents and in water below 38°C. HPC however shares the interesting property of thermal gelation with MC[204] and other cellulose ethers[205]; the mechanism of that gelation is discussed in the MC section. As a result of this gelation, HPC is insoluble in water above 45°C. The polymer is available in a wide range of viscosity types, providing a large range of solution properties in water and ethanol. Its thermoplastic properties will be described in more detail later in this section, but they do permit extrusion, use in film and coatings, and heat sealing. The presence of both hydrophilic (OH) and hydrophobic (hydrocarbon) portions of the molecule leads to miscibility with a number of plasticizers and other polymers[206].

HPC is primarily supplied by two manufacturers, Ashland Specialty Ingredients and Nippon Soda Co., Ltd. Ashland provides different grades of HPC trademarked as Klucel™; within the pharmaceutical grade there are 7 viscosity types designated as H, M, G, J, L, E and EL. HPC products are also characterized by particle size, with regular particle size materials suitable for use in wet processing, and finer "X-grind" material for dry processing. **Table 2.4** gives the water and ethanol viscosity specifications of pharmaceutical grade for each available viscosity type[201]. Nippon Soda Nisso™ HPC is available in 5 viscosity types, and the aqueous viscosity info can be found in **Table 2.5**[207].

Table 2.4: Klucel HPC Viscosity Types, Viscosities (cps), and Molecular Weights.

Klucel Pharmaceutical Grade	Viscosities of aqueous solutions, cps				M_w**
	1%*	2%*	5%*	10%*	
ELF					~40,000
EF and EXF				300-600	~80,000
LF and LXF			75-150		95,000
JF and JXF			150-400		370,000
GF and GXF		150-400			140,000
MF and MXF		4000-6500			850,000
HF and HXF	1500-3000				1,150,000
Pharmaceutical Grade	Viscosities of anhydrous ethanol solutions, cps				M_w**
	1%*	2%*	5%*	10%*	
ELF					40,000
EF and EXF				150-700	80,000
LF and LXF			25-150		95,000
JF and JXF			75-400		370,000
GF and GXF		75-400			140,000
MF and MXF		3000-6000			850,000
HF and HXF	1000-4000				1,150,000

*All viscosities are determined at 25°C using a Brookfield LVF viscometer with spindle and speed combinations depending on viscosity level

**Weight average molecular weight determined by size exclusion chromatography.

Table 2.5: Nisso HPC Viscosity Types and Viscosities (cps).

Nisso HPC type	SSL	SL	L	M	H
Viscosity @ 20°C/2% aq	2-2.9	3-5.9	6-10	150-400	1000-4000
M_w	~40,000	~100,000	~140,000	~620,000	~910,000

It is interesting that HPC is thermoplastic, unlike the other high-volume cellulose ether prepared by epoxide ring-opening, HEC. HPC is significantly more hydrophobic than HEC; HPC has a reported T_g of ~130°C[208] and can be processed by virtually all fabrication methods used for plastics. Importantly, HPC has rather good thermal stability, not beginning to decompose until ca. 300ºC[209] (as quantified by thermogravimetric analysis (TGA)); HEC decomposition begins in the vicinity of 200ºC. Therefore, for HPC there is a processing window of sufficient width to make melt processing a practical alternative. Injection-and compression-molding; blow-molding; injection foam molding, vacuum forming and extrusion of film, sheet, foam profiles and filament have been demonstrated in conventional plastic equipment, using pelletized molding powder. The melt flow behavior of HPC depends in predictable fashion upon its molecular weight, with lower MW grades having higher melt flow indices (**Figure 2.6**)[201].

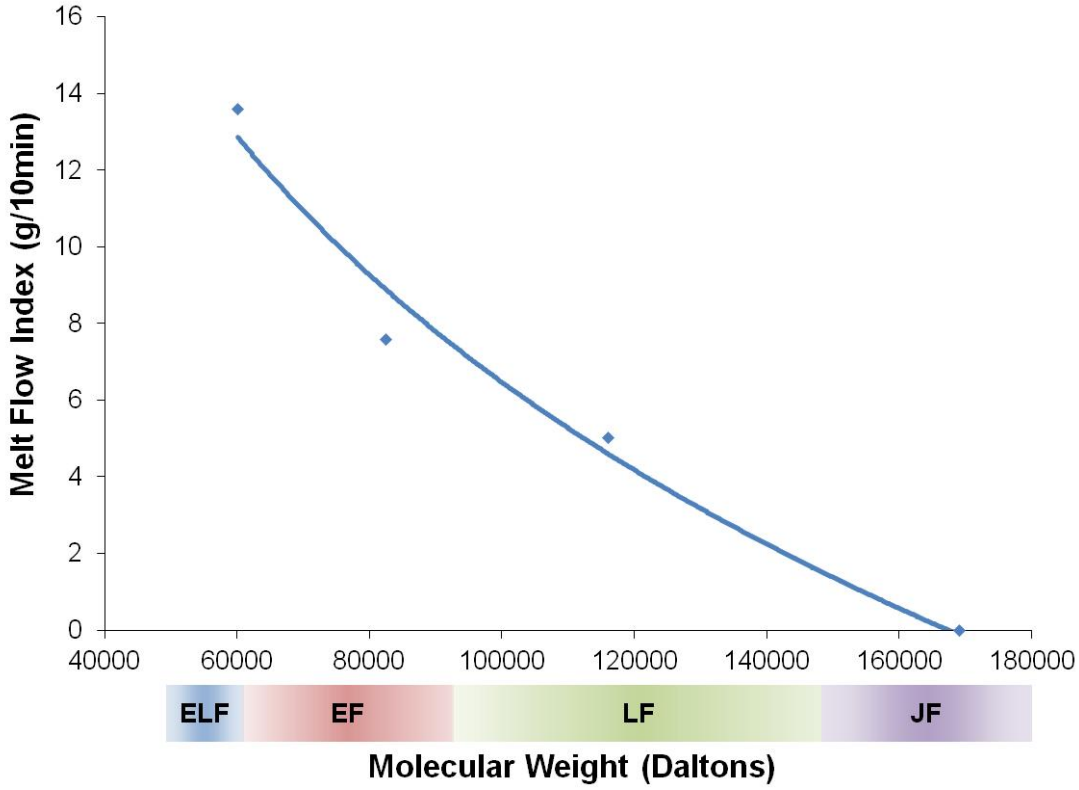

Figure 2.6: Melt flow index of HPC as a function of MW at 150°C.

HPC is, like many other cellulose derivatives, a good film former, and its films are somewhat less brittle than those from cellulose and certain of its derivatives because of the relatively hydrophobic oligo(hydroxypropyl) substituents. These properties make it a useful material for fabrication of films and sheets by conventional extrusion techniques. HPC coatings have also been extruded onto paper, fabrics, food products and other substrates. The HPC T_g value of 130ºC is relatively high vs. those of most synthetic polymers, but is in a range similar to those of many other cellulose ethers and esters. The relatively high T_g means that HPC films stay in the glassy phase (non-tacky) even when humidity is rather high and/or even when containing a plasticizer (or drug that plasticizes the film). HPC films can be of interest for packaging for the reasons cited above, as well as for the ability to heat seal due to their thermoplastic nature, their insolubility in hydrocarbons (like oils and fats), and their relatively low oxygen permeability (common to most polysaccharides and many derivatives thereof). Although extrusion of some HPC grades can lead to impractical melt viscosities[210], the addition of plasticizers can reduce

melt viscosity to more moderate levels; in some cases drug molecules themselves are plasticizers for HPC and can obviate the need for added plasticizer. Plasticizers increase film flexibility, reduce heat-seal temperatures, and increase impact resistance and elongation. HPC is compatible with plasticizers including propylene glycol, citrate esters and ethers, glycerin, stearic acid, oleic acid, and polymeric plasticizers such as PEG at concentrations up to at least 5%[210].

2.3.5.2 HPC Pharmaceutical applications

It is useful to discuss a few selected applications of HPC to highlight how its structure and properties have been exploited in specific ways.

HPC is frequently employed as a tablet binder, because of its high Tg (typical of cellulose derivatives), its thermal plasticity, relatively broad compatibility due to its balance of hydrophilic and hydrophobic properties, and its resulting organic solvent or aqueous solubility. These properties allow tablet preparation using a variety of formulation techniques. It has been found that levels of ca. 2-8% HPC in the formulation by weight act to bind the tablet, affording fast release, whereas higher levels of HPC (ca. 20-30%) promote the formation of a gel layer upon exposure to water, thereby affording extended release (*vide infra*)[211]. Picker-Freyer and Dürig have studied physical mechanical and tablet properties of HPC both in pure form and in mixtures. They observed that compactibility and plasticity increase as molecular weight and particle size decrease. Conversely, elastic deformation is more pronounced at higher molecular weight and particle size[211].

Fine particle size grades of HPC (ca. 80 mm mean size) are most suitable for dry binder applications, while regular particle size grades (ca. 250 mm mean size) are more readily dispersible, making them more useful in solution binding applications.

Skinner et al. have evaluated fine-particle HPC as a roller compaction binder in pharmaceutical applications using poorly compressible acetaminophen (APAP) as a model drug. The fine-particle HPC was incorporated into the formula at 4%, 6%, and 8% w/w levels, and tablets were evaluated for capping, hardness, friability, ejection force,

and drug dissolution. Using HPC at these binder levels could overcome capping and friability problems and achieve optimal tablet dosage forms[212].

As a polysaccharide derivative with considerable water affinity, HPC is useful for preparing physical mixture matrix tablets. When fine particle size HPC grades are used in matrix tablets, a gel layer forms rapidly upon contact with water. The gel layer retards the release of active ingredients, either by diffusion or erosion. HPC levels of at least 20% of the matrix are usually sufficient to obtain gel-controlled release[213]. For poorly soluble drugs, where erosion is the predominant release mechanism, low molecular weight grades of HPC are most suitable. Higher molecular weight grades provide long-lasting gels for diffusion-controlled release of more highly soluble drugs.

Drug release from HPC matrices is sensitive to HPC molecular weight, particle size, and drug/polymer proportions; co-excipients may also impact release profiles. In a study aiming to attain 100% drug release of caffeine after 24 h from HPC tablet matrices, it was shown that increasing HPC/caffeine ratios significantly decreased caffeine release rate[214].

A comparative study on rates of hydration and matrix erosion of high molecular weight grades of HEC and HPC, and of release of chlorpheniramine maleate from tablets made from physical blends of drug and polymer, was carried out by Roy and Rohera[215]. HEC matrices swelled faster than HPC matrices, but importantly they also eroded much faster than the HPC tablets. Drug release from HEC matrices occurred by non-Fickian transport, i.e., a combination of drug diffusion and polymer erosion and swelling, while drug release from these HPC matrices was controlled primarily by diffusion through pores and channels in the formed HPC gel structure. A higher polymer level was needed in the case of HEC vs. HPC matrices to sustain drug release for up to 12 h, due to the greater hydrophilicity of HEC.

Saša et al. investigated the surface properties of cellulose ethers by inverse gas chromatography and correlated with drug release from their matrix tablets. They found that the relative polarity of the cellulose ethers was HEC > HPMC > HPC, which correlated well with their water sorption and with the swelling degree of polymer matrices. Unfortunately they failed to report the MS and DS values of the three polymers

used by the same terminology, making it difficult to do detailed structure-property relationship evaluation. Release of pentoxifylline and vancomycin from the cellulose ether matrices followed the same order as the polarity of polymers. They found that drug release from HPC is governed mainly by Fickian diffusion, whereas from HEC relaxation of polymer chains is also important[216].

Uekama et. al used combinations of β-cyclodextrin and HPC to develop bi-layer controlled release tablets for poorly soluble compounds[217,218]. For a rapidly releasing portion, hydrophilic β-cyclodextrin derivatives were employed to form a water-soluble complex. The pH-independent slow release was attained by use of HPC or HPC/EC matrices. An optimal formulation of a double-layer tablet was obtained by the combination of each fraction.

The thermal stability of HPC and its ability to be melt-extruded have led to applications in melt granulation, and hot-melt extrusion for both immediate and prolonged release. The following examples illustrate its utility in these applications.

Lakshman et al. explored a melt granulation process using a twin-screw extruder to combine the hydrophilic, poorly compactible drug metformin HCl (METF) with HPC as the polymeric excipient, seeking to develop a high-dose tablet with low friability and also the ability to form combination tablets. Drug–polymer powder mixtures were melt granulated at a temperature above HPC T_g, but below metformin T_m. In comparison with wet granulation and solvent granulation, melt granulation provided a robust manufacturing process with highest compactability and lowest friability, that was insensitive to changes in atmospheric moisture level. HPC permitted formulation of decreased tablet size of the high-dose drugs; it was remarkable in fact that < 10% by weight HPC was sufficient to achieve compactability and friability targets. HPC was found to be superior to HPMC in this instance due to enhanced hardness, and to HEC due to enhanced drug release rate[219].

As a cellulose ether that is both organic solvent soluble, and melt extrudable, HPC is a potential fit for the most commonly used methods (e.g., spray drying and melt extrusion) for preparing amorphous solid dispersions (ASD) of drugs in order to enhance solubility

and bioavailability. A number of investigators have reported exploring HPC as an ASD matrix polymer.

Inoue and co-workers examined a variety of polymers as ASD matrices for the immunosuppressant drug cyclosporine A (CsA)[220], and their study provides insights about the relative merits of HPC for ASD. They found that HPC formed amorphous dispersions with CsA, even at > 75% drug in the ASD. Other cellulose ethers including MC and HPMC also formed ASDs at similar levels of drug, but the dissolution rate from the HPC formulation was faster and the supersaturation achieved was much greater. The rate of release was related to HPC molecular weight, with polymers of Mw of 70,000 or less releasing CsA almost immediately, while delayed release was observed with high Mw HPC (250K – 400K). It may be that the relative hydrophobicity of HPC (solubility parameters MC 22.7, HPMC 21.5, HPC 21.1 $MPa^{1/2}$)[221,222] enhances interactions with the hydrophobic drug, promoting stabilization against recrystallization.

The heterogeneity of the HPC structure can be an advantage in ASD, since it essentially eliminates any tendency for HPC to crystallize. Studies of HPC vs. PEG in ASD of felodopine[223] showed that felodopine release from the PEG matrix was much faster and more complete due to faster dissolution of the very hydrophilic PEG. However, the PEG in these ASDs showed a clear tendency to crystallize, which would be unacceptable variation in a marketed formulation, whereas the HPC showed no such tendency as shown by XRD and DSC.

Mohammed et al. reported the use of HPC for drug solubilization[224]. The authors evaluated HPC for solubility enhancement of ketoprofen by forming a solid dispersion in HPC matrix via hot-melt extrusion, which is attractive for ASD since no organic solvents are involved. Drug release from extruded pellets was found to be dependent on HPC molecular weight, with faster release observed at lower molecular weight HPC (40K vs. 80K M_w). Tablets compressed from milled extrudates exhibited rapid release, and addition of mannitol further enhanced the release by forming micro-pores and increasing extrudate porosity.

When higher molecular weight grades of HPC are used for ASD or other controlled release formulations using extrusion, plasticizers can be used to reduce melt viscosity, thus facilitating the extrusion process (**Figure 2.7**)[199].

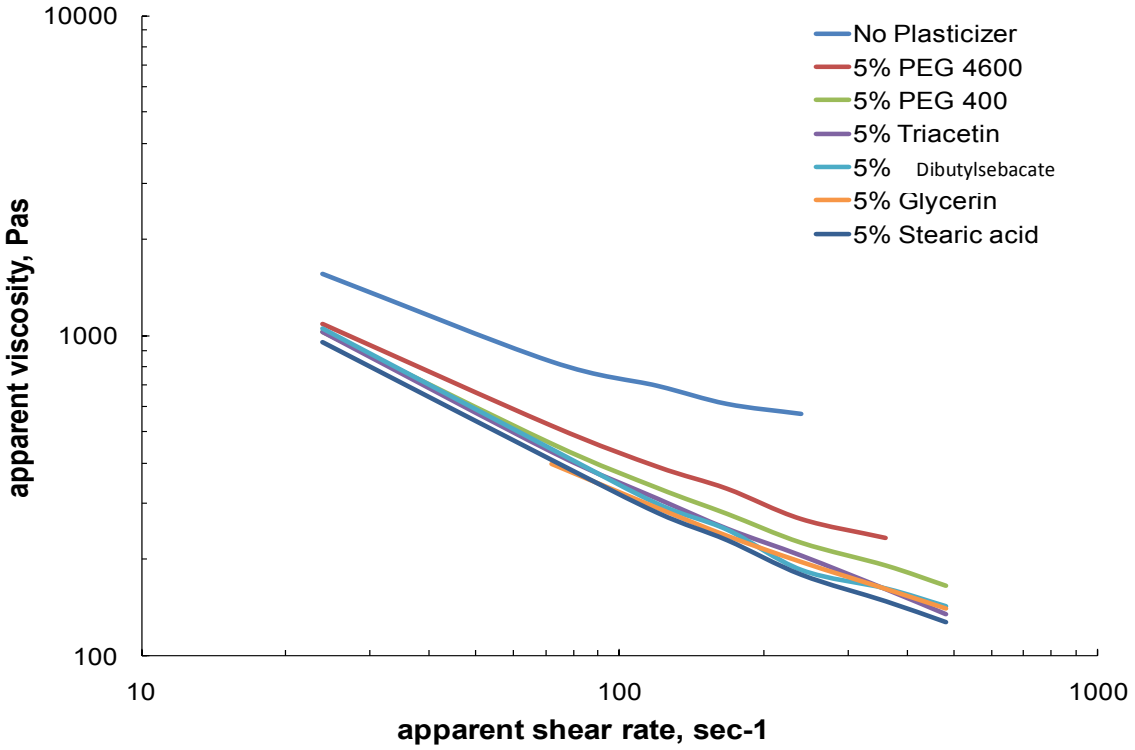

Figure 2.7: Effect of plasticizer on melt viscosity of HPC (M_w ~ 850,000) at 180°C.

A study by Repka et al. illustrated some of the issues with melt extrusion of HPC/drug formulations. They investigated HPC/drug extrusion in the presence of plasticizers including PEG 8000 (2%), triethyl citrate (TEC, 2%), acetyltributyl citrate (ATBC, 2%), and PEG 400 (1%). In addition, either hydrocortisone (HC) 1% or chlorpheniramine maleate (CPM) 1% was incorporated into the films as a model drug. One issue was that while the T_g values predictably decreased with the inclusion of drugs and plasticizers, the T_g values were not stable over 6 months aging; the authors did not report investigations of whether this was due to plasticizer loss, phase separation, or other cause. Importantly, the authors reported that a consistent film of HPC could not be extruded in the absence of drugs or plasticizers due to excessive melt viscosity[210]. The authors also carefully

examined extrudates containing hydrocortisone and chlorpheniramine by HPLC. They found profound degradation of hydrocortisone, as shown by the appearance of impurity peaks; degradation of chlorpheniramine was less prominent but still detectable. In another study, the authors investigated the potential of extruded HPC films for transdermal applications, by measuring moisture absorption, physical-mechanical and bioadhesive properties of extruded HPC containing plasticizers including polyethylene glycol (PEG), poly(acrylic acid) (Carbomer), cross-linked poly(acrylic acid) (Polycarbophil), and methyl methacrylate/*n*-butyl methacrylate/dimethylaminoethyl methacrylate co-polymer (Eudragit E-100). The film containing 5% Polycarbophil had the highest force of adhesion and the highest elongation at adhesive failure *in vivo*. The authors hypothesized that in this film hydrogen bonding with the polymers of the skin is enhanced by the presence of Polycarbophil due to its high carboxylic acid content[225].

2.4 Cellulose Ether Esters

2.4.1 Carboxymethylcellulose Acetate Butyrate (CMCAB)

2.4.1.1 CMCAB Synthesis and general properties

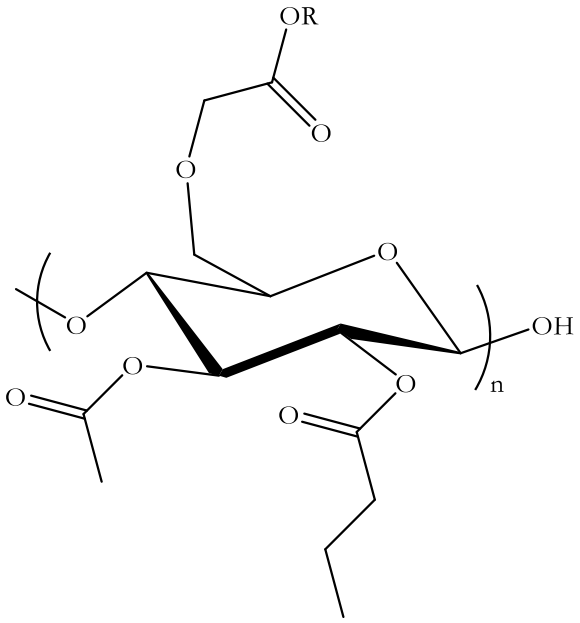

Figure 2.8: The chemical structure of CMCAB (R=H or $-CH_2COOH$).

Hydrophobically modified CMC derivatives, prepared by esterification of CMC hydroxyl groups with carboxylic acids, have been explored for waterborne coatings and as drug delivery polymers. CMCAB synthesis by reaction of CMC with acetic and butyric anhydrides under strong acid catalysis has been reported by Eastman Chemical Co.[226]. DS values obtained depend in predictable fashion upon the reaction conditions and reactant mole ratios. The resulting CMCAB polymer (**Figure 2.8**) has three substituent types (other than hydrogen), with DS (CMC) of 0.33, DS butyrate (Bu) 1.64, and DS acetyl (Ac) of 0.44. The carboxymethyl groups impart pH sensitivity; the polymer swells at neutral pH or higher, that is at the pH of the intestines.

2.4.1.2 CMCAB Pharmaceutical applications

CMCAB has potential use in drug delivery systems in different dosage forms, playing roles such as matrix, binder, or film former with poorly water soluble drugs, e.g. ibuprofen, glyburide, griseofulvin[227], and clarithromycin,[36] as well as with water soluble drugs such as fexofenadine HCl [227] and moderately soluble drugs like rifampin. CMCAB solid dispersions can be prepared through spray drying, co-precipitation, film casting, or solvent rotary evaporation[227]. Extrusion of CMCAB has not been reported and may be difficult, since the high T_g (137°C) polymer contains both free OH and carboxyl groups, and may be prone to cross-linking during thermal extrusion.

Ibuprofen tablets directly compressed with CMCAB gave zero order release of ibuprofen, and this otherwise modestly soluble drug displayed much higher solution concentrations upon release from a CMCAB matrix at pH 6.8. *In vitro* experiments showed that zero order release was prolonged for more than 20 hours, promising for a simple, once-daily form of ibuprofen. Edgar et al. studied controlled release of ibuprofen, glyburide, griseofulvin and fexofenadine HCl from CMCAB ASDs prepared by different techniques, which showed pH-controlled release and enhanced drug solution concentration. For some formulations, zero order drug release (ibuprofen-CMCAB solid dispersion) and enhanced stabilization against drug crystallization were afforded.

Clarithromycin/CMCAB ASDs were investigated in order to increase solubility of the drug and also prevent its degradation at acidic pH.[36] It was found that ASD in CMCAB afforded considerable protection against clarithromycin decomposition at low pH; as a result, a total of approximately 55% of the drug was released intact during simulated passage through the absorptive zone of the GI tract (vs. 0% for clarithromycin in the absence of polymer, or in ASD with HPMCAS). Similarly, CMCAB/rifampin ASDs were prepared in order to increase rifampin bioavailability, and investigated by *in vitro* dissolution studies. The hydrophobic protonated CMCAB matrix prevented any measurable drug release under gastric (pH 1.2) simulating conditions, but at pH 6.8, upon deprotonation of the CMCAB carboxyls and resulting matrix swelling, the CMCAB ASDs released around 70% of the rifampin intact within 8 hours, showing an initial burst release upon pH switch to 6.8[228].

2.4.2 Hydroxypropyl Methyl Cellulose Acetate Succinate (HPMCAS)

2.4.2.1 HPMCAS Synthesis and general properties

HPMCAS is a complex co-polymer prepared by reaction of HPMC with acetic and succinic anhydrides. Many more than four types of moiety excluding hydrogen (acetyl, succinoyl, methyl, the isomeric hydroxypropyl groups, and the many possible permutations of oligo(hydroxypropyl) groups, not to mention the possibility of the oligo(hydroxypropyl) groups being capped by acetate or succinate esters) are presumably relatively randomly substituted around the AHG ring and along and between chains. HPMCAS has low water solubility at acidic pH due to the relatively hydrophobic methoxy and acetate groups, but swells when its succinate groups (4-14%) are ionized at intestinal pH (6-7.5). There are also HPMCAS grades with higher % succinate groups (14-18%) that can ionize at lower pH (5.5-6)[229]. Due to its amphiphilic nature, it is a favored polymer for use in ASD formulations with hydrophobic drugs. HPMCAS, along with cellulose acetate trimellitate (CAT), cellulose acetate phthalate (CAP), hydroxypropyl cellulose acetate phthalate (HPCAP), hydroxypropyl methyl cellulose acetate phthalate (HPMCAP), and methylcellulose acetate phthalate (MCAP) were patented by Pfizer Inc. for their ability to increase drug solution concentration and hence bioavailability from ASDs, and their use in pH-controlled drug delivery systems[230].

2.4.2.2 HPMCAS Pharmaceutical Applications

HPMCAS has now been used as the matrix polymer in many ASDs of poorly water soluble drugs, in order to increase their solution concentrations and prevent recrystallization, including AMG 517[231], nifedipine[232], felodipine[233], quercetin[234], naringenin[235], clarithromycin[36] and itraconazole[236].

HPMCAS was identified as the most efficient polymer among HPMC, hypromellose phthalate (HPMCP), methacrylic acid/ethyl acrylate copolymer (MAEA), and povidone

(PVP) for nifedipine stabilization in ASDs. ASD in HPMCAS increased nifedipine solution concentration, and prevented its recrystallization after dissolution at pH 6.8[232].

HPMCAS can be combined with drugs by solvent-free (thermal extrusion) methods, or by co-dissolution followed by spray drying or other methods of isolation from solution[236,237]. HPMCAS bulk physicochemical properties are not strongly affected by hot melt extrusion, but the polymer does lose some acetic and succinic acid moieties during extrusion, potentially leading to longer dissolution times due to the loss of ionizable succinate groups. Lower molecular weight HPMCAS is relatively more suitable to thermal processing than higher molecular weight grades because of its lower processing temperature (160-180°C); as a result it loses few carboxylic acid groups and did not exhibit reduction in dissolution time[238]. Felodipine solid dispersions with HPMCAS were prepared by both spray drying and hot melt extrusion. HPMCAS has a T_g of 120°C and begins to degrade at ca. 200°C (Mw 17,000-20,000). In this study, materials were extruded at 130°C. Alternatively, HPMCAS/felodipine solutions in acetone were spray dried at 65°C at 1:1, 1:2, and 1:3 polymer to drug ratios. The spray dried particles released drug faster than the melt-extruded formulations, which is likely due in part to the large surface area of the spray dried particles, thereby enhancing contact with the dissolution medium. On the other hand, the 1:1 drug:polymer ratio melt extruded samples had higher stability against recrystallization than spray dried particles[237]. Taylor et al. showed by mid-infrared studies that HPMCAS more effectively prevented crystallization of certain model drugs (quercetin and naringenin) than HPMC, CMCAB, or poly(acrylic acid) (PAA)[235].

2.5 Conclusions

Both cellulose ethers and cellulose ether esters have been applied to pharmaceutical formulations and have great utility that can be systematically related to their structural features. Etherification of cellulose, and in some cases subsequent esterification, can provide polymers with enhanced water solubility, amphiphilicity, at high DS(alkyl) hydrophobicity, increased thermoplasticity, high glass transition temperature, compressibility, and compatibility with drugs, to name just a few pharmaceutically useful

properties. All of these properties can be controlled by modulation of substituent type and DS/MS in predictable fashion, as we demonstrate in this review. The investigations discussed herein show that these renewable-based polymer derivatives can increase drug bioavailability, thereby decreasing drug costs, variability, dosage form size, and potentially side effects of the formulation relative to the crystalline drug. To date the scope of available cellulose ethers has been limited by the demands of the standard aqueous processes in which strong alkali catalysts are used. Electrophiles for reaction with cellulose must possess some water solubility, be able to penetrate swollen cellulose fibers, and react sufficiently slowly with water or alkali. There is a strong need for modern, practical synthetic methods that can expand the scope of available cellulose ethers and the functional groups they may contain, such as by elaboration of ω-unsaturated alkyl groups via olefin cross methastasis[239]. We anticipate that cellulose ethers and cellulose ether esters will continue to grow in importance to pharmaceutical formulators as a result of their appropriate structural, toxicity, performance, and renewability characteristics.

2.6 References

(1) S. Yamanaka; K. Watanabe; N. Kitamura; M. Iguchi; S. Mitsuhashi; Y. Nishi; Uryu, M. The Structure and Mechanical Properties of Sheets Prepared from Bacterial Cellulose. *J. Mater. Sci.* **1989**, *24*, 3141–3145.

(2) Klemm, D.; Heublein, B.; Fink, H. P.; Bohn, A. Cellulose: Fascinating Biopolymer and Sustainable Raw Material. *Angew Chem Int Ed Engl* **2005**, *44*, 3358–3393.

(3) El-Sakhawy, M.; Kamel, S.; Salama, A.; Sarhan, H. A. Carboxymethyl Cellulose Acetate Butyrate: A Review of the Preparations, Properties, and Applications. *J Drug Deliv* **2014**, *2014*, 575969.

(4) Cellulose as a Nanostructured Polymer: A Short Review. *BioResources* **2008**, *3*, 1403–1418.

(5) Liu, H.; Cherniawski, B. P.; Ritchie, E. T.; Taylor, L. S.; Kevin J. Edgar, G. A. I. Synthesis and Structure–property Evaluation of (1) Liu, H.; Cherniawski, B. P.; Ritchie, E. T.; Taylor, L. S.; Kevin J. Edgar, G. A. I. Synthesis and Structure–

property Evaluation of Cellulose ω-Carboxyesters for Amorphous Solid Dispersions. Carbohydr Pol. *Carbohydr Polym* **2012**.

(6) Chandra R.; Rustgi R. Biodegradable Polymers. *Prog. Polym. Sci.* **1998**, *23*, 1273–1335.

(7) Cunha, A. G.; Gandini, A. Turning Polysaccharides into Hydrophobic Materials: A Critical Review. Part 1. Cellulose. *Cellulose* **2010**, *17*, 875–889.

(8) Edgar K. J; Buchanan C. M; Debenham J. S; Rundquist P. A; Seiler B. D; Shelton M. C; Tindall D. Advances in Cellulose Ester Performance and Application . *Prog. Polym. Sci.* **2001**, *26*, 1605–1688.

(9) Alderman, D. A. A Review of Cellulose Ethers in Hydrophilic Matrices for Oral Controlled-Release Dosage Forms. Ht. *Int. J. Pharm. Tech. Prod. Mfr.* **1984**, *5*, 1–9.

(10) T.M. Aminabhavia; G. V. Patilb; R.H. Balundgic; S.F. Harlapurd; F.V. Manvie; Bhaskarf, C. A Review on the Sustained Release of Cardiovascular Drugs through Hydroxypropyl Methylcellulose and Sodium Carboxymethylcellulose Polymers. *Des. Monomers Poymers* **1998**, *1*, 347–372.

(11) Shojaei, A. Buccal Mucosa As A Route For Systemic Drug Delivery: A Review. *J Pharm Pharm Sci.* **1998**, *1*, 15–30.

(12) Murtaza, G. Ethylcellulose Microparticles: A Review. *Acta Pol Pharm* **2012**, *69*, 11–22.

(13) S. Kamel; N. Ali; K. Jahangir; S. M. Shah; El-Gendy, A. A. Pharmaceutical Significance of Cellulose: A Review. *eXPRESS Polym. Lett.* **2008**, *2*, 758–778.

(14) Schulz, G. J. Grinding Process for High Viscosity Cellulose Ethers, 1989.

(15) Miller, K. S.; Krochta, J. M. Oxygen and Aroma Barrier Properties of Edible Films: A Review. *Trends Food Sci. Technol.* **1997**, *8*, 228–237.

(16) Cha, D. S.; Chinnan, M. S. Biopolymer-Based Antimicrobial Packaging: A Review. *Crit Rev Food Sci Nutr* **2004**, *44*, 223–237.

(17) Gardnera, D. J.; Oportob, G. S.; Millsc, R.; Samir, A. S. Adhesion and Surface

Issues in Cellulose and Nanocellulose. *J Adhes. Sci Technol.* **2008**, *22*, 545–567.

(18) Petit, J. Y.; Wirquin, E. Evaluation of Various Cellulose Ethers Performance in Ceramic Tile Adhesivemortars. *Int. J. Adhes. Adhes.* **2013**, *40*, 202–209.

(19) Cellulose Ethers Market By Derivative [Methyl, Ethyl & Carboxymethyl Cellulose] & Application [Pharmaceuticals, Personal Care, Construction, Food & Beverages, Surface Coatings & Paints] – Global Trends & Forecasts to 2017 http://www.marketsandmarkets.com/Market-Reports/cellulose-ethers-market-782.html.

(20) Mazeau, K.; Heux, L. Molecular Dynamics Simulations of Bulk Native Crystalline and Amorphous Structures of Cellulose. *J. Phys. Chem. B* **2003**, *107*, 2394–2403.

(21) Voiges, K.; Adden, R.; Rinken, M.; Mischnick, P. Critical Re-Investigation of the Alditol Acetate Method for Analysis of Substituent Distribution in Methyl Cellulose. *Cellulose* **2012**, *19*, 993–1004.

(22) Volkert, B.; Wagenknecht, W. Substitution Patterns of Cellulose Ethers - Influence of the Synthetic Pathway. *Macromol. Symp.* **2008**, *262*, 97–118.

(23) Mischnick, P. Challenges in Structure Analysis of Polysaccharide Derivatives. *Cellulose* **2002**, *8*, 245–257.

(24) Mischnick, P. *Mass Spectrometric Characterization of Oligo- and Polysaccharides and Their Derivatives*; Hakkarainen, M., Ed.; Advances in Polymer Science; Springer Berlin Heidelberg: Berlin, Heidelberg, 2012; Vol. 248.

(25) Heinze, T.; Koschella, A. Carboxymethl Ethers of Cellulose and Stach- A Review. *Macromol. Symp.* **2005**, *223*, 13–40.

(26) Koschella, A.; Klemm, D. Silylation of Cellulose Regiocontrolled by Bulky Reagents and Dispersity in the Reaction Media. *Macromol. Symp.* **1997**, *120*, 115–125.

(27) Fox, S. C.; Li, B.; Xu, D.; Edgar, K. J. Regioselective Esterification and Etherification of Cellulose: A Review. *Biomacromolecules* **2011**, *12*, 1956–1972.

(28) Lorand, E. J. Cellulose Ethers Variations of Physical Properties with Composition.

Ind. Eng. Chem. **1938**, *30*, 527–530.

(29) Serlin, M. J.; Orme, M. L.; MacIver, M.; Green, G. J.; Sibeon, R. G.; Breckenridge, A. M. The Pharmacodynamics and Pharmacokinetics of Conventional and Long-Acting Propranolol in Patients with Moderate Hypertension. *Br J Clin Pharmacol* **1983**, *15*, 519–527.

(30) Brazel, C. S.; Peppas, N. A. Modeling of Drug Release from Swellable Polymers. *Eur. J. Pharm. Biopharm.* **2000**, *49*, 47–58.

(31) O'Donnell, P. *The Williams Dictionary of Biomaterials*; The Liverpool University Press: Liverpool L69 3BX, 1999.

(32) Safari J.; Zarnegar, Z. Advanced Drug Delivery Systems: Nanotechnology of Health Design A Review. *J Saudi Chem Soc* **2014**, *18*, 85–99.

(33) Posey-Dowty, J. D.; Watterson, T. L.; Wilson, A. K.; Edgar, K. J.; Shelton, M. C.; Jr., L. R. L. Zero-Order Release Formulations Using a Novel Cellulose Ester. *Cellulose* **2007**, *14*, 73–83.

(34) Arca, H. C.; Mosquera-Giraldo, L. I.; Pereira, J. M.; Sriranganathan, N.; Taylor, L. S.; Edgar, K. J. Rifampin Stability and Solution Concentration Enhancement through Amorphous Solid Dispersion in Cellulose ω-Carboxyalkanoate Matrices. *J Pharm Sci* **2016**.

(35) Li, B.; Wegiel L.A.; Taylor L.S.; Edgar, K. J. Stability and Solution Concentration Enhancement of Resveratrol by Solid Dispersion in Cellulose Derivative Matrices. *Cellulose* **2013**, *20*, 1249–1260.

(36) Pereira, J. M.; Mejia-Ariza, R.; Ilevbare, G. A.; McGettigan, H. E.; Sriranganathan, N.; Taylor, L. S.; Davis, R. M.; Edgar, K. J. Interplay of Degradation, Dissolution and Stabilization of Clarithromycin and Its Amorphous Solid Dispersions. *Mol Pharm* **2013**, *10*, 4640–4653.

(37) Bigucci, F.; Abruzzo, A.; Cerchiara, T.; Gallucci, M. C.; Luppi, B. Formulation of Cellulose Film Containing Permeation Enhancers for Prolonged Delivery of Propranolol Hydrocloride. *Drug Dev Ind Pharm* **2014**, 1–9.

(38) Gupta, V.; Singh, S.; Srivarstava, M.; Ahmad, H.; Pachauri, S. D.; Khandelwal,

K.; Dwivedi, P.; Dwivedi, A. K. Effect of Polydimethylsiloxane and Ethylcellulose on in Vitro Permeation of Centchroman from Its Transdermal Patches. *Drug Deliv* **2014**.

(39) Fini, A.; Bergamante, V.; Ceschel, G. C. Mucoadhesive Gels Designed for the Controlled Release of Chlorhexidine in the Oral Cavity. *Pharmaceutics* **2011**, *3*, 665–679.

(40) Sushma, M.; Raju, Y. P.; Sundaresan, C. R.; Vandana, K. R.; Kumar, N. V; Chowdary, V. H. Transmucosal Delivery of Metformin- a Comprehensive Study. *Curr Drug Deliv* **2014**, *11*, 172–178.

(41) Murdande, S. B.; Pikal, M. J.; Shanker, R. M.; Bogner, R. H. Aqueous Solubility of Crystalline and Amorphous Drugs: Challenges in Measurement. *Pharm Dev Technol* **2011**, *16*, 187–200.

(42) Williams, H. D.; Trevaskis, N. L.; Charman, S. A.; Shanker, R. M.; Charman, W. N.; Pouton, C. W.; Porter, C. J. Strategies to Address Low Drug Solubility in Discovery and Development. *Pharmacol Rev* **2013**, *65*, 315–499.

(43) N. Shah D. Choi, H. Chokshi, Malick A.W., H. S. *Amorphous Solid Dispersions Theory and Practice*; Rathbone, M., Ed.; Advances in Delivery Science and Technology: London, 2014.

(44) Hancock, B. C.; Zografi, G. Characteristics and Significance of the Amorphous State in Pharmaceutical Systems. *J Pharm Sci* **1997**, *86*, 1–12.

(45) Ilevbare, G. A. .; Liu, H. .; Edgar, K. J. .; Taylor, L. S. Maintaining Supersaturation in Aqueous Drug Solutions: Impact of Different Polymers on Induction Times. *Cryst. Growth Des.* **2013**, *13*, 740–751.

(46) Heinze, T.; Liebert, T.; Klüfers, P.; Meister, F. Carboxymethylation of Cellulose in Unconventional Media. *Cellulose* **1999**, *6*, 153–165.

(47) McCormick, C. L.; Callais, P.; Hutchinson, B. Solution Studies of Cellulose in Lithium Chloride and N,N-Dimethylacetamide. *Macromolecules* **1985**, *18*, 2394–2401.

(48) Dawsey, T. R.; McCormick, C. L. The Lithium Chloride/Dimethylacetamide

Solvent for Cellulose: A Literature Review. *Polym. Rev.* **1990**, *30*, 405–440.

(49) Heinze, T.; Erler, U.; Nehls, I.; Klemm, D. Determination of the Substituent Pattern of Heterogeneously and Homogeneously Synthesized Carboxymethyl Cellulose by Using High-Performance Liquid Chromatography. *Die Angew. Makromol. Chemie* **2003**, *215*, 93–106.

(50) P.N. Bhandaria; D.D. Jonesb; Hannac, M. A. Carboxymethylation of Cellulose Using Reactive Extrusion. *Carbohydr Polym* **2012**, *87*, 2246–2254.

(51) Limbert, T.; Klemm, D.; Heinze, T. Synthesis and Carboxymethylation of Organo-Soluble Trifluoroacetates and Formates of Cellulose. *J. Macromol. Sci. Part A* **1996**, *33*, 613–626.

(52) Garrett, Q.; Simmons, P. A.; Xu, S.; Vehige, J.; Zhao, Z.; Ehrmann, K.; Willcox, M. Carboxymethylcellulose Binds to Human Corneal Epithelial Cells and Is a Modulator of Corneal Epithelial Wound Healing. *Invest Ophthalmol Vis Sci* **2007**, *48*, 1559–1567.

(53) He, F.; Zhao, D. Manipulating the Size and Dispersibility of Zerovalent Iron Nanoparticles by Use of Carboxymethyl Cellulose Stabilizers. *Env. Sci Technol* **2007**, *41*, 6216–6221.

(54) Varshosaz, J.; Dehghan, Z. Development and Characterization of Buccoadhesive Nifedipine Tablets. *Eur J Pharm Biopharm* **2002**, *54*, 135–141.

(55) Badwaik, L. S.; Borah, P. K.; Deka, S. C. Antimicrobial and Enzymatic Antibrowning Film Used as Coating for Bamboo Shoot Quality Improvement. *Carbohydr Polym* **2014**, *103*, 213–220.

(56) Saha, S.; Tomaro-Duchesneau, C.; Daoud, J. T.; Tabrizian, M.; Prakash, S. Novel Probiotic Dissolvable Carboxymethyl Cellulose Films as Oral Health Biotherapeutics: In Vitro Preparation and Characterization. *Expert Opin Drug Deliv* **2013**, *10*, 1471–1482.

(57) Shah, S. U.; Shah, K. U.; Rehman, A.; Khan, G. M. Investigating the in Vitro Drug Release Kinetics from Controlled Release Diclofenac Potassium-Ethocel Matrix Tablets and the Influence of Co-Excipients on Drug Release Patterns. *Pak J Pharm*

Sci **2011**, *24*, 183–192.

(58) Panda, R. R.; Tiwary, A. K. Formulation and Optimization of Osmotically Controlled Release Tablets of Glipizide: Hot Melt Granulation. *Ther Deliv* **2010**, *1*, 763–774.

(59) Sotthivirat, S.; Haslam, J. L.; Lee, P. I.; Rao, V. M.; Stella, V. J. Release Mechanisms of a Sparingly Water-Soluble Drug from Controlled Porosity-Osmotic Pump Pellets Using Sulfobutylether-Beta-Cyclodextrin as Both a Solubilizing and Osmotic Agent. *J. Pharm. Sci.* **2009**, *98*, 1992–2000.

(60) Chen, R. N.; Ho, H. O.; Yu, C. Y.; Sheu, M. T. Development of Swelling/floating Gastroretentive Drug Delivery System Based on a Combination of Hydroxyethyl Cellulose and Sodium Carboxymethyl Cellulose for Losartan and Its Clinical Relevance in Healthy Volunteers with CYP2C9 Polymorphism. *Eur J Pharm Sci* **2010**, *39*, 82–89.

(61) Varshosaz, J.; Tavakoli, N.; Eram, S. A. Use of Natural Gums and Cellulose Derivatives in Production of Sustained Release Metoprolol Tablets. *Drug Deliv* **2006**, *13*, 113–119.

(62) Majid Khan, G.; Zhu, J. B. Ibuprofen Release Kinetics from Controlled-Release Tablets Granulated with Aqueous Polymeric Dispersion of Ethylcellulose II: Influence of Several Parameters and Coexcipients. *J Control Release* **1998**, *56*, 127–134.

(63) Rahmani-Neishaboor, E.; Jallili, R.; Hartwell, R.; Leung, V.; Carr, N.; Ghahary, A. Topical Application of a Film-Forming Emulgel Dressing That Controls the Release of Stratifin and Acetylsalicylic Acid and Improves/prevents Hypertrophic Scarring. *Wound Repair Regen* **2013**, *21*, 55–65.

(64) Ghanbarzadeha, B.; Almasia, H.; Entezamib, A. A. Physical Properties of Edible Modified Starch/carboxymethyl Cellulose Films. *Innov. Food Sci. Emerg. Technol.* **2010**, *11*, 697–702.

(65) Qiu, X.; Leporatti, S.; Donath, E.; Möhwald, H. Studies on the Drug Release Properties of Polysaccharide Multilayers Encapsulated Ibuprofen Microparticles.

Langmuir **2001**, *17*, 5375–5380.

(66) Jiménez-Castellanos, M. R.; Ziaa, H.; Rhodesa, C. T. Design and Testing in Vitro of a Bioadhesive and Floating Drug Delivery System for Oral Application. *Int J Pharm* **1994**, *105*, 65–70.

(67) K.V.Ranga Rao; Buri, P. A Novel in Situ Method to Test Polymers and Coated Microparticles for Bioadhesion. *Int J Pharm* **1989**, *52*, 265–270.

(68) Varshosaz, J.; Tavakoli, N.; Roozbahani, F. Formulation and in Vitro Characterization of Ciprofloxacin Floating and Bioadhesive Extended-Release Tablets. *Drug Deliv* **2006**, *13*, 277–285.

(69) Parmar Viram J.; Lumbhani A N.; Vijayalakshmi P.; Jha, S. FORMULATION DEVELOPMENT AND EVALUATION OF BUCCAL FILMS OF CARVEDILOL. *int J Pharm Scince Res.* **2010**, *1*, 149–156.

(70) Semalty, M.; Semalty, A.; Kumar, G. Formulation and Characterization of Mucoadhesive Buccal Films of Glipizide. *Indian J Pharm Sci* **2008**, *70*, 43–48.

(71) Dortunc, B.; Ozer, L.; Uyanik, N. Development and in Vitro Evaluation of a Buccoadhesive Pindolol Tablet Formulation. *Drug Dev Ind Pharm* **1998**, *24*, 281–288.

(72) Ali, J.; Khar, R.; Ahuja, A.; Kalra, R. Buccoadhesive Erodible Disk for Treatment of Oro-Dental Infections: Design and Characterisation. *Int J Pharm* **2002**, *238*, 93–103.

(73) Perioli, L.; Ambrogi, V.; Rubini, D.; Giovagnoli, S.; Ricci, M.; Blasi, P.; Rossi, C. Novel Mucoadhesive Buccal Formulation Containing Metronidazole for the Treatment of Periodontal Disease. *J Control Release* **2004**, *95*, 521–533.

(74) Emami J.; Varshosaz J.; N., S. Development and Evaluation of Controlled-Release Buccoadhesive Verapamil Hydrochloride Tablets. *DARU J. Pharm. Sci.* **2008**, *16*, 60–69.

(75) Parvez N.; Ahuja A. Development and Evaluation of Muco-Adhesive Buccal Tablets of Lignocaine Hydrochloride. *Indian J Pharm Sci* **2002**, *64*, 563–567.

(76) Mohammed, F. A.; Khedr, H. Preparation and in Vitro/in Vivo Evaluation of the Buccal Bioadhesive Properties of Slow-Release Tablets Containing Miconazole Nitrate. *Drug Dev Ind Pharm* **2003**, *29*, 321–337.

(77) Ali, J.; Khar, R. K.; Ahuja, A. Formulation and Characterisation of a Buccoadhesive Erodible Tablet for the Treatment of Oral Lesions. *Pharmazie* **1998**, *53*, 329–334.

(78) Sudhakar, Y.; Kuotsu, K.; Bandyopadhyay, A. K. Buccal Bioadhesive Drug Delivery--a Promising Option for Orally Less Efficient Drugs. *J Control Release* **2006**, *114*, 15–40.

(79) Inactive Ingredient Search for Approved Drug Products.

(80) Vehige, J. G.; Simmons, P. A.; Anger, C.; Graham, R.; Tran, L.; Brady, N. Cytoprotective Properties of Carboxymethyl Cellulose (CMC) When Used prior to Wearing Contact Lenses Treated with Cationic Disinfecting Agents. *Eye Contact Lens* **2003**, *29*, 177–180.

(81) Alam, M. A.; Ahmad, F. J.; Khan, Z. I.; Khar, R. K.; Ali, M. Development and Evaluation of Acid-Buffering Bioadhesive Vaginal Tablet for Mixed Vaginal Infections. *AAPS PharmSciTech* **2007**, *8*, E109.

(82) Sharma, G.; Jain, S.; Tiwary, A. K.; Kaur, G. Once Daily Bioadhesive Vaginal Clotrimazole Tablets: Design and Evaluation. *Acta Pharm* **2006**, *56*, 337–345.

(83) Genc, L.; Oguzlar, C.; Guler, E. Studies on Vaginal Bioadhesive Tablets of Acyclovir. *Pharmazie* **2000**, *55*, 297–299.

(84) Karasulu, H. Y.; Hilmioglu, S.; Metin, D. Y.; Guneri, T. Efficacy of a New Ketoconazole Bioadhesive Vaginal Tablet on Candida Albicans. *Farmaco* **2004**, *59*, 163–167.

(85) Denham W.S.; Woodhouse H. The Methylation of Cellulose. *J. Chem. Soc., Trans.,* **1913**, *103*, 1735–1742.

(86) Heuser E.; Neuenstein W. Zur Kenntnis Der Hydrocellulose. *Cellulosechemie* **1922**, *3*, 89–96.

(87) Bock, L. H. Water Soluble Cellulose Ethers. *Ind. Eng. Chem.* **1937**, *29*, 985–988.

(88) Houghton, A.; Martin, C. Manufacture of Methyl Cellulose, 1942.

(89) Keary, C. M. Characterization of METHOCEL Cellulose Ethers by Aqueous SEC with Multiple Detectors. *Carbohydr Polym* **2001**, *45*, 293–303.

(90) Kondo, T. The Relationship between Intramolecular Hydrogen Bonds and Certain Physical Properties of Regioselectively Substituted Cellulose Derivatives. *J. Polym. Sci. part B; Polym. Phys.* **1997**, *35*, 717–723.

(91) Sarkar, N. Kinetics of Thermal Gelation of Methylcellulose and Hydroxypropylmethylcellulose in Aqueous Solutions. *Carbohydr Polym* **1995**, *26*, 195–203.

(92) Li, L. Thermal Gelation of Methylcellulose in Water: Scaling and Thermoreversibility. *Macromolecules* **2002**, *35*, 5990–5998.

(93) Balaghi, S.; Edelby, Y.; Senge, B. Evaluation of Thermal Gelation Behavior of Different Cellulose Ether Polymers by Rheology. *AIP Conf. Proc.* **2014**, *1593*.

(94) Takahashi, S. I.; Fujimoto, T.; Miyamoto, T.; Inagaki, H. Relationship between Distribution of Substituents and Water Solubility of O-Methyl Cellulose. *J. Polym. Sci. Part A Polym. Chem.* **1987**, *25*, 987–994.

(95) Landoll, L. M. Modified Nonionic Cellulose Ethers. US4228277 A, October 14, 1980.

(96) Nyström, C.; Mazur, J.; Sjögren, J. Studies on Direct Compression of Tablets II. The Influence of the Particle Size of a Dry Binder on the Mechanical Strength of Tablets ☆. *Int. J. Pharm.* **1982**, *10*, 209–218.

(97) Sahoo, G. P.; Bhui, D. K.; Bar, H.; Sarkar, P.; Samanta, S.; Pyne, S.; Misra, A. Synthesis and Characterization of Gold Nanoparticles Adsorbed in Methyl Cellulose Micro Fibrils. *J Mol. Liq.* **2010**, *155*, 91–95.

(98) Kanig, J. L.; Goodman, H. Evaluative Procedures for Film-Forming Materials Used in Pharmaceutical Applications. *J. Pharm. Sci.* **1962**, *51*, 77–83.

(99) Nerurkar, J.; Jun, H. W.; Price, J. C.; Park, M. O. Controlled-Release Matrix

Tablets of Ibuprofen Using Cellulose Ethers and Carrageenans: Effect of Formulation Factors on Dissolution Rates. *Eur J Pharm Biopharm* **2005**, *61*, 56–68.

(100) Sharma, V.; Chopra, H. Role Of Taste And Taste Masking Of Bitter Drugs In Pharmaceutical Industries An Overview . *Int J Pharm Pharm. Sci* **2010**, *2*, 14–18.

(101) Debeaufort, F.; Voilley, A. Methyl Cellulose-Based Edible Films and Coatings I. Effect of Plasticizer Content on Water and 1-Octen-3-Ol Sorption and Transport. *Cellulose* **1995**, *2*, 205–2013.

(102) Debeaufort, F.; Voilley, A. Methylcellulose-Based Edible Films and Coatings: 2. Mechanical and Thermal Properties as a Function of Plasticizer Content. *J. Agric. Food Chem.* **1997**, *45*, 685−689.

(103) Arvanitoyannis, I.; Biliaderis, C. G. Physical Properties of Polyol-Plasticized Edible Blends Made of Methyl Cellulose and Soluble Starch. *Carbohydr Polym* **1999**, *38*, 47–58.

(104) Olabisi, O.; Robeson, L. M.; Shaw, M. T. *Polymer-Polymer Miscibility*; Academic Press.: New York, 1979.

(105) Chan, L. W.; Wong, T. W.; Chua, P. C.; York, P.; Heng, P. W. Anti-Tack Action of Polyvinylpyrrolidone on Hydroxypropylmethylcellulose Solution. *Chem Pharm Bull* **2003**, *51*, 107–112.

(106) Li, C. L.; Martini, L. G.; Ford, J. L.; Roberts, M. The Use of Hypromellose in Oral Drug Delivery. *J Pharm Pharmacol* **2005**, *57*, 533–546.

(107) Arisz, P. W.; Thai, H. T. T.; Boon, J. J.; Salomons, W. G. Changes in Substituent Distribution Patterns during the Conversion of Cellulose toO-(2-Hydroxyethyl) Celluloses. *Cellulose* **1996**, *3*, 45–61.

(108) Haque, A.; Richardson, R. K.; Morris, E. R.; Gidley, M. J.; Caswell, D. C. Thermogelation of Methylcellulose. Part II: Effect of Hydroxypropyl Substituents. *Carbohydr Polym* **1993**, *22*, 175–186.

(109) Dow Chemical Co. An Introduction to METHOCEL Cellulose Ethers http://www.dow.com/dowwolff/en/pdf/192-01062.pdf.

(110) Rekhi G.S.; S.S., J. Ethylcellulose - A Polymer Review. *Drug Dev Ind Pharm* **1995**, *21*, 61–77.

(111) Ford, J. L. Thermal Analysis of Hydroxypropylmethylcellulose and Methylcellulose: Powders, Gels and Matrix Tablets. *Int J Pharm* **1999**, *179*, 209–228.

(112) Hanhijarvi, K.; Majava, T.; Kassamakov, I.; Heinamaki, J.; Aaltonen, J.; Haapalainen, J.; Haeggstrom, E.; Yliruusi, J. Scratch Resistance of Plasticized Hydroxypropyl Methylcellulose (HPMC) Films Intended for Tablet Coatings. *Eur J Pharm Biopharm* **2010**, *74*, 371–376.

(113) Liu, Z.; Li, J.; Nie, S.; Liu, H.; Ding, P.; Pan, W. Study of an alginate/HPMC-Based in Situ Gelling Ophthalmic Delivery System for Gatifloxacin. *Int J Pharm* **2006**, *315*, 12–17.

(114) Melia, C. D. Hydrophilic Matrix Sustained Release Systems Based on Polysaccharide Carriers. *Crit Rev Ther Drug Carr. Syst* **1991**, *8*, 395–421.

(115) Jaipal, A.; Pandey, M. M.; Charde, S. Y.; Sadhu, N.; Srinivas, A.; Prasad, R. G. Controlled Release Effervescent Buccal Discs of Buspirone Hydrochloride: In Vitro and in Vivo Evaluation Studies. *Drug Deliv* **2014**, 1–7.

(116) Drozen M.S. GRAS Notification for Hydroxypropyl Methylcellulose http://www.accessdata.fda.gov/scripts/fcn/gras_notices/grn000213.pdf.

(117) Thackaberry, E. A.; Kopytek, S.; Sherratt, P.; Trouba, K.; McIntyre, B. Comprehensive Investigation of Hydroxypropyl Methylcellulose, Propylene Glycol, Polysorbate 80, and Hydroxypropyl-Beta-Cyclodextrin for Use in General Toxicology Studies. *Toxicol Sci* **2010**, *117*, 485–492.

(118) USP Front Matter: Excipients. USP30 NF 25. **2007**.

(119) Al-Tabakha, M. M. HPMC Capsules: Current Status and Future Prospects. *J Pharm Pharm Sci* **2010**, *13*, 428–442.

(120) Ashland. Pharmaceutical Excipients and Coating Systems http://www.ashland.com/Ashland/Static/Documents/AAFI/PRO_250-72D_Excipients_and_Tablet_Coating.pdf.

(121) Dow Chemical. METHOCEL Cellulose Ethers Techical Handbook http://www.dow.com/dowwolff/en/pdf/192-01062.pdf.

(122) Ashland Inc. Benecel TM hydroxypropyl methlcellulose for personal care http://www.ashland.com/Ashland/Static/Documents/ASI/PC_10642_Benecel_HPMC.pdf (accessed Jul 3, 2015).

(123) Shin-Etsu Chemical Co., L. Metolose (Hypromellose* & Methylcellulose) http://www.metolose.jp/e/pharmaceutical/metolose.shtml.

(124) The Dow Chemical Co. METHOCEL™ Cellulose Ethers http://www.dow.com/personalcare/technologies/rheology/methocel.htm.

(125) Ashland Inc. BenecelTM methylcellulose, hypromellose and methylhydroxyethyl cellulose (Number 4391-15) http://www.ashland.com/Ashland/Static/Documents/ASI/Pharmaceutical/PDS_4391_Benecel_Methylcellulose_and_Hypromellose.pdf.

(126) Viriden, A.; Larsson, A.; Wittgren, B. The Effect of Substitution Pattern of HPMC on Polymer Release from Matrix Tablets. *Int J Pharm* **2010**, *389*, 147–156.

(127) Viriden, A.; Wittgren, B.; Andersson, T.; Larsson, A. The Effect of Chemical Heterogeneity of HPMC on Polymer Release from Matrix Tablets. *Eur J Pharm Sci* **2009**, *36*, 392–400.

(128) Viriden, A.; Abrahmsen-Alami, S.; Wittgren, B.; Larsson, A. Release of Theophylline and Carbamazepine from Matrix Tablets--Consequences of HPMC Chemical Heterogeneity. *Eur J Pharm Biopharm* **2011**, *78*, 470–479.

(129) Ford, J. L.; Rubinstein, M. H.; Hogan, J. E. Propranolol Hydrochloride and Aminophylline Release from Matrix Tablets Containing Hydroxypropylmethylcellulose. *Int J Pharm* **1985**, *24*, 339–350.

(130) Ford, J. L.; Rubinstein, M. H.; Hogan, J. E. Formulation of Sustained Release Promethazine Hydrochloride Tablets Using Hydroxypropyl-Methylcellulose Matrices. *Int J Pharm* **1985**, *24*, 327–338.

(131) Vueba, M. L.; Batista de Carvalho, L. A.; Veiga, F.; Sousa, J. J.; Pina, M. E. Influence of Cellulose Ether Polymers on Ketoprofen Release from Hydrophilic

Matrix Tablets. *Eur J Pharm Biopharm* **2004**, *58*, 51–59.

(132) Campos-Aldrete, M. E. Influence of the Viscosity Grade and the Particle Size of HPMC on Metronidazole Release from Matrix Tablets. *Eur. J. Pharm. Biopharm.* **1997**, *43*, 173–178.

(133) Pradhan, R.; Budhathoki, U.; Thapa, P. Formulation of Once a Day Controlled Release Tablet of Indomethacin Based on HPMC-Mannitol. *Kathmandu Univ. J. Sci. Eng. Technol.* **2008**, *4*.

(134) Nochos, A.; Douroumis, D. In Vitro Release of Bovine Serum Albumin from alginate/HPMC Hydrogel Beads. *Carbohydr Polym* **2008**, *74*, 451–457.

(135) Rasenack, N.; Hartenhauer, H.; Muller, B. W. Microcrystals for Dissolution Rate Enhancement of Poorly Water-Soluble Drugs. *Int J Pharm* **2003**, *254*, 137–145.

(136) Law, S. L.; Kayes, J. B. Adsorption of Non-Ionic Water-Soluble Cellulose Polymers at the Solid-Water Interface and Their Effect on Suspension Stability. *Int J Pharm* **1983**, *15*, 251–260.

(137) Patil, S.; Kuchekar, B.; Chabukswar, A.; Jagdale, S. Formulation and Evaluation of Extended-Release Solid Dispersion of Metformin Hydrochloride. *J Young Pharm* **2010**, *2*, 121–129.

(138) Pradhan, R.; Kim, Y. I.; Chang, S. W.; Kim, J. O. Preparation and Evaluation of Once-Daily Sustained-Release Coated Tablets of Tolterodine-L-Tartrate. *Int J Pharm* **2014**, *460*, 205–211.

(139) Pygall, S. R.; Kujawinski, S.; Timmins, P.; Melia, C. D. Mechanisms of Drug Release in Citrate Buffered HPMC Matrices. *Int J Pharm* **2009**, *370*, 110–120.

(140) Avalle, P.; Pygall, S. R.; Gower, N.; Midwinter, A. The Use of in Situ near Infrared Spectroscopy to Provide Mechanistic Insights into Gel Layer Development in HPMC Hydrophilic Matrices. *Eur. J. Pharm. Sci.* **2011**, *43*, 400–408.

(141) Hardy, I. J.; Cook, W. G.; Melia, C. D. Compression and Compaction Properties of Plasticised High Molecular Weight Hydroxypropylmethylcellulose (HPMC) as a Hydrophilic Matrix Carrier. *Int J Pharm* **2006**, *311*, 26–32.

(142) Benecel Hypromellose (HPMC) and Methlycellulose (MC) - Low viscosity grades http://www.ashland.com/products/benecel-methylcellulose-and-hypromellose.

(143) Obara, S.; Kokubo, H. *Application of HPMC and HPMCAS to Aqueous Film Coating of Pharmaceutical Dosage Forms, Aqueous Polymeric Coatings for Pharmaceutical Dosage Forms, Informa Healthcare*; 2008.

(144) J.T. Heinaimaiki; V.M. Lehtola; P. Nikupaavo; Yliruusi, J. K. The Mechanical and Moisture Permeability Properties of Aqueous-Based Hydroxypropyl Methylcellulose Coating Systems Plasticized with Polyethylene Glycol. *Int J Pharm.* **1994**, *112*, 191–196.

(145) Roy, A.; Ghosh, A.; Datta, S.; Das, S.; Mohanraj, P.; Deb, J.; Bhanoji Rao, M. E. Effects of Plasticizers and Surfactants on the Film Forming Properties of Hydroxypropyl Methylcellulose for the Coating of Diclofenac Sodium Tablets. *Saudi Pharm J* **2009**, *17*, 233–241.

(146) G.S. MacLeod; J.T. Fell; J.H. Collett; H.L. Sharma; Smith, A. M. Selective Drug Delivery to the Colon Using Pectin:chitosan:hydroxypropyl Methycellulose Film Coated Tablets. *Int. J. Pharm.* **1999**, *187*, 251–257.

(147) G.S. MacLeod J.H. Collett, J. T. F. An in Vitro Investigations into the Potential for Biomodal Drug Release from Petin/chitosan HPMC-Coated Tablets. *Int. J. Pharm.* **1999**, *188*, 11–18.

(148) Adibkia, K.; Barzegar-Jalalia, M.; Maheri-Esfanjanib, H.; Ghanbarzadehb, S.; Shokrib, J.; Sabzevarie, A.; Javadzadeha, Y. Physicochemical Characterization of Naproxen Solid Dispersions Prepared via Spray Drying Technology. *Powder Technol.* **2013**, *246*, 448–455.

(149) Raffin, R. P.; Jornada, D. S.; Re, M. I.; Pohlmann, A. R.; Guterres, S. S. Sodium Pantoprazole-Loaded Enteric Microparticles Prepared by Spray Drying: Effect of the Scale of Production and Process Validation. *Int J Pharm* **2006**, *324*, 10–18.

(150) Kumar, S.; Xu, X.; Gokhale, R.; Burgess, D. J. Formulation Parameters of Crystalline Nanosuspensions on Spray Drying Processing: A DoE Approach. *Int J Pharm* **2014**, *464*, 34–45.

(151) Verreck, G.; Six, K.; Van den Mooter, G.; Baert, L.; Peeters, J.; Brewster, M. E. Characterization of Solid Dispersions of Itraconazole and Hydroxypropylmethylcellulose Prepared by Melt Extrusion--Part I. *Int J Pharm* **2003**, *251*, 165–174.

(152) Six, K.; Berghmans, H.; Leuner, C.; Dressman, J.; Van Werde, K.; Mullens, J.; Benoist, L.; Thimon, M.; Meublat, L.; Verreck, G.; Peeters, J.; Brewster, M.; Van den Mooter, G. Characterization of Solid Dispersions of Itraconazole and Hydroxypropylmethylcellulose Prepared by Melt Extrusion, Part II. *Pharm Res* **2003**, *20*, 1047–1054.

(153) Zhao, M.; Barker, S. A.; Belton, P. S.; McGregor, C.; Craig, D. Q. Development of Fully Amorphous Dispersions of a Low T(g) Drug via Co-Spray Drying with Hydrophilic Polymers. *Eur J Pharm Biopharm* **2012**, *82*, 572–579.

(154) Repka, M. A.; Gutta, K.; Prodduturi, S.; Munjal, M.; Stodghill, S. P. Characterization of Cellulosic Hot-Melt Extruded Films Containing Lidocaine. *Eur J Pharm Biopharm* **2005**, *59*, 189–196.

(155) Xu, S.; Dai, W. G. Drug Precipitation Inhibitors in Supersaturable Formulations. *Int J Pharm* **2013**, *453*, 36–43.

(156) Yamashita, K.; Nakate, T.; Okimoto, K.; Ohike, A.; Tokunaga, Y.; Ibuki, R.; Higaki, K.; Kimura, T. Establishment of New Preparation Method for Solid Dispersion Formulation of Tacrolimus. *Int J Pharm* **2003**, *267*, 79–91.

(157) Agarwal, V.; Mishra, B. Design, Development, and Biopharmaceutical Properties of Buccoadhesive Compacts of Pentazocine. *Drug Dev Ind Pharm* **1999**, *25*, 701–709.

(158) Taylan, B.; Capan, Y.; Guven, O.; Kes, S.; Hincal, A. A. Design and Evaluation of Sustained-Release and Buccal Adhesive Propranolol Hydrochloride Tablets. *J Cont Release* **1996**, *38*, 11–20.

(159) El- Nabarawi, M. A.; Makky, A. M.; El-Setouhy, D. A.; Abd-Elmoniem, R. A.; Amin, M. G.; Jasti, B. A. Fabrication, Evaluation And Preliminary Clinical Study Of Bi-Layer Orobuccal Devices Containing Ketorolac Tromethamine And

Chlorhexidine Hcl For Treatment Of Oral Inflammation. *Int. J. Pharm. Pharm. Sci.* **2014**, *6*, 851–857.

(160) BERMOCOLL® Cellulose Ethers http://www.elotex.com/cellulose-ethers-products.

(161) Hosny, E. A.; Elkheshen, S. A.; Saleh, S. I. Buccoadhesive Tablets for Insulin Delivery: In-Vitro and in-Vivo Studies. *Boll Chim Farm* **2002**, *141*, 210–217.

(162) Yoo, J. W.; Dharmala, K.; Lee, C. H. The Physicodynamic Properties of Mucoadhesive Polymeric Films Developed as Female Controlled Drug Delivery System. *Int J Pharm* **2006**, *309*, 139–145.

(163) Valenta, C. The Use of Mucoadhesive Polymers in Vaginal Delivery. *Adv Drug Deliv Rev.* **2005**, *57*, 1692–1712.

(164) SR Bhat; Shivakumar, H. G. Bioadhesive Controlled Release Clotrimazole Vaginal Tablets. *Trop. J. Pharm. Res.* **2010**, *9*, 339–346.

(165) Bilensoy, E.; Rouf, M. A.; Vural, I.; Sen, M.; Hincal, A. A. Mucoadhesive, Thermosensitive, Prolonged-Release Vaginal Gel for Clotrimazole:beta-Cyclodextrin Complex. *AAPS PharmSciTech* **2006**, *7*, E38.

(166) Leon Lilienfeld. Process of Making a New Type of Cellulose Derivatives. US 1589606 A, June 22, 1926.

(167) Lilienfeld, A. Manufacture of Cellulose Derivatives. US2265917 A, December 9, 1941.

(168) Donges, R. Non-Ionic Cellulose Ethers. *Br. Polym. J.* **1990**, *23*, 315–326.

(169) Company, T. D. C. Ethycellulose Polymers Technical Handbook http://msdssearch.dow.com/PublishedLiteratureDOWCOM/dh_004f/0901b8038004fb7c.pdf?filepath=/192-00818.pdf&fromPage=GetDoc.

(170) Dow Chemical Co. ETHOCEL Ethylcellulose Technical review http://msdssearch.dow.com/PublishedLiteratureDOWCOM/dh_08e5/0901b803808e5465.pdf?filepath=dowwolff/pdfs/noreg/198-02293.pdf&fromPage=GetDoc.

(171) Murtaza G.; Ahmad A.; Waheed A. A.; M., N. A. Salbutamol Sulphate-

Ethylcellulose Microparticles: Formulation and in-Vitro Evaluation with Emphasis on Mathematical Approaches. *DARU* **2009**, *17*, 209–217.

(172) Finelli L.; Scandola M.; P., S. Biodegradation of Blends of Bacterial poly(3-Hydroxybutyrate) with Ethyl Cellulose in Activated Sludge and in Enzymatic Solution. *Macromol. Chem. Phys.* **1998**, *199*, 695–703.

(173) Huang, J.; Wigent, R. J.; Schwartz, J. B. Nifedipine Molecular Dispersion in Microparticles of Ammonio Methacrylate Copolymer and Ethylcellulose Binary Blends for Controlled Drug Delivery: Effect of Matrix Composition. *Drug Dev Ind Pharm* **2006**, *32*, 1185–1197.

(174) Khan, G. M.; Meidan, V. M. Drug Release Kinetics from Tablet Matrices Based upon Ethylcellulose Ether-Derivatives: A Comparison between Different Formulations. *Drug Dev Ind Pharm* **2007**, *33*, 627–639.

(175) Gohel, M. C.; Nagori, S. A. Fabrication of Modified Transport Fluconazole Transdermal Spray Containing Ethyl Cellulose and Eudragit RS100 as Film Formers. *AAPS PharmSciTech* **2009**, *10*, 684–691.

(176) Muschert, S.; Siepmann, F.; Leclercq, B.; Carlin, B.; Siepmann, J. Prediction of Drug Release from Ethylcellulose Coated Pellets. *J Control Release* **2009**, *135*, 71–79.

(177) Avanço, G. B.; Bruschi, M. L. Preparation and Characterisation of Ethylcellulose Microparticles Containing Propolis. *Rev. Ciênc. Farm. Básica Apl.,* **2008**, *29*, 129–135.

(178) Chemical, C. D. Product specification sheet for Ethocel FP Ethylcellulose polymers http://msdssearch.dow.com/PublishedLiteratureDOWCOM/dh_0171/0901b80380171e50.pdf?filepath=/198-02001.pdf&fromPage=GetDoc.

(179) Vynckier, A. K.; Dierickx, L.; Saerens, L.; Voorspoels, J.; Gonnissen, Y.; De Beer, T.; Vervaet, C.; Remon, J. P. Hot-Melt Co-Extrusion for the Production of Fixed-Dose Combination Products with a Controlled Release Ethylcellulose Matrix Core. *Int J Pharm* **2014**, *464*, 65–74.

(180) Verhoeven, E.; De Beer, T. R.; Van den Mooter, G.; Remon, J. P.; Vervaet, C. Influence of Formulation and Process Parameters on the Release Characteristics of Ethylcellulose Sustained-Release Mini-Matrices Produced by Hot-Melt Extrusion. *Eur J Pharm Biopharm* **2008**, *69*, 312–319.

(181) Verhoeven, E.; De Beer, T. R.; Schacht, E.; Van den Mooter, G.; Remon, J. P.; Vervaet, C. Influence of Polyethylene Glycol/polyethylene Oxide on the Release Characteristics of Sustained-Release Ethylcellulose Mini-Matrices Produced by Hot-Melt Extrusion: In Vitro and in Vivo Evaluations. *Eur J Pharm Biopharm* **2009**, *72*, 463–470.

(182) Zhang, Z. Y.; Ping, Q. N.; Xiao, B. Microencapsulation and Characterization of Tramadol-Resin Complexes. *J Control Release* **2000**, *66*, 107–113.

(183) Desai, R. P.; Neau, S. H.; Pather, S. I.; Johnston, T. P. Fine-Particle Ethylcellulose as a Tablet Binder in Direct Compression, Immediate-Release Tablets. *Drug Dev Ind Pharm* **2001**, *27*, 633–641.

(184) Shah, S.; Shah, K.; Jan, S. U.; Ahmad, K.; Rehman, A.; Hussain, A.; Khan, G. M. Formulation and in Vitro Evaluation of Ofloxacin-Ethocel Controlled Release Matrix Tablets Prepared by Wet Granulation Method: Influence of Co-Excipients on Drug Release Rates. *Pak J Pharm Sci* **2011**, *24*, 255–261.

(185) Wahab A; Khan G.M.; Akhlaq M.; Khan N.R.; Hussain A.; Zeb A.; Rehman A.; Shah K.U. Pre-Formulation Investigation and in Vitro Evaluation of Directly Compressed Ibuprofen-Ethocel Oral Controlled Release Matrix Tablets: A Kinetic Approach. *African J. Pharm. Pharmacol.* **2011**, *5*, 2118–2127.

(186) Sanchez-Lafuente, C.; Furlanetto, S.; Fernandez-Arevalo, M.; Alvarez-Fuentes, J.; Rabasco, A. M.; Faucci, M. T.; Pinzauti, S.; Mura, P. Didanosine Extended-Release Matrix Tablets: Optimization of Formulation Variables Using Statistical Experimental Design. *Int J Pharm* **2002**, *237*, 107–118.

(187) Sanchez-Lafuente, C.; Teresa Faucci, M.; Fernandez-Arevalo, M.; Alvarez-Fuentes, J.; Rabasco, A. M.; Mura, P. Development of Sustained Release Matrix Tablets of Didanosine Containing Methacrylic and Ethylcellulose Polymers. *Int J*

Pharm **2002**, *234*, 213–221.

(188) Badshah, A.; Subhan, F.; Rauf, K.; Bukhari, N. I.; Shah, K.; Khan, S.; Ahmed, Z.; Khan, I. Development of Controlled-Release Matrix Tablet of Risperidone: Influence of Methocel(R)- and Ethocel(R)-Based Novel Polymeric Blend on in Vitro Drug Release and Bioavailability. *AAPS PharmSciTech* **2011**, *12*, 525–533.

(189) Pollock, D. K. Influence of Filler/binder Composition on the Properties of an Inert Matrix CR System. *Proc. Int. Symp. Control. Release Bioact. Mater.* **1997**, *24*, 481–482.

(190) Iqbal, Z.; Babar, A.; Ashraf, M. Controlled-Release Naproxen Using Micronized Ethyl Cellulose by Wet-Granulation and Solid-Dispersion Method. *Drug Dev Ind Pharm* **2002**, *28*, 129–134.

(191) Eichie F.L.; Okor R.S. Parameters to Be Considered in the Simulation of Drug Release from Aspirin Crystals and Their Microcapsules. *Trop. J. Pharm. Res.* **2002**, *1*, 99–110.

(192) Dailey O.D.; Dowler C.C. Polymeric Microcapsules of Cyanazine: Preparation and Evaluation of Efficacy. *J. Agric. Food Chem* **1998**, *46*, 3823–3827.

(193) Mastiholimath, V. S.; Dandagi, P. M.; Gadad, A. P.; Mathews, R.; Kulkarni, A. R. In Vitro and in Vivo Evaluation of Ranitidine Hydrochloride Ethyl Cellulose Floating Microparticles. *J Microencapsul* **2008**, *25*, 307–314.

(194) Palmieri G. F.; Wehrle P. Evaluation of Ethylcellulose-Coated Pellets Optimized Using the Approach of Taguchi. *Drug Dev Ind Pharm* **1997**, *23*, 1069–1077.

(195) Milojevic S.; Newton J.M.; Cummings J.H.; Gibson G.R.; Botham R.L.; Ring S.G.; Stockham M.; Allwood M.C. Amylose as a Coating for Drug Delivery to the Colon: Preparation and in Vitro Evaluation Using 5-Aminosalicylic Acid Pellets. *J. Control. Release* **1996**, *38*, 75–84.

(196) Sinha, V. R.; Kumria, R. Microbially Triggered Drug Delivery to the Colon. *Eur J Pharm Sci* **2003**, *18*, 3–18.

(197) Quinten, T.; De Beer, T.; Vervaet, C.; Remon, J. P. Evaluation of Injection Moulding as a Pharmaceutical Technology to Produce Matrix Tablets. *Eur. J.*

Pharm. Biopharm. **2009**, *71*, 145–154.

(198) De Brabander, C.; Vervaet, C.; Remon, J. P. Development and Evaluation of Sustained Release Mini-Matrices Prepared via Hot Melt Extrusion. *J Control Release* **2003**, *89*, 235–247.

(199) Verhoeven, E.; Vervaet, C.; Remon, J. P. Xanthan Gum to Tailor Drug Release of Sustained-Release Ethylcellulose Mini-Matrices Prepared via Hot-Melt Extrusion: In Vitro and in Vivo Evaluation. *Eur J Pharm Biopharm* **2006**, *63*, 320–330.

(200) De Brabander, C.; Van Den Mooter, G.; Vervaet, C.; Remon, J. P. Characterization of Ibuprofen as a Nontraditional Plasticizer of Ethyl Cellulose. *J Pharm Sci* **2002**, *91*, 1678–1685.

(201) Klucel Hydroxypropylcellulose Physical and chemical properties http://www.ashland.com/Ashland/Static/Documents/ASI/PC_11229_Klucel_HPC.pdf (accessed Sep 9, 2015).

(202) Guo, J.-H.; Skinner, G. .; Harcum, W. .; Barnum, P. . Pharmaceutical Applications of Naturally Occurring Water-Soluble Polymers. *Pharm. Sci. Technolo. Today* **1998**, *1*, 254–261.

(203) Imeson, A. *Thickening and Gelling Agents for Food*; Springer Science & Business Media, 2012.

(204) Kobayashi, K.; Huang, C.; Lodge, T. P. Thermoreversible Gelation of Aqueous Methylcellulose Solutions. *Macromolecules* **1999**, *32*, 7070–7077.

(205) Kamitakahara, H.; Funakoshi, T.; Nakai, S.; Takano, T.; Nakatsubo, F. Synthesis and Structure/property Relationships of Regioselective 2-O-, 3-O- and 6-O-Ethyl Celluloses. *Macromol. Biosci.* **2010**, *10*, 638–647.

(206) Dubolazov, A. V; Nurkeeva, Z. S.; Mun, G. A.; Khutoryanskiy, V. V. Design of Mucoadhesive Polymeric Films Based on Blends of Poly(acrylic Acid) and (Hydroxypropyl)cellulose. *Biomacromolecules* **2006**, *7*, 1637–1643.

(207) Nisso HPC http://www.nissoexcipients.com/ (accessed Sep 9, 2015).

(208) Crowley, M. M.; Zhang, F.; Repka, M. A.; Thumma, S.; Upadhye, S. B.; Battu, S.

K.; McGinity, J. W.; Martin, C. Pharmaceutical Applications of Hot-Melt Extrusion: Part I. *Drug Dev. Ind. Pharm.* **2008**, *33*, 909–926.

(209) El-Zaher, N. A.; Osiris, W. G. Thermal and Structural Properties of Poly(vinyl Alcohol) Doped with Hydroxypropyl Cellulose. *J. Appl. Polym. Sci.* **2005**, *96*, 1914–1923.

(210) Repka, M. A.; Gerding, T. G.; Repka, S. L.; McGinity, J. W. Influence of Plasticizers and Drugs on the Physical-Mechanical Properties of Hydroxypropylcellulose Films Prepared by Hot Melt Extrusion. *Drug Dev. Ind. Pharm.* **1999**, *25*, 625–633.

(211) Picker-Freyer, K. M.; Dürig, T. Physical Mechanical and Tablet Formation Properties of Hydroxypropylcellulose: In Pure Form and in Mixtures. *AAPS PharmSciTech* **2007**, *8*, E92.

(212) Skinner, G. W.; Harcum, W. W.; Barnum, P. E.; Guo, J. H. The Evaluation of Fine-Particle Hydroxypropylcellulose as a Roller Compaction Binder in Pharmaceutical Applications. *Drug Dev. Ind. Pharm.* **1999**, *25*, 1121–1128.

(213) Klucel Hydroxypropylcellulose Hydrophilic Matrix System http://www.ashland.com/Ashland/Static/Documents/ASI/PC_10691_Klucel_HPC.pdf (accessed Oct 9, 2015).

(214) Teixeira, A. Z. A. Hydroxypropylcellulose Controlled Release Tablet Matrix Prepared by Wet Granulation: Effect of Powder Properties and Polymer Composition. *Brazilian Arch. Biol. Technol.* **2009**, *52*, 157–162.

(215) Sinha Roy, D.; Rohera, B. D. Comparative Evaluation of Rate of Hydration and Matrix Erosion of HEC and HPC and Study of Drug Release from Their Matrices. *Eur. J. Pharm. Sci.* **2002**, *16*, 193–199.

(216) Sasa, B.; Odon, P.; Stane, S.; Julijana, K. Analysis of Surface Properties of Cellulose Ethers and Drug Release from Their Matrix Tablets. *Eur. J. Pharm. Sci.* **2006**, *27*, 375–383.

(217) Uekama, K.; Matsubara, K.; Abe, K.; Horiuchi, Y.; Hirayama, F.; Suzuki, N. Design and in Vitro Evaluation of Slow-Release Dosage Form of Piretanide:

Utility of β-Cyclodextrin:cellulose Derivative Combination as a Modified-Release Drug Carrier. *J. Pharm. Sci.* **1990**, *79*, 244–248.

(218) Wang, Z.; Horikawa, T.; Hirayama, F.; Uekama, K. Design and In-Vitro Evaluation of a Modified-Release Oral Dosage Form of Nifedipine by Hybridization of Hydroxypropyl-β-Cyclodextrin and Hydroxypropylcellulose. *J. Pharm. Pharmacol.* **1993**, *45*, 942–946.

(219) Lakshman, J. P.; Kowalski, J.; Vasanthavada, M.; Tong, W.-Q.; Joshi, Y. M.; Serajuddin, A. T. M. Application of Melt Granulation Technology to Enhance Tabletting Properties of Poorly Compactible High-Dose Drugs. *J. Pharm. Sci.* **2011**, *100*, 1553–1565.

(220) Onoue, S.; Sato, H.; Ogawa, K.; Kawabata, Y.; Mizumoto, T.; Yuminoki, K.; Hashimoto, N.; Yamada, S. Improved Dissolution and Pharmacokinetic Behavior of Cyclosporine A Using High-Energy Amorphous Solid Dispersion Approach. *Int. J. Pharm.* **2010**, *399*, 94–101.

(221) Sakellariou, P.; Rowe, R. C.; White, E. F. T. The Solubility Parameters of Some Cellulose Derivatives and Polyethylene Glycols Used in Tablet Film Coating. *Int. J. Pharm.* **1986**, *31*, 175–177.

(222) Arca, H. C.; Mosquera-Giraldo, Laura Taylor, L. S.; Edgar, K. J. Synthesis and Characterization of Alkyl Cellulose ω-Carboxyesters for Amorphous Solid Dispersion. *Carbohydr Polym* **2015**.

(223) Ozeki, T.; Yuasa, H.; Kanaya, Y. Application of the Solid Dispersion Method to the Controlled Release of Medicine. IX. Difference in the Release of Flurbiprofen from Solid Dispersions with Poly(ethylene Oxide) and Hydroxypropylcellulose and the Interaction between Medicine and Polymers. *Int. J. Pharm.* **1997**, *155*, 209–217.

(224) Mohammed, N. N.; Majumdar, S.; Singh, A.; Deng, W.; Murthy, N. S.; Pinto, E.; Tewari, D.; Durig, T.; Repka, M. A. Klucel^{TM} EF and ELF Polymers for Immediate-Release Oral Dosage Forms Prepared by Melt Extrusion Technology. *AAPS PharmSciTech* **2012**, *13*, 1158–1169.

(225) Repka, M. A.; McGinity, J. W. Physical–mechanical, Moisture Absorption and Bioadhesive Properties of Hydroxypropylcellulose Hot-Melt Extruded Films. *Biomaterials* **2000**, *21*, 1509–1517.

(226) Allen, J. M.; Wilson, A. K.; Lucas, P. L.; Curtis, L. G. Carboxyalkyl Cellulose Esters. US5668273, 1996.

(227) Shelton, M. C. .; Posey-Dowty, J. D. .; Lingerfelt, L. R. .; Kirk, S. K. .; Klein, S. .; Edgar, K. J. *Enhanced Dissolution of Poorly Soluble Drugs from Solid Dispersions in Carboxymethylcellulose Acetate Butyrate Matrices*; American Chemical Society, 2009; Vol. 1017.

(228) Casterlow, S. A. Characterization and Pharmacokinetics of Rifampicin Laden Carboxymethylcellulose Acetate Butyrate Particles, Virginia Tech, 2012.

(229) AquaSolve ^{TM} Hypromellose Acetate Succinate (HPMCAS) http://www.ashland.com/Ashland/Static/Documents/ASI/PC_12474_AquaSolve_HPMCAS.pdf (accessed Jan 1, 2015).

(230) Curatolo, W. J.; Nightingale, J. A. S.; Shanker, R. M.; Sutton, S. C. Solubility in Small Intestines; Hydroxypropyl Methyl Cellulose Acetate Succinate Polymer and Zwitterion Drug; US6548555 B1, April 15, 2003.

(231) Kennedy, M.; Hu, J.; Gao, P.; Li, L.; Ali-Reynolds, A.; Chal, B.; Gupta, V.; Ma, C.; Mahajan, N.; Akrami, A.; Surapaneni, S. Enhanced Bioavailability of a Poorly Soluble VR1 Antagonist Using an Amorphous Solid Dispersion Approach: A Case Study. *Mol Pharm* **2008**, *5*, 981–993.

(232) Tanno, F.; Nishiyama, Y.; Kokubo, H.; Obara, S. Evaluation of Hypromellose Acetate Succinate (HPMCAS) as a Carrier in Solid Dispersions. *Drug Dev Ind Pharm* **2004**, *30*, 9–17.

(233) Konno, H.; Handa, T.; Alonzo, D. E.; Taylor, L. S. Effect of Polymer Type on the Dissolution Profile of Amorphous Solid Dispersions Containing Felodipine. *Eur J Pharm Biopharm* **2008**, *70*, 493–499.

(234) Li, B.; Konecke, S.; Harich, K.; Wegiel, L.; Taylor, L. S.; Edgar, K. J. Solid Dispersion of Quercetin in Cellulose Derivative Matrices Influences Both

Solubility and stabilityLi B, Konecke S, Harich K, et Al (2013) Solid Dispersion of Quercetin in Cellulose Derivative Matrices Influences Both Solubility and Stability. Carbohy. *Carbohydr Polym* **2013**, *92*, 2033–2040.

(235) Wegiel LA; Mauer LJ; Edgar KJ; Taylor, L. S. Mid-Infrared Spectroscopy as a Polymer Selection Tool for Formulating Amorphous Solid Dispersions. *J Pharm Pharmacol.* **2014**, *66*, 244–255.

(236) Lang, B.; McGinity, J. W.; Williams 3rd, R. O. Dissolution Enhancement of Itraconazole by Hot-Melt Extrusion Alone and the Combination of Hot-Melt Extrusion and Rapid Freezing--Effect of Formulation and Processing Variables. *Mol Pharm* **2014**, *11*, 186–196.

(237) Mahmah, O.; Tabbakh, R.; Kelly, A.; Paradkar, A. A Comparative Study of the Effect of Spray Drying and Hot-Melt Extrusion on the Properties of Amorphous Solid Dispersions Containing Felodipine. *J Pharm Pharmacol* **2014**, *66*, 275–284.

(238) Sarode, A. L.; Obara, S.; Tanno, F. K.; Sandhu, H.; Iyer, R.; Shah, N. Stability Assessment of Hypromellose Acetate Succinate (HPMCAS) NF for Application in Hot Melt Extrusion (HME). *Carbohydr. Polym.* **2014**, *101*, 146–153.

(239) Dong, Y.; Edgar, K. J. Imparting Functional Variety to Cellulose Ethers via Olefin Cross-Metathesis. *Polym. Chem.* **2015**, *6*, 3816–3827.

Chapter 3. Rifampin Stability and Solution Concentration Enhancement through Amorphous Solid Dispersion in Cellulose ω-Carboxyalkanoate Matrices

Adapted from "Arca, H. C.; Mosquera-Giraldo, L. I.; Pereira, J. M.; Sriranganathan, N.; Taylor, L. S.; Edgar, K. J. *J Pharm Sci* 2016 Submitted."

3.1 Abstract

Tuberculosis (TB) is the second most deadly infectious disease in the world; approximately 2 billion people are currently latently infected with the causative agent *Mycobacterium tuberculosis*. Approximately 8 million new cases and 2 million deaths due to TB are recorded annually[1]. Rifampicin or Rifampin (Rif) is a vital first line TB treatment drug that requires high dose (600 mg 1x/day) application to achieve its moderate, variable bioavailability. These issues can be explained by Rif instability at gastric pH, moderate solubility at neutral pH, polymorphism, and stimulation of its own metabolism. To overcome these obstacles, we developed new cellulose based oral drug delivery systems aiming to increase and make more consistent Rif solubility and bioavailability. ASDs of Rif with cellulose ω-carboxyalkanoates (cellulose acetate suberate, cellulose acetate propionate adipate, and cellulose acetate butyrate sebacate) were prepared, and compared with crystalline Rif and carboxymethyl cellulose acetate butyrate ASD controls. Cellulose w-carboxyalkanoate ASDs prevented acid-catalyzed degradation in conditions mimicking the acidic stomach, and provided complete release of intact Rif at intestinal pH. Rif incorporation into ASD in these novel cellulose derivative matrices creates the potential for convenient, robust, consistent, and high Rif oral bioavailability for treatment of TB.

3.2 Introduction

Tuberculosis is an infectious disease caused by the *M. tuberculosis* bacterium. As is common for mycobacterial diseases, *M. tuberculosis* infects macrophages[2] and it is therefore difficult to kill intracellular *M. tuberculosis* with antimicrobials. As a result, treatment is lengthy (ca. 6 months), and requires daily administration of multiple drugs, leading to complex treatment regimes and relatively poor patient compliance to complex dosage schedules. The infection is readily transmitted, as pulmonary TB patients create aerosols by coughing, sneezing, and talking. As a result, *M. tuberculosis* infection is remarkably common globally; approximately 2 billion people,

that is to say 1/3 of all humans on the planet, are infected. Fortunately, infection does not always or immediately lead to symptomatic TB. In 2012, 8.6 million people developed TB and 0.45 million of them developed multi-drug resistant TB (MTB), while in that year TB killed 1.3 million people (including 0.32 million who were co-infected with HIV)[3]. While TB can be cured through antimicrobial therapy, the long course of treatment and the prevalence of the disease in countries with limited resources and infrastructure mean that effective delivery and completion of therapy are major barriers to disease cure[4]. TB is also a threat to more developed countries, due to the prevalence of MTB[5], development of which can be promoted by patient non-compliance, and co-infection with HIV[6,7]. Indeed, the importance of compliance issues is underlined by the fact that they are addressed routinely, by "directly observed therapy" (DOT) regimes[8], in spite of the effort and expense involved. TB can be described as a deadly, transmittable, widely prevalent disease for which current drug therapeutic regimes are lengthy and not well adhered to, leading to growing problems with patient adherence, the development of MDR and extensively drug resistant (XDR) strains.

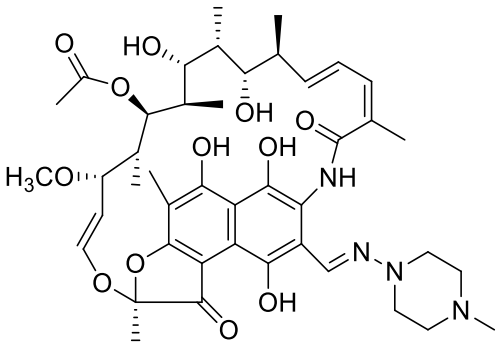

Figure 3.1: The chemical structure of Rif.

Rif is a key component of standard multidrug combination TB therapies in which its role is thought to be, at least in part, killing bacteria that emerge from dormancy after the onset of treatment[9]. It is frequently given in combination with ethambutol, pyrazinamide, and isoniazid for the first two months, and then in combination with isoniazid for the last four months of therapy[6]. Rif (**Figure 3.1**) is a semi-synthetic derivative of rifamycin B[10]. It is active against bacteria due to its ability to inhibit RNA polymerase[11]. Rif has interesting characteristics; it is zwitterionic due to the fact that it possesses both a basic amine on the piperazine ring (pKa 7.9)

as well as an acidic *p*-hydroxynaphthyl ketone (pKa 1.7) moiety. Rif permeates well through the enterocytes[12] and is quite soluble under the acidic conditions of the stomach (solubility ca. 125 mg/mL at pH 1.2[13]), leading to reasonably high bioavailability (50-70%)[14]. On the other hand, Rif is not very chemically stable in acidic environments, degrading by hydrolysis of the azomethine imine linkage to liberate 1-amino-4-methylpiperazine[15]. In addition, release of Rif under the neutral pH conditions of the small intestine is modest and variable[14]. Rif solubility in water has been reported to be between 1.51 mg and 1.74 mg/mL, and dissolution rate can vary depending on the crystal morphology[16]. Inconsistent performance of Rif formulations may also be caused by Rif polymorphism, since two crystalline and one amorphous form have been reported[17].

Solubility in physiological media is one of the key parameters affecting bioavailability; Rif is classified as a Biopharmaceutical Classification System (BCS) Class II drug, poorly soluble and highly permeable[18]. Amorphous solid dispersion has emerged as one of the most promising methods for generating high (supersaturated) solution concentrations of otherwise poorly soluble drugs[19,20], particularly those that are highly crystalline in pure form. The Taylor and Edgar laboratories have collaborated to synthesize and evaluate a series of cellulose w-carboxyalkanoates that are specifically designed for high performance as ASD matrix polymers[21,22]. These polymers have already been demonstrated to strongly inhibit crystal growth and nucleation, and to generate supersaturated solutions of a broad variety of drug structures including protease inhibitors like ritonavir[23], non nucleoside reverse transcriptase inhibitors (NNRTI) like efavirenz[24], and, highly pertinent for this work, the macrolide antibiotic clarithromycin[25]. We selected from among the set of new polymers two that have previously been shown to have high performance in ASDs (cellulose acetate suberate (CASub) and cellulose acetate adipate propionate (CAAdP))[21,24,26], as well as another promising cellulose w-carboxyalkanoate chosen because it is more hydrophobic than the others (cellulose acetate butyrate sebacate (CABSeb)). In addition, we selected as a positive control a carboxy-containing cellulose ester that has been previously demonstrated to be an effective ASD polymer, and that showed promise in our preliminary experiments towards Rif ASD (carboxymethylcellulose acetate butyrate, CMCAB)[27]. Structures of these polymers are presented in **Figure 3.2**.

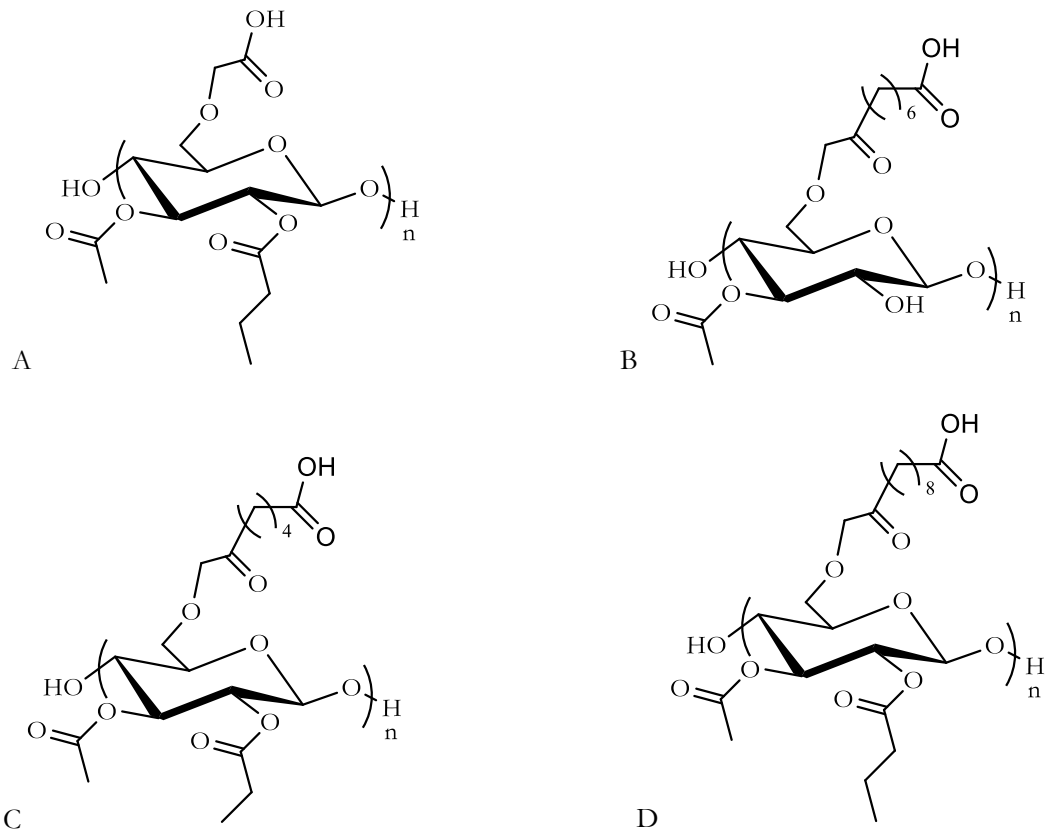

Figure 3.2: Chemical structures of CMCAB (A), CASub (B), CAAdP (C) and CABSeb (D). These structures are not meant to convey regioselective substitution; depictions of substituent location are merely for convenience and clarity of depiction.

ASD is one of the most effective methods for addressing issues of suboptimal drug solubility and oral bioavailability. In ASDs, the drug is dispersed into an amorphous polymer matrix in order to create a polymer-drug miscible blend, where there is no crystalline drug, and recrystallization is inhibited by polymer-drug interactions[28]. The amorphous drug has higher energy than in the crystalline form, thus reducing the energy barrier to drug dissolution. Therefore, higher solution concentrations (supersaturated solutions) are attained. It is also necessary that the ASD polymers should retard drug recrystallization from the dissolution medium after drug release[21,29].

Our hypothesis is that by preparing ASDs of Rif using the relatively hydrophobic cellulose w-carboxyalkanoates we have designed for use in ASD, we can significantly reduce the extent of release in the low pH environment of the stomach, preventing loss of Rif due to hydrolysis at low

pH. We further hypothesize that ASD formulation, by eliminating Rif crystallinity (MP ca. 188ºC), will enhance solution concentration at the neutral pH of the small intestine. If our hypothesis is correct, we may expect overall enhanced and robust release of intact Rif, resulting in consistently high solution concentrations and bioavailability regardless of the acidity of the stomach, potentially permitting significant Rif dose reduction and reducing bioavailability variation. We report herein tests of this hypothesis *in vitro* by preparation of the appropriate Rif ASDs and thorough examination of their performance in dissolution testing under the relevant pH regimes.

3.3 Experimental

3.3.1 Materials

Rif was purchased from Sigma. CMCAB 641-0.2 (approximate MW 22,000, degree of substitution (DS) (butyrate) = 1.64, DS (acetate) = 0.44, and DS (carboxymethyl) = 0.33), cellulose acetate propionate (CAP-504-0.2, DS (acetate) = 0.04, DS (propionate) = 2.09) M_n = 15,000 as previously reported[25], cellulose acetate butyrate (CAB-553-0.4, DS (butyrate)= 1.99, DS (acetate)= 0.14) M_n = 20,000 as previously reported[23], and cellulose acetate (CA 320S, DS (acetate) = 1.82) M_n = 50,000) as previously reported[30] were obtained from Eastman Chemical Company (Kingsport, Tennessee). Acetonitrile (HPLC-grade), tetrahydrofuran (THF), reagent ethanol, potassium phosphate monobasic, and sodium hydroxide (NaOH) were purchased from Fisher Scientific and used as received. Suberic acid, sebacic acid, adipic acid, methyl ethyl ketone (MEK), *p*-toluenesulfonic acid (PTSA), triethylamine (Et_3N), oxalyl chloride, and anhydrous THF were purchased from ACROS Organics. 1,3-Dimethyl-2-imidazolidinone (DMI) was purchased from ACROS Organics and dried over 4 Å molecular sieves. Water was purified by reverse osmosis and ion exchange using a Barnstead RO pure ST (Barnstead/Thermolyne, Dubuque, IA, USA) purification system.

3.3.2 Methods

3.3.2.1 Synthesis of cellulose derivatives:

CAAdP (synthesized as previously reported[31]; procedures summarized below)

Preparation of monobenzyl adipate: Adipic acid (73 g, 0.5 mol), benzyl alcohol (81 g, 0.75 mol), PTSA (0.95 g, 5 mmol), and toluene (200 mL) were stirred in a flask equipped with Dean-Stark trap and heated at reflux for 3 h. The resulting mixture was cooled to room temperature, water (200 mL) was added, and the pH adjusted to 8 with 6M NaOH. The aqueous layer was separated, mixed with ether (150 mL), and the pH adjusted to 2 with 6M HCl. The ether layer was separated and concentrated under reduced pressure at 40°C, affording the product as a colorless oil. ^{1}H NMR ($CDCl_3$); 1.68 (m, 4H), 2.36 (m, 4H), 5.09 (s, 2H), and 7.32 (m, 5H).

Preparation of monobenzyl adipoyl chloride: A solution of monobenzyl adipate (20 g, 80 mmol), DMF (3 drops), and 200 mL dichloromethane was cooled in a round bottomed flask to 0°C. Oxalyl chloride (25.4 g, 200 mmol) was slowly added and then the solution stirred for 2 h at room temperature. The solvent was removed under reduced pressure, 20 mL toluene was added, and then it was concentrated again under reduced pressure. The product was a yellow oil (36 g). ^{1}H NMR ($CDCl_3$): 1.73 (m, 4 H), 2.39 (t, 2 H), 2.90 (t, 2 H), 5.12 (s, 2 H), 7.32 (m, 5 H).

Similar procedures were followed to synthesize monobenzyl suberoyl chloride (^{1}H NMR ($CDCl_3$): 1.34 (m, 4H), 1.66 (m, 4H), 2.36 (t, 2H), 2.86 (t, 2H), 5.12 (s, 2H), 7.35 (m, 5H)), and monobenzyl sebacoyl chloride (^{1}H NMR ($CDCl_3$): 1.30 (m, 8H), 1.67 (m, 4H), 2.35 (t, 2H), 2.86 (t, 2H), 5.11 (s, 2H), 7.35 (m, 5H).

Monobenzyl CAAdP synthesis: CAP (1 g, 3.52 mmol) was dissolved in MEK (20 mL), Et_3N (1.06 mL, 7.74 mmol, 2.2 equiv) was added all at once, then monobenzyl adipoyl chloride (1.78 g, 7.04 mmol, 2 equiv) was added. After 20 hours at 60°C under nitrogen, the reaction mixture was cooled, then added to ethanol (250 mL) to precipitate the product, which was isolated by vacuum filtration, then washed with 200 mL water. The product was characterized by ^{1}H NMR. d 1.02-1.20 (m, $COCH_2\underline{CH_3}$ of propionate), 1.66 (broad s, $COCH_2\underline{CH_2}\underline{CH_2}CH_2CO$ of adipate), 2.16-2.35 (m, $CO\underline{CH_2}CH_3$ of propionate, $COCH_3$ of acetate and $CO\underline{CH_2}CH_2CH_2\underline{CH_2}CO$ of adipate), 3.25-5.24 (cellulose backbone), 5.10 ($\underline{CH_2}C_6H_5$), 7.33 ($CH_2\underline{C_6}\underline{H_5}$). DS by ^{1}H-NMR: adipate 0.6, propionate 2.09, acetate 0.04.

Monobenzyl CABSeb was synthesized as previously reported[23] by a procedure similar to that used for CAAdP, by reaction of CAB-553-0.4 (1.00 g, 3.26 mmol) with monobenzyl sebacoyl chloride (1 equiv).

Monobenzyl CASub was synthesized as previously reported[23] by reaction of CA 320S (1.00 g, 4.19 mmol) with monobenzyl suberoyl chloride (2.61 g, 8.38 mmol, 2 equiv) in 20 mL DMI and triethylamine (1.29 mL, 9.22 mmol, 2.2 equiv).

Example procedure for hydrogenolysis of benzyl esters: Benzyl CAAdP (1 g, 2.77 mmol) was dissolved in 100 mL THF, then $Pd(OH)_2/C$ (500 mg) was added. The mixture was stirred at high speed under H_2 atmosphere in a high-pressure reactor (Parr reactor Model 4848) at 120-psi bar pressure for 24 hours at room temperature. Products were isolated by filtering through Celite, removing the solvent under reduced pressure, and then precipitating in ethanol (50 mL).

^{1}H NMR CAAdP ($CDCl_3$, yield 88%): d 1.02-1.20 (m, $COCH_2\underline{CH_3}$ of propionate), 1.66 (broad s, $COCH_2$- $\underline{CH_2}\underline{CH_2}CH_2CO$ of adipate), 2.16-2.35 (m, $CO\underline{CH_2}CH_3$ of propionate, $COCH_3$ of acetate and $CO\underline{CH_2}CH_2CH_2\underline{CH_2}CO$ of adipate), 3.25-5.24 (cellulose backbone). DS by ^{1}H NMR: adipate 0.6, propionate 2.09, acetate 0.04.

^{1}H NMR CASub (DMSO, yield 80%): d 1.2 ($COCH_2CH_2\underline{CH_2}\underline{CH_2}CH_2CH_2CO$ of suberate), 1.4-1.6 ($COCH_2\underline{CH_2}CH_2CH_2\underline{CH_2}CH_2CO$ of suberate), 2.10–2.46 ($CO\underline{CH_2}CH_2CH_2CH_2CH_2\underline{CH_2}CO$ of suberate, and $COCH_3$ of acetate), 3.00-5.20 (cellulose backbone). DS by ^{1}H NMR: suberate 0.65, acetate 1.8.

^{1}H NMR CABSeb (DMSO, yield 79%): d 0.75-1.10 ($COCH_3$ of acetate), 1.2-1.4 ($COCH_2CH_2\underline{CH_2}\underline{CH_2}\underline{CH_2}\underline{CH_2}CH_2CH_2CO$ of sebacate), 1.45-1.7 ($COCH_2\underline{CH_2}CH_2CH_2CH_2CH_2\underline{CH_2}CH_2CO$ of sebacate), 2.0-2.45 ($CO\underline{CH_2}CH_2CH_2CH_2CH_2CH_2CH_2\underline{CH_2}CO$ of sebacate, $COCH_2CH_2CH_3$ of butyrate, and $COCH_3$ of acetate), 2.80-5.30 (cellulose backbone). DS by ^{1}H NMR: sebacate 0.3, butyrate 1.99, acetate 0.14.

3.3.2.2 Preparation of ASDs by spray drying: In each case 2 g total of drug and polymer was dissolved in 80 mL THF at room temperature. First, polymer (CMCAB, CAAdP, or CABSeb; weight 1.7 g) was magnetically stirred in THF for 15 h, at which point it was completely dissolved. Rif (weight 0.3 g) was then added to the solution and stirred for 20 min, protected from light. ASDs were prepared by spray drying the polymer/Rif solutions using a nitrogen-blanketed spray dryer (Buchi B-290). Instrument parameters were as follows: inlet temperature

80°C, outlet temperature 65°C, aspirator rate 80%, compressed nitrogen height 30 mm and nozzle cleaner 2.

A similar procedure was followed to prepare CASub spray dried dispersions, except that acetone was used as solvent.

3.3.2.3 Preparation of physical mixtures: Physical mixtures were prepared by grinding weighed portions of Rif and polymer with a mortar and pestle.

3.3.2.4 Rif quantification by High-Performance Liquid Chromatography (HPLC): An Agilent 1200 series HPLC comprising a quaternary pump, online degasser, autosampler, and Agilent Chemstation LC 3D software was used in reversed phase mode using an Eclipse XDB-C18 column (4.6 × 150 mm i.d., particle size 5 μm). Mobile phase was 50% potassium phosphate monobasic buffer (0.01 M, pH 5.5) and 50% acetonitrile (V/V). Flow rate was 1.5 mL/min, and column temperature was 30°C. UV detection at 254 nm was used and the retention time for Rif was 3.4 min.

3.3.2.5 Powder X-ray diffraction (XRD): X-ray powder diffraction patterns were measured with a Bruker D8 Discover X-ray Defractometer with a Lynxeye detector and a KFL CU 2K Xray source. Samples were run with a 1 mm slit window. The experiments were conducted with a scan range from 10° to 50° 2θ.

3.3.2.6 Differential scanning calorimetry (DSC): DSC analyses were performed on a TA Instruments Q2000 apparatus. Dry samples (5 mg) were loaded in Tzero^{TM} aluminum pans. Each sample was equilibrated at 20°C and then heated to 200°C at 20°C/min. Then samples were quench-cooled to -50°C and reheated to 200°C at 20°C/min. T_g values were recorded as the step-change inflection point from second heating scans.

3.3.2.7 Infrared analysis: Infrared spectra were obtained in transmission mode using a Bruker Optics Vertex 70 model IR Spectrophotometer (MA, U.S.A). 64 scans were collected for each sample over the wavenumber region 400 - 4000 cm^{-1}. The amorphous RIF sample was prepared by a spin coating method, RIF was dissolved in methanol, added into a coverslip and spun at 1000 rpm using a spin coater KW-4A (Chemat Technology Inc. Northridge, CA). The solid samples Rif, 15% RIF: 85% CMCAB, and CMCAB were evaluated using an attenuated total

reflectance accessory (Golden gate ATR, Specac Ltd., Slough, England). The samples and detector were purged with dry air to avoid contact with moisture.

3.3.2.8 Calculation of ASD drug loading: ASD sample (5 mg) was dissolved in THF (10 mL). Then concentration of Rif was measured by HPLC and quantified according to a standard curve.

3.3.2.9 Scanning electron microscopy (SEM): Particle size and morphology were analyzed on a LEO 1550 field emission scanning electron microscope (FESEM). Powder samples were spread on double-faced adhesive tape and coated with a very thin gold palladium layer (sputter coater Cressington 208HR) for 1 min. 5kV was used for excitation.

3.3.2.10 Solubility parameter calculation: Solubility parameters provide information about the relative polymer hydrophobicity. These were calculated by the Fedors method[32] (Equation 1), using a procedure similar to the one reported by Babcock et al[33]. The calculation includes the energy of vaporization (E), molar volume (V) and the degree of substitution (DS) for the diverse chemical entities.

$$\delta = \sqrt{\frac{\sum E\ (J*mol^{-1})}{\sum V\ (cm^3*m^{-1})}} \quad \text{Equation 1}$$

For compounds with T_g and T_m above room temperature a correction to account for differences in the molar volume (v_i) (Equation 2) was applied. In these equations n is the number of main chain skeletal atoms in the smallest repeating unit[32]. For cellulose polymers, n is equal to 7 (6 atoms in the ring and the oxygen bonded to the adjacent monomer). Details about the SP calculation can be found in the supplementary information of the paper by Dong *et al.* [34].

$$\Delta v_i = 2\times n,\ n \geq 3 \quad \text{Equation 2}$$

3.3.2.11 *In Vitro* release from drug dispersions: Dissolution studies were conducted in 250 mL jacketed flasks at 37 °C. Volumes were kept constant by adding a volume of fresh buffer solution equal to that of each withdrawn aliquot. Samples were protected from light during the experimentation and prior to analysis.

3.3.2.11.1 Rif release profile from ASDs at pH 6.8: Dissolution medium (100 mL 0.05 M potassium phosphate pH 6.8 buffer) was placed in each dissolution flask and magnetically stirred

at 300 rpm. ASD sample (6.7 mg) or Rif (1 mg) was then added to each flask. Every 0.5 h (during first 2 h) and then every 1.0 h for 8 hours, 1 mL samples were obtained from each dissolution flask. Each sample was centrifuged at 13,000 rpm for 10 min, then 0.5 mL of the supernatant was transferred to a HPLC vial and analyzed immediately.

3.3.2.11.2 pH switch dissolution experiment: HCl (100 mL, 1N, pH 1.2) was placed in a dissolution flask and magnetically stirred at 300 rpm. The ASD sample (6.7 mg) was dispersed into the solution and aliquots were withdrawn every 0.5 h for 4 h (2 h at pH 1.2 and 2 h at pH 6.8; adjustment to 6.8 was made by adding saturated Na_2CO_3 solution (approximately 1 mL)). After 4 h, sampling frequency decreased to 1/h. Samples were processed as described above.

3.3.2.11.3 Rif stabilization by CMCAB ASD during pH switch dissolution experiment: HCl (100 mL, 1N, pH 1.2) was placed in a dissolution flask and magnetically stirred at 300 rpm. The CMCAB ASD sample (6.7 mg contains 1 mg Rif) was dispersed into the solution, after 2 h pH was adjusted to 6.8 by adding saturated Na_2CO_3 solution (approximately 1 mL). After 6 h, a 1 mL sample was centrifuged at 13,000 rpm for 10 min and 0.5 mL of the supernatant was transferred to an HPLC vial and analyzed immediately. 100 mL THF was added to the dissolution flask and stirred at 37°C for 10 min. Then a 1 mL sample was transferred to a HPLC vial and analyzed immediately.

3.4. Results

3.4.1 Cellulosic polymers

We employed cellulose w-carboxyalkanoates, varying structure, solubility parameter, and DS(CO_2H) in order to determine the impact of these key parameters[24] on Rif ASD formation and ultimately release; we were hopeful of achieving miscible ASDs based on results with the related macrolide antibiotic clarithromycin[25]. We employed CMCAB as a positive control since it had previously been shown to be an effective ASD polymer[35,36], and since preliminary experiments[27] had shown that it could effectively form Rif ASDs. Physical mixtures of Rif and the individual polymers were used as negative controls. The synthetic scheme for cellulose ω-carboxyalkanoates[23,30,31] CAAdP, CABSeb, and CASub is shown in **Figure 3.3**. Polymer properties are summarized in **Tables 3.1** and **3.2**. Each of these polymers has a high glass transition temperature (T_g), helpful for keeping the formulation T_g above ambient temperature

even under hot and humid ambient conditions, and each has a substantial DS(CO_2H), expected to provide the impetus for Rif release at the neutral pH of the small intestine but to remain un-ionized and thus inhibit Rif release under low gastric pH conditions.

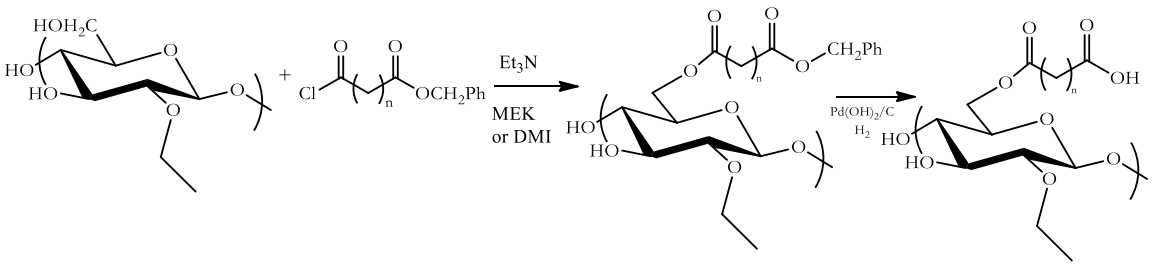

Figure 3.3: Syntheses of CAAdP (n = 4, R = H, acetyl, propionyl, adipoyl), CASub (n = 6, R = H, acetyl, suberoyl), and CABSeb (n = 8, R = H, acetyl, butyryl, sebacoyl).

Table 3.1: Solubility Parameters of cellulose derivatives and Rif.

Polymer	Solubility Parameter ($MPa^{1/2}$)	T_g (°C)
CMCAB	23.03	141[25]
CAAdP	22.79	116[22, 25]
CASub	23.72	101[22, 23]
CABSeb	22.29	88[22, 23]
Rif	20.76[37]	-

3.4.2 Preparation and solid state characterization of Rif ASDs

Solid dispersions of Rif with four cellulose derivatives (CMCAB, CAAdP, CASub and CABSeb) were prepared by spray-drying. Drug loading of 15% was targeted based on previous experience with clarithromycin[25] and other drugs[24,37] indicating that this should be a reasonable and achievable level. CABSeb is the most hydrophobic of the polymers examined, and as such we were concerned that drug release might be too slow from this very hydrophobic matrix. Therefore we also examined a 25% Rif loading level in CABSeb dispersions; Rif (solubility parameter 20.76 $MPa^{1/2}$ [38]) is more hydrophilic than CABSeb, so higher Rif levels are likely to lead to drug-controlled, more rapid release.

Table 3.2. Summary of ASD and physical mixture (PM) properties

Polymer Type	DS (CO_2H)	DS (Other)	Solubility Parameter ($MPa^{1/2}$)	Drug Load (Wt %)	Polymer T_g (°C)	ASD T_g (°C)	PM T_g (°C)
CAAdP	0.6	Pr 2.09 Ac 0.04	22.79	15%	116	118	116
CASub	0.66	Ac 1.82	23.72	15%	101	139	159
CMCAB	0.3	CM 0.33 Bu 1.64 Ac 0.44	23.03	15%	141	141	141
CABSeb	0.33	Bu 1.99 Ac 0.14	22.29	15%	88	89	90
CABSeb	0.33	Bu 1.99 Ac 0.14	22.29	25%	88	89	91

We have previously synthesized cellulose ω-carboxyalkanoate polymers with various DS values and types of ω-carboxy substituents. In these studies we employ CASub of DS(Sub) 0.66 and CAAdP of DS(Ad) 0.6 due to their promising performance in induction time and crystal growth

experiments with diverse poorly intrinsically soluble drug substances (e.g. celecoxib, efavirenz, and ritonavir)[22,24]. We employ CABSeb with lower DS(w-carboxyalkanoate) than the CAAdP or CASub against which it is compared; higher DS(Seb) is not readily accessible under our standard conditions because of the lower nucleophilicity of the CAB substrate and the steric bulk of the sebacoyl chloride reagent. Polymer properties are summarized in **Table 3.2** and, the drug load efficiencies are presented in **Table 3.3**.

Table 3.3: Drug loading of spray-dried Rif/polymer dispersions

	CAAdP	**CABSeb (15%)**	**CABSeb (25%)**	**CMCAB**	**CASub**
Drug load Target (%)	15.0	15.0	25.0	15.0	15.0
Drug load measured (%)	14.8	14.4	23.6	13.5	14.8
Drug load Efficiency (%)	98.8	96.3	94.5	90.0	98.9

3.4.2.1 DSC Results

Polymer/Rif spray-dried blends and physical mixtures were first characterized by DSC in order to determine whether crystalline Rif was present. Neither purchased Rif, nor Rif obtained by solvent casting and grinding showed a glass transition by DSC. It is known that isolation of amorphous Rif is challenging; for example Panchagnula *et al*. reported that Rif prepared by freeze drying from solution (in an attempt to prepare amorphous drug) does not display a distinct T_g by DSC[39]. DSC thermograms of CMCAB and CAAdP polymers, as well as their physical mixtures and spray-dried dispersions with Rif are shown in **Figure 3.4**. **Table 3.1** summarizes polymer T_g values; T_g values of polymer/Rif physical mixtures and spray-dried dispersions are presented in **Table 3.2**. Single glass transition temperatures were evident for the pure polymers, physical mixtures and spray-dried dispersions, and the values were all within 1-2°C of the polymer-only value. None of the spray-dried polymeric dispersions of Rif display either Rif crystallization or melting transitions. It is interesting to note that the physical mixtures, in which the Rif cannot possibly be amorphously dispersed, also display only one T_g. Clearly changes in glass transitions in DSC thermograms are not highly useful in determining the degree of interaction between these polymers and Rif, as they are for many other drug-polymer

dispersions [40].

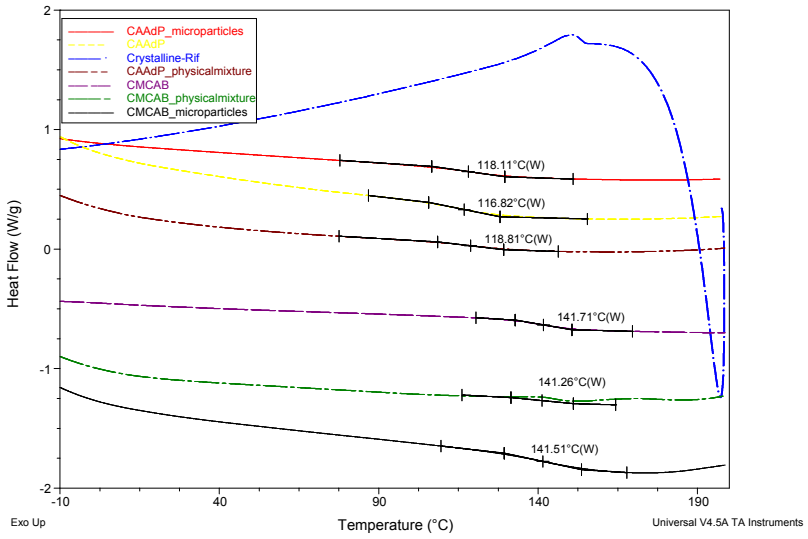

Figure 3.4: DSC thermograms of polymers, polymer/Rif amorphous dispersions and physical mixtures, and Rif.

3.4.2.2 XRD results

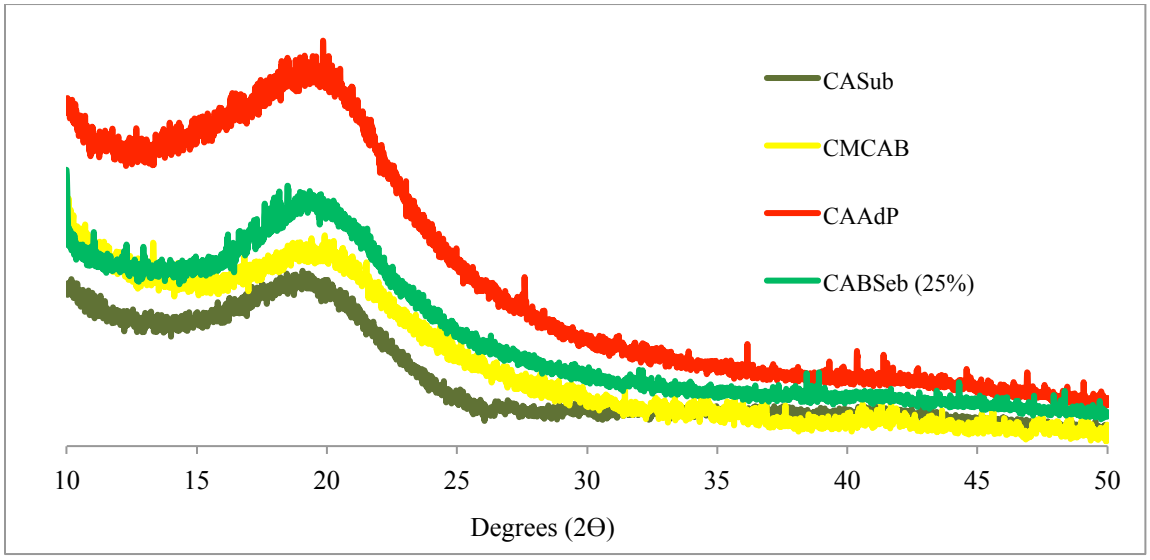

Figure 3.5: XRD spectra of spray dried dispersions in CASub, CABSeb, CAAdP and CMCAB.

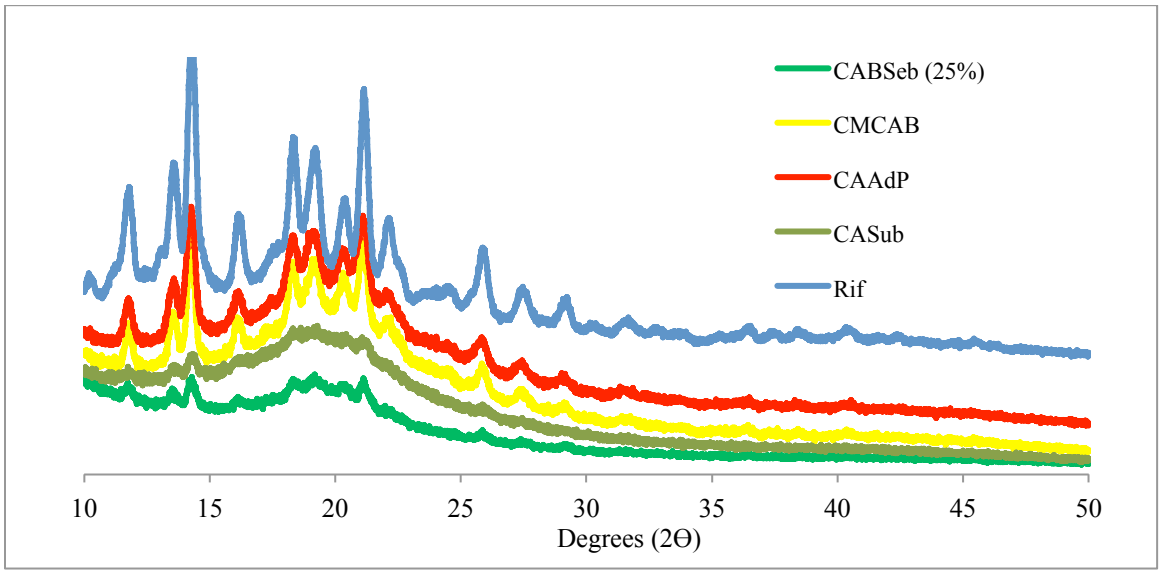

Figure 3.6: XRD spectra of Rif and its physical mixtures with CASub, CABSeb, CAAdP and CMCAB.

XRD spectra of the polymers, spray-dried Rif/polymer blends, physical polymer/Rif mixtures, and crystalline Rif are presented in **Figures 3.5** and **3.6**. Purchased, crystalline Rif shows its characteristic, sharp peaks, including particularly sharp reflections at 2Θ values of 14° and 21°. The XRD diffractograms of all spray-dried dispersions (**Figure 3.5**) show amorphous halos in that range and lack the sharp peaks of crystalline Rif (**Figure 3.6**). The small sharp peaks in CAAdP and CABSeb dispersions do not match up with Rif reflections and are believed to be the result of random noise. In contrast, all physical polymer/Rif mixtures (**Figure 3.6**) display the peaks of crystalline Rif; clearly it is not amorphous in these physical mixtures.

3.4.2.3 FTIR analysis

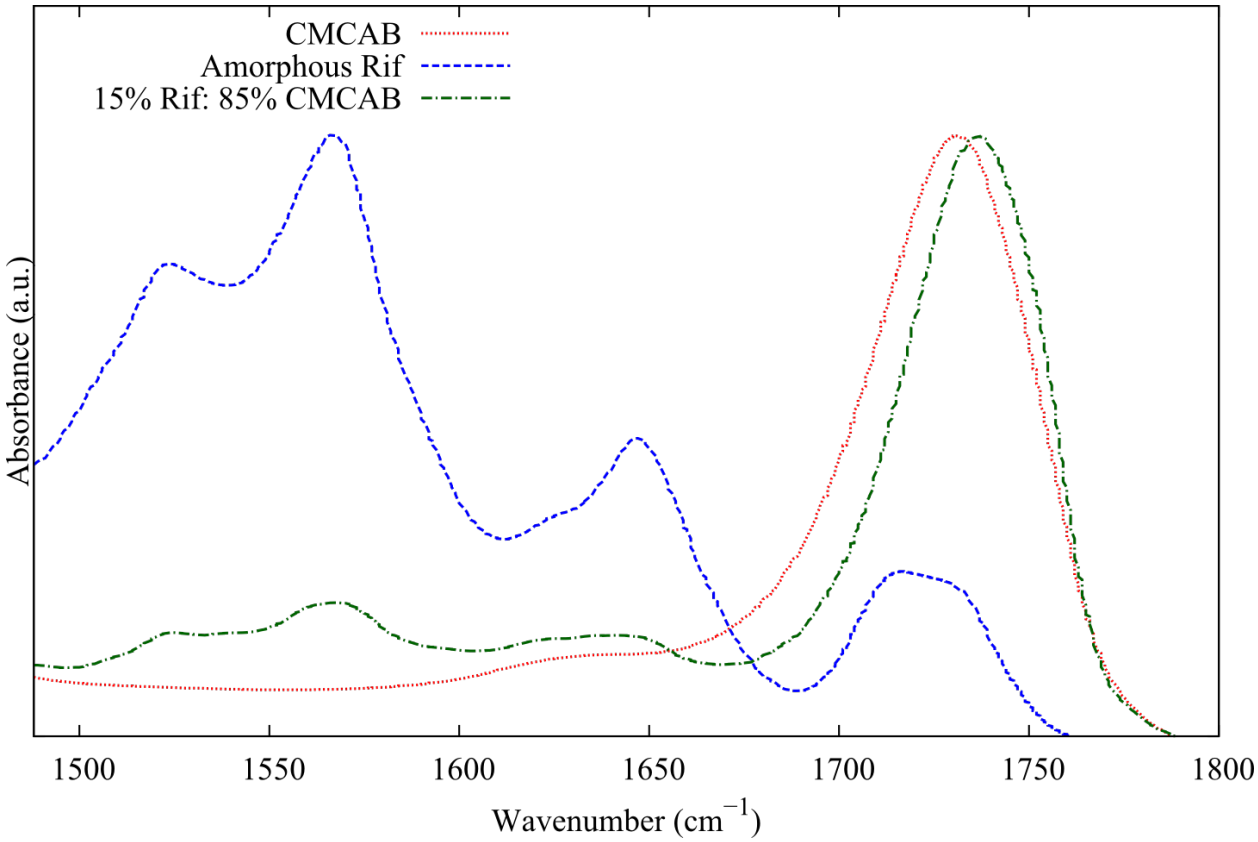

Figure 3.7 (A): FTIR spectra of pure Rif, pure CMCAB, and 15% spray-dried dispersion of Rif in CMCAB, wavenumber 1500-1800 cm^{-1}.

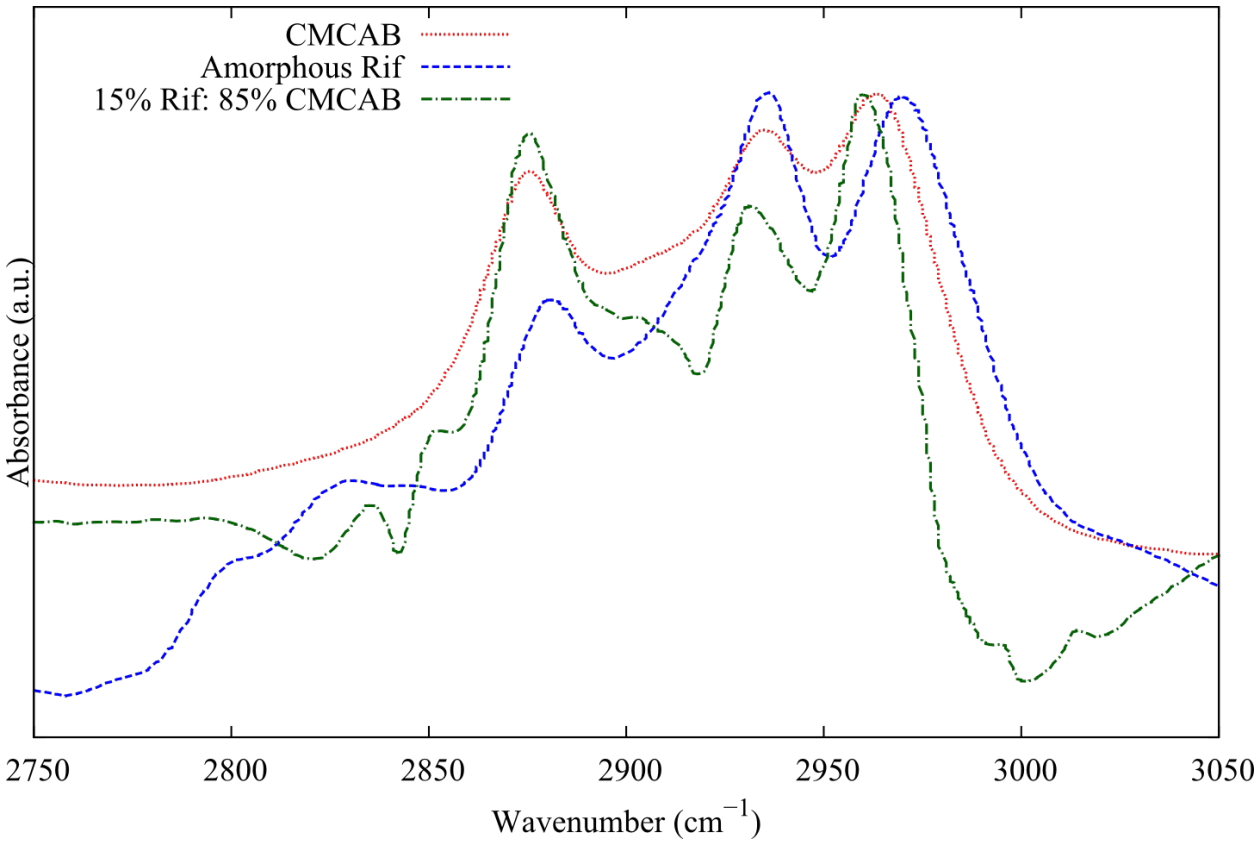

Figure 3.7 (B): FTIR spectra of pure Rif, pure CMCAB, and 15% spray-dried dispersion of Rif in CMCAB, wavenumber 2750-3050 cm^{-1}.

Because DSC was not useful for proving that Rif was amorphous in the spray-dried dispersions, we wished to supplement the clear XRD evidence with additional data from FTIR[41]. We selected the CMCAB dispersion for study, since commercial CMCAB was available in quantity. **Figure 3.7** shows the FTIR spectra of amorphous Rif, CMCAB, and a 15% Rif dispersion in CMCAB, in the CH and carbonyl stretching regions. Subtle changes in the spectrum are indicative of a miscible system and of intermolecular interactions between the two components. For example, the carbonyl peak of pure CMCAB is shifted to a slightly higher wavenumber in the presence of a small amount of Rif, which suggests that its hydrogen bond environment has changed. Likewise, there are some changes in the pattern of the Rif carbonyl stretching vibrations, which are also suggestive of drug-polymer interactions. These cannot be accounted for simply by the presence of the polymer, which has minimal absorption below 1675 cm^{-1}. Similarly, there are some changes in the CH stretching region that cannot be recreated by simply summing the

contributions from the pure amorphous drug and polymer, suggesting that the environment of each component is changed, as would occur in a miscible system.

3.4.2.4 SEM Analysis

Morphology of spray-dried blends and physical mixtures was examined by SEM. **Figure 3.8** presents images of spray-dried Rif/polymer blends at 5K magnification to illustrate particle sizes and morphology. Spray-dried particle sizes range from 2-15 µm for CAAdP, CASub and CABSeb. CMCAB has a slightly larger particle size range of 2-25 µm. They all have corrugated morphology; the particles look crushed and collapsed, typical of spray-dried ASDs. Polysaccharide-based spray dried particles usually display apparent surface indentation [25,42]. Rod-like crystalline Rif [43] was not observed in any of the spray-dried dispersion images (**Figure 3.8**), while it is observed in the physical mixtures (Sup Data), further supporting the hypothesis that Rif is amorphous in these dispersions.

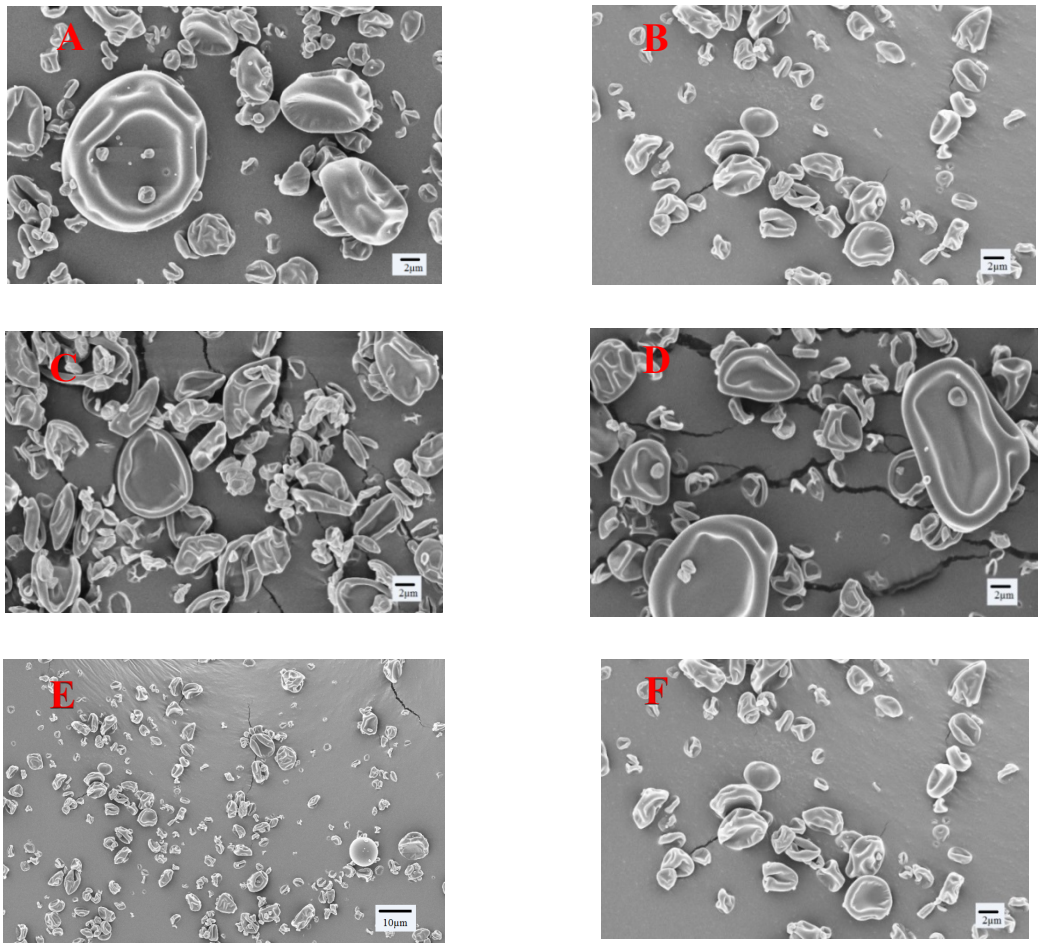

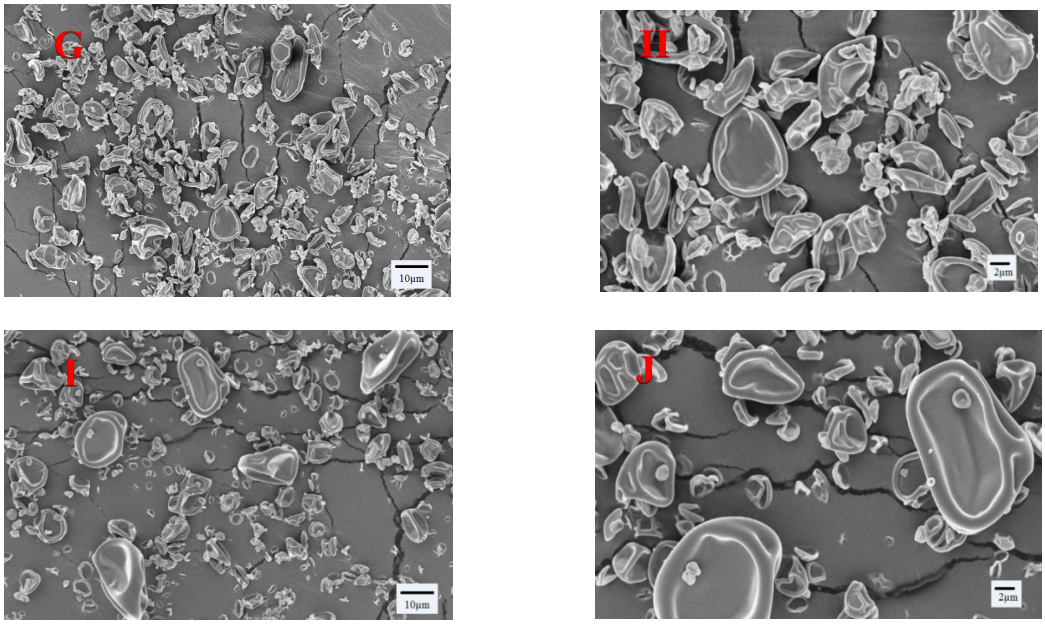

Figure 3.8: SEM images of Rif/polymer spray-dried dispersions at 5Kx magnification: CABSeb (A), CAAdP (B), CASub (C), CMCAB (D); and ASDs at 2Kx (E, G and I) and 5Kx magnification (F, H and J): CAAdP (E, F), CASub (G, H) and CMCAB (I, J)

The preponderance of the XRD, DSC, FTIR, and SEM evidence supports the hypothesis that Rif is amorphous in all of the spray-dried polymer dispersions prepared.

3.4.3 Dissolution Studies

3.4.3.1 Rif dissolution from ASDs at pH 6.8

Initially we chose to test the rate and extent of Rif dissolution at intestinal pH and under sink conditions. Rif dissolution was measured in phosphate buffer at pH 6.8 and 37 °C over 8 h; profiles are presented in **Figure 3.9**.

In most cases Rif release rates from cellulose derivative ASDs at pH 6.8 were similar to the dissolution rate of crystalline Rif. The stability of dissolved Rif against degradation was greater in every ASD than it was for pure Rif. CAAdP gave the best performance, reaching 91% release after 5h and showing essentially complete stability against Rif degradation. CASub is relatively hydrophilic among the set of polymers studied and as a result released Rif rapidly, approaching

100% release within 30 min. However, its stabilization of Rif against degradation appeared to be inferior to that of CAAdP; dissolved Rif decreased to 60% of available drug by the 8h mark. HPLC chromatograms are presented where we can see the growing degradation peak as time passes (Sup Data).

The CMCAB ASD also gave promising results, releasing 80% of the Rif and providing strong stabilization against degradation. It is interesting to note that release from the ASD in hydrophobic (solubility parameter 19.62) CABSeb, even at 25% Rif, is almost nil. Apparently swelling due to carboxyl ionization is insufficient to cause substantial Rif release for this polymer, which has relatively low DS of ω-carboxyalkanoyl substituent in addition to its low solubility parameter.

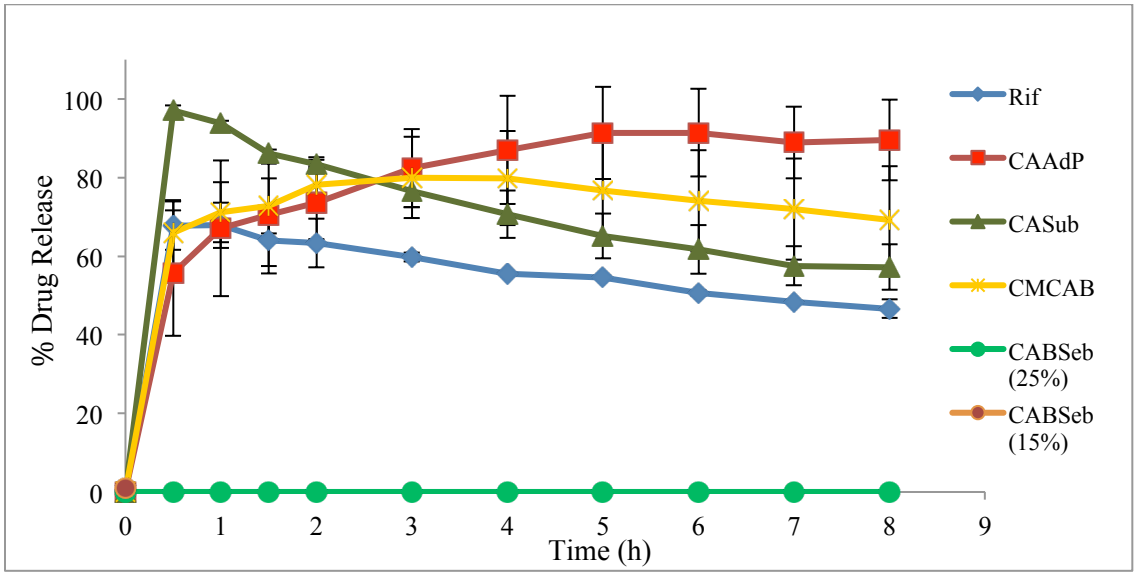

Figure 3.9: Dissolution profiles of Rif and Rif/polymer ASDs (pH 6.8, 37°C). Error bars indicate one standard deviation (n = 3).

3.4.3.2 pH switch experiment

A key element of our hypothesis is that we can enhance Rif bioavailability by protecting it against dissolution (and hence degradation) in the stomach, based on the known Rif instability under acidic conditions (*vide supra*), and create concentrated solutions in the small intestine such that the entire dose is absorbed intact. Therefore, it was important for us to carry out dissolution experiments under more realistic conditions, in which the dosage form first experienced acidic

gastric pH, then the neutral pH of the intestines. Such an experiment had already proven its illuminatory power in our studies of the related, acid-unstable macrolide clarithromycin[25].
In this study, ASDs were first exposed to pH 1.2 HCl solution for 2h to mimic gastric conditions. Then medium pH was increased to 6.8 (Na_2CO_3) in order to mimic the intestinal environment, and measurements continued for a further 6 h. **Figure 3.10** shows the data obtained, indicating intact drug remaining in solution vs. time.

As with clarithromycin, this type of experiment was very revealing with regard to behavior of Rif ASDs. Since crystalline Rif has good solubility in acid due to its basic piperazine moiety, it dissolved immediately at pH 1.2, reaching a maximum of ca. 65% release within 30 min. However, the concentration of dissolved Rif then rapidly decreased at gastric pH. From the HPLC analysis, we could clearly see that the cause of this observed decrease was acid-catalyzed chemical decomposition (Sup Data). None of the cellulose derivative ASDs released any observable amount of Rif at gastric pH, supporting our hypothesis with regard to Rif protection against release, and thus acid-catalyzed hydrolysis at gastric pH.

After the switch to intestinal pH (6.8), the results were equally illuminating. The amount of initially crystalline Rif remaining in solution at the pH switch (ca. 40%) remained in solution; no further degradation occurred, but no further dissolution either. In contrast, carboxyl ionization and associated swelling caused rapid release of amorphous Rif from all cellulose-based ASDs, in each case reaching a stable concentration higher than that observed from pure Rif. CASub and CAAdP were particularly effective at generating high Rif concentrations, achieving greater than 90% release. Note that this experiment was carried out under sink conditions so that these results reflect effective release and protection against chemical degradation, rather than levels of supersaturation.
Polymer solubility parameters (**Table 3.1**) provide insight about relative hydrophobicity[22], enabling consideration of the influence of this polymer property on Rif dissolution profiles, although it must be noted that these calculations do not take into consideration carboxyl group ionization. CABSeb is the most hydrophobic and CMCAB is the least hydrophobic among the polymers in this study. Polymer hydrophobicity decreases in the following order: CABSeb > CAAdP > CASub > CMCAB. Properties (DS(CO_2H) and other DS values) of these polymers are listed in **Table 3.2**. CABSeb has the lowest aqueous solubility, as expected due to its

hydrophobicity. The Rif release results (**Figure 3.10**) clearly depend at least in part upon polymer matrix hydrophobicity. Release from the very hydrophobic CABSeb matrix is virtually nil at 15% Rif in the ASD, and is delayed significantly in the more hydrophilic 25% Rif ASD (beginning to release at approximately 2h after the shift to pH 6.8). The ASD in the relatively hydrophilic CMCAB (solubility parameter 23.03) does release Rif faster than does the CABSeb ASD, reaching ca. 60% Rif release after 6h in the pH change study, and not releasing Rif (could not be detected) at pH 6.8. It is also clear that DS(CO_2H) has an influence upon release and stabilization, as would be expected; the polymers highest in DS(CO_2H) are CASub and CAAdP, and these polymers provide the highest Rif release (both > 90% after 6h) as well as strong stabilization once released. Overall, given adequate DS(CO_2H) and hydrophobicity that is not overly high, CASub and CAAdP provided excellent performance with regard to enhanced release and stabilization of intact Rif in these pH-switch experiments, much better than that observed from crystalline Rif itself. They released nearly 95% of available intact Rif, with maximum levels stable all the way to the end of the experiment, implying very little degradation. Clearly the release behavior from CABSeb, though suboptimal for oral delivery of Rif, is also of interest; such delayed release, if observed with other drugs, could be useful for delivery to the distal small intestine or to the colon. There is a notable difference in Rif release behavior from a CABSeb matrix in the pH 6.8 release study (no observed release, **Figure 3.9**) vs. the pH switch study (**Figure 3.10**) where delayed but substantial Rif release is observed at pH 6.8. Clearly this is related to the initial low pH exposure in the pH switch experiment, but we have not yet carried out detailed mechanistic investigations.

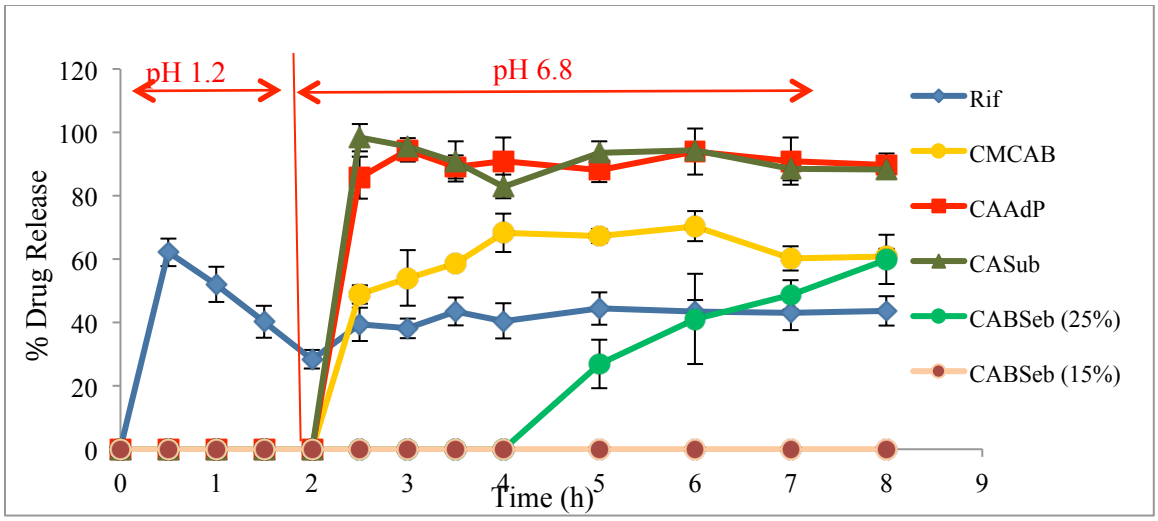

Figure 3.10: Rif dissolution from pH switch experiment under sink conditions; pH 1.2 for 2 h, then pH 6.8 for 6h. Error bars indicate one standard deviation (n = 3).

In addition to the pH change study, we separately investigated the intact Rif content of CMCAB ASD remaining at the end of the pH switch study (2h in acidic pH followed by 6 h small intestine pH); analysis of the soluble Rif at this point showed that 96% of the drug was still intact and in solution. The very low extent of Rif degradation in these cellulose ester ASDs is of particular interest (and obvious potential value), since it implies not only almost complete prevention of Rif release in gastric pH, but also that HCl infiltration into the ASD does not cause significant degradation in the amorphous solid phase over the duration of these experiments.

3.5 Conclusions

The results of these experiments confirmed our hypothesis that these cellulose w-carboxyalkanoate ASDs (and CMCAB) effectively prevent Rif release at gastric pH, and enhance release at small intestine pH, thereby protecting Rif against chemical degradation, thus creating the potential for bioavailability enhancement *in vivo*. The combination of adequate hydrophilicity and aqueous solubility of CASub and CAAdP, and their adequate DS(CO_2H) (ca. 0.6), provide high concentrations of Rif upon the change from gastric to small intestinal pH. These polymers protect Rif against gastric release to a remarkable extent, especially considering the relatively good Rif solubility in acidic media. They then provide relatively stable Rif

concentrations after release, throughout the duration of these experiments; the duration was selected to be slightly longer than the average time the dosage form would be expected to spend in the stomach and small intestine combined. Therefore, interactions between the drug and the polymer are critical for both Rif chemical stabilization and controlled release, and the release behaviors observed are somewhat predictable based on readily calculated, measured, and controlled properties like solubility parameters and DS(CO_2H).

Confirmation of this hypothesis is highly encouraging with regard to enhanced oral delivery of Rif. The ability to protect Rif against degradation regardless of the actual pH in an individual's stomach, and potentially to generate solution concentrations high and robust enough to guarantee near complete bioavailability, could permit dose reduction, cost reduction, reduced patient-to-patient and dose-to-dose variability, reduced fed/fasted differences, and overall may provide much more effective treatment of tuberculosis throughout the lengthy 6-month treatment regime. Reduced side effects are also possible but this would have to be explored (as would all of these potential benefits) in clinical trials. The delayed Rif release observed from ASDs containing the very hydrophobic CABSeb at high drug concentrations also creates the potential for exciting scenarios, if also successful upon application to other drugs whose release in the lower intestinal tract would be therapeutically beneficial.

The potential for these cellulose ω-carboxyalkanoate ASDs to enhance Rif bioavailability, as well as other potential advantages revealed by the results described herein, are under active investigation in our laboratories.

3.6 Acknowledgments

We thank the Eastman Chemical Company for their kind donation of the cellulose ester starting materials. We thank the Macromolecules Innovation Institute and the Institute for Critical Technologies and Applied Science at Virginia Tech for their support, facilities and funding. We also thank Steve McCartney (Nanoscale Characterization and Fabrication Laboratory, Virginia Tech) for his help in taking SEM images, and Rick Caudill (Sustainable Biomaterials, Virginia Tech) for XRD study.

3.7 References

(1) Gelperina, S.; Kisich, K.; Iseman, M. D.; Heifets, L. The Potential Advantages of Nanoparticle Drug Delivery Systems in Chemotherapy of Tuberculosis. *Am. J. Respir. Crit. Care Med.* **2005**, *172*, 1487–1490.

(2) Smith, I. Mycobacterium Tuberculosis Pathogenesis and Molecular Determinants of Virulence. *Clin. Microbiol. Rev.* **2003**, *16*, 463–496.

(3) Global Tuberculosis Report 2013 http://www.who.int/tb/publications/global_report/en/.

(4) Panchagnula, R.; Agrawal, S. Biopharmaceutic and Pharmacokinetic Aspects of Variable Bioavailability of Rifampicin. *Int. J. Pharm.* **2004**, *271*, 1–4.

(5) Farmer, P.; Kim, J. Y. Community Based Approaches to the Control of Multidrug Resistant Tuberculosis: Introducing "DOTS-Plus". *BMJ* **1998**, *317*, 671–674.

(6) Zumla, A.; Nahid, P.; Cole, S. T. Advances in the Development of New Tuberculosis Drugs and Treatment Regimens. *Nat. Rev. Drug Discov.* **2013**, *12*, 388–404.

(7) Mukherjee, J. S.; Rich, M. L.; Socci, A. R.; Joseph, J. K.; Viru, F. A.; Shin, S. S.; Furin, J. J.; Becerra, M. C.; Barry, D. J.; Kim, J. Y.; Bayona, J.; Farmer, P.; Smith Fawzi, M. C.; Seung, K. J. Programmes and Principles in Treatment of Multidrug-Resistant Tuberculosis. *Lancet* **2004**, *363*, 474–481.

(8) Weis, S. E.; Slocum, P. C.; Blais, F.; King, B.; Nunn, M.; Mathney, B.; Gomez, E.; Foresman, B. The Effect of Directly Observed Therapy on the Rates of Drug Resistance and Relapse in Tuberculosis. *N. Engl. J. Med.* **1994**, *330*, 1179–1184.

(9) Ellard, G. A.; Fourie, P. B. Rifampicin Bioavailability: A Review of Its Pharmacology and the Chemotherapeutic Necessity for Ensuring Optimal Absorption. *Int. J. Tuberc. Lung. Dis.* **1999**, *3*, 301–321.

(10) Lester, W. Rifampin: A Semisynthetic Derivative of Rifamycin--a Prototype for the Future. *Annu. Rev. Microbiol.* **1972**, *26*, 85–102.

(11) Konno, K.; Oizumi, K.; Oka, S. Mode of Action of Rifampin on Mycobacteria. II. Biosynthetic Studies on the Inhibition of Ribonucleic Acid Polymerase of Mycobacterium Bovis BCG by Rifampin and Uptake of Rifampin- 14 C by Mycobacterium Phlei. *Am.*

Rev. Respir. Dis. **1973**, *107*, 1006–1012.

(12) Biganzoli, E.; Cavenaghi, L. A.; Rossi, R.; Brunati, M. C.; Nolli, M. L. Use of a Caco-2 Cell Culture Model for the Characterization of Intestinal Absorption of Antibiotics. *Farm.* **1999**, *54*, 594–599.

(13) Agrawal, S.; Panchagnula, R. Dissolution Test as a Surrogate for Quality Evaluation of Rifampicin Containing Fixed Dose Combination Formulations. *Int. J. Pharm.* **2004**, *287*, 97–112.

(14) Becker, C.; Dressman, J. B.; Junginger, H. E.; Kopp, S.; Midha, K. K.; Shah, V. P.; Stavchansky, S.; Barends, D. M. Biowaiver Monographs for Immediate Release Solid Oral Dosage Forms: Rifampicin. *J. Pharm. Sci.* **2009**, *98*, 2252–2267.

(15) Prankerd R.J.; Waiters J.M.; Parnes J.H. Kinetics for Degradation of Rifampicin, an Azomethine-Containing Drug Which Exhibits Reversible Hydrolysis in Acidic Solutions. *Int. J. Pharm.* **1992**, *78*, 59–67.

(16) Henwood, S. Q.; de Villiers, M. M.; Liebenberg, W.; Lotter, A. P. Solubility and Dissolution Properties of Generic Rifampicin Raw Materials. *Drug Dev. Ind. Pharm.* **2000**, *26*, 403–408.

(17) Pelizza, G.; Nebuloni, M.; Ferrari, P.; Gallo, G. G. Polymorphism of Rifampicin. *Farmaco. Sci.* **1977**, *32*, 471–481.

(18) Biopharmaceutics Classification System (BCS) -based biowaiver applications : anti-tuberculosis medicines http://apps.who.int/prequal/info_applicants/BE/BW_TB_2009February.pdf (accessed Oct 11, 2015).

(19) N. Saffoon; R. Uddin; N. H. Huda; Sutradhar, K. B. Enhancement of Oral Bioavailability and Solid Dispersion: A Review. *J. Appl. Pharm. Sci.* **2011**, *1*, 13–20.

(20) Chiou, W. L.; Riegelman, S. Pharmaceutical Applications of Solid Dispersion Systems. *J. Pharm. Sci.* **1971**, *60*, 1281–1302.

(21) Ilevbare, G. A.; Liu, H.; Edgar, K. J. Understanding Polymer Properties Important for Crystal Growth Inhibition – Impact of Chemically Diverse Polymers on Solution Crystal Growth of Ritonavir. *Cryst. Growth Des.* **2012**, *12*, 3133–3143.

(22) Ilevbare, G. A. .; Liu, H. .; Edgar, K. J. .; Taylor, L. S. Maintaining Supersaturation in Aqueous Drug Solutions: Impact of Different Polymers on Induction Times. *Cryst. Growth Des.* **2013**, *13*, 740–751.

(23) Liu, H.; Ilevbare, G. A.; Cherniawski, B. P.; Ritchie, E. T.; Taylor, L. S.; Edgar, K. J. Synthesis and Structure-Property Evaluation of Cellulose Omega-Carboxyesters for Amorphous Solid Dispersions. *Carbohydr. Polym.* **2014**, *100*, 116–125.

(24) Ilevbare, G. A.; Liu, H.; Edgar, K. J.; Taylor, L. S. Impact of Polymers on Crystal Growth Rate of Structurally Diverse Compounds from Aqueous Solution. *Mol. Pharm.* **2013**, *10*, 2381–2393.

(25) Pereira, J. M.; Mejia-Ariza, R.; Ilevbare, G. A.; McGettigan, H. E.; Sriranganathan, N.; Taylor, L. S.; Davis, R. M.; Edgar, K. J. Interplay of Degradation, Dissolution and Stabilization of Clarithromycin and Its Amorphous Solid Dispersions. *Mol. Pharm.* **2013**, *10*, 4640–4653.

(26) Ilevbare, G. A.; Liu, H.; Edgar, K. J.; Taylor, L. S. Inhibition of Solution Crystal Growth of Ritonavir by Cellulose Polymers – Factors Influencing Polymer Effectiveness. *CrystEngComm* **2012**, *14*, 6503–6514.

(27) Casterlow, S. A. Characterization and Pharmacokinetics of Rifampicin Laden Carboxymethylcellulose Acetate Butyrate Particles, Virginia Tech, 2012.

(28) Leuner, C.; Dressman, J. Improving Drug Solubility for Oral Delivery Using Solid Dispersions. *Eur. J. Pharm. Biopharm.* **2000**, *50*, 47–60.

(29) Alonzo, D. E.; Zhang, G. G. Z.; Zhou, D. L.; Gao, Y.; Taylor, L. S. Understanding the Behavior of Amorphous Pharmaceutical Systems during Dissolution. *Pharm. Res.* **2010**, *27*, 608–618.

(30) Kar, N.; Liu, H.; Edgar, K. J. Synthesis of Cellulose Adipate Derivatives. *Biomacromolecules* **2011**, *12*, 1106–1115.

(31) Liu, H. Y.; Kar, N.; Edgar, K. J. Direct Synthesis of Cellulose Adipate Derivatives Using Adipic Anhydride. *Cellulose* **2012**, *19*, 1279–1293.

(32) Fedors, R. F. A Method for Estimating Both the Solubility Parameters and Molar Volumes of Liquids. *Polym. Eng. Sci.* **1974**, *14*, 147–154.

(33) Babcock, W. C.; Friesen, D. T.; Lyon, D. K.; Miller, W. K.; Smithey, D. T. Pharmaceutical Compositions with Enhanced Performance. WO 2005115330 A2, December 8, 2005.

(34) Dong, Y.; Mosquera-Giraldo, L. I.; Taylor, L. S.; Edgar, K. J. Amphiphilic Cellulose Ethers Designed for Amorphous Solid Dispersion via Olefin Cross-Metathesis. *Biomacromolecules* **2015**, acs.biomac.5b01336.

(35) Posey-Dowty, J. D.; Watterson, T. L.; Wilson, A. K.; Edgar, K. J.; Shelton, M. C.; Jr., L. R. L. Zero-Order Release Formulations Using a Novel Cellulose Ester. *Cellulose* **2007**, *14*, 73–83.

(36) Shelton, M. C. .; Posey-Dowty, J. D. .; Lingerfelt, L. R. .; Kirk, S. K. .; Klein, S. .; Edgar, K. J. *Enhanced Dissolution of Poorly Soluble Drugs from Solid Dispersions in Carboxymethylcellulose Acetate Butyrate Matrices*; American Chemical Society, 2009; Vol. 1017.

(37) Li, B.; Wegiel L.A.; Taylor L.S.; Edgar, K. J. Stability and Solution Concentration Enhancement of Resveratrol by Solid Dispersion in Cellulose Derivative Matrices. *Cellulose* **2013**, *20*, 1249–1260.

(38) Schierholz, J. M. Physico-Chemical Properties of a Rifampicin-Releasing Polydimethylsiloxane Shunt. *Biomaterials* **1997**, *18*, 635–641.

(39) Agrawal, S.; Ashokraj, Y.; Bharatam, P. V; Pillai, O.; Panchagnula, R. Solid-State Characterization of Rifampicin Samples and Its Biopharmaceutic Relevance. *Eur. J. Pharm. Sci.* **2004**, *22*, 127–144.

(40) Li, B.; Harich, K.; Wegiel, L.; Taylor, L. S.; Edgar, K. J. Stability and Solubility Enhancement of Ellagic Acid in Cellulose Ester Solid Dispersions. *Carbohydr. Polym.* **2013**, *92*, 1443–1450.

(41) Konno, H.; Taylor, L. S., Influence of different polymers on the crystallization tendency of molecularly dispersed amorphous felodipine. *J. Pharm. Sci.* **2006,** *95*, 2692-2705.

(42) Yin, L.; Hillmyer, M. A. Preparation and Performance of Hydroxypropyl Methylcellulose Esters of Substituted Succinates for in Vitro Supersaturation of a Crystalline Hydrophobic Drug. *Mol. Pharm.* **2014**, *11*, 175–185.

(43) Kockro, R. A.; Hampl, J. A.; Jansen, B.; Peters, G.; Scheihing, M.; Giacomelli, R.; Kunze, S.; Aschoff, A. Use of Scanning Electron Microscopy to Investigate the Prophylactic Efficacy of Rifampin-Impregnated CSF Shunt Catheters. *J. Med. Microbiol.* **2000**, *49*, 441–450.

Chapter 4. Rifampin Stability and Solution Concentration Enhancement Study with Cellulose Esters *in vivo*

4.1 Abstract

Tuberculosis (TB) is a disease caused mainly by *Mycobacterium tuberculosis* (MTB); approximately 2 billion people are currently latently infected in the world. Rifampicin (Rif) is a first line drug used throughout the treatment period of six to eight months although it exhibits low and variable bioavailability. This research study of Rif amorphous solid dispersions (ASDs) with cellulose ω-carboxyalkanoates (cellulose acetate suberate (CASub), cellulose acetate propionate Adipate (CAAdP), and cellulose acetate butyrate sebacate (CABSeb)) were compared with our previous study of crystalline Rif and carboxymethyl cellulose acetate butyrate (CMCAB) ASD to prevent acid degradation and to provide pH triggered release. In this study, the investigation continued with CMCAB and CAAdP ASDs to compare with the crystalline Rif in *in vivo* study with mice for 96 h after a single oral dose. The CMCAB ASD showed higher bioavailability than the pure drug application while CAAdP ASD did not show any improvement. The variation in the *in vitro* and *in vivo* results can be related to the physiological differences and poor gastrointestinal animal model for humans.

4.2 Introduction

Tuberculosis is an infectious disease caused by the *Mycobacterium tuberculosis* and requires long-term treatment (ca. 6 months) with a daily administration of multiple drugs, leading to complex treatment regimen and relatively poor patient compliance due to complex dosage schedules and toxicity of the drugs. The high incidence of side effects such as loss of appetite, nausea or vomiting, skin rash, drug fever or hepatitis[1] and the need for multiple drugs to be taken, the patients default the chemotherapy. The discontinuation of medication leads to increased incidence of multi-drug resistant strains. Although the issues with the compliance issues has been addressed routinely by "Directly Observed therapy" (DOT) in spite of its expense, it is known that 90 % of the patients default the chemotherapy that can lead to relapses and development of multidrug resistant strains of TB. In 2013, 9.6 million people developed TB, 1.5 million died and 480,000

people developed multi drug resistant TB[2]. These are alarming statistics besides, infection is readily transmitted. According to the world health organization, approximately 2 billion people are already infected but do not show the symptoms immediately[3,4]. In case of an immune suppression due to stress or HIV, such patients can develop the disease, the main reason for the concerns in the western countries. In fact 1 out of every 3 deaths due to HIV is caused by TB[3] complication and at least 11 million of the 33 million HIV infected people are already infected with *M. tuberculosis*[4].

Rif is a first line drug for TB treatment (**Figure 4.1**), which has been in the market for more than 50 years, frequently given in combination with ethambutol, pyrazinamide, and isoniazid for the first two months, and then in combination with isoniazid for the last four months of chemotherapy. Rif is zwitterionic since it possesses both a basic amine on the piperazine ring (pKa 7.9) and an acidic *p*-hydroxynaphthyl ketone (pKa 1.7) moiety. Rif with 1.51 - 1.74 mg/mL solubility at neutral pH, permeates well through the enterocyte[5]. Therefore it is a BCS Class II drug (low solubility high permeability) with variable bioavailability (50-70%[6]) although it is quite soluble in the acidic pH (125 mg/ml at pH 1.2)[7]. The decreased bioavailability of Rif has been explained by changes in the crystalline structure of Rif, excipients, degradation in the acidic pH, absorption and metabolism[8]. Therefore we prepared new polymeric carriers (excipients) that prevent degradation, break crytsallinity, stabilize the metastable drug and release at the neutral pH to overcome the low bioavailability problem[9].

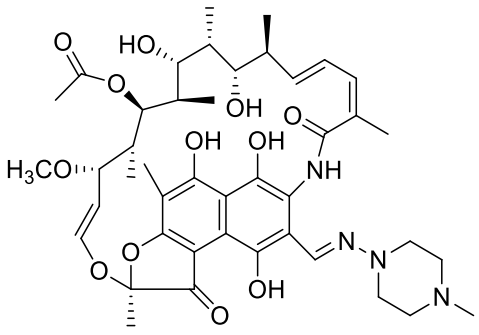

Figure 4.1: Rif Chemical Structure.

ASD is a very efficient method to increase solubility of the crystalline drugs since they generate supersaturated solutions that dissolve drugs faster and increases oral bioavailability[10–12]. It is essential to create a molecular dispersion of the drug in polymeric matrix that has high T_g to limit drug mobility thereby retard crystallization to solid state, and should have enough aqueous solubility to prevent recrystallization after the release. In addition, there must be good polymer-drug interaction to prevent crystallization of the metastable drug. Cellulose esters are suitable polymers due to their low toxicity, decomposition products, stability, miscibility with a wide range of active pharmaceutical ingredients, and ability to form ASDs. In addition to these properties, it is also important to have pH triggered release to protect the drug from the acidic environment of the stomach and prevent related side effects but releasing the drug in the small intestine as a result of the ionization of carboxylic acid groups. The Edgar lab published a range of cellulose ω-carboxyalkanoates for ASD purposes such as CAAdP that has potential for miscibility with hydrophobic drugs due to its hydrocarbon chain of the adipate group and the alkyl groups[13–15], and the Taylor and Edgar laboratories investigated the performance of cellulose w-carboxyalkanoates specifically designed as ASD matrix polymers and it has already been shown that the polymers are very efficient in inhibiting crystal growth and nucleation, and to generate ASD formulations to increase solubility of a variety of hydrophobic drugs including but not limited to chlaritromycin[10], quercetin[16], ritonavir[17,18], curcumin[19,20], resveratrol[21,22] and efavirenz[23]. In addition, a carboxy containing commercial cellulose ester has been previously demonstrated to be an effective ASD polymer both *in vitro* and *in vivo*, and that showed promising results in our preliminary experiments towards Rif ASD CMCAB[24]. After that, Rif solubility enhancement and acid degradation prevention was also demonstrated by a range of cellulose w-carboxyalkanoates (CAAdP, cellulose acetate suberare, cellulose acetate butyrate sebacate, CABSeb) and CMCAB *in vitro*[9] that shows immediate drug release (95%) from CAAdP ASD. In addition, it has been shown in literature before that CMCAB is a very powerful commercial polymer for ASD formulations and controlled release of both low soluble drugs such as ellagic acid[25] and curcumin[20] and, relatively more soluble drugs such as fexofenadine HCl, ibuprofen and acetylsalicylic acid[26]. Therefore in this study, we continued the research effort with CAAdP and CMCAB

ASDs compared with crystalline Rif. Structures of these polymers are presented in **Figure 4.2**.

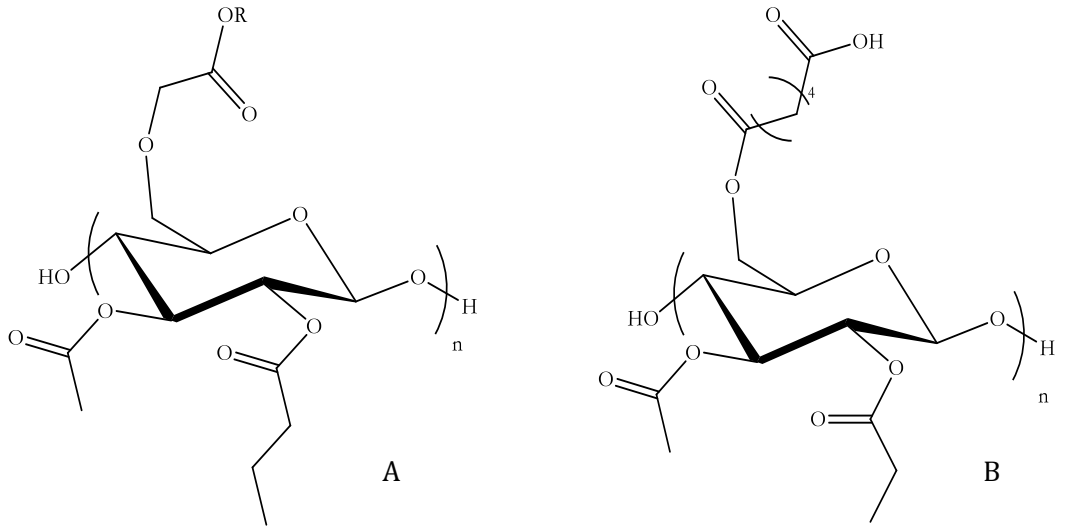

Figure 4.2: Chemical structures of CMCAB (A), and CAAdP (B). These structures are not meant to convey regioselective substitution; depictions of substituent location are merely for convenience and clarity of depiction. R= -H or -CH_2COOR

Our hypothesis is that the ASDs have the potential to prevent bioavailability variation and to reduce the Rif dosing, dosing intervals, treatment time of MTB and minimize Rif associated adverse affects, thus increasing patient compliance while maintaining inhibitory concentrations necessary to kill the bacterium. Therefore the Rif encapsulated CMCAB and CAAdP spray dried particles compared to that of free drug were tested when given a single oral dose to a mouse model. We report here the Rif ASDs performance compared with Rif *in vivo* for 96 h.

4.3. Experimental

4.3.1 Materials

Rif was purchased from Sigma-Aldrich (St Louis, MO). CMCAB 641-0.2 (approximate MW 22,000, degree of substitution (DS) (butyrate) = 1.64, DS (acetate) = 0.44, and DS (carboxymethyl) = 0.33), and cellulose acetate propionate (CAP-504-0.2, DS (acetate) =

0.04, DS (propionate) = 2.09) M_n = 15,000 as previously reported[10] were obtained from Eastman Chemical Company (Kingsport, Tennessee). Acetonitrile (HPLC-grade), tetrahydrofuran (THF), reagent ethanol, potassium phosphate monobasic, and sodium hydroxide (NaOH) were purchased from Fisher Scientific and used as received. Adipic acid, methyl ethyl ketone (MEK), *p*-toluenesulfonic acid (PTSA), triethylamine (Et_3N), and oxalyl chloride were purchased from ACROS Organics. Water was purified by reverse osmosis and ion exchange using a Barnstead RO pure ST (Barnstead/Thermolyne, Dubuque, IA, USA) purification system. Water, acetonitrile and formic acid were LC-MS grade (Spectrum Chemicals, New Brunswick, NJ, USA) and ascorbic acid were from Sigma-Aldrich (St Louis, MO), and d3-Rif was from Toronto Research Chemicals (Toronto, ON, Canada). All microfuge tubes were cleaned with glass-distilled ethanol prior to use.

4.3.2 Methods

4.3.2.1 Synthesis of Cellulose Derivatives

CAAdP (synthesized as previously reported[27]; procedures summarized below)

Preparation of monobenzyl adipate: Adipic acid (73 g, 0.5 mol), benzyl alcohol (81 g, 0.75 mol), PTSA (0.95 g, 5 mmol), and toluene (200 mL) were stirred in a flask equipped with Dean-Stark trap and heated at reflux for 3 h. After cooling to room temperature, water (200 mL) was added, and the pH adjusted to 8 with 6M NaOH. The aqueous layer was separated, mixed with ether (150 mL), and the pH was adjusted to 2 with 6M HCl. The ether layer was separated, concentrated under reduced pressure at 40°C, and obtained the product as a colorless oil. Yield 48.1% (51g, 216 mmol) ^{1}H NMR ($CDCl_3$); 1.68 (m, 4H), 2.36 (m, 4H), 5.09 (s, 2H), and 7.32 (m, 5H).

Preparation of monobenzyl adipoyl chloride: A solution of monobenzyl adipate (20 g, 80 mmol), DMF (3 drops), and 200 mL dichloromethane was cooled in a round bottomed flask to 0°C, oxalyl chloride (25.4 g, 200 mmol) was added drop wise and then the solution stirred for 3 h at room temperature. The solvent was removed under reduced pressure, 10 mL toluene was added, and then it was concentrated again under reduced pressure at 50°C. The product was a yellow oil. Yield 75% (16 g, 63 mmol) ^{1}H NMR

($CDCl_3$): 1.73 (m, 4 H), 2.39 (t, 2 H), 2.90 (t, 2 H), 5.12 (s, 2 H), 7.32 (m, 5 H).

Monobenzyl CAAdP synthesis: CAP (1 g, 3.52 mmol) was dissolved in MEK (20 mL), Et_3N (1.06 mL, 7.74 mmol, 2.2 eq) was added all at once, then monobenzyl adipoyl chloride (1.78 g, 7.04 mmol, 2 eq) was added. After 20 hours at 60°C under nitrogen, the reaction mixture was cooled, then added to ethanol (250 mL) to precipitate the product, which was isolated by vacuum filtration, then washed with 200 mL water. Then it dissolved in 20 ml THF and reprecipitated in 400 ml hexane. The white product was characterized by ^{1}H NMR. Yield 80% (1.2 g, 2.8 mmol) d 1.02-1.20 (m, $COCH_2\underline{CH_3}$ of propionate), 1.66 (broad s, $COCH_2\underline{CH_2}\underline{CH_2}CH_2CO$ of adipate), 2.16-2.35 (m, $CO\underline{CH_2}CH_3$ of propionate, $COCH_3$ of acetate and $CO\underline{CH_2}CH_2CH_2\underline{CH_2}CO$ of adipate), 3.25-5.24 (cellulose backbone), 5.10 ($\underline{CH_2}C_6H_5$), 7.33 ($CH_2\underline{C_6}\underline{H_5}$). DS by ^{1}H-NMR: adipate 0.6, propionate 2.09, acetate 0.04.

Hydrogenolysis of benzyl CAAdP: Monobenzyl CAAdP (1 g, 2.77 mmol) was dissolved in 100 mL THF, then $Pd(OH)_2/C$ (500 mg) was added. The mixture was stirred at high speed under H_2 atmosphere in a high-pressure reactor (Parr reactor Model 4848) at 120-psi bar pressure for 24 hours at room temperature. Products were isolated by filtering through Celite, removing the solvent under reduced pressure, and then precipitating in ethanol (50 mL).

^{1}H NMR CAAdP ($CDCl_3$, yield 78%, 0.65 g, 1.71 mmol): d 1.02-1.20 (m, $COCH_2\underline{CH_3}$ of propionate), 1.66 (broad s, $COCH_2$- $\underline{CH_2}\underline{CH_2}CH_2CO$ of adipate), 2.16-2.35 (m, $CO\underline{CH_2}CH_3$ of propionate, $COCH_3$ of acetate and $CO\underline{CH_2}CH_2CH_2\underline{CH_2}CO$ of adipate), 3.25-5.24 (cellulose backbone). DS by ^{1}H NMR: adipate 0.6, propionate 2.09, acetate 0.04.

4.3.2.2 Preparation of Rif containing CMCAB and CAAdP ASDs

In each case 2 g total of Rif and polymer was dissolved in 80 mL THF at room temperature. Firstly, polymer (1.7 g of CMCAB or CAAdP) was magnetically stirred in THF for 15 h, at which point it was completely dissolved. Rif (weight 0.3 g) was then added to the solution and stirred for 20 min, protected from light. ASDs were prepared by

spray drying the polymer/Rif solutions using a nitrogen-blanketed spray dryer (Buchi B-290) and the instrument parameters were as follows: inlet temperature 80°C, outlet temperature 65°C, aspirator rate 80%, compressed nitrogen height 30 mm and nozzle cleaner 2.

4.3.2.3 Powder X-Ray Diffraction

X-ray powder diffraction patterns were measured with a Bruker D8 Discover X-ray Defractometer with a Lynxeye detector and a KFL CU 2K Xray source. Samples were run with a 1 mm slit window. The experiments were conducted with a scan range from 10° to 50° 2θ.

4.3.2.4 Animals

Approximately 5 week-old fifty-one BABL/c female mice weighing ~25 g were received from Harlan Laboratories (Dublin, VA). All of the mice were acclimated for two weeks in the animal housing facility of the Infectious Disease Unit in the College of Veterinary Medicine, as per protocol (IACUC #13-043-CVM) approved by Virginia Tech Institutional Animal Care and Use Committee (IACUC).

4.3.2.5 *In vivo* experimental design, Dosing Schedule and Sample Collection

Almost 24 h before experimental study mice were housed (5 mice per cage) in cages (Techniplast, Philadelphia, PA). Mice were given commercial pellet diet and water ad libitum. Ten hours before experimental study food was removed from all mice and animals were randomly divided into three groups as follows: Group 1 with 17 mice were orally gavaged with Rif; Group 2 with 17 mice were orally gavaged with spray dried formulated Rif/CMCAB; and Group 3 with 17 mice were orally gavaged with Rif/CAAdP ASDs and untreated two extra mice from each group were pre-bled before the start of the experiment. A single dose equivalent to 125 mg/kg body weight of Rif (2.9 mg/mouse) were dispersed in PBS (3600ul PBS) administered by oral gavage. Material safety data information from Science lab Inc. reports an oral LD_{50} for Rif in mice as 500mg/kg and previous study of Samantha Casterlow showed 250 mg/ml

application results were too high for a mice because of toxicity (high Rif content of urine and mild to moderate signs of damage to the glomeruli according to histopathology results)[24] therefore we chose to work with 125 mg/ml as a safe concentration. Then under general anaesthesia blood samples were collected retro-orbitally from 3 mice from each group into heprinized tubes at 0, 2, 4, 6, 8, 10, 12, 18, 24, 36, 48, 60, 72, 84 and 96 h. The mice were bled in tandem so that only two bleeds were performed per mouse with in 96 hours of experiment. Then the blood samples were centrifuged at 6708 x g for 10 min for separation of plasma and transferred into clean vials and centrifuged once more at 6708 x g for 10 minutes to remove any red blood cells. The supernatant clear plasma was collected carefully and stored in dark at -20°C until analysis.

4.3.2.6 LCMS Analysis for Biological Samples

Twenty microliters of each diluted sample were injected onto a Jupiter 4 µ Proteo 90 Å 50 x 0.5 mm reversed phase column (Phenomenex) using a G1313A 1100 series autosampler (Agilent). The HPLC gradient was developed utilizing a Tempo nano MDLC (Eksigent) and column effluent was introduced into a 4000 QTrap mass spectrometer (ABSciex) utilizing a TurboIonSpray (TIS) electrospray source. Solvents A and B were water and acetonitrile, respectively, each supplemented with 0.1 % (v/v) formic acid. A flow rate of 20 µl/min was maintained throughout a 30 minute gradient separation where the initial conditions were 80% A and 20 % B. These conditions were maintained for 5 minutes after injection followed by a linear gradient from 80 % A to 20 % A over 10 minutes. The 20 % A was maintained for 5 minutes followed by a linear gradient back to 80 % A and a re-equilibration at 80 % A for 5 minutes prior to injection of the next sample. Data acquisition conditions for the mass spectrometer were: ion spray 5400 V, source temperature 120°C, interface heater on, CAD gas high, entrance potential 10 V and curtain gas, ion source gas 1 and ion source gas 2 were set to 10, 10 and 20, respectively. Rif was quantified utilizing the transition intensity for 823.4 to 791.5 (DP 91, CE 25, CXP 12) following normalization to the transition intensity for the internal standard d_3-Rif 826.5 to 794.4 (DP 101, CE 25, CXP 12). A calibration curve was generated by measuring transition intensities for samples containing 40 ng/ml d_3-Rif and from 0.2 to 78100 ng/ml Rif. Samples from several early time points exceeded the

maximum amount used to generate the calibration curve and were analyzed again following a 100-fold dilution.

4.3.2.7 Sample Processing

Serum samples were thawed by heating (37˚C, 3 min) and then mixed using a vortex mixer prior to transferring an aliquot (50 µl) to a clean microfuge tube (2 mL). Samples were then diluted by adding methanol (200 µL) that contained ascorbic acid (1 mg/mL) and d_3-Rif (500 ng/ml). The samples were again mixed using a vortex mixer and incubated on ice for 30 minutes. Precipitated protein was collected at the bottom of the microfuge tube by centrifugation at room temperature at (13000xg, 10 min) and 100 µl of the supernatant from each sample was carefully transferred to amber autosampler vials. Samples were further diluted by adding 900 µl of methanol:water (1:1, v/v).

4.3.2.8 Statistical analysis

The data were analyzed by Student's unpaired t-test by JMP. Free drug and ASD treatment groups were compared.

4.4 Results

4.4.1 Cellulose Derivatives as polymeric matrix

We decided to investigate CMCAB and a cellulose ω-carboxyalkanoates, CAAdP, for ASD preparation in *in vivo* study because of their previous promising results in increasing solution concentration of Rif *in vitro*[9]. Both of the polymers have a high glass transition temperature (T_g), that will keep the metastable drug trapped above the ambient temperature even under hot and humid conditions, and each has a substantial DS(CO_2H), expected to release Rif at the neutral pH of the small intestine but to remain unionized and thus inhibit the release under acidic pH conditions as shown *in vitro* before.

Both CAAdP and CMCAB provided excellent performance with regard to enhanced release and stabilization of intact Rif in pH-switch dissolution experiments *in vitro*, much better than that observed from crystalline Rif itself. CMCAB released 70% of the drug and CAAdP released nearly 95% of available intact Rif, with maximum levels stable till

the end of the experiment, implying very little degradation. On the other hand, crystalline Rif remaining in solution was 40% at the end of the experiment. In addition, the amount of intact Rif content was shown as 96%, which proved very low extent of Rif degradation in the cellulose ester ASDs. Therefore it was decided to extend the study by an *in vivo* experiment.

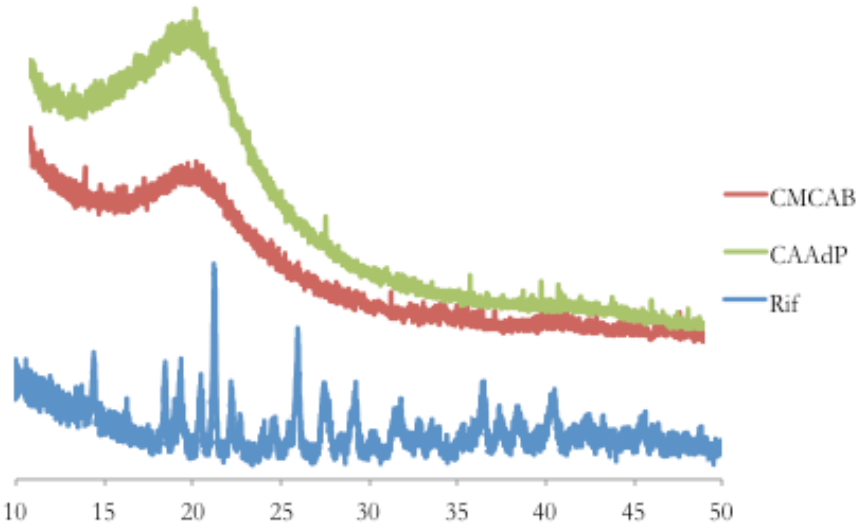

Figure 4.3: XRD results of spray dried dispersions in CAAdP and CMCAB and crystalline Rif.

XRD spectra of the spray-dried Rif/polymer blends and the crystalline Rif are presented in **Figure 4.3**. Crystalline Rif shows its characteristic sharp peaks, including particularly sharp reflections at 2Θ values of 14° and 21° while the spray dried drug polymer blends show amorphous halos in that range and lack the sharp peaks of crystalline Rif. We did not perform further characterizations since we already completed them in our previous paper.

4.4.2 Rif Plasma drug profiles

In vivo drug release studies were carried out in mouse by oral administration of a single dose of CMCAB ASD and CAAdP ASD containing Rif and crystalline Rif. Subsequently, the plasma levels of Rif were recorded at different time intervals (0, 2, 4, 6, 8, 10, 12, 18, 24, 36, 48, 60, 72, 84 and 96 h). Free Rif and CMCAB ASD particles

demonstrated a maximum concentration of Rif 2h after the administration (**Figure 4.4**) while CAAdP ASD reached to the max in 4h. The C_{max} values were presented on **Table 4.1.**

Table 4.1: Summary of average C_{max} values of Rif and ASDs after a single oral application.

	Rif (ng/ml)	CMCAB (ng/ml)	CAAdP (ng/ml)
C_{max}	76517	132544	61822
T_{max}	2h	2h	4h

The Rif blood concentrations were presented in three figures as **Figure 4.4** shows time points 2 to 10h, **Figure 4.5** shows 10 to 24 h and **Figure 4.6** shows time points 24 to 96 h, for better illustration.

CMCAB ASD had higher Rif blood concentrations than CAAdP ASD and crystalline drug throughout the experiment, but the difference become statistically significant after 36h ($P < 0.001$). The bioavailability of CMCAB between 36 and 96 h is 2.6 fold higher than crystalline Rif at the same time points that implies that the CMCAB ASDs releases Rif slowly in intestines and thereby have longer time in the blood stream and has the potential to decrease drug application frequency. The higher Rif concentration of the CMCAB ASDs resulted in higher bioavailability when compared with the free Rif and CAAdP ASDs as shown in **Table 4.2**. CMCAB and free Rif are reaching to undetectable limits at 96 h while CAAdP were at very low concentration after 60h from the single oral application.

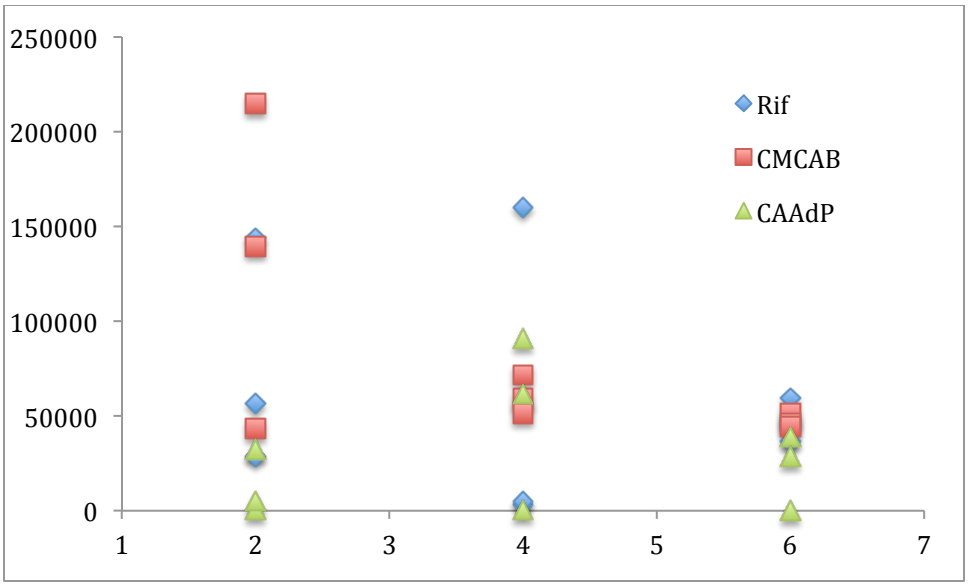

Figure 4.4: Plasma drug profile following a single 125 mg/kg oral administration of Rif and Rif containing CMCAB and CAAdP ASDs. Each formulation treatment group is noted with a different color line, n=3 for each time point, time points: 2 to 10 h.

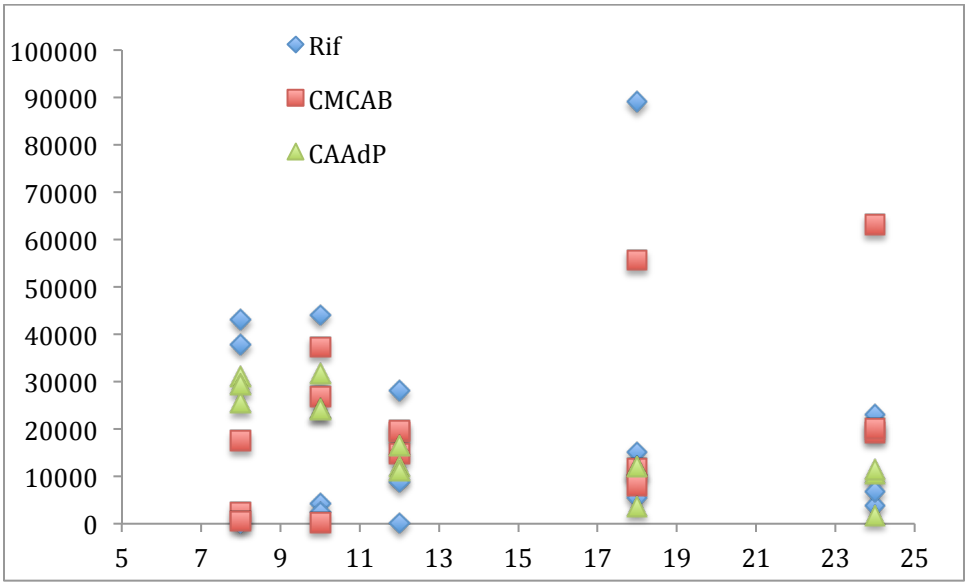

Figure 4.5: Plasma drug profile following a single 125 mg/kg oral administration of Rif and Rif containing CMCAB and CAAdP ASDs. Each formulation treatment group is noted with a different color line, n=3 for each time point, time points: 10 to 24 h.

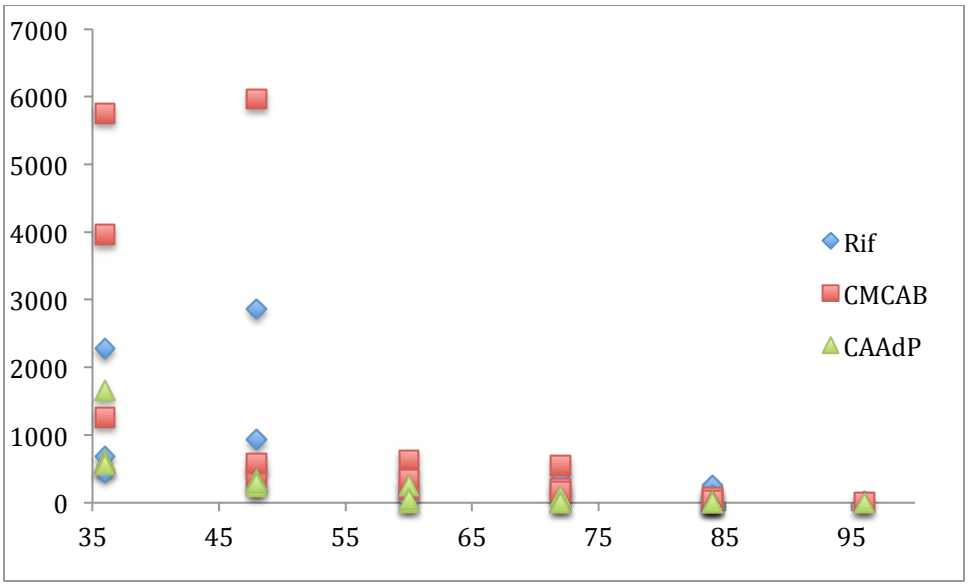

Figure 4.6: Plasma drug profile following a single 125 mg/kg oral administration of Rif and Rif containing CMCAB and CAAdP ASDs. Each formulation treatment group is noted with a different color line, n=3 for each time point, time points: 24 to 96 h.

Table 4.2: Bioavailability of the CMCAB ASD, CAAdP ASD and Crystalline Rif at different concentrations.

Time points of bioavailability calculation	Rif AUC (ng/ml/h)	CMCAB ASDs AUC (ng/ml/h)	CAAdP ASDs AUC (ng/ml/h)
0- 96 h	2177	2690	1510
0-36 h	2562	2650	1464
36-96 h	97	234	45

Although CMCAB ASDs had very promising results and provided increase in bioavailability of the drug relative to the free Rif application, it was quite surprising to see that CAAdP ASD had almost half of the crystalline Rif bioavailability. We have shown that CAAdP can release almost 95% of the amorphous drug immediately *in vitro* but it did not follow the same trend *in vivo,* which leads to the conclusion that there is no correlation between the *in vitro* and *in vivo* behavior of the drug delivery system. The

lower delivery of the CAAdP ASD can be because of the limited time during the interaction with water and lower pH of the mouse small intestine. In addition, mouse stomach pH is 4.0 (fasted) and the intestinal pH is lower than that in man, <pH 5.2 in the mouse[28]. Instead of mouse, dogs would be a better model since their pH profile of the GI track is very similar to that of humans[29]. Higher pH of stomach will limit crystalline Rif degradation, which is the one of the main reason for the decrease in bioavailability in human. Besides, pH 5.2 or lower is not high enough to ionize the carboxylic acid groups (>6 pH is convenient) that will help the polymeric matrix to interact with water to swell and release the amorphous drug, on the other hand human small intestine pH is 6.0 to 7.2 (about pH 6 in the duodenum and 6 to about pH 7.4 in the terminal ileum)[30] that should be excellent conditions for the ionization of our polymers as it has been shown *in vitro*.

4.5 Conclusions

Rif encapsulated CMCAB and CAAdP spray dried particles compared to that of free Rif were tested when given a single oral dose in a mouse model. The results indicate that the Rif CMCAB ASD was able to increase bioavailability of Rif compared to that of the free drug form at the same concentration in a mouse model, especially after 36 h that is 2.4 fold bioavailability increase. Therefore, these ASD particles may have the potential to the reduce Rif dose in a pill and frequency of medication thus price of the both medication and treatment can be decreased. Thus the approach has a great potential to have an impact on TB patients, especially in the third world countries. In addition, decrease in the drug dose can decrease Rif associated adverse affects, thus increasing patient compliance.

4.6 References

(1) Yee, D.; Valiquette, C.; Pelletier, M.; Parisien, I.; Rocher, I.; Menzies, D. Incidence of Serious Side Effects from First-Line Antituberculosis Drugs among Patients Treated for Active Tuberculosis. *Am. J. Respir. Crit. Care Med.* **2003**, *167*, 1472–1477.

(2) WHO | Tuberculosis http://www.who.int/mediacentre/factsheets/fs104/en/ (accessed Apr 17, 2016).

(3) WHO | 10 facts about tuberculosis http://www.who.int/features/factfiles/tuberculosis/en/ (accessed Apr 17, 2016).

(4) Harrington, M. From HIV to Tuberculosis and Back Again: A Tale of Activism in 2 Pandemics. *Clin. Infect. Dis.* **2010**, *50 Suppl 3*, S260–S266.

(5) Biganzoli, E.; Cavenaghi, L. A.; Rossi, R.; Brunati, M. C.; Nolli, M. L. Use of a Caco-2 Cell Culture Model for the Characterization of Intestinal Absorption of Antibiotics. *Farm.* **1999**, *54*, 594–599.

(6) Becker, C.; Dressman, J. B.; Junginger, H. E.; Kopp, S.; Midha, K. K.; Shah, V. P.; Stavchansky, S.; Barends, D. M. Biowaiver Monographs for Immediate Release Solid Oral Dosage Forms: Rifampicin. *J. Pharm. Sci.* **2009**, *98*, 2252–2267.

(7) Agrawal, S.; Panchagnula, R. Dissolution Test as a Surrogate for Quality Evaluation of Rifampicin Containing Fixed Dose Combination Formulations. *Int. J. Pharm.* **2004**, *287*, 97–112.

(8) Panchagnula, R.; Agrawal, S. Biopharmaceutic and Pharmacokinetic Aspects of Variable Bioavailability of Rifampicin. *Int. J. Pharm.* **2004**, *271*, 1–4.

(9) Arca, H. C.; Mosquera-Giraldo, L. I.; Pereira, J. M.; Sriranganathan, N.; Taylor, L. S.; Edgar, K. J. Rifampin Stability and Solution Concentration Enhancement through Amorphous Solid Dispersion in Cellulose ω-Carboxyalkanoate Matrices. *J Pharm Sci* **2016**.

(10) Pereira, J. M.; Mejia-Ariza, R.; Ilevbare, G. A.; McGettigan, H. E.; Sriranganathan, N.; Taylor, L. S.; Davis, R. M.; Edgar, K. J. Interplay of Degradation, Dissolution and Stabilization of Clarithromycin and Its Amorphous Solid Dispersions. *Mol Pharm* **2013**, *10*, 4640–4653.

(11) Liu, H.; Taylor, L. S.; Edgar, K. J. The Role of Polymers in Oral Bioavailability Enhancement; a Review. *Polymer (Guildf).* **2015**, *77*, 399–415.

(12) Singhal, D.; Curatolo, W. Drug Polymorphism and Dosage Form Design: A

Practical Perspective. *Adv. Drug Deliv. Rev.* **2004**, *56*, 335–347.

(13) Liu, H. Y.; Ilevbare, G. A.; Cherniawski, B. P.; Ritchie, E. T.; Taylor, L. S.; Edgar, K. J. Synthesis and Structure-Property Evaluation of Cellulose Omega-Carboxyesters for Amorphous Solid Dispersions. *Abstr. Pap. Am. Chem. Soc.* **2013**, *245*.

(14) Liu, H. Y.; Kar, N.; Edgar, K. J. Direct Synthesis of Cellulose Adipate Derivatives Using Adipic Anhydride. *Cellulose* **2012**, *19*, 1279–1293.

(15) Kar, N.; Liu, H.; Edgar, K. J. Synthesis of Cellulose Adipate Derivatives. *Biomacromolecules* **2011**, *12*, 1106–1115.

(16) Li, B.; Konecke, S.; Harich, K.; Wegiel, L.; Taylor, L. S.; Edgar, K. J. Solid Dispersion of Quercetin in Cellulose Derivative Matrices Influences Both Solubility and Stability. *Carbohydr Polym* **2013**, *92*, 2033–2040.

(17) Ilevbare, G. A.; Liu, H. Y.; Edgar, K. J.; Taylor, L. S. Understanding Polymer Properties Important for Crystal Growth Inhibition-Impact of Chemically Diverse Polymers on Solution Crystal Growth of Ritonavir. *Cryst. Growth Des.* **2012**, *12*, 3133–3143.

(18) Ilevbare, G. A.; Liu, H.; Edgar, K. J.; Taylor, L. S. Inhibition of Solution Crystal Growth of Ritonavir by Cellulose Polymers – Factors Influencing Polymer Effectiveness. *CrystEngComm* **2012**, *14*, 6503–6514.

(19) Wegiel, L. A.; Zhao, Y.; Mauer, L. J.; Edgar, K. J.; Taylor, L. S. Curcumin Amorphous Solid Dispersions: The Influence of Intra and Intermolecular Bonding on Physical Stability. *Pharm. Dev. Technol.* **2014**, *19*, 976–986.

(20) B. Li; S. Konecke; L.A. Wegielb; L.S. Taylor; K.J. Edgar. Both Solubility and Chemical Stability of Curcumin Are Enhanced by Solid Dispersion in Cellulose Derivative Matrices. *Carbohydr Polym* **2013**, *98*, 1108–1116.

(21) Wegiel, L. A.; Mauer, L. J.; Edgar, K. J.; Taylor, L. S. Crystallization of Amorphous Solid Dispersions of Resveratrol during Preparation and Storage-

Impact of Different Polymers. *J Pharm Sci* **2013**, *102*, 171–184.

(22) Li, B.; Wegiel, L. A.; Taylor, L. S.; Edgar, K. J. Stability and Solution Concentration Enhancement of Resveratrol by Solid Dispersion in Cellulose Derivative Matrices. *Cellulose* **2013**, *20*, 1249–1260.

(23) Ilevbare, G. A.; Liu, H.; Edgar, K. J.; Taylor, L. S. Impact of Polymers on Crystal Growth Rate of Structurally Diverse Compounds from Aqueous Solution. *Mol Pharm* **2013**, *10*, 2381–2393.

(24) Casterlow, S. A. Characterization and Pharmacokinetics of Rifampicin Laden Carboxymethylcellulose Acetate Butyrate Particles, Virginia Tech, 2012.

(25) Li, B.; Harich, K.; Wegiel, L.; Taylor, L. S.; Edgar, K. J. Stability and Solubility Enhancement of Ellagic Acid in Cellulose Ester Solid Dispersions. *Carbohydr Polym* **2013**, *92*, 1443–1450.

(26) Posey-Dowty, J. D.; Watterson, T. L.; Wilson, A. K.; Edgar, K. J.; Shelton, M. C.; Jr., L. R. L. Zero-Order Release Formulations Using a Novel Cellulose Ester. *Cellulose* **2007**, *14*, 73–83.

(27) Kar, N.; Liu, H.; Edgar, K. J. Synthesis of Cellulose Adipate Derivatives. *Biomacromolecules* **2011**, *12*, 1106–1115.

(28) McConnell, E. L.; Basit, A. W.; Murdan, S. Measurements of Rat and Mouse Gastrointestinal pH, Fluid and Lymphoid Tissue, and Implications for in-Vivo Experiments. *J. Pharm. Pharmacol.* **2008**, *60*, 63–70.

(29) Dressman, J. B. Comparison of Canine and Human Gastrointestinal Physiology. *Pharm. Res.* **1986**, *3*, 123–131.

(30) Fallingborg, J. Intraluminal pH of the Human Gastrointestinal Tract. *Dan. Med. Bull.* **1999**, *46*, 183–196.

Chapter 5. Amorphous solid dispersions of multiple anti-HIV drugs: impacts of drugs on each other's solution concentrations, and mechanisms thereof

5.1 Abstract

Human immunodeficiency virus (HIV) infection is a life threating disease that can give rise to acquired immunodeficiency syndrome (AIDS), a condition in which the immune system breaks down. Highly Active Anti Retroviral Therapy (HAART) is a combination therapy recommended by WHO in order to suppress HIV and prevent development of AIDS by the application of three or more drugs in combination. It is highly desirable for multidrug combinations to be co-formulated into single dosage forms where possible, to promote patient convenience and adherence to dosage regimens. Such co-formulation can be convenient when amorphous solid dispersions (ASDs) are prepared. We investigated multi-drug ASDs of several model anti-HIV drugs (ritonavir (Rit), etravirine (Etra) and efavirenz (Efa)) in cellulosic polymer matrices. Our hypothesis was that the presence of multiple drugs would reduce crystallization tendency from the ASD, thereby providing stable formulations for solution concentration enhancement. We explored cellulose esters that we have designed as effective ASD polymers, cellulose acetate suberate (DS_{Sub} 0.9, CASub) and cellulose acetate adipate propionate (DS_{Ad} 0.9, CAAdP), comparing with commercial cellulosic polymers 6-carboxyl cellulose acetate butyrate (CCAB) and carboxymethylcellulose acetate butyrate (CMCAB). We succeeded in preparing three drug ASDs containing high drug loadings (45% drug total; 15% of each drug); each polymer tested was effective at stabilizing the amorphous drugs in the solid phase, as demonstrated by XRD, SEM and DSC studies. These ASDs were shown in dissolution studies to release each anti-HIV drug over a 8-hour period at pH 6.8, affording supersaturated solutions of each drug as expected, but unexpectedly failing in some cases to reach the maximum possible supersaturation. In a second set of dissolution studies (pH 6.8), the cause of the observed solution concentration limitations was investigated by studying release from single- and two-drug ASDs. These dissolution studies showed that concentrations of Rit, Etra and Efa achieved from three-drug ASDs were higher than those achieved from crystalline drugs, but that there was a decrease in the achieved drug concentration of both Rit and Efa when they dissolved together. Interestingly, Etra

solution concentration was enhanced by the presence of Rit and Efa in the ASD. We demonstrate that these effects have to do primarily with solution interactions between the anti-HIV drugs, rather than resulting from the drugs influencing each other's release rate, and we suggest that such observations may indicate an important, previously inadequately recognized, and general phenomenon for multi-drug ASDs of hydrophobic drugs.

5.2 Introduction

Human immunodeficiency virus (HIV) is a retrovirus that can be transmitted through contact with body fluids of an infected person, including blood or breast milk. According to the World Health Organization (WHO), 37 million people were infected globally in 2015; in that year 2.1 million new HIV infections were discovered and 1.1 million people lost their lives due to AIDS, which results from HIV infection.[1] No cure is currently available for HIV infection, but fortunately the Herculean efforts of biologists, chemists, and physicians since the first identification of HIV and AIDS in the early 1980s have provided a remarkable level of understanding of the biology of this virus, and a suite of therapeutic drugs that in most cases can suppress its harmful effects over the course of a lifetime[2–4]. Development of a combination therapy comprising three or more anti-HIV drugs with different drug mechanisms, called Highly Active Anti Retroviral Therapy (HAART), was a major advance in control of HIV infection and prevention of progression to AIDS, as HAART therapy effectively suppresses HIV, prevents development of resistant strains[5,6], and enhances patient compliance.[7,8] HIV virus suppression is made more difficult by the heterogeneity of the viral population.[9] HIV reverse transcriptases are prone to error by base substitutions, duplications and insertions, which result in nearly one mutation per cycle of infection[5] , potentially leading to drug resistance. It is more unlikely that mutations will lead to resistance to all drugs in the combination HAART therapy.

Non-nucleoside reverse-transcriptase inhibitors (NNRTI), such as Etra and Efa, bind to and inhibit the reverse-transcriptase enzyme, which is essential for retroviral replication. Etra, a second generation NNRTI used for the treatment of HIV-1, has a high genetic

barrier to viral resistance, so that clinically significant resistance develops only as a result of a large number of critical mutations; Etra therefore continues to be effective even in the presence of common NNRTI mutations.[10] PIs such as Rit block protease enzymes that are essential for cleavage of long polypeptide chains in order to activate them. Thus HAART therapy attacks HIV through multiple mechanisms, thereby enhancing efficacy and retarding the development of resistant strains.

Although HAART formulations were first approved by FDA more than a decade ago[11], HIV treatment is still problematic. In developing countries, the price of the medications is not affordable for many patients, and support for treatment from foundations and governments has not proved adequate to get needed drug therapy to all patients. Additional therapeutic challenges include patient non-compliance to lifelong, multi-pill therapeutic regimes in environments where medical care is difficult, and potential for significant side effects.[12]

Oral administration is essential for practical, daily, lifelong treatment of HIV patients. Most of the more than 25 anti-HIV drugs approved by FDA[11,13] for oral administration have low solubility in water (0.1-10 mg/ml), limiting the rate and the extent of drug absorption. While other methods have been used to increase solubility of anti-HIV drugs[14–17], ASD has particular value for enhancing drug solution concentration and thereby enhancing bioavailability. ASD works by trapping the drug in a polymer matrix, creating a metastable, molecular dispersion of drug in polymer, thereby eliminating the drug crystal lattice energy as a barrier to drug dissolution; therefore supersaturated drug solutions are formed. Because this methodology creates supersaturated solutions rather than enhancing thermodynamic solubility (as cyclodextrin and solvent approaches do, for example), ASDs also enhance permeation across the enterocytes and thus reduce both solubility and permeation barriers to bioavailability. Since ASDs are often prepared starting with an organic solvent solution of drug and polymer, and converting to particulate ASD by methods including spray-drying or film casting, it would seem to be particularly well-suited to formation of multi-drug molecular dispersions in one or more polymers (melt extrusion is another popular ASD formation technique, which could be equally well suited to formation of multi-drug dispersions).

Our starting hypothesis was that formation of ASDs containing multiple drugs should be advantageous, since the presence of the "other" drug(s) would tend to inhibit crystallization of any one-drug component, thereby enhancing ASD stability against crystallization[18]. This could in turn permit higher drug loading, and/or faster drug release. We felt that confirmation of this hypothesis would be particularly valuable for HIV drug treatment, since it could permit reduction in drug usage and expense, potentially expanding the number of patients treated for a given amount of expenditure. We further felt that successful multidrug formulations could enhance patient compliance, and that the reduced doses might even diminish certain side effects. We chose ritonavir, efavirenz, and etravirine as model drugs for this study due to their oral administration, low solubilities, low bioavailabilities, and ready availability, realizing that this particular three-drug combination is not necessarily the ideal anti-HIV drug treatment regime.

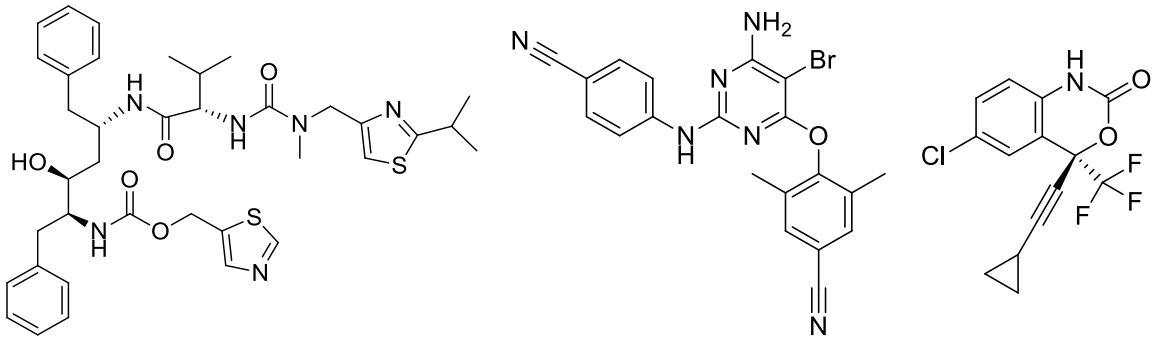

Figure 5.1: Chemical structures of Rit, Etra and Efa, respectively.

We chose to explore ASDs with CASub and CAAdP, which were designed and developed in the Edgar and Taylor laboratories as high-performance ASD polymers. Each of these cellulose w-carboxyalkanoates has high solvent solubility, high glass transition temperature (T_g), and demonstrated ability to form amorphous dispersions with at least some of these model drugs. We chose to compare them to currently or formerly commercial cellulosic polymers that have promise in ASD, namely CMCAB[19] and CCAB.[20] CMCAB has been shown repeatedly to be an effective polymer for ASD, while the chemical features of CCAB (high T_g, good solubility, carboxyl groups for release trigger and to enhance specific interactions with drug molecules) are of interest for that purpose in our laboratory.

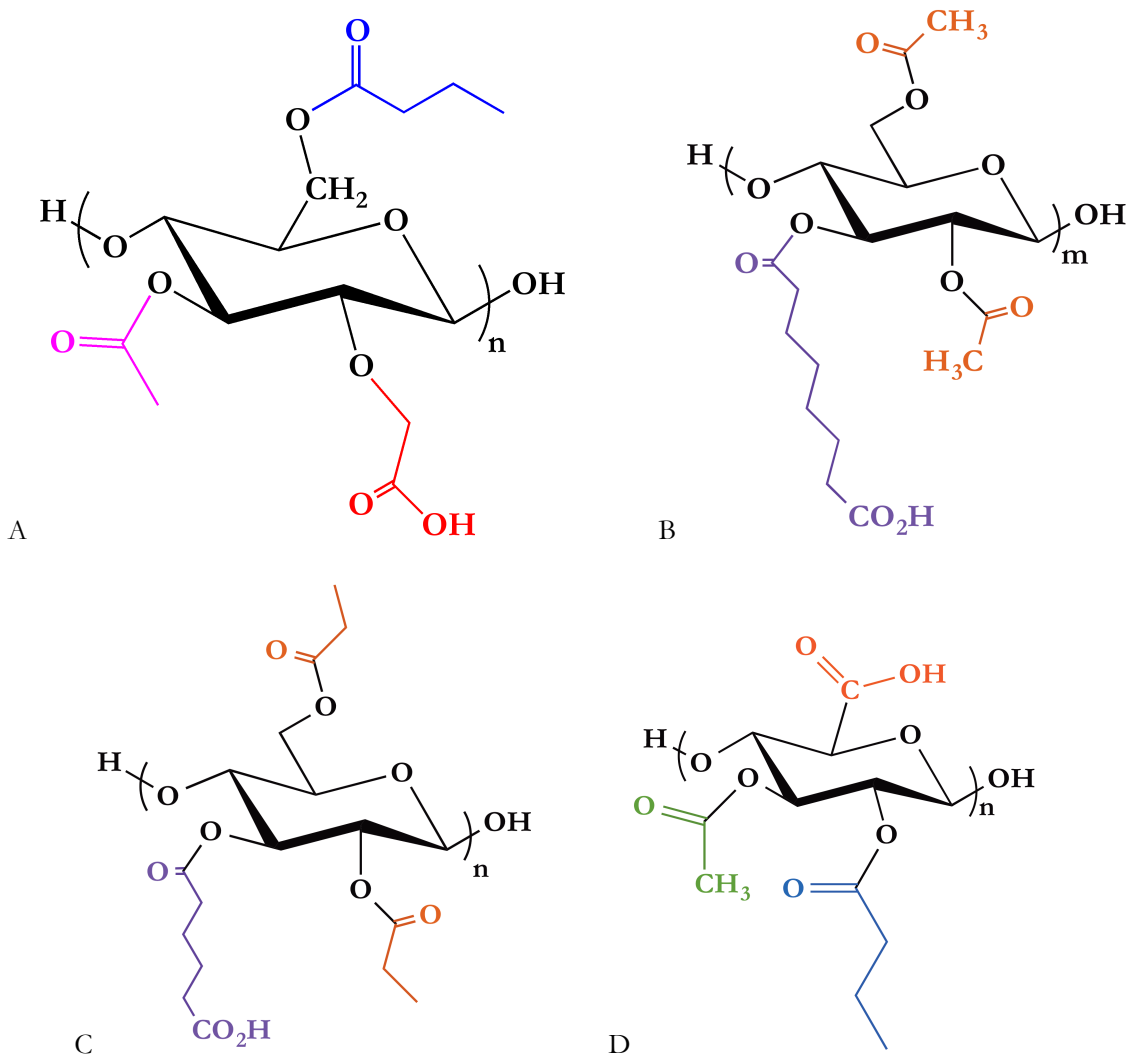

Figure 5.2: Chemical structures of CMCAB (A), CASub (B), CAAdP (C) and CCAB (D). These structures are not meant to convey regioselective substitution; depictions of substituent location are merely for convenience and clarity of depiction (except for CCAB carboxyl which is exclusively at C-6)

ASDs of hydrophobic drugs, like these, can be plagued by poor drug release. Surfactants are often useful for improving drug release from ASDs.[21] d-α-Tocopheryl polyethylene glycol 1000 succinate (TPGS) is a nonionic surfactant that is also a weak inhibitor of P-glycoprotein (P-gp), TPGS forms micelles above its critical micelle concentration (0.02%), thereby solubilizing some lipophilic actives, in some cases increasing their oral

bioavailability (in some cases the P-gp inhibitory activity can also contribute).[22–24]

Table 5.1: Physicochemical properties of polymers.

Polymer Type	DS (CO_2H)	DS (Other)	Solubility Parameter ($MPa^{1/2}$)	Drug Load (Wt %)	Polymer T_g (°C)	3-drug ASD T_g (°C)
CAAdP	0.9	Pr 2.09 Ac 0.04	22.79	15% Etra 15% Efa 15% Rit	116	58
CASub	0.9	Ac 1.82	23.72	15% Etra 15% Efa 15% Rit	101	58
CMCAB	0.3	CM 0.33 Bu 1.64 Ac 0.44	23.03	15% Etra 15% Efa 15% Rit	141	77
CCAB	(56.2 mg KOH/g) 0.28	Bu 1.62 Ac 0.06	24.44	15% Etra 15% Efa 15% Rit	134	74

We report herein investigations to test our hypothesis by attempts to form ASDs of the three model anti-HIV drugs (Etra, Efa and Rit) with the selected cellulosic polymers, CMCAB, CCAB, CASub (degree of substitution (DS) Sub 0.9) and CAAdP (DS Ad 0.9), and to evaluate the extent and rate of release of each drug from the ASD, as well as the extent of supersaturation achieved. We report also the interesting and unexpected drug interactions that we encountered, the influence of added TPGS, the consequences of those

interactions with regard to supersaturation of each individual drug, and our initial investigations of the mechanism leading to the observed effects.

5.3 Experimental

5.3.1 Materials

Etravirine, ritonavir and efavirenz were purchased from Attix Pharmaceuticals (Toronto, Canada). Cellulose acetate propionate (CAP-504-0.2) DS (acetate) = 0.04, DS (propionate) = 2.09) M_n = 15,000; cellulose acetate (CA-320S) DS (acetate) = 1.82) M_n = 50,000; CMCAB (CAS 641-0.2, approximate MW 22,000, degree of substitution (DS) (butyrate) = 1.64, DS (acetate) = 0.44, and DS (carboxymethyl) = 0.33)); and CCAB (cellouronic acid acetate butyrate or 6-carboxy cellulose acetate butyrate, MW 252,000, degree of substitution (DS) (butyrate) = 1.62, DS (acetate) = 0.06, and DS (carboxylic acid) = (56.2 mg KOH/g) 0.28) were from Eastman Chemical Company (Kingsport, Tennessee); polymers were dried in a vacuum oven at 50°C overnight before use. Acetonitrile (HPLC-grade), tetrahydrofuran (THF), benzyl alcohol, toluene, dichloromethane, *N*, *N*-dimethylformamide (DMF), ethanol, potassium phosphate monobasic, and sodium hydroxide (NaOH) were purchased from Fisher Scientific and used as received. Suberic acid, sebacic acid, adipic acid, methyl ethyl ketone (MEK), 1,3-dimethyl-2-imidazolidinone (DMI) (dried over 4Å molecular sieves), *p*-toluenesulfonic acid (PTSA), triethylamine (Et_3N) and oxalyl chloride were purchased from ACROS Organics. Palladium hydroxide was purchased from Sigma Aldrich. Water was purified by reverse osmosis and ion exchange using the Barnstead RO pure ST (Barnstead/Thermolyne, Dubuque, IA, USA) purification system.

5.3.2 Methods

5.3.2.1 Synthesis of CAAdP (DS 0.9) and CASub (DS 0.9): CAAdP was synthesized as previously reported[25], and summarized in the sup data.

^{1}H NMR of monobenzyl adipate ($CDCl_3$); 1.68 (m, 4H), 2.36 (m, 4H), 5.09 (s, 2H), and 7.32 (m, 5H).

^{1}H NMR of monobenzyl adipoyl chloride ($CDCl_3$): 1.73 (m, 4 H), 2.39 (t, 2 H), 2.90 (t, 2 H), 5.12 (s, 2 H), 7.32 (m, 5 H).

Similar procedures were followed to synthesize monobenzyl suberoyl chloride (^{1}H NMR ($CDCl_3$): 1.34 (m, 4H), 1.66 (m, 4H), 2.36 (t, 2H), 2.86 (t, 2H), 5.12 (s, 2H), 7.35 (m, 5H)).

^{1}H NMR of CAAdP monobenzyl ester ($CDCl_3$): d 1.02_1.20 (m, $COCH_2\underline{CH_3}$ of propionate), 1.66 (broad s, $COCH_2\underline{CH_2}\underline{CH_2}CH_2CO$ of adipate), 2.16-2.35 (m, $CO\underline{CH_2}CH_3$ of propionate, $COCH_3$ of acetate and $CO\underline{CH_2}CH_2CH_2\underline{CH_2}CO$ of adipate), 3.25-5.24 (cellulose backbone), 5.10 ($\underline{CH_2}C_6H_5$), 7.33 ($CH_2\underline{C_6}\underline{H_5}$). DS by ^{1}H NMR ($CDCl_3$): adipate 0.9, propionate 2.09, acetate 0.04.

Characterization of final products: ^{1}H NMR CAAdP (DMSO): 1.02-1.20 (m, $COCH_2\underline{CH_3}$ of propionate), 1.66 (broad s, $COCH_2$- $\underline{CH_2}\underline{CH_2}CH_2CO$ of adipate), 2.16-2.35 (m, $CO\underline{CH_2}CH_3$ of propionate, $COCH_3$ of acetate and $CO\underline{CH_2}CH_2CH_2\underline{CH_2}CO$ of adipate), 3.25-5.24 (cellulose backbone). DS by ^{1}H NMR: adipate 0.9, propionate 2.09, acetate 0.04.

^{1}H NMR CASub (DMSO): 1.2 ($COCH_2CH_2\underline{CH_2}\underline{CH_2}CH_2CH_2CO$ of suberate), 1.4-1.6 ($COCH_2\underline{CH_2}CH_2CH_2\underline{CH_2}CH_2CO$ of suberate), 2.10–2.46 ($CO\underline{CH_2}CH_2CH_2CH_2\underline{CH_2}CO$ of suberate, and $COCH_3$ of acetate), and 3.00–5.20 (cellulose backbone).

5.3.2.2 Preparation of ASDs by Solvent Casting and Grinding: Each formulation was prepared to total 1 g material, including polymer and drug(s). Three drug formulations (0.15 g of each drug and 0.55 g of polymer), two drug formulations, (0.15 g of each drug and 0.70 g of polymer) and single drug formulations (0.15 g drug and 0.85 g polymer) were each dissolved in 50 mL THF at room temperature. Three-drug samples that included surfactant were prepared with 0.15 g of each drug, 0.15 g of TPGS, and 0.4 g polymer, and were likewise dissolved in 50 mL THF at room temperature. From each

solution a film was cast upon a Teflon surface; each film was air-dried at 50°C. Each film was then peeled from the Teflon surface and placed into a Micro-Mill® (Scienceware®, Wayne, NJ 07470 USA) apparatus with dry ice, then milled for 5 min in order to prepare the dispersion in powder form.

5.3.2.3 Rit, Efa and Etra Detection by HPLC: Drug analyses employed an Agilent 1200 series HPLC consisting of a quaternary pump, online degasser, autosampler, and Agilent Chemstation LC 3D software. Analyses were conducted in reversed phase mode using an Eclipse XDB-C18 column (4.6 × 150 mm i.d., particle size 5 μm). A gradient analytical method was used employing acetonitrile and 0.05M phosphate buffer (pH 5.55). The acetonitrile proportion was 40% for 1 min, then raised to 60% for 14 min, then reduced to 40% in 1 min, remaining at 40% for 4 min. Flow rate was 1.5 mL/min, column temperature was 25°C, sample injection volume was 5 μL, UV detection was at 240 nm, and retention times observed were 10.49 min, 11.57 and 13.80 for Rit, Efa and Etra, respectively.

5.3.2.4 Powder XRD: X-ray powder diffraction patterns were measured with a Shimadzu XRD 6000 diffractometer (Shimadzu Scientific Instruments, Columbia, Maryland) using film samples. The instrument was calibrated relative to a silicon standard, which has a characteristic peak at 28.44° 2θ. Divergence and scattering slits were set at 1.0 mm, and the receiving slit was set at 10 iris. The experiments were conducted with a scan range from 10° to 50° 2θ.

5.3.2.5 ^{1}H NMR: 1-5 mg sample was dissolved in 1 ml NMR solvent ($CDCl_3$ or $(CD_3)_2SO$) and 0.7 ml of it transferred to NMR tubes. Proton NMR spectra were acquired on an INOVA 400 spectrometer operating at 400 MHz at room temperature by 32 scans.

5.3.2.6 DSC: DSC analyses were performed on a TA Instruments Q200. Dry samples (5 mg) were loaded in Tzero^{TM} aluminum pans. Each sample was equilibrated at -50°C and then heated to 190°C at 20 °C/min. Samples were then quench cooled to -50°C, then reheated to 190°C at 20°C/min. T_g values were recorded as the step-change inflection

point from 2nd heating scans.

5.3.2.7 SEM: Particle size and morphology were analyzed on a LEO 1550 field emission scanning electron microscope (FESEM). The samples were spread on double faced adhesive tape and coated with a very thin gold palladium layer (sputter coater Cressington 208HR) for 1 min. 5kV was used for excitation.

5.3.2.8 *In Vitro* Drug Release from ASDs: Dissolution studies were conducted in 250 mL jacketed flasks, using circulating ethylene glycol/water (1:1) in order to keep the flasks and accordingly the buffer temperature at 37°C. The volume of 0.05M phosphate buffer (pH 6.8) was 100 mL for each flask; volume was kept constant during the experiment by replacing each aliquot (1 mL) withdrawn by an equal volume of fresh buffer solution. All of the dissolutions experiments were conducted at supersaturated conditions for all of the drugs. Efa has the highest water solubility among the three drugs we studied therefore calculations were according to Efa supersaturation at 37°C; 25 fold supersaturated conditions were used for Efa and the drug content kept constant for the other two drugs for comparison.

5.3.2.8.1. Experiment A: Dissolution Study to Evaluate Drug Release Profiles: PBS buffer (0.05 M, 100 mL, pH 6.8) was placed in the dissolution flask. Drug-containing ASD (166 mg) or 25 mg of each pure drug (25 mg Efa, 25 mg Etra and 25 mg Rit together) was placed into the dissolution flask and magnetically stirred at 400 rpm. Samples (1 mL each) were withdrawn initially every 0.5 h (during first 2 h), and then every 1 h for the following 6 hours. Each sample was centrifuged at 13,000 rpm for 10 min, then 0.5 mL supernatant from the top of the centrifuge vial was transferred to an HPLC vial and analyzed immediately.

2-drug experiments were conducted with a similar protocol where 166 mg ASD (containing 15% of 2 drugs) were placed into a dissolution flask and compared with 25 mg of two-drugs (50 mg drug in total, drugs tested together) dissolution.

5.3.2.8.2 Experiment B: Evaluation of Drug-Drug Solution Interactions: A single drug ASD (166 mg) was dispersed into PBS buffer solution (0.05 M, 100 mL, pH 6.8) and stirred 8 h at 400 rpm. Afterwards, another single drug ASD (166 mg) was added to the buffer and aliquots were withdrawn at 1, 2 and 8 hours thereafter. Each sample was centrifuged at 13,000 rpm for 10 min, then 0.5 ml supernatant from the top of the centrifuge vial was transferred to a HPLC vial and analyzed immediately.

5.4 Results

5.4.1 Characterization of ASDs

Solid dispersions of the anti-HIV drugs Etra, Efa and Rit were prepared by solvent casting and subsequent micro-milling of the resulting films, using cellulose derivative matrices (CMCAB, CCAB, CAAdP (DS 0.9) and CASub (DS 0.9)). These one-drug dispersions (**Figure 5.2**) were prepared with 15% drug loads, in order to determine whether each drug could form an ASD with each polymer, and whether such ASDs would afford supersaturated solutions of the individual drugs. Key physical properties and categories of each of these poorly soluble drugs are summarized in **Table 5.2**. We initially explored whether the one-drug dispersions were amorphous by solid-state characterization, using XRD, DSC and SEM, comparing as appropriate vs. pure drug.

Etra, Efa and Rit are crystalline drugs, showing sharp, characteristic XRD peaks (Figure **5.3**). XRD diffraction patterns of the three one-drug formulations showed no sharp peaks; instead each exhibited an amorphous halo, as shown in **Figure S5.1** (sup data). Furthermore all two- (**Figure S5.3**, sup data) and three-drug (CCAB and CMCAB **Figure 5.4**; CASub and CAAdP, **Figure S5.2** (sup data)) dispersions also showed amorphous haloes but no crystalline diffraction peaks, conforming that all of these are amorphous dispersions.

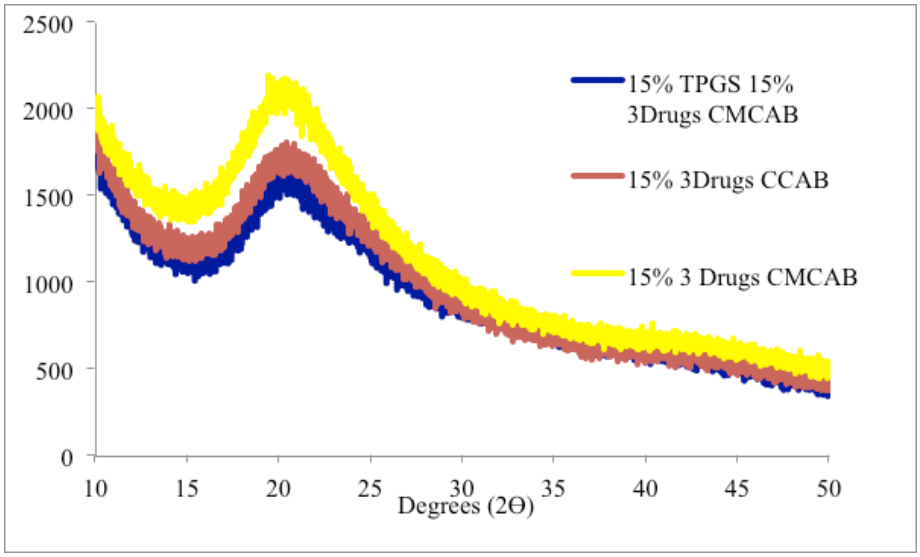

Figure 5.3: The XRD spectra of 15% 3 Drugs (15% Etra, 15% Efa and 15% Rit) ASDs prepared with CMCAB, CCAB and 15%TPGS in CMCAB. 15% 3 Drugs CASub and 15% 3 Drugs CAAdP XRD results are presented in sup data.

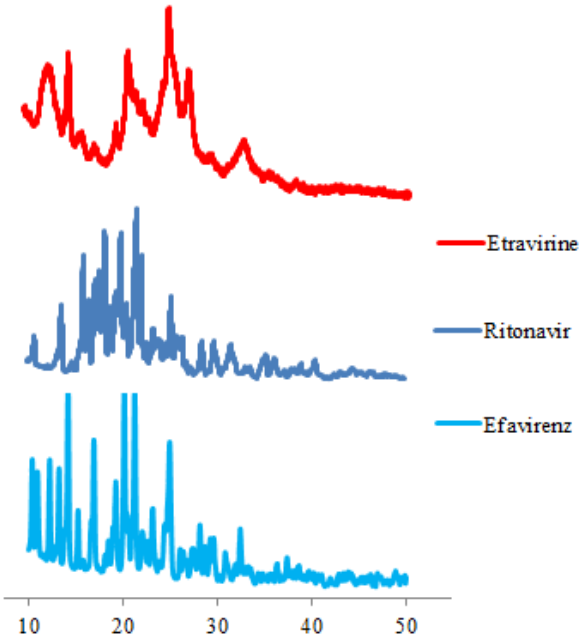

Figure 5.4: XRD spectra of crystalline Etra, Efa and Rit.

Table 5.2: The physicochemical properties of Etra, Efa and Rit.

Property	**Etra**	**Efa**	**Rit**
Molecular weight (g mol^{-1})	435.2	315.7	720.9
pK_a	3.5[26]	10.2	1.8 and 2.6[27]
Log P	5.2	4.7	5.6
Solubility Parameter ($MPa^{1/2}$)		21.89	20.03
Melting point (°C)	260.0	139.0	122.7
T_g of Amorphous Drug (°C)	99[28]	33[29]	50
Theoretical Amorphous Solubility (μg ml^{-1})	3	19.8[30]	20.6[30]
Experimental Amorphous Solubility (μg ml^{-1})	2.7	12.3	19.8
Tg (°C)	100 [26]	46[29]	50[31]
Drug Mechanism	NNTRI	NNRTI	PI
BCS	Class IV	Class II	Class IV
Recommended Dose	200 mg	600 mg	600 mg

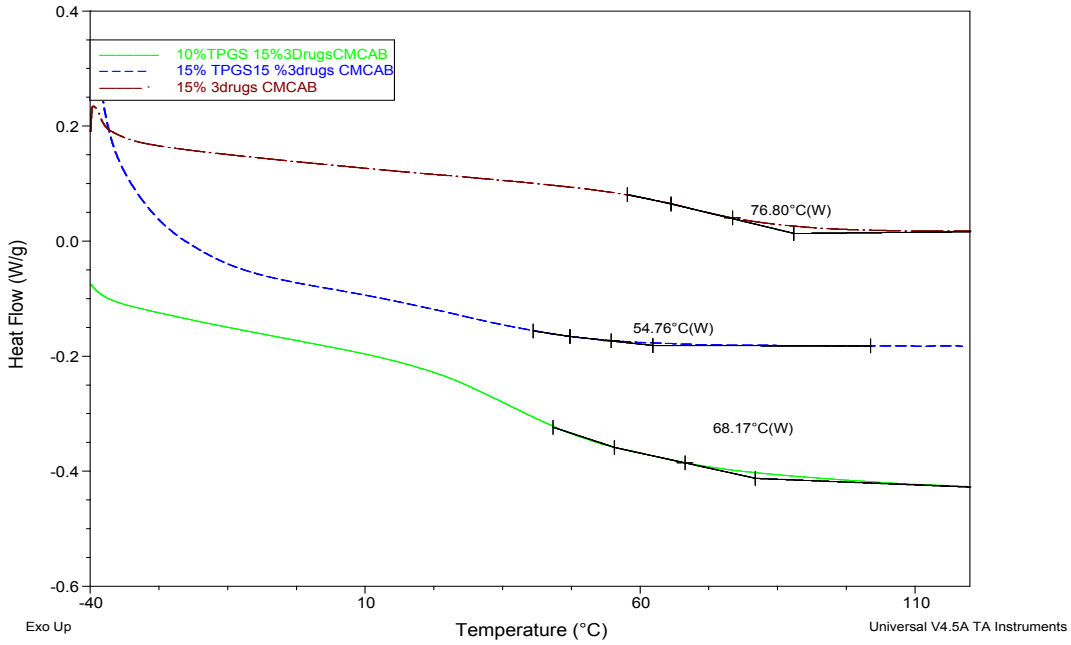

Figure 5.5: DSC thermograms of three drug CCAB and CMCAB formulations.

Thermal analysis is also a useful tool for quantifying drug-polymer miscibility; partial miscibility can lead to instability since concentrated drug domains can promote recrystallization and instability. If polymer and the drug(s) are miscible, a single T_g that ranges between the T_g values of pure components should be recorded. Theoretical T_g values were calculated according to the Gordon-Taylor equation,:

$$T_{g\ mix} = \frac{(Tg1\ W1 + Tg2\ W2)}{(W1 + W2)}$$

where T_g is the glass transition temperature, and W_1 and W_2 are the weight fractions of the components. Experimentally calculated and theoretical T_g values were close to one another (sup data), thermal properties of the crystalline drugs were presented in **Table 5.2**. DSC thermograms of the drug combinations show (**Figure 5.5**) the absence of drug melting endotherms or crystallization exotherms, which with the single T_g values confirms complete drug-polymer miscibility in every 3-drug dispersion, consistent with the XRD results.

5.4.2 Release profiles of anti-HIV drugs at pH 6.8:

Having established that the dispersions were amorphous, even with all three drugs present and even with as much as 45% drug vs. only 55% polymer, we investigated the dissolution properties of the anti-HIV drugs from single- and three-drug ASDs at small intestine pH. In these experiments the conditions were chosen to create supersaturation of each drug (if the drug were completely released), since this is necessary to evaluate the ability of the polymer to stabilize supersaturated drug solutions against recrystallization. We utilized HPLC to measure drug concentration, having developed a method that gave us baseline separation of the three peaks from the anti-HIV drugs. We began by experiments in which one ASD (containing 1-3 drugs) was added to pH 6.8 phosphate buffer in a jacketed flask, with dissolution at 37°C monitored by sampling and HPLC analysis for 8 h.

5.4.2.1 Three drug formulations of commercial polymers vs. crystalline drugs:

The dissolution results of three drugs containing CMCAB and CCAB ASDs were presented for Rit, Efa and Etra solution concentrations in **Figure 5.7, 5.8** and **5.9**, respectively. As will be clear from the results it is convenient to discuss the results by individual drug, since there are complex phenomena involved and this approach provides the clearest way to approach the data. We also separate out the 3-drug ASD results by commercial vs. lab-prepared cellulose derivative matrix polymers, primarily because of the fact that there are already many curves to compare in each figure and we feel that comparison is easier for the reader using a somewhat higher number of groupings but less curves per group. During the experiment, each dissolution flask contains all three drugs together for 8h at pH 6.8.

Rit dissolution results (**Figure 5.6**) clearly show enhancement of Rit solution concentration vs. crystalline drug, with approximately the maximum attainable supersaturation (20-fold) being achieved from a CMCAB ASD, when Rit is the only drug present. On the other hand, from the 3-drug ASDs, we observed 2-fold Rit supersaturation from the CCAB ASD, and 1.5-fold from the CMCAB ASD, all in relation to the thermodynamic solubility of crystalline Rit measured by us using the same

methodology. In each case release of the amorphous drug is rapid, quickly reaching a plateau and leveling off, as is common for ASD formulations[32,33]. The supersaturation appeared to be stable throughout the 8h experiment in the presence of either CCAB or CMCAB, significantly in excess of the time the formulation would typically spend in the small intestine. Likewise, significant Rit supersaturation is evident from the 3-drug combination using CAAdP as the matrix polymer; in this case approximately 1.7-fold supersaturation is observed, higher than for CMCAB but not as great as that observed for CCAB. Surprisingly, from CASub 3-drug ASDs (CASub is slightly more hydrophilic than is CAAdP), only slight Rit supersaturation was observed, not statistically significant. The fact that Rit supersaturation and stabilization were observed from these 1- and 3-drug ASDs was very encouraging, but the observation of reduced supersaturation from the multidrug ASD was unexpected and of concern, and would require further investigation.

Crystalline Efa has considerably higher water solubility than does Rif (approximately 6-7 fold higher), in keeping with its higher calculated solubility parameter. Perhaps as a result, Efa solubility was not aided by ASD. Examination of results from 3-drug ASDs in the commercial polymers (**Figure 5.7**) shows that ASD in the relatively hydrophobic CCAB or CMCAB polymer matrices actually reduced Efa solution concentrations achieved from the 3-drug ASDs, in comparison with the crystalline drug. Similarly, the ω-carboxyalkanoate CASub afforded significantly lower Efa concentration from its 3-drug ASD (**Figure 5.10**). On the other hand, CAAdP 3-drug ASD provided approximately the same Efa solution concentration as from crystalline drug (**Figure 5.10**). Overall dispersion in the 3-drug polymer ASDs investigated did not provide solubility advantage for Efa, and single drug ASD of Efa in CMCAB (**Figure 5.13**) likewise actually reduced Efa solution concentration vs. crystalline drug.

Etra is the least water-soluble of the three anti-HIV drugs examined, indeed being so low as to be hard to measure reliably; the thermodynamic solubility of Etra at pH 6.8 was below our HPLC detection limit, and has been described as less than 1 mL in the literature[26]. Etra solution concentration from CMCAB and CCAB 3-drug ASDs was significantly higher than that achieved from crystalline drug, showing steady release throughout the experiment and reaching 0.74 and 0.12 μg/ml after 8h from CMCAB and

CCAB ASDs, respectively. These concentrations are modest to be sure, but are quantifiable by our method and show significant improvement. However, crystalline Etra concentration was not measureable by our HPLC as a result of its very low water solubility. Unlike Etra and Rit, crystalline Efa solution concentration was higher (9.8 μg/ml) than those from three drug ASD formulations, 5.8 and 5.0 μg/ml from CMCAB and CCAB, respectively. Both of the ASD formulations and the crystalline drug generated immediate release and kept the concentration constant for 8h.

In addition to the CMCAB and CCAB ASDs, TPGS formulation was prepared with CMCAB that affords the highest concentration for three of the drugs for more then 3 fold increase of Rit concentration (4.9 μg/ml) and 1.3 fold increase of Efa relative to the crystalline drug (12.9 μg/ml), as well as a continued release for 8 h. Moreover, the Etra solution concentration was reached to 2.4 μg/ml that is very close to the highest experimental amorphous solution concentration of this drug (2.7 μg/ml). It is necessary to emphasize that 15% TPGS three drugs CMCAB ASD can increase the solution concentration of all the three drugs, even Efa, which had crystalline drug concentration higher than the other ASD formulations.

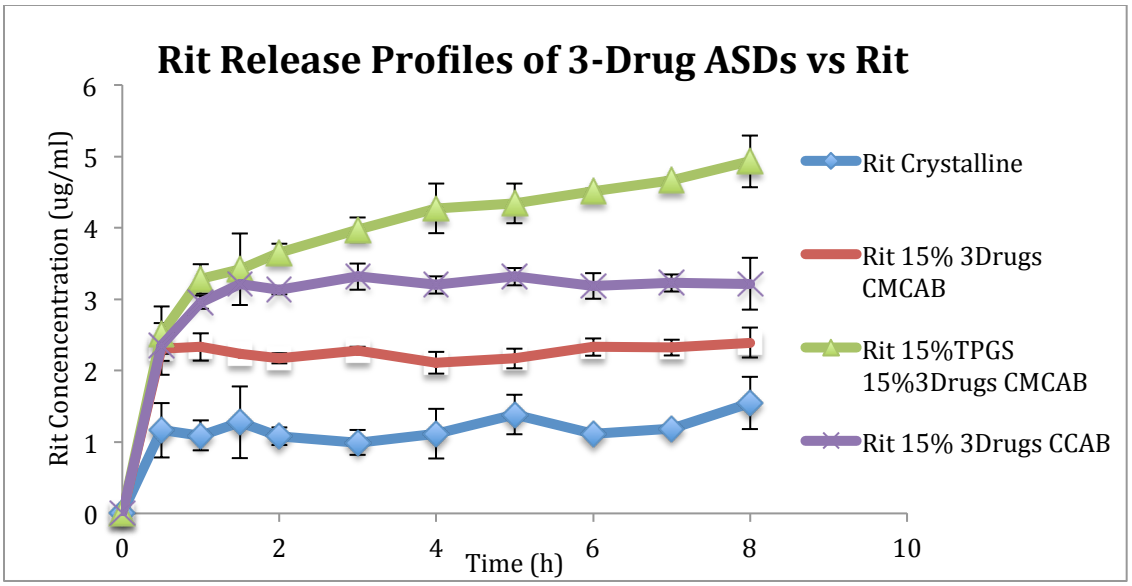

Figure 5.6: Dissolution profiles of crystalline Rit, Rit/Efa/Etra/CMCAB ASD, Rit/Efa/Etra/ CCAB ASDs (15% of each drug) and TPGS Rit/Efa/Etra/CMCAB ASD for 8h (pH 6.8, 37°C). Error bars indicate one standard deviation (n = 3) and only Rit concentration was presented in this figure.

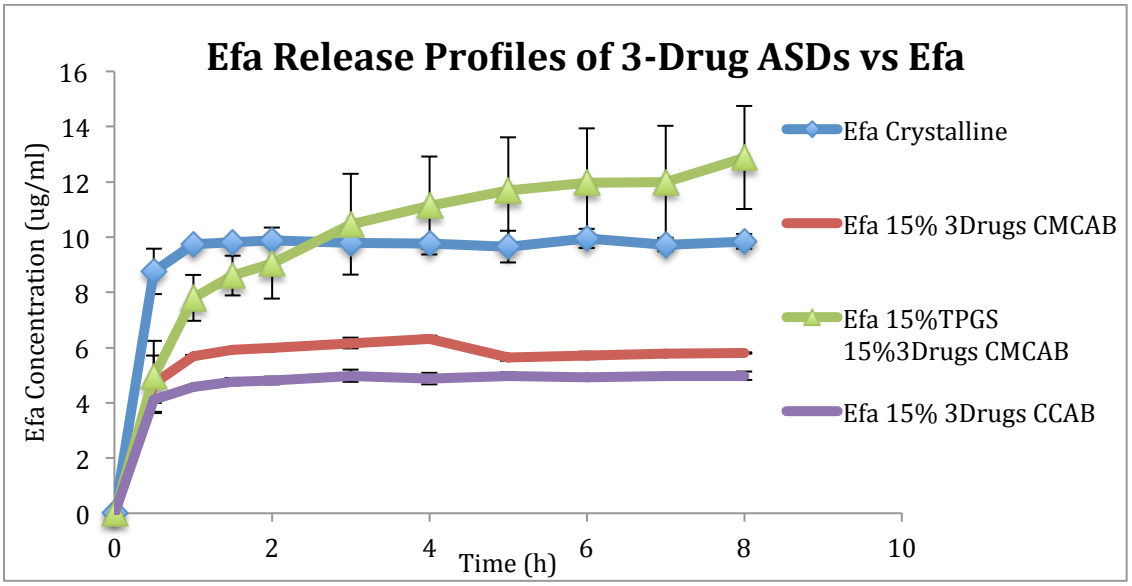

Figure 5.7: Dissolution profiles of crystalline Efa, Rit/Efa/Etra/CMCAB ASD, Rit/Efa/Etra/CCAB ASDs (15% each drug) and TPGS Rit/Efa/Etra/CMCAB ASD for 8h (pH 6.8, 37°C). Error bars indicate one standard deviation (n = 3) and only Efa solution concentration was presented in this figure.

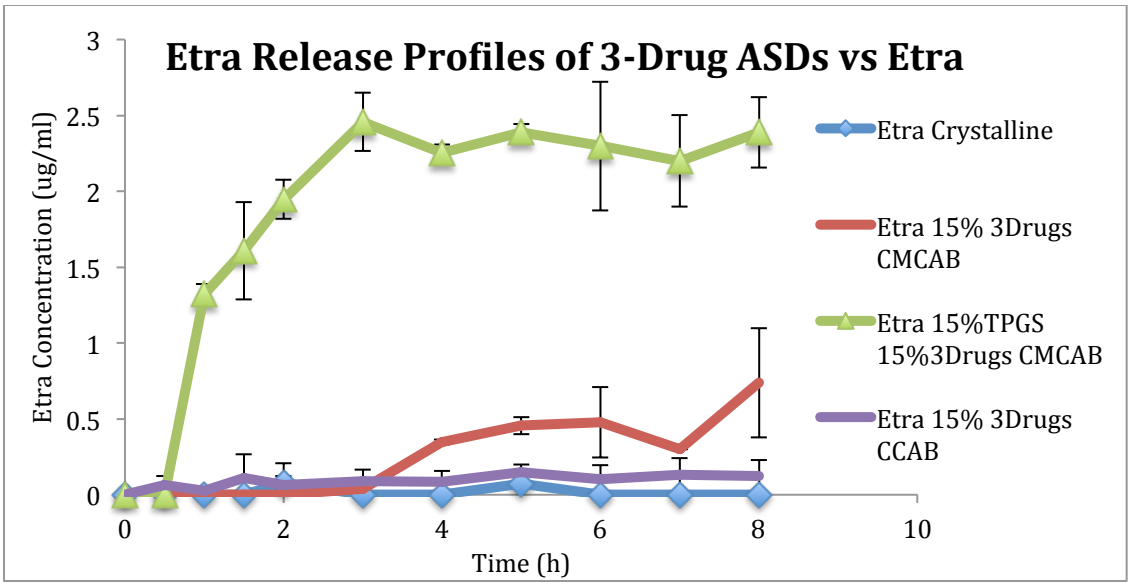

Figure 5.8: Dissolution profiles of crystalline Etra, Rit/Efa/Etra/CMCAB ASD, Rit/Efa/Etra/ CCAB ASDs (15% each drug) and TPGS Rit/Efa/Etra/CMCAB ASD for 8h (pH 6.8, 37°C). Error bars indicate one standard deviation (n = 3) and only Etra concentration was presented in this figure.

5.4.2.2 Three drug formulations of omega-carboxyl esters (n=3) compared with crystalline drug:

The dissolution results of three drugs containing CAAdP ASD and CASub ASD, and crystalline drugs (for comparison) were presented for Rit, Efa and Etra solution concentrations in **Figure 5.9, 5.10** and **5.11**, respectively. During the experiment, each dissolution flask contains all three drugs together for 8h at pH 6.8 similar to the protocol of 3.2.1 formulations.

The polymer dependent increase of Rit and Efa solution concentrations from CAAdP and CASub ASDs generated immediate release and stabilized the concentration for 8h. On the other hand, Etra has a continuous release profile from CAAdP ASD.

As presented on **Figure 5.9**, Rit solution concentration of CAAdP ASD was 1.45 fold higher than the crystalline drug itself but interestingly CASub ASD did not perform

better than the crystalline drug in spite of its amorphous morphology. The release profile trend of Rit is similar to that of Etra, where the Etra solution concentration of the CAAdP ASD (2 μg/ml) was higher than that of the crystalline drug and the CASub ASD, which was not different than the crystal Etra. On the other hand, the Efa solution concentration of the CAAdP ASD was similar to the crystalline drug (9.9 μg/ml) while the concentration was lower from the CASub ASD (6.7 μg/ml). According to these results, three drugs CAAdP ASD was the best formulation among all the three drugs formulations (without surfactant) to increase the drug solubility since both Rit and Etra concentrations were higher than the crystalline drugs and, the amorphous Efa concentration was similar to the drug itself. Although three drugs CMCAB ASD has higher Rit solution concentration than the three drugs CAAdP ASD, the Efa and Etra releases were lower from the CMCAB formulation.

Although the drugs were amorphous in ASD formulations, it was interesting to observe the concentrations lower than the crystalline drugs in some cases. Besides, when we compared the measured amorphous concentrations of the drugs from the three drug ASDs with the literature values (**Table 5.1**), the recorded concentrations were lower. Therefore, single drug and double drug CMCAB ASD formulations (**Figures 5.12-5.14**) were prepared to understand why the three drug formulations were leading to lower solution concentrations.

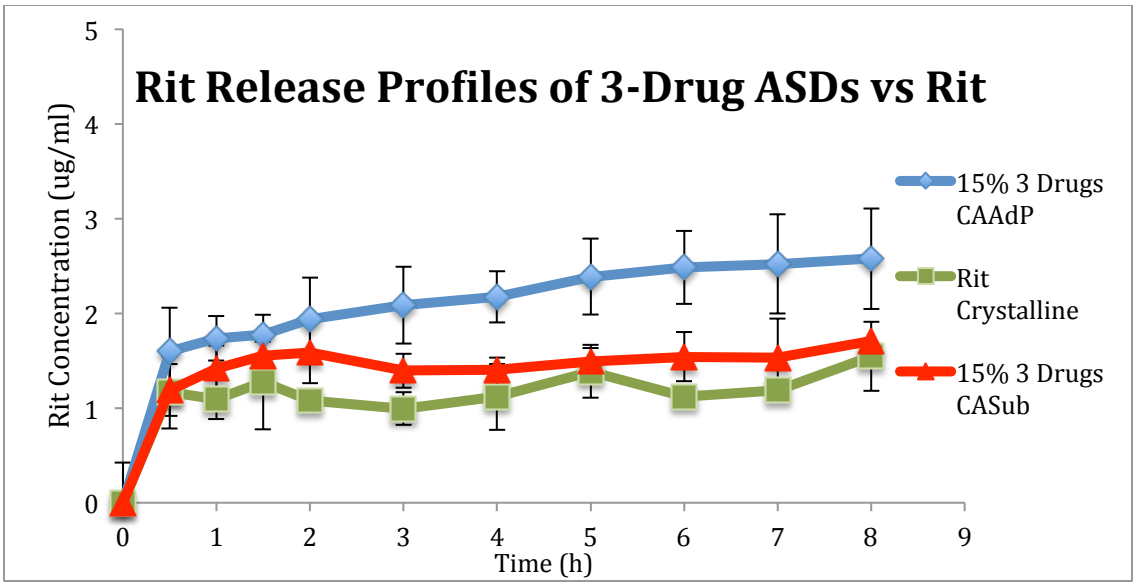

Figure 5.9: Dissolution profiles of crystalline Rit and Rit/Efa/Etra/CASub or CAAdP ASDs (15% each drug) for 8h (pH 6.8, 37°C). Error bars indicate one standard deviation (n = 3) and only Rit solution concentration was presented in this figure.

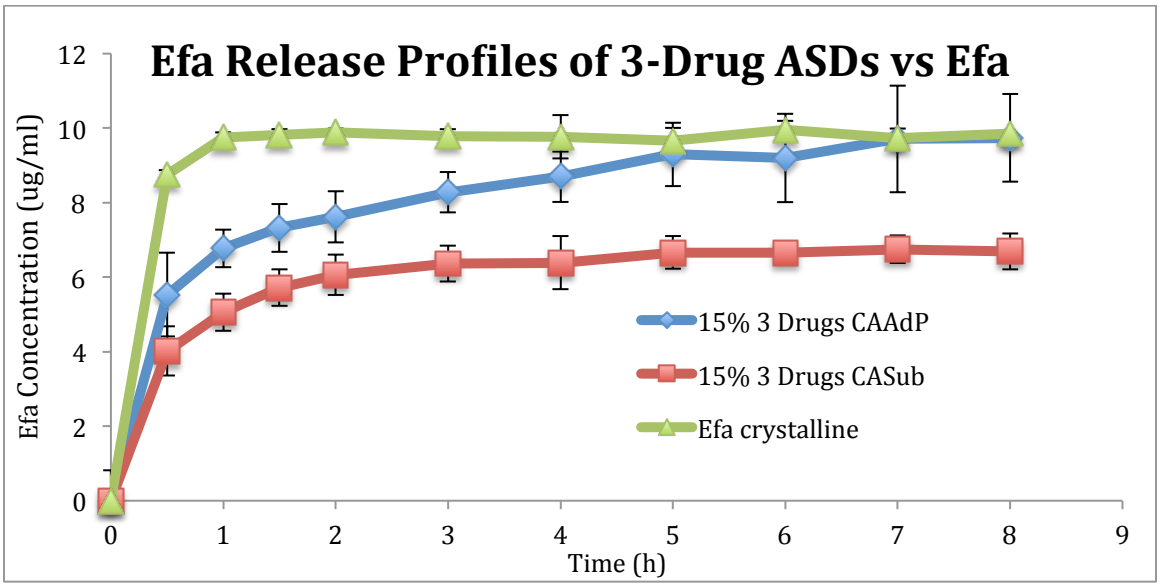

Figure 5.10: Dissolution profiles of crystalline Efa and Rit/Efa/Etra/CASub or CAAdP ASDs (15% each drug) for 8h (pH 6.8, 37°C). Error bars indicate one standard deviation (n = 3) and only Efa concentration was presented in this figure.

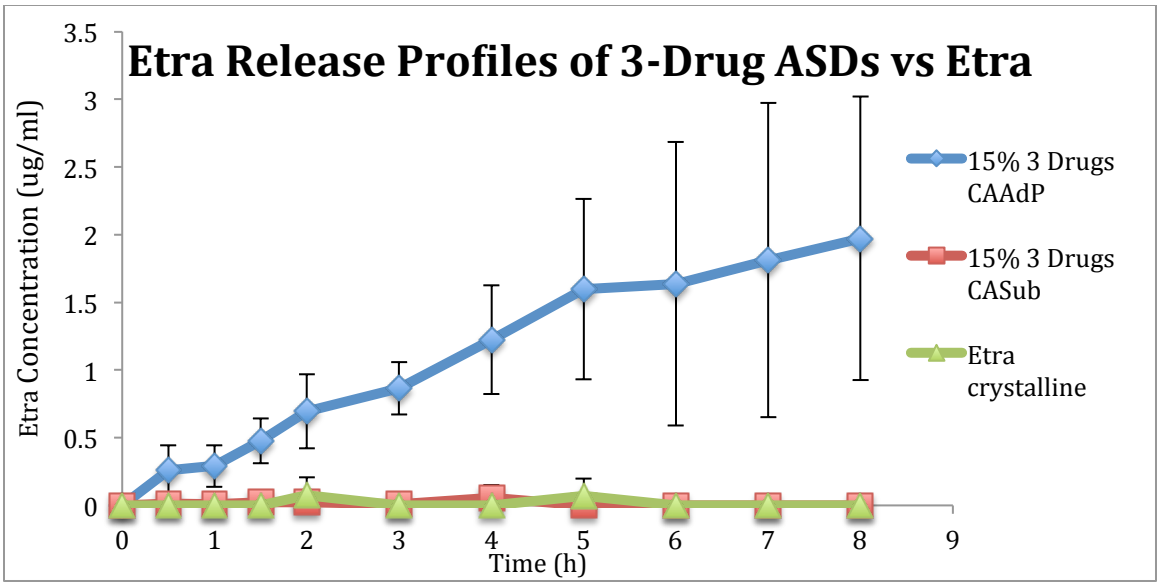

Figure 5.11: Dissolution profiles of crystalline Etra and Rit/Efa/Etra/CASub or CAAdP ASDs (15% each drug) for 8h (pH 6.8, 37°C). Error bars indicate one standard deviation (n = 3) and only Etra concentration was presented in this figure.

5.4.2.3 Single and double drug formulations (n=3) compared with crystalline drug:

The dissolution results of single and double drugs containing CMCAB ASDs and, crystalline drugs (for comparison) were presented for Rit, Efa and Etra solution concentrations in **Figure 5.12**, **5.13** and **5.14**, respectively.

Rit concentration from the 15% Rit CMCAB (single drug ASD) formulation reached to 20 µg/ml, similar to the reported amorphous concentration values (**Table 5.1**). On the other hand, the solution concentration of the 15% Rit 15% Etra and 15% Rit 15% Efa formations could not reach to this concentration, recorded 12.95 µg/ml and 5.7 µg/ml, respectively (**Figure 5.12**). The decrease in the concentration of the Rit might be explained with the solubility suppression by the second drug; since the solution cannot maintain high concentrations of the both drugs that might limit releasing and dissolving high content of them together. However, the single drug formulation can achieve the highest amorphous solution concentration of the drug, which shows that the ASD has the capability to reach to this concentration in the provided dissolution conditions but not the two drug formulations. Another interesting point about the drug interactions in the multi

drug systems is that the higher Rit concentration of 15% Rit 15% Etra ASD than 15% Rit 15% Efa ASD might be related with the solubility differences between the Etra and Efa, where the lower solubility of Etra might allow higher concentrations of Rit while relatively more soluble Efa does not. Moreover, dissolution results of three drug formulations support the idea, where the Rit concentration was lower than the 2 drug formulations, 5 μg/ml, that might be result of the two-drug solubility suppression effect leading to a lower Rit concentration.

Efa two drug formulations follow the same trend with the Rit dissolution profiles, as presented on **Figure 5.13**. 15% Efa 15% Etra has higher Efa solution concentration than 15% Efa 15% Rit CMCAB ASD that might be related with the lower solubility of Etra than Rit, limiting the suppression of the Efa and leading to higher concentration of Efa. Besides, 15% Efa CMCAB ASD and 15%Efa 15% Etra CMCAB ASD has similar dissolution profiles which implies that Etra does not have a drastic negative effect on the solubility of Efa, unlike Rit (**Figure 5.13**). Moreover, the comparison between the three drugs CMCAB ASD (**Figure 5.7**) and the 15% Rit 15% Efa CMCAB ASD dissolution (**Figure 5.13**) profiles support this idea where the addition of Etra to the formulation did not effect the concentration of Efa (5.7 μg/ml). However, Rit addition decreased the Efa concentration drastically.

Unlike Efa and Rit, all of the Etra ASD formulations had a continuous release for 8h and multi drug formulations had a positive effect on Etra solubility as shown on **Figure 5.14**. The single drug CMCAB ASD had a higher Etra concentration (0.35 μg/ml) than the crystalline Etra but lower than the two drug formulations, 15% Etra 15%Efa CMCAB and 15% Etra 15% Rit CMCAB, 0.79 μg/ml and 1.15 μg/ml, respectively. According to the dissolution profiles and final concentration, addition of Rit and Efa increased the Etra concentration separately. Moreover, three drug formulations had a higher Etra solution concentration than the two drug ASD formulations, implying that both Rit and Efa are increasing the solution concentration of Etra.

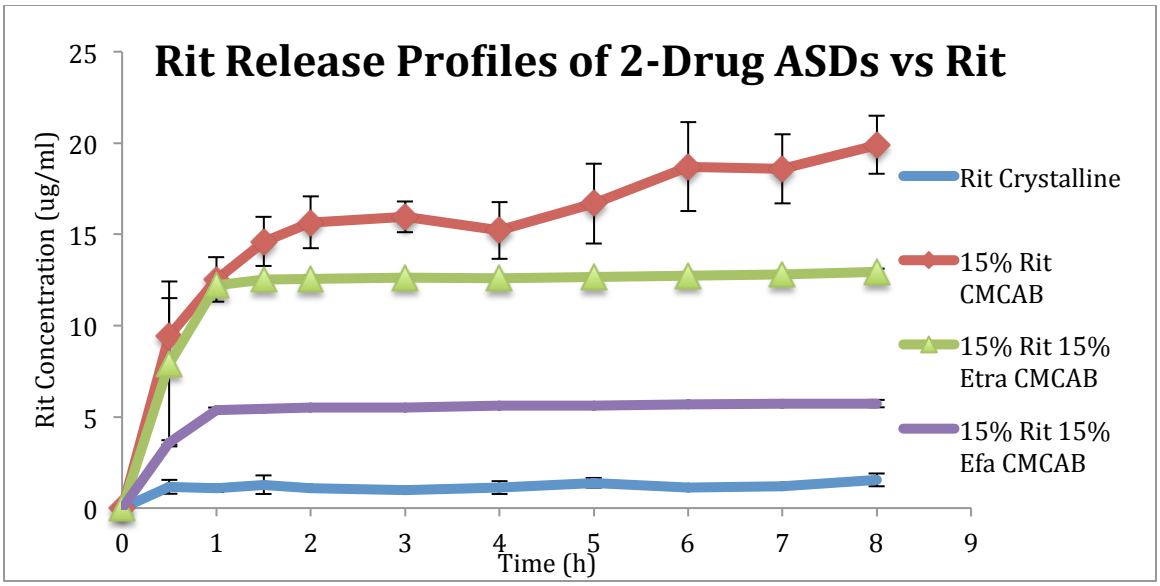

Figure 5.12: Dissolution profiles of crystalline Rit, 15% Rit CMCAB ASD and 2-drug CMCAB ASDs (15% of each drug) were presented for 8h (pH 6.8, 37°C). Error bars indicate one standard deviation (n = 3) and only Rit concentrations were presented in this figure.

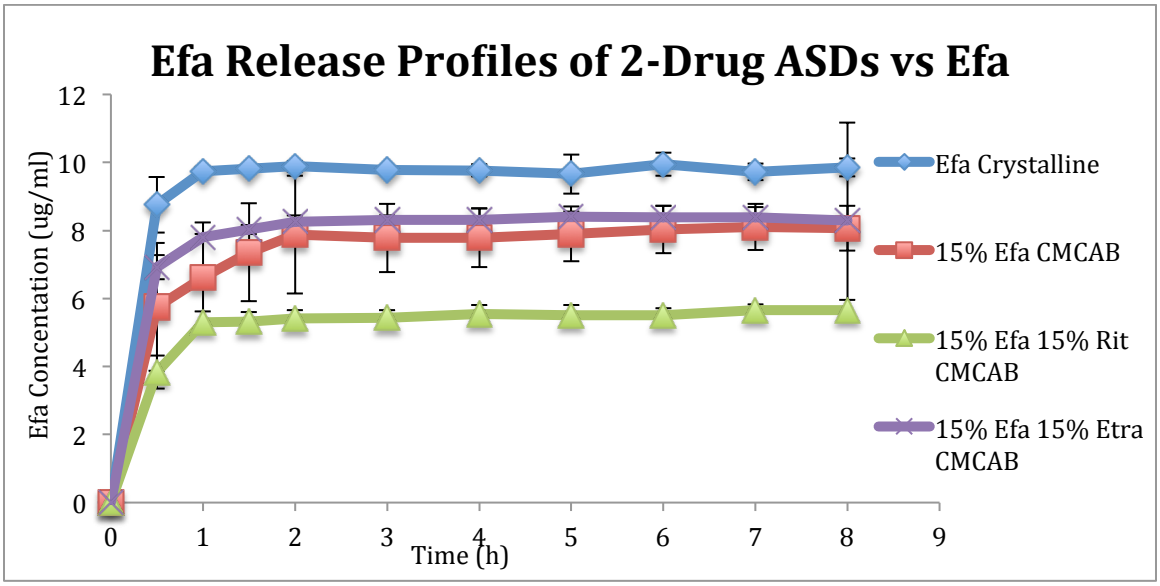

Figure 5.13: Dissolution profiles of crystalline Efa, 15% Efa CMCAB ASD and 2-drug CMCAB ASDs (15% of each drug) were presented for 8h (pH 6.8, 37°C). Error bars indicate one standard deviation (n = 3) and only Efa concentrations were presented in this figure.

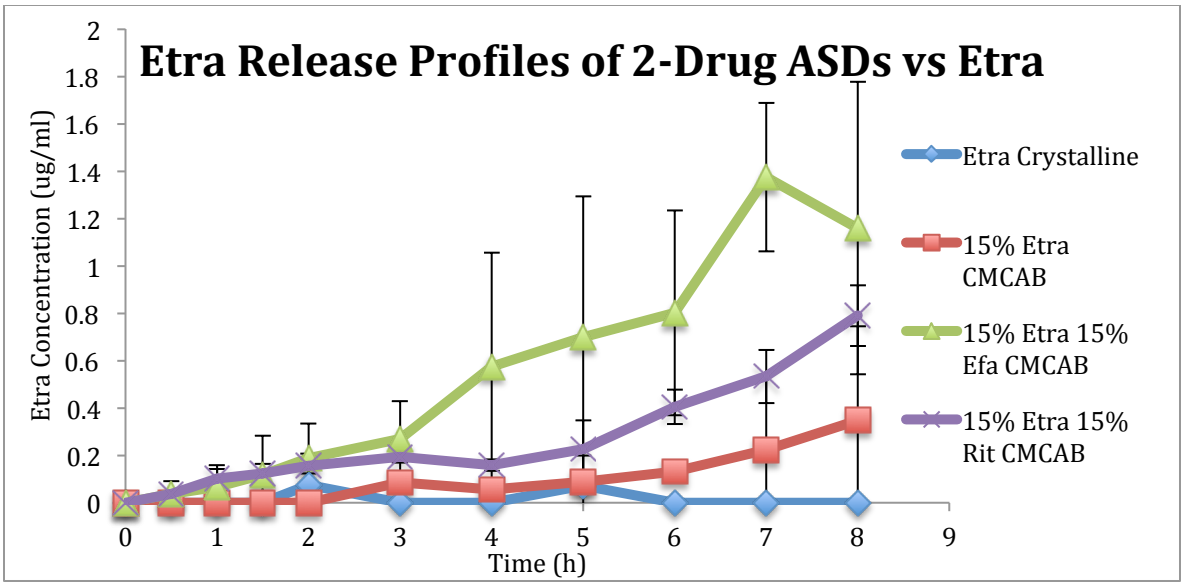

Figure 5.14: Dissolution profiles of crystalline Etra, 15% Etra CMCAB ASD and 2-drug CMCAB ASDs (15% of each drug) were presented for 8h (pH 6.8, 37°C). Error bars indicate one standard deviation (n = 3) and only Etra concentrations were presented in this figure.

5.4.2.4 Single drug ASD addition into another single drug ASD dissolution vs. single drug ASD Dissolution to understand drug solubility effect on Rit and Efa:

As shown on the previous sections, Rit and Efa solution concentrations of multidrug ASDs were lower than the Rit and Efa single drug formulations (**Figure 5.6, 5.7, 5.9, 5.10, 5.12** and **5.13**), independent of the polymer. The idea of Efa and Rit solution concentrations were suppressed in multidrug systems can be challenged with the approach that the drug release can be blocked by the drug to drug or drug to polymer interactions in the ASD and, as a result of that drugs might not be able to released. To be able to eliminate the concerns about the release properties of the ASD formulations, a new set of experiments were designed, where a single drug ASD was tested first for 8h to release the drug and reach to the highest amorphous solution concentration, 19.9 µg/ml for Rit and 8 µg/ml for Efa. Then another single drug ASD was added to the formulation that contains a different drug than the first formulation to observe the second drug effect on the released one. Finally, the concentrations of both drugs were recorded for another 8h (**Figure 5.15**, **5.16**, **5.17** and **5.18**).

Efa and Etra effect on Rit solution concentration were presented on **Figure 5.15** and **5.16**. As shown on both of the graphs, Rit was released from ASD, reached to the concentration of 19.9 μg/ml after 8h, then either 15% Efa 85% CMCAB or 15% Etra 85% CMCAB formulation were added. After that Rit concentration was decreased immediately as the second drug concentration was increasing. These results shows that solution cannot maintain the amorphous concentrations of the two drugs together that leads to the reduction of the dissolved drug content. When Efa CMCAB ASD was added, Rit solution concentration was decreased to 8 μg/ml and when Etra CMCAB ASD was added, it was 15.3 μg/ml (**Figure 5.16**). If Etra concentration were higher (0.8 μg/ml), Rit concentration would be lower (12.9 μg/ml) (compare **Figure 5.12** and **5.14** with **Figure 5.16**), which gives us the control over the concentrations we would like to achieve. Moreover, Efa follows the same suppressing trend with Etra since it is also reducing the solution concentration of Rit. When Efa was dissolved (3.3 μg/ml), Rit concentration was decreased to 8 μg/ml from 19.9 μg/ml. In other words, both Etra and Efa can decrease the solution concentration of Rit. As Etra or Efa concentration gets higher, Rit solution concentration decreases.

Dissolved Efa behaves similar to Rit, since its concentration was also reduced when interacted with a second drug as shown on **Figures 5.17** and **5.18**. Firstly, 15% Efa 85% CMCAB ASD released the drug for 8h, reached the Efa concentration to 8.2 μg/ml, then either 15% Rit 85% CMCAB or 15% Etra 85% CMCAB formulations were added, after that Efa concentrations were decreased to 3.5 μg/ml and 4.8 μg/ml, respectively. Since the drugs were released first, the lower concentrations were not related with the release abilities of the ASDs, but the solubility suppression effect of the drugs. These results explain why the solution concentrations of the three drug formulations showed lower Efa and Rit concentrations then the single formulations.

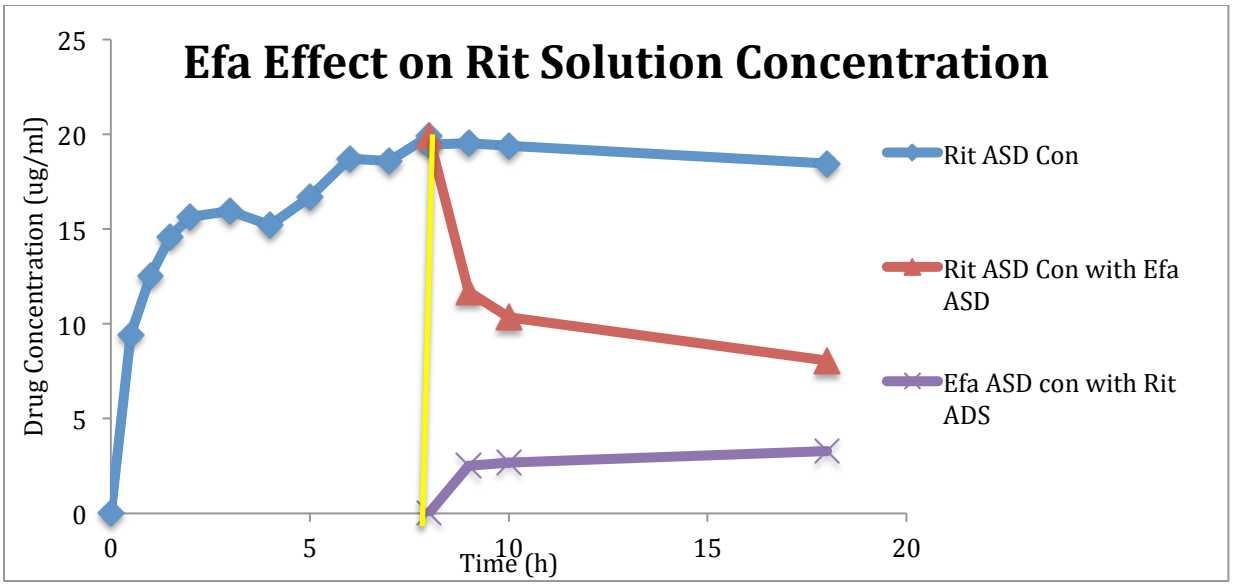

Figure 5.15: Dissolution at pH 6.8 started with 15% Rit CMCAB ASD formulation. After 8h, 15% Efa CMCAB ASD was added to 15% Rit CMCAB ASD and, Efa (purple) and Rit (Red) concentrations were recorded for another 8h. 15% Rit CMCAB ASD release was presented (blue) for 16h for comparison.

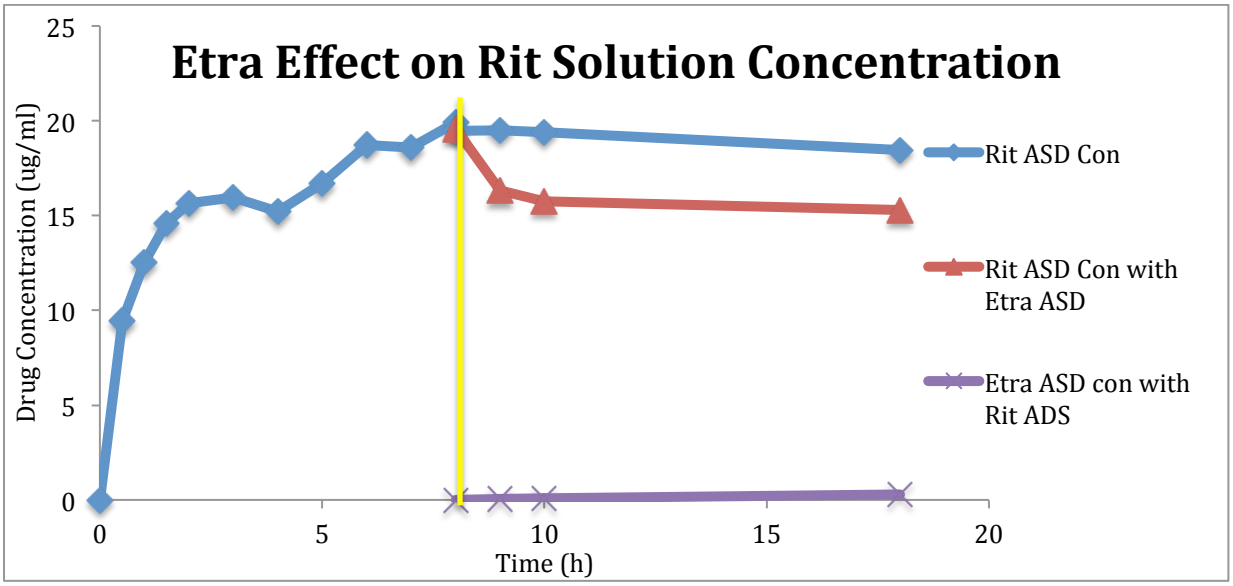

Figure 5.16: Dissolution at pH 6.8 started with 15% Rit CMCAB ASD formulation. After 8h, 15% Etra CMCAB ASD was added to 15% Rit CMCAB ASD and, Etra (purple) and Rit (Red) concentrations were recorded for another 8h. 15% Rit CMCAB ASD release was presented (blue) for 16h for comparison.

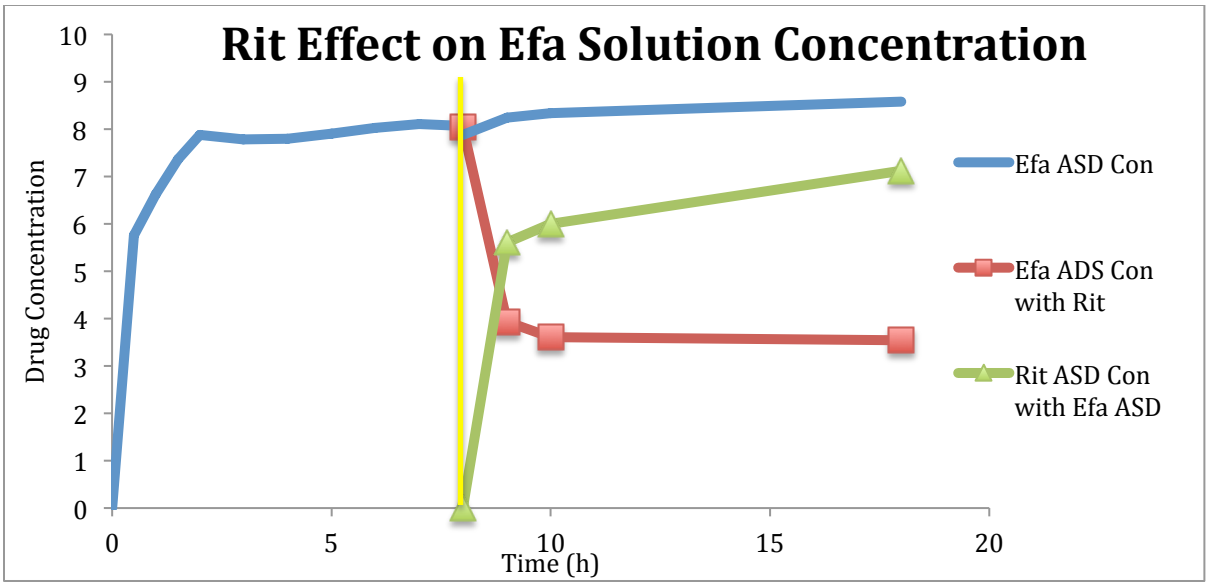

Figure 5.17: Dissolution at pH 6.8 started with 15% Efa CMCAB ASD formulation. After 8h, 15% Rit CMCAB ASD was added to 15% Efa CMCAB ASD and, Efa (red) and Rit (green) concentrations were recorded for another 8h. 15% Efa CMCAB ASD release was presented (blue) for 16h for comparison.

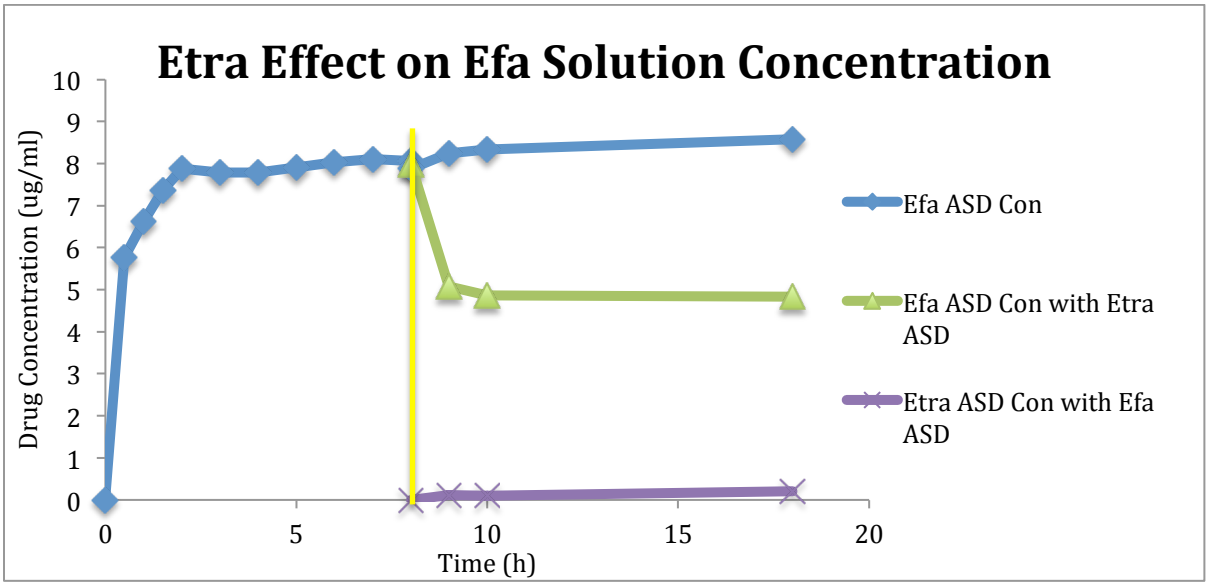

Figure 5.18: Dissolution at pH 6.8 started with 15% Efa CMCAB ASD formulation. After 8h, 15% Etra CMCAB ASD was added to 15% Efa CMCAB ASD and, Efa (green) and Etra (purple) concentrations were recorded for another 8h. 15% Efa CMCAB ASD release was presented (blue) for 16h for comparison.

5.5 Conclusions

It was shown that three drug ASD formulations can be prepared with a very high drug content (45%) and the amorphous morphology can be obtained with all of the cellulose derivatives even after the addition of TPGS. Moreover, we showed that the three drug formulations have higher Rit and Etra solution concentrations from ASDs than the crystalline Rit and Etra. Among the three drug formulation dissolution studies, CAAdP has highest solution concentrations of the three drugs combined without the use of surfactant. Besides, addition of TPGS can further increase the solution concentration of the three drugs.

We also tested two drug and single drug formulations to understand drug to drug suppression effect and concluded that Rit and Efa concentrations decreases when Etra, Efa or Rit was added to the dissolution since two or more drugs can not be dissolved at the higher concentrations together but they suppressed each others solubility. On the other hand, Rit and Efa increased Etra solution concentration.

We also know that as the second drug concentration (Rit, Efa or Etra) was increasing, Efa and Rit concentrations were decreasing that limits the highest drug concentration of multi drug formulations. In other words, we can have the control to decide the concentrations of the drugs such as increase Rit concentration to decrease Efa solution concentration. However, we need more investigation to understand how the drug-to-drug interaction is progressing, what is the role of polymer in preventing the decrease of concentrations and also how different is the suppression effect of one drug than the other.

5.6 Acknowledgments

We thank the Eastman Chemical Company for their kind donations of the cellulose ester starting materials. We thank Macromolecules and Interfaces Institute and the Institute for Critical Technologies and Applied Science at Virginia Tech for their support, facilities and funding. We also thank Steve McCartney (Nanoscale Characterization and Fabrication Laboratory, Virginia Tech) for his help in taking SEM images, and Ann Noris (Sustainable Biomaterials, Virginia Tech) for XRD study.

5.7 References

(1) WHO-HIV Department. Global Summary of the AIDS Epidemic http://www.who.int/hiv/data/epi_core_dec2014.png?ua=1.

(2) Gallo, R. C.; Montagnier, L. Prospects for the Future. *Science (80-.).* **2002**, *298*, 1730–1731.

(3) Mehellou, Y.; De Clercq, E. Twenty-Six Years of Anti-HIV Drug Discovery: Where Do We Stand and Where Do We Go? *J. Med. Chem.* **2010**, *53*, 521–538.

(4) Fauci, A. S. HIV and AIDS: 20 Years of Science. *Nat. Med.* **2003**, *9*, 839–843.

(5) Clavel, F.; Hance, A. J. HIV Drug Resistance. *N Engl J Med* **2004**, *350*, 1023–1035.

(6) Vandamme, A. M.; Van Vaerenbergh, K.; De Clercq, E. Anti-Human Immunodeficiency Virus Drug Combination Strategies. *Antivir. Chem. Chemother.* **1998**, *9*, 187–203.

(7) Gulick, R.; Mellors, J.; Havlir, D.; Eron, J. J.; Gonzalez, C.; McMahon, D.; Richman, D.; Valentine, F.; Jonas, L.; Meibohm, A. Treatment with Indinavir, Zidovudine, and Lamivudine in Adults with Human Immunodeficiency Virus Infection and Prior Antiretroviral Therapy — NEJM. *N Engl J Med* **1997**, *337*, 734–739.

(8) Hammer, S. M.; Squires, K. E.; Hughes, M. D.; Grimes, J. M.; Demeter, L. M.; Currier, J. S.; Eron, J.; Feinberg, J. E.; Balfour, H. H.; Deyton, L. R.; Chodakewitz, J. A.; Fischl, M. A.; John P. Phair, Pedneault, L.; NguyenBach-Yen; Cook, J. C. A Controlled Trial of Two Nucleoside Analogues plus Indinavir in Persons with Human Immunodeficiency Virus Infection and CD4 Cell Counts of 200 per Cubic Millimeter or Less — NEJM. *N Engl J Med* **1997**, *337*, 725–733.

(9) Meyerhans, A.; Cheynier, R.; Albert, J.; Seth, M.; Kwok, S.; Sninsky, J.; Morfeldt-Månson, L.; Asjö, B.; Wain-Hobson, S. *Temporal Fluctuations in HIV Quasispecies in Vivo Are Not Reflected by Sequential HIV Isolations.*; 1989; Vol. 58, pp 901–910.

(10) Scholler-Gyure, M.; Kakuda, T. N.; Raoof, A.; De Smedt, G.; Hoetelmans, R. M. Clinical Pharmacokinetics and Pharmacodynamics of Etravirine. *Clin Pharmacokinet* **2009**, *48*, 561–574.

(11) HIV Treatment FDA Apprved HIV Medicines http://aidsinfo.nih.gov/education-materials/fact-sheets/21/58/fda-approved-hiv-medicines.

(12) Ammassari, A.; Murri, R.; Pezzotti, P.; Trotta, M. P.; Ravasio, L.; De Longis, P.; Lo Caputo, S.; Narciso, P.; Pauluzzi, S.; Carosi, G.; Nappa, S.; Piano, P.; Izzo, C. M.; Lichtner, M.; Rezza, G.; Monforte, A.; Ippolito, G.; d'Arminio Moroni, M.; Wu, A. W.; Antinori, A. Self-Reported Symptoms and Medication Side Effects Influence Adherence to Highly Active Antiretroviral Therapy in Persons with HIV Infection. *J. Acquir. Immune Defic. Syndr.* **2001**, *28*, 445–449.

(13) De Clercq, E. Anti-HIV Drugs: 25 Compounds Approved within 25 Years after the Discovery of HIV. *Int. J. Antimicrob. Agents* **2009**, *33*, 307–320.

(14) Vasconcelos, T.; Sarmento, B.; Costa, P. Solid Dispersions as Strategy to Improve Oral Bioavailability of Poor Water Soluble Drugs. *Drug Discov Today* **2007**, *12*, 1068–1075.

(15) Sharma, P.; Garg, S. Pure Drug and Polymer Based Nanotechnologies for the Improved Solubility, Stability, Bioavailability and Targeting of Anti-HIV Drugs. *Adv. Drug Deliv. Rev.* **2010**, *62*, 491–502.

(16) Rajput, L.; Sanphui, P.; Desiraju, G. R. New Solid Forms of the Anti-HIV Drug Etravirine: Salts, Cocrystals, and Solubility. *Cryst. Growth Des.* **2013**, *13*, 3681–3690.

(17) Sosnik, A.; Chiappetta, D. A.; Carcaboso, A. M. Drug Delivery Systems in HIV Pharmacotherapy: What Has Been Done and the Challenges Standing Ahead. *J. Control. Release* **2009**, *138*, 2–15.

(18) Pereira, J. M.; Mejia-Ariza, R.; Ilevbare, G. A.; McGettigan, H. E.; Sriranganathan, N.; Taylor, L. S.; Davis, R. M.; Edgar, K. J. Interplay of Degradation, Dissolution and Stabilization of Clarithromycin and Its Amorphous Solid Dispersions. *Mol Pharm* **2013**, *10*, 4640–4653.

(19) Guo, Y.; Luo, J.; Tan, S.; Otieno, B. O.; Zhang, Z. The Applications of Vitamin E TPGS in Drug Delivery. *Eur. J. Pharm. Sci.* **2013**, *49*, 175–186.

(20) Varma, M. V. S.; Panchagnula, R. Enhanced Oral Paclitaxel Absorption with Vitamin E-TPGS: Effect on Solubility and Permeability in Vitro, in Situ and in Vivo. *Eur. J. Pharm. Sci.* **2005**, *25*, 445–453.

(21) Tang, X.; Liang, Y.; Feng, X.; Zhang, R.; Jin, X.; Sun, L. Co-Delivery of Docetaxel and Poloxamer 235 by PLGA-TPGS Nanoparticles for Breast Cancer Treatment. *Mater. Sci. Eng. C. Mater. Biol. Appl.* **2015**, *49*, 348–355.

(22) Pooja, D.; Kulhari, H.; Singh, M. K.; Mukherjee, S.; Rachamalla, S. S.; Sistla, R. Dendrimer-TPGS Mixed Micelles for Enhanced Solubility and Cellular Toxicity of Taxanes. *Colloids Surf. B. Biointerfaces* **2014**, *121*, 461–468.

(23) De Melo-Diogo, D.; Gaspar, V. M.; Costa, E. C.; Moreira, A. F.; Oppolzer, D.; Gallardo, E.; Correia, I. J. Combinatorial Delivery of Crizotinib-Palbociclib-Sildenafil Using TPGS-PLA Micelles for Improved Cancer Treatment. *Eur. J. Pharm. Biopharm.* **2014**, *88*, 718–729.

(24) Kar, N.; Liu, H.; Edgar, K. J. Synthesis of Cellulose Adipate Derivatives. *Biomacromolecules* **2011**, *12*, 1106–1115.

(25) Haoyu Liu Benjamin P. Cherniawski, Earl T. Ritchie, Lynne S. Taylor, Kevin J. Edgar, G. A. I. Synthesis and Structure–property Evaluation of Cellulose Ω-Carboxyesters for Amorphous Solid Dispersions. *Carbohydr Polym* **2012**.

(26) Qi, S.; Weuts, I.; De Cort, S.; Stokbroekx, S.; Leemans, R.; Reading, M.; Belton, P.; Craig, D. Q. An Investigation into the Crystallisation Behaviour of an Amorphous Cryomilled Pharmaceutical Material above and below the Glass Transition Temperature. *J Pharm Sci* **2010**, *99*, 196–208.

(27) Sathigari, S. K.; Radhakrishnan, V. K.; Davis, V. A.; Parsons, D. L.; Babu, R. J. Amorphous-State Characterization of Efavirenz--Polymer Hot-Melt Extrusion Systems for Dissolution Enhancement. *J Pharm Sci* **2012**, *101*, 3456–3464.

Chapter 6. Synthesis and characterization of alkyl cellulose ω-carboxyesters for amorphous solid dispersion

Adapted from "Arca, H. C.; Mosquera-Giraldo, L. I.; Taylor, L. S.; Edgar, K. J. *Cellulose* 2016 Submitted."

6.1 Abstract

Poor drug solubility and consequently poor bioavailability are major impediments to new drug innovation (development of new drugs), and they limit the performance of many existing drugs. In recent years amorphous solid dispersion (ASD) has emerged as one of the most effective approaches for enhancing drug solution concentration, and thereby bioavailability, including in many marketed drug formulations. Recently efforts have been under way in several laboratories to design new ASD polymers, rather than relying on polymers that are already in FDA-approved formulations, but were not designed as ASD polymers. We describe here the design and synthesis of a new class of polymers, alkyl cellulose ω-carboxyesters, for ASD formulation. We synthesize these polymers by reaction of cellulose alkyl ethers with monoprotected (benzyl ester), monofunctional long chain acid chlorides, followed by protecting group removal using mild hydrogenolysis to form the target alkyl cellulose ω-carboxyalkanoate. These new amphiphilic polymers have high glass transition temperatures (T_g), tunable carboxyl content for controlling release pH and drug-polymer interactions, and certain members of this new group of amphiphilic cellulose ether esters are shown to be successful at forming ASDs with the important model drug ritonavir. These ASDs efficiently release ritonavir at small intestine pH, creating the maximum attainable amorphous solubility (20 mg/mL), and maintaining it for a time period substantially greater than normal residence time in the absorptive region of the stomach and small intestine. Members of this new class of alkyl cellulose ω-carboxyester amphiphiles show great potential as ASD polymers for enhancing oral bioavailability of otherwise poorly soluble drugs.

6.2 Introduction

Poor solubility of existing pharmaceutical active compounds significantly restricts their effectiveness, since drugs must be presented to the enterocytes in solution in order for

them to be absorbed. Poor solubility is also an important roadblock to the development of new active compounds, since by some estimates as many as 70% of compounds under development have poor water solubility [1]; this can lead to poor bioavailability and candidate failure. Formation of polymer/drug ASDs has become increasingly important in recent years as it is an effective method for increasing solubility of otherwise poorly soluble, crystalline drugs (Biopharmaceutical Classification System (BCS) Types II and IV) in order to increase bioavailability [2]. Successful ASD creates a molecular dispersion of drug in a polymer matrix, preventing drug crystallization in the solid phase, and eliminates the heat of fusion as an energy barrier to drug dissolution. Properly designed ASD polymers release the drug in response to an external stimulus (often the stimulus is the pH change in moving from the acidic stomach to the neutral small intestine), creating supersaturated drug solutions. These polymers should also have sufficient aqueous solubility so as to be able to interact with and stabilize the drug in solution after drug release, preventing premature de-supersaturation. These supersaturated solutions from ASDs thereby attack both major impediments to drug bioavailability recognized by the BCS; solubility and permeation (supersaturation from ASDs, unlike most other drug solubilization methods, increases the chemical potential of the drug across the epithelium and so enhances permeation)[3]. Certain polymer design elements are key to achieving adequate formulation stability [4]. Strong polymer-drug interactions (often via hydrogen bonding), good polymer-drug miscibility due to polymer hydrophobic groups and polymer moieties that promote specific polymer-drug interactions, and high polymer glass transition values (T_g) promote formulation stability [5,6]. In addition, the polymer should have a drug release mechanism, such as dissolution or swelling in water at neutral pH [7–9].

A few cellulose ether esters have been previously studied as ASD polymers. They could be advantaged, since ether linkages are stable under any physiological conditions, and since alkyl ether substituents are inherently more hydrophobic than their ester counterparts. Carboxymethylcellulose acetate butyrate (CMCAB) has been studied in various drug delivery formulations as a matrix, binder, coating material, or film former with poorly water-soluble drugs such as curcumin[10], glyburide, griseofulvin, and ibuprofen, where it can provide zero order release properties [11], as well as with more

water-soluble drugs such as rifampin [12] and fexofenadine HCl [13]. CMCAB is suitable for multiple ASD preparation methods such as solvent evaporation film casting [11], spray drying [12] and solvent rotary evaporation [11]. Although CMCAB has proven to be a promising ASD polymer, and has a number of attractive material properties (e.g. pH-responsive, high T_g, carboxyl content, fundamentally hydrophobic) for use in ASDs, the possibility of crosslinking during its synthesis creates a concern. CMCAB is synthesized by esterification of water-soluble carboxymethylcellulose (CMC) with carboxylic acid anhydrides in the presence of strong acid (e.g. sulfuric acid) catalyst. This type of methodology for synthesis of cellulose ether esters is problematic since it requires the desired esterification to proceed under strong acid catalysis on a polymer backbone that is polyfunctional with respect both to alcohol and acid groups; therefore crosslinking to form inter-chain ester linkages can lead to network formation, insolubility, and loss of processability. Such approaches should be avoided.

HPMCAS is a commercial cellulose ether ester of strong recent interest for use in ASDs. It is a water dispersible polymer at acidic pH due to its amphiphilic nature. On the other hand, at the neutral pH of the intestines, the succinate groups are ionized; as a result, HPMCAS is pH-responsive and has slight water-solubility at neutral pH (17.7 mg/ml at pH 6.8) [7]. With its balance of hydrophobic and hydrophilic groups, HPMCAS is miscible with many hydrophobic drugs, and forms strong specific hydrogen bond interactions. HPMCAS is also a high T_g polymer (T_g = 120 °C, MW 18,000) [12]. For these reasons, HPMCAS has been used in ASD formulations of drugs including indomethacin [14], itraconazole [14], curcumin [10], felodipine [15], nifedipine [16] and griseofulvin [14,17]. HPMCAS has been employed to formulate many pharmaceutical active materials [18–20] such as duloxetine [21]. HPMCAS is most often formulated into ASDs by spray-drying [10] and other solution methods [22], though recently investigations of HPMCAS hot melt extrusion have been reported [14]. It is important to note that HPMCAS has an extraordinarily complex structure as a result of its multiple functional groups and the fact that during reaction of cellulose with propylene oxide, oligo(hydroxypropyl) substituents of various lengths and compositions are appended, leading to a copolymer comprising an enormous number of different monosaccharides (certainly a much higher number than 7^3 (> 7 substituent types (-OH, -OCH_3, -$OCOCH_3$, -$OCH_2CH(OH)CH_3$, -$OCOCH_2CH_2COOH$, -

$OCH_2CH(OCOCH_3)CH_3$, $-OCH_2CH(OCOCH_2CH_2COOH)CH_3$) at the three hydroxyl positions), or 343 different monosaccharides). This makes it a remarkable challenge to analyze or have confidence in the detailed structure of a given HPMCAS polymer.

Previously, the Edgar group reported that cellulose w-carboxyesters containing adipate, suberate or sebacate groups were useful ASD polymers [23,24]. As the length of the hydrocarbon chain increases, polymer hydrophobicity increases, thus leading to increasing miscibility with hydrophobic drugs. In our previous studies, it was shown that cellulose acetate adipate propionate (CAAdP) and cellulose acetate suberate (CASub) were effective and efficient inhibitors of both crystal growth (G. A. Ilevbare, Liu, Edgar, & Taylor, 2012) and nucleation (Ilevbare, Liu, Edgar, & Taylor, 2013) of the hydrophobic anti-HIV drug, ritonavir [27]. We also showed that CAAdP and CASub were useful polymers for ASD formulation of a structurally diverse variety of other poorly soluble drugs including the flavonoids curcumin [10,28], quercetin [29] and resveratrol [8], and the macrolide antibiotics clarithromycin [7] and rifampicin [12,30]. These are very promising ASD polymers and the cited studies have provided significant insight into ASD polymer structure-property-performance relationships. However, the diversity of drug and drug candidate structures, increasingly challenging formulation requirements, and the need for deeper understanding of these fundamental relationships inspired us to seek further for even higher performance polymers, in particular further exploring the possibilities of cellulose ether esters.

In order to make cellulose ether esters, it is most practical to attach the ether groups first, then esterify, since etherification is always carried out under alkaline conditions that would saponify any ester groups present [31]. Appending ester substituents containing terminal carboxyl groups (e.g ω-carboxyalkanoate substituents) cannot be carried out by acid-catalyzed reaction of a cellulose ether with a dicarboxylic acid synthon, because this would result in crosslinking between pendent carboxyl and free hydroxyl groups. Most past methods for appending ω-carboxyalkanoate groups like succinate (McCormick, Dawsey, 1990) and phthalate [32] have involved ring opening of cyclic anhydrides under mild base catalysis, conditions that do not favor crosslinking. However, these methods are not possible for diacid chain lengths longer than C6 (adipate), because longer chain

lengths do not form stable cyclic anhydrides. Even adipic anhydride, though it can be synthesized and isolated, is a problematic electrophile for synthesis of cellulose ω-carboxyalkanoates because of its propensity for homopolymerization). Therefore our hypothesis is that by a two-step protocol; 1) esterification with a mono-benzyl protected, mono-activated dicarboxylic acid and 2) removal of the protecting group via hydrogenolysis, crosslinking can be avoided and a variety of cellulose ether ω-carboxyalkanoate esters can be synthesized. This protocol is analogous to the method that was successful for the synthesis of cellulose alkanoate ω-carboxyalkanoate esters in previous work from our laboratory [24]. We further hypothesize that these new amphiphilic cellulose ether ω-carboxyalkanoates will be of particular utility in ASD formulations, since they are in some cases based on cellulose ethers that are rather hydrophilic, and thus the ether ester products may be expected to have faster release rates than more hydrophobic derivatives that have been previously examined. We report herein the results of efforts to make such cellulose derivatives and of preliminary *in vitro* testing to determine their potential as ASD polymers.

6.3 Experimental

6.3.1 Materials

Methylcellulose (MC) (M_n= 40,000; manufacturer reported DS(Me) = 1.6 - 1.9) was obtained from Sigma-Aldrich (Saint Louis, MO) and ethyl cellulose (manufacturer reported 48 - 49.5% ethoxy content; DS(Et) = 2.46 - 2.58; 5% (wt.) concentration of the polymer has 40-52 cps viscosity at 25°C) (commercial name EC-N50 PHARM, abbreviated EC in this manuscript) were from Ashland Inc., Wilmington, DE. Polymers were dried under reduced pressure at 50°C overnight prior to use. Other purchased reagents were used as received. Suberic acid, sebacic acid, adipic acid, methyl ethyl ketone (MEK), *p*-toluenesulfonic acid (PTSA), triethylamine (Et_3N), oxalyl chloride, anhydrous pyridine, phenyl isocyanate and tetrahydrofuran were purchased from Acros Organics (Pittsburgh, PA). Toluene, benzyl alcohol, *N*,*N*-dimethylformamide (DMF), dichloromethane, sodium hydroxide, potassium phosphate monobasic and sodium bicarbonate were purchased from Thermo Fisher Scientific (Asheville, NC). The

hydrogenolysis catalyst $Pd(OH)_2/C$ was obtained from Sigma–Aldrich (Saint Louis, MO) and ritonavir was purchased from Attix Pharmaceuticals (Toronto, Canada).

6.3.2 Methods

6.3.2.1 Hydroxyl group carbanilation

Carbanilation was conducted according to the procedure of Malm et al. [33]. Dried EC (0.5 g) was dissolved in 5 mL of anhydrous pyridine. Phenyl isocyanate (0.5 mL) was then added and stirred at 100°C for 2 h. After 2 h, the mixture was cooled to room temperature and added to 500 mL of water to precipitate the product. The precipitate was collected and dissolved in 10 mL of THF and re-precipitated in water. The product was re-dissolved and precipitated four times. When the purification was over, the white product was dried in a vacuum oven at 50°C overnight.

Ethyl cellulose carbanilate: ^{1}H NMR ($CDCl_3$): 1.14 (CH_3 of ethyl group), 3.00–5.20 (cellulose backbone and CH_2 of ethyl group), 6.8-7.6 (C_6H_5).

A similar protocol was followed for carbanilation of MC. MC (0.1 g) dissolved in 5 mL dry pyridine and reacted with 0.5 mL of phenyl isocyanate at 100°C for 2 h. After the reaction, the polymer was precipitated in 500 mL of ethanol, washed with 500 mL of water, dissolved in 10 mL of THF and re-precipitated in 500 mL of ethanol.

Methyl cellulose carbanilate: ^{1}H NMR ($CDCl_3$): 3.00–5.20 (cellulose backbone and CH_3 of methyl group), 6.8-7.6 (C_6H_5).

6.3.2.2 Synthesis of monobenzyl adipate

Monobenzyl adipate was prepared according to the procedure of Kar [23]. Adipic acid (73 g, 0.5 mol), benzyl alcohol (81 g, 0.75 mol), PTSA (0.95 g, 5 mmol), and toluene (200 mL) were combined in a one neck flask equipped with a Dean-Stark trap, and the resulting solution was heated at reflux for approximately 4 h. The mixture was heated (above 110°C) until the theoretical amount of H_2O (13.5 mL, 0.75 mol) was obtained from the Fischer esterification of adipic acid that will form monobenzy adipate, dibenzyl

adipate and adipic acid (diacid). In order to separate monobenzyl adipate from the mixture, we used phase separation method at different pH environments. First, the solution was cooled to room temperature after the reaction, 200 mL of H_2O was added, and the pH was adjusted to 9.0 with 6N NaOH. By this means, dibenzyl adipate will stay in the organic solvent but ionized monobenzyl adipate and adipic acid will transfer to the aqueous layer (water). The aqueous layer was separated and washed with ether (2 X 100 mL) to remove dibenzyl adipate residues, then 200 mL of ethyl ether was added, and the pH of the aqueous layer was adjusted to 2.0 with 6N HCl. Thus the adipic acid stays in the water but the monobenzyl adipate transfers to the organic solvent. The ether layer was separated, and washed with 50 mL of 1M $NaHCO_3$ for 15 min to remove impurities. Then the ether layer was separated, concentrated under reduced pressure, and filtered. Monobenzyl adipate (41 % yield) was dried under vacuum at 40°C as a colorless oil: ^{1}H NMR ($CDCl_3$): 1.68 (m, 4 H), 2.36 (m, 4 H), 5.09 (s, 2 H), and 7.32 (m, 5 H).

Similar protocols were followed to synthesize monobenzyl sebacate (white solid, yield 31.35 g, 0.12 mol, 19% yield) and monobenzyl suberate (colorless oil, yield 16.96 g, 0.058 mol, 24% yield).

^{1}H NMR of monobenzyl suberate. ($CDCl_3$): 1.33 (m, 4H), 1.63 (m, 4H), 2.33 (m, 4H), 5.11 (s, 2H), 7.34 (m, 5H).

^{1}H NMR of monobenzyl sebacate ($CDCl_3$): 1.29 (m, 8H), 1.62 (m, 4H), 2.33 (m, 4H), 5.11 (s, 2H), 7.35 (m, 5H).

6.3.2.3 Synthesis of monobenzyl adipoyl chloride

Monobenzyl adipoyl chloride was prepared according to Liu [23,24]. Monobenzyl adipate (0.068 mol, 15.00 g) was dissolved in dichloromethane (300 mL) in a one-neck flask while stirring, then 5 drops of DMF was added. The solution was cooled in an ice bath to 0°C and oxalyl chloride (24.42 mL, 5.6 eq) was added slowly via an addition funnel. The ice bath was then removed and the solution stirred at room temperature. Completion of gas formation indicated the end of the reaction, at which point the solvent was removed

under reduced pressure. Toluene (15 mL) was added and the product was concentrated again under reduced pressure at 50°C for 1 h. Yield: 90% (0.04 mol, 13.5 g). ^{1}H NMR ($CDCl_3$): 1.73 (m, 4 H), 2.39 (t, 2 H), 2.90 (t, 2 H), 5.12 (s, 2 H), 7.32 (m, 5 H).

Similar procedures were followed to synthesize monobenzyl sebacoyl and monobenzyl suberoyl chlorides.

Monobenzyl sebacoyl chloride. Yield: 95% (0.046 mol, 14.35 g). ^{1}H NMR ($CDCl_3$): 1.30 (m, 8H), 1.67 (m, 4H), 2.35 (t, 2H), 2.86 (t, 2H), 5.11 (s, 2H), 7.35 (m, 5H).

Monobenzyl suberoyl chloride. Yield: 90% (0.051 mol, 14.54 g). ^{1}H NMR ($CDCl_3$): 1.34 (m, 4H), 1.66 (m, 4H), 2.36 (t, 2H), 2.86 (t, 2H), 5.12 (s, 2H), 7.35 (m, 5H).

6.3.2.4 Preparation of benzyl ethyl cellulose adipate/suberate/sebacate

EC (0.2 g, 0.887 mmol) was dissolved in DMF (20 mL), and the solution was heated to 90 °C with stirring under nitrogen. Triethylamine (1.25 mL, 8.87 mmol, 10 eq) was added to the solution. Monobenzyl adipoyl chloride (1.8 g, 7.096 mmol, 8 eq), monobenzyl suberoyl chloride (2.0 g, 7.096 mmol, 8 eq) or monobenzyl sebacoyl chloride (2.2 g, 7.096 mmol, 8 eq) was added dropwise and allowed to react at 90 °C for 20 h. The reaction mixture was cooled and transferred to pre-wetted dialysis tubing (MWCO 3500), then dialyzed against ethanol for 2 d, followed by dialysis against water for 1 d. The aqueous solution then was freeze-dried for 2 d.

Benzyl EC adipate (0.258 g, 0.75 mmol, yield 85%): ^{1}H NMR ($CDCl_3$): 1.14 (CH_3 of ethyl group), 1.33 (broad s, $COCH_2\underline{CH_2}\underline{CH_2}CH_2CO$ of adipate), 1.66 (broad s, $CO\underline{CH_2}CH_2CH_2\underline{CH_2}CO$ of adipate), 3.00–5.20 (cellulose backbone and CH_2 of ethyl group), 5.03 ($\underline{CH_2}C_6H_5$), 7.35 ($CH_2\underline{C_6H_5}$).

Benzyl EC suberate (0.262 g, 0.73 mmol, yield 83%): ^{1}H NMR ($CDCl_3$): 1.14 (CH_3 of ethyl group), 1.33 (broad s, $COCH_2CH_2\underline{CH_2}\underline{CH_2}CH_2CH_2CO$ of suberate), 1.66 (broad s, $COCH_2\underline{CH_2}CH_2CH_2\underline{CH_2}CH_2CO$ of suberate), 2.10–2.54 ($CO\underline{CH_2}CH_2CH_2CH_2CH_2\underline{CH_2}CO$ of suberate, 3.00–5.20 (cellulose backbone and CH_2 of ethyl group), 5.11 ($\underline{CH_2}C_6H_5$), 7.35 ($CH_2\underline{C_6H_5}$).

Benzyl EC sebacate (0.26 g, 0.69 mmol, yield 79%). ^{1}H NMR ($CDCl_3$): 1.14 (CH_3 of ethyl group), 1.30 ($COCH_2CH_2\underline{CH_2}\underline{CH_2}\underline{CH_2}\underline{CH_2}CH_2CH_2CO$ of sebacate), 1.63 ($COCH_2\underline{CH_2}CH_2CH_2CH_2CH_2\underline{CH_2}CH_2CO$ of sebacate), 2.13–2.44 ($CO\underline{CH_2}CH_2CH_2CH_2CH_2CH_2CH_2\underline{CH_2}CO$ of sebacate, 3.00–5.20 (cellulose backbone and CH_2 of ethyl group), 5.11 ($\underline{CH_2}C_6H_5$), 7.35 ($CH_2\underline{C_6H_5}$).

6.3.2.5 Preparation of benzyl methyl cellulose adipate/suberate/sebacate

MC (0.2 g, 1.07 mmol) was dissolved in DMF (20 mL), and the solution was heated to 90°C with stirring under nitrogen for 2 h. Triethylamine (1.5 mL, 10.7 mmol, 10 eq) was added to the solution. Monobenzyl adipoyl chloride (2.18 g, 8.55 mmol, 8 eq), monobenzyl suberoyl chloride (2.42 g, 8.55 mmol, 8 eq) or monobenzyl sebacoyl chloride (2.66 g, 8.55 mmol, 8 eq) was added dropwise and allowed to react at 90°C for 20 h. Then the reaction mixture was cooled and added to 400 mL ethanol to precipitate the product. The product was collected by filtration, redissolved in a minimal amount of THF and reprecipitated in 400 mL hexane. The product was recovered by filtration, then the precipitate was reslurried with 500 mL of water for 1 h and filtered. The filtered product was redissolved in a minimal amount of THF and reprecipitated into 400 mL ethanol. The product was collected by filtration, then was dried under reduced pressure at 50 °C overnight.

Benzyl MC adipate yield. (0.36 g, 0.84 mmol, 79 % yield). ^{1}H NMR (DMSO-d_6): 1.3 (broad s, $COCH_2\underline{CH_2}\underline{CH_2}CH_2CO$ of adipate), 1.66 (broad s, $CO\underline{CH_2}CH_2CH_2\underline{CH_2}CO$ of adipate), 3.00–5.20 (cellulose backbone and CH_3 of methyl group), 5.03 ($\underline{CH_2}C_6H_5$), 7.35 ($CH_2\underline{C_6H_5}$).

Benzyl MC suberate yield. (0.38 g, 0.842 mmol, 79 % yield). ^{1}H NMR (DMSO-d_6): 1.3 ($COCH_2CH_2\underline{CH_2}\underline{CH_2}CH_2CH_2CO$ of suberate), 1.6 ($COCH_2\underline{CH_2}CH_2CH_2\underline{CH_2}CH_2CO$ of suberate), 2.10–2.45 ($CO\underline{CH_2}CH_2CH_2CH_2CH_2\underline{CH_2}CO$ of suberate, 3.00–5.20 (cellulose backbone and CH_3 of methyl group), 5.11 ($CH_2C_6H_5$), 7.35 ($CH_2C_6H_5$).

Benzyl MC sebacate yield. (0.44 g, 0.96 mmol, 90 % yield). ^{1}H NMR (DMSO-d_6): 1.2 ($COCH_2CH_2\underline{CH_2CH_2CH_2CH_2}CH_2CH_2CO$ of sebacate), 1.45 ($COCH_2\underline{CH_2}CH_2CH_2CH_2CH_2\underline{CH_2}CH_2CO$ of sebacate), 2.05–2.52 ($CO\underline{CH_2}CH_2CH_2CH_2CH_2CH_2CH_2\underline{CH_2}CO$ of sebacate,, 3.00–5.20 (cellulose backbone and CH_3 of methyl group), 5.11 ($CH_2C_6H_5$), 7.35 ($CH_2C_6H_5$).

6.3.2.6 $Pd(OH)_2/C$ catalyzed hydrogenolysis of the benzyl ethyl cellulose ω-carboxyalkanoate esters and benzyl methyl cellulose adipate

In 100 mL of THF, 0.2 g of benzyl cellulose ether ester was dissolved and 200 mg of palladium hydroxide on carbon was added. Then the mixture was charged to a Parr reactor and hydrogenolysis was conducted under hydrogen at 120 psi for 2 d. After the reaction, the solution was filtered through Celite and concentrated under reduced pressure. The oil was precipitated in 400 mL hexane, collected by filtration, and dried at 50°C overnight. Yields and ^{1}H NMR spectral data of representative products are listed below.

Ethyl cellulose adipate (0.55 g, 0.23 mmol, 39% yield). ^{1}H NMR ($CDCl_3$): 1.14 (CH_3 of ethyl group), 1.33 (broad s, $COCH_2\underline{CH_2CH_2}CH_2CO$ of adipate), 1.66 (broad s, $CO\underline{CH_2}CH_2CH_2\underline{CH_2}CO$ of adipate), 3.00–5.20 (cellulose backbone and CH_2 of ethyl group).

Methyl cellulose adipate (0.042 g, 0.12 mmol, 26 % yield). ^{1}H NMR ($CDCl_3$): 1.3 (broad s, $COCH_2\underline{CH_2CH_2}CH_2CO$ of adipate), 1.61 (broad s, $CO\underline{CH_2}CH_2CH_2\underline{CH_2}CO$ of adipate), 3.00–5.20 (cellulose backbone and CH_3 of methyl group).

6.3.2.7 $Pd(OH)_2/C$ catalyzed hydrogenolysis of benzyl methyl cellulose suberate and sebacate

Benzyl methyl cellulose w-carboxyalkanoate (0.2 g) was dissolved in DMI (100 mL) in a round bottom flask with a magnetic stirrer, and 200 mg of palladium hydroxide on carbon was added. Then air in the flask was removed by vacuum, a balloon filled with hydrogen gas was attached, and hydrogenolysis was conducted at 55°C for 2 d. After 2d, the solution was filtered through Celite and new catalyst was added (200 mg). The same

protocol was repeated, with reaction time of 1 d. Then the catalyst was removed by filtration through Celite, and the filtrate concentrated under reduced pressure. The oil was precipitated in 400 mL hexane, the solid product isolated by filtration, and dried at 50°C overnight. Yields and ^{1}H NMR spectral data of a representative product are listed below.

Methyl cellulose suberate (0.035 g, 0.095 mmol, 22 % yield). ^{1}H NMR (DMSO-d_6): 1.33 ($COCH_2CH_2\underline{CH_2}\underline{CH_2}CH_2CH_2CO$ of suberate), 1.6 ($COCH_2\underline{CH_2}CH_2CH_2\underline{CH_2}CH_2CO$ of suberate), 2.10–2.45 ($CO\underline{CH_2}CH_2CH_2CH_2CH_2\underline{CH_2}CO$ of suberate, 3.00–5.20 (cellulose backbone and CH_3 of methyl group).

Methyl cellulose sebacate (0.045 g, 0.0117 mmol, 27 % yield). ^{1}H NMR (DMSO-d_6): 1.3 ($COCH_2CH_2\underline{CH_2}\underline{CH_2}\underline{CH_2}\underline{CH_2}CH_2CH_2CO$ of sebacate), 1.62 ($COCH_2\underline{CH_2}CH_2CH_2\underline{CH_2}CH_2CO$ of sebacate), 2.11–2.45 ($CO\underline{CH_2}CH_2CH_2CH_2CH_2\underline{CH_2}CO$ of sebacate, 3.00–5.20 (cellulose backbone and CH_3 of methyl group).

6.3.2.8 NMR Spectroscopy

^{1}H NMR spectra were acquired using 32 scans in DMSO-d_6 or $CDCl_3$ solvent (e.g. 5 mg/mL) on a Bruker Avance 500 spectrometer operating at 500 MHz at 25°C in standard 5 mm o.d. tubes. A drop of trifluoroacetic acid was added to DMSO-d_6 in order to shift the water peak downfield. ^{13}C NMR spectra were obtained on a Bruker Avance 500 spectrometer with a minimum of 15,000 scans at a concentration of 25-40 mg/mL, at 80°C.

6.3.2.9 FTIR

FTIR spectra were obtained using a Thermo Electron Nicolet 8700 instrument in transmission mode. Samples were prepared as KBr (90 mg) pellets with 1 mg of polymer by compressing in the sample holder between two screws to form a disk. Thirty-two scans were obtained for each spectrum.

6.3.2.10 Determination of polymer solubility in solvent

A sample of each ethyl cellulose derivative (3 mg) was dispersed in 2 mL of solvent (THF, acetone, methanol, ethanol, isopropanol, DMSO and DMAc) at 25°C and mixed

for 1 h. If the sample did not dissolve, the mixture was heated to the solvent boiling point, then kept stirring till it cooled to room temperature. Solubility was determined by visual observation of solution clarity.

6.3.2.11 Degree of polymerization determination

Protocol for EC derivatives: Size exclusion chromatography (SEC) was carried out in THF at 1 mL/min at 30°C on two Agilent PLgel 10 μm MIXED-B columns connected in series with a Wyatt Dawn Heleos 2 light scattering detector and a Wyatt Optilab Rex refractive index detector. No calibration standards were used, and d*n*/d*c* values were obtained by assuming 100% mass elution from the columns.

Protocol for MC derivatives: Column set consists of two Shodex KF-801 columns connected in series with a guard column of the same stationary phase. Chloroform mobile phase maintained at 35°C. Isocratic pump (Water 515 HPLC Pump, from Waters Technologies) and 717 Waters autosampler for injection with multi-angle laser light scattering detector (mini-DAWN from Wyatt Technology Corp) operating at a wavelength of 658 nm and refractive index detector at 880 nm (Waters 410, Waters Technology). Shodex polystyrene standards were used for calibrations.

6.3.2.12 DSC

Thermal analysis employed a TA Q2000 differential scanning calorimeter (TA Instruments, New Castle, DE). The instrument was calibrated for enthalpy and temperature using indium and tin. Nitrogen (50 mL/min) was used as the purge gas. Sample (3-5 mg) were added into aluminum Tzero sample pans, with a pinhole. Modulated DSC was used, the samples were equilibrated at -10 °C for 5 minutes isothermally, and then were heated at a rate of 5°C/min, with a modulation amplitude of 1°C min^{-1} every 60 seconds. Ethyl cellulose samples were heated from -10 °C to 190 °C, while for methylcellulose samples the temperature range was -10 to 240 °C.

6.3.2.13 SP calculations

Solubility parameters provide information about relative polymer hydrophobicity. They were calculated by the Fedors method [34] (Equation S1), using a procedure similar to that

reported by Babcock et al. [35]. The calculation includes the energy of vaporization, molar volume and degree of substitution for the diverse chemical features.

$$\delta = \sqrt{\frac{\sum \mathrm{E}\ (\mathrm{J}*\mathrm{mol}^{-1})}{\sum \mathrm{V}\ (\mathrm{cm}^3*\mathrm{m}^{-1})}}$$ Equation S1

For compounds with T_g and T_m above room temperature a correction to account for differences in the molar volume (Equation S2) was applied, where n is the number of main chain skeletal atoms in the smallest repeating unit [34]. For cellulose polymers, n is equal to 7 (6 atoms in the ring and the oxygen bonded to the next monomer).

$\Delta v_i = 2n, n \geq 3$ Equation S2

Some of the groups are constant for all cellulose-based polymers, and independent of the DS: 1 ring closure, 5 -CH, 1 -CH_2 and 2 –O–. In contrast, the substituent groups vary for each polymer. The electronic supplementary information shows a sample calculation for methyl cellulose adipate.

6.3.2.14 ASD preparation by solvent casting

Ritonavir (0.035 g) and polymer (0.2 g) (15% w/w ratio) were dissolved in 50 mL of THF. The solvent was evaporated on a Teflon® surface by air and films were detached from the surface upon drying.

6.3.2.15 XRD

X-ray diffraction patterns were obtained using a Shimadzu XRD 6000 diffractometer (Shimadzu Scientific Instruments, Columbia, Maryland). The instrument was calibrated using a silicon standard with a characteristic peak at 28.44° 2θ. Divergence and scattering slits were set at 1.0 mm, and the receiving slit was set at 10 iris. The experiments were conducted with a scan range from 10 to 50° 2θ. Scanning speed was 5°/min.

6.3.2.16 Ritonavir detection by HPLC

An Agilent 1200 series HPLC system consisting of Agilent Chemstation LC 3D software and reversed phase mode using an Eclipse XDB-C18 column (4.6 × 150 mm i.d., particle size 5 μm) was used. Eluant gradient was employed using acetonitrile and 0.05M phosphate buffer (pH 5.55) at 1.5 mL/min flow rate for 20 min. The acetonitrile

proportion was 40% for 1 min, raised to 60% for 14 min, reduced back to 40% in 1 min and maintained at 40% for 4 min. The column temperature was 25°C, sample injection volume was 5 μL and a UV detector at 240 nm was used. The retention time of ritonavir was 10.4 min.

6.3.2.17 *In vitro* drug release of ritonavir from ASDs at pH 6.8

Films (13 mg film, 15 fold supersaturation, 15% ritonavir loaded ASD) were dispersed in 100 mL of 0.05M PBS buffer at pH 6.8 (prepared according to US Pharmacopeia). The solution was stirred at 400 rpm and the temperature was kept at 37 °C. Aliquots (0.5 mL) were withdrawn every hour and replaced with 0.5 mL of buffer to maintain constant volume in the dissolution flask. Each sample was centrifuged at 13 x 10^3 *g* for 10 min. Ritonavir concentration was determined by HPLC analysis of a sample of the supernatant immediately after centrifugation, and the drug concentration was calculated according to a standard curve prepared with 0, 1.56, 3.125, 6.25, 12.5 and 25 μg/ml standards in acetonitrile.

6.4 Results

6.4.1 Carbanilation of Cellulose Ethers

We selected commercially cellulose alkyl ether starting materials since they were readily available and the alkyl groups would provide desired hydrophobicity to promote miscibility with hydrophobic drugs. It was essential to determine the precise degree of substitution (DS) of OH groups (DS(OH)) of the methyl cellulose and ethyl cellulose commercial samples used, so that we could understand the efficiency of attachment of the ω-carboxyalkanoyl groups; residual backbone hydroxyl groups in the final product could also significantly impact ASD and other properties. We chose reaction of the free hydroxyl groups with phenyl isocyanate for determining the DS(OH) available for esterification since it has long been known that phenyl isocyanate reacts rapidly and completely with cellulosic hydroxyl groups [33]. Cellulose ethers were reacted with excess phenyl isocyanate in pyridine at elevated temperatures to form tricarbanilates quantitatively (EC example in **Figure 6.1**), as previously confirmed by elemental analysis

[36,37]. DS(carbanilate) was determined by ^{1}H NMR (**Figure 6.2**), by integration of the aromatic protons, well separated from the cellulose backbone and alkyl group resonances, using the integration ratios of the aromatic peaks and cellulose backbone/cellulose ether peaks. The final products have very good solvent solubility that helps the characterization of methyl cellulose derivative since it was soluble in water but not in many common organic solvents before the reaction.

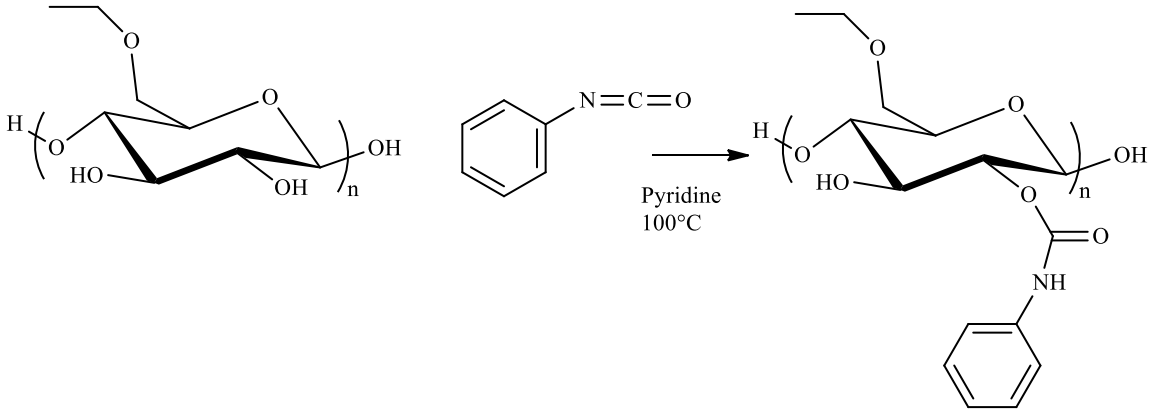

Figure 6.1: Carbanilation reaction of ethyl cellulose for quantification of DS(OH). Structures in this and all schemes are not meant to convey regioselective substitution; depictions of substituent location are merely for convenience and clarity of depiction.

The DS(OH) values so measured, along with other measured and calculated properties of the starting cellulose ethers we used, are presented in **Table 6.1**. Both cellulose ethers used have substantial DS(OH), so that in theory we should be able to attach adequate DS(ω-carboxyalkanoate) to determine the structure-property relationship with regard to ASD. Unfortunately EC with DS(OH) equivalent to that of the MC used was not commercially available.

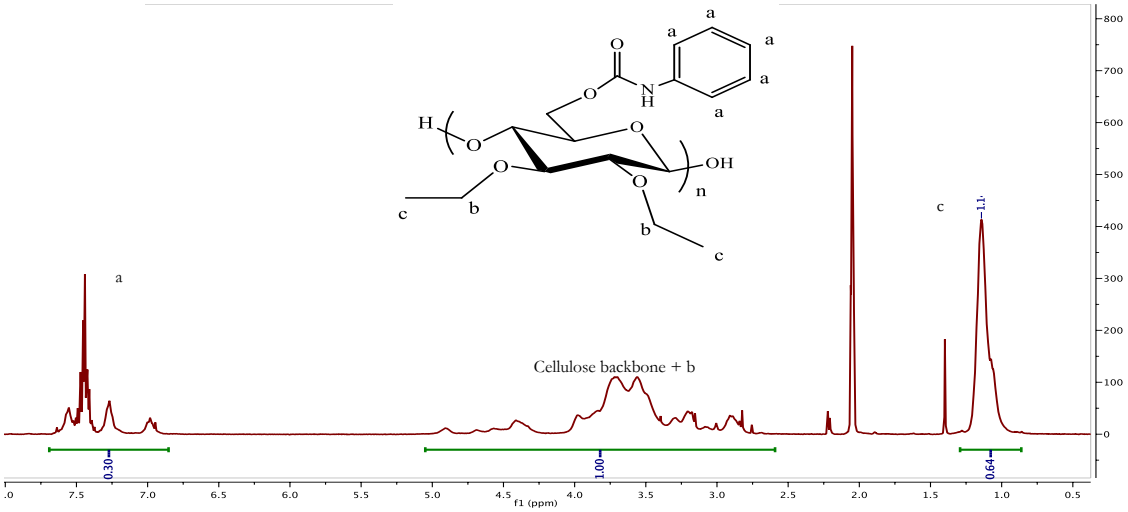

Figure 6.2: ^{1}H NMR spectrum of EC carbanilate in acetone-d_6.

Table 6.1: Measured/Calculated Unmodified Cellulose Ether Properties

Sample	**Ether Group**	**DS (alkyl)**	**DS (OH)**	**T_g (°C)**	**Solubility Parameter ($MPa^{1/2}$)**
1	Ethyl (EC)	2.3	0.7	142	21.24
2	Methyl (MC)	1.8	1.2	207	25.02

6.4.2 Synthesis and characterization of cellulose ether ω-carboxyalkanoates

In our previous investigations of cellulose ester adipate/suberate/sebacate synthesis, direct reaction of cellulose esters with commercial or conventionally prepared

(Albertsson, Lundmark, 1990) adipic anhydride led to crosslinking due to the contaminant poly(adipic anhydride). Therefore, in our attempts to synthesize alkyl cellulose **ω**-carboxyalkanoates, attachment of the **ω**-carboxyalkanoate moiety was carried out by initial reaction of cellulose with a monofunctional, monoprotected reagent, followed by deprotection, as had proven successful in the case of cellulose alkanoate w-carboxyalkanoate esters (Liu, Ilevbare, Cherniawski, Ritchie, Taylor, & Edgar (2014)). Monoprotected reagents were prepared as previously reported; diacid was reacted with benzyl alcohol by Fischer esterification, and the monobenzyl ester was separated from diacid and dibenzyl ester co-products by phase separations at appropriate pH values. Then, the monobenzyl ester was converted into monobenzyl ester acid chloride by reaction with oxalyl chloride. The resulting monobenzyl ester monoacid chlorides were reacted with the cellulose ether in an appropriate solvent, using pyridine as catalyst and acid scavenger (**Figure 6.3**).

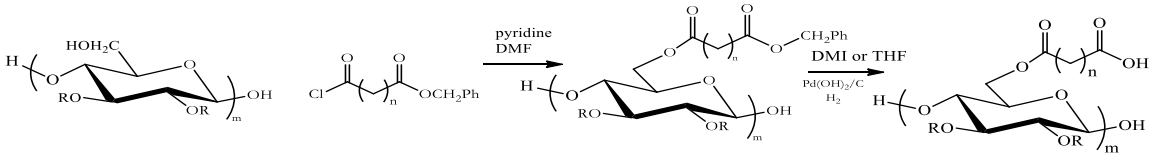

Figure 6.3: The synthesis scheme of ethyl ether cellulose derivatives.

Commercial EC (DS(Et) 2.3) is soluble in many common organic solvents including tetrahydrofuran (THF), methyl ethyl ketone (MEK), 1,3-dimethyl-2-imidazolidinone (DMI), pyridine, DMF and DMSO. We chose DMF as reaction solvent since it is known to promote nucleophilic displacement reactions, and since it would permit use of relatively high temperatures if needed given the poor nucleophilicity of cellulosic hydroxyls. On the other hand, MC esterification was more problematic since MC is soluble in water, but not soluble in most common organic solvents. Fortunately MC is soluble in the polar aprotic solvent DMF, so MC esterification was also performed in DMF; we employed 90°C reaction temperature for both EC and MC, with reaction times of 20h in each case.

Ester DS values of the benzyl protected MC and EC ω-carboxyalkanoates were readily determined by ^{1}H NMR spectroscopy (**Figure 6.4**). DS was calculated by integrating the

cellulose backbone region, which also included the benzyl methylene protons, and the methylene protons of the ethyl groups in the case of EC, and calculating the ratio of backbone integral to that of the phenyl protons of the benzyl protecting groups. Reactions of these relatively highly substituted cellulose ethers were somewhat sluggish (the 2- and 6-OH groups tend to be most reactive in conventional cellulose etherification, so that a significant proportion of the residual OH groups are less reactive 3-OH groups) [38,39], thus excess acylating reagent was needed to reach desired DS in a reasonable reaction time. For example, using 3 eq. each of catalyst and acid chloride afforded relatively low w-carboxyalkanoate DS values (e.g. DS (Ad) = 0.2 obtained by reaction with EC under these conditions), that likely would not be sufficient for strong ASD performance (data not shown). Indeed, the low DS MC esters obtained in this way were insoluble in both organic solvents and water. On the other hand, when we employed 10 eq. catalyst and 8 eq. acid chloride, DS(ω-carboxyalkanoate) values higher than 0.5 were obtained. Therefore these higher levels of catalyst and reactant equivalents were used to synthesize the EC and MC derivatives listed in **Table 6.2**. Under these conditions, for each alkyl cellulose and each w-carboxyalkanoate reagent explored, the DS(ester) obtained was higher than 0.5, approaching complete esterification of the available OH groups in the case of EC. In addition, our experience from cellulose ester ω-carboxyester shows that higher DS of ω-carboxyester group often affords better ASD performance, in terms of drug release and recrystallization prevention.

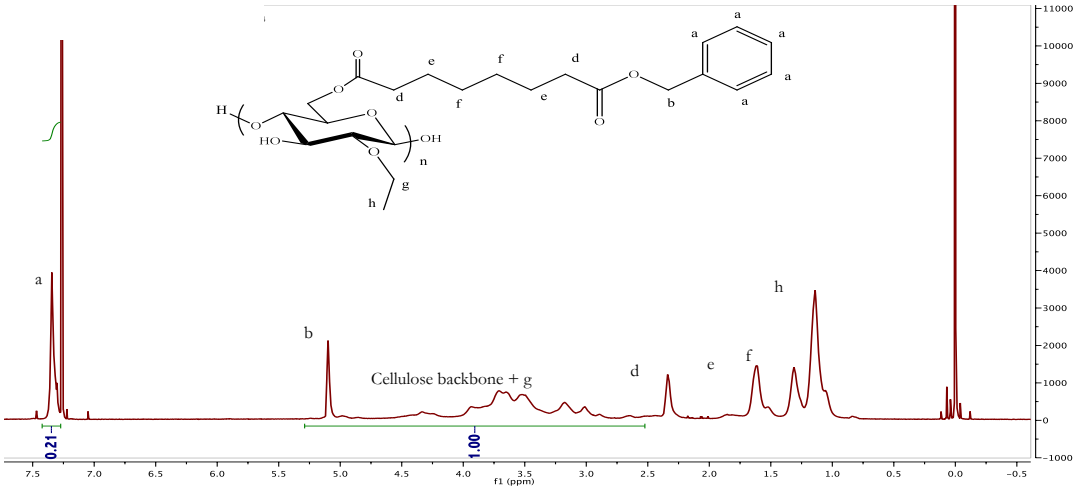

Figure 6.4: ^{1}H NMR spectrum of benzyl ECSub ($CDCl_3$).

The ^{13}C NMR spectrum of benzyl MCAd (**Figure 6.5**) confirmed successful esterification. We studied acylation conversion in detail using the benzyl ester, since it was more soluble in the NMR solvent than was the product carboxylic acid. Particularly diagnostic were the carbonyl resonance at 172.7 ppm, those for aromatic carbons at 136.8 and 128.7 ppm, and the benzyl carbon at 65.7 ppm, diagnostic for successful esterification since they are not present in the starting MC. In addition, we can identify the adipate hydrocarbon chain peaks at 33.9 and 24.37 ppm.

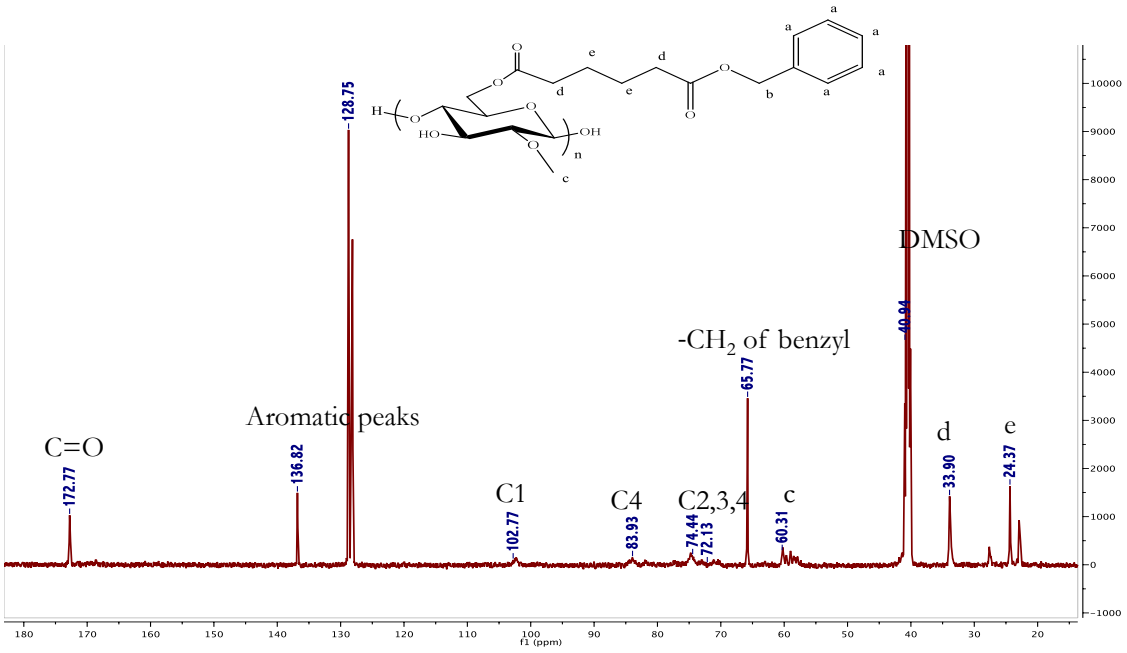

Figure 6.5: ^{13}C NMR of benzyl MCAd in DMSO-d_6.

Heterogeneously catalyzed hydrogenolysis to remove the protective benzyl groups of EC derivatives was performed in THF, in which the benzyl w-carboxyalkanoate derivatives were readily soluble, under moderate H_2 pressure ($Pd(OH)_2/C$ catalyst, room temperature, 2 d, 80 psi H_2). Catalytic hydrogenations of cellulose derivatives can be difficult, in part because of the steric bulk of the rigid cellulose backbone that may interfere with interaction with the heterogeneous catalyst surface. In this case, ^1H NMR spectra of the products show complete hydrogenolysis of all derivatives studied, confirmed by the disappearance of the benzylic and aromatic signals.

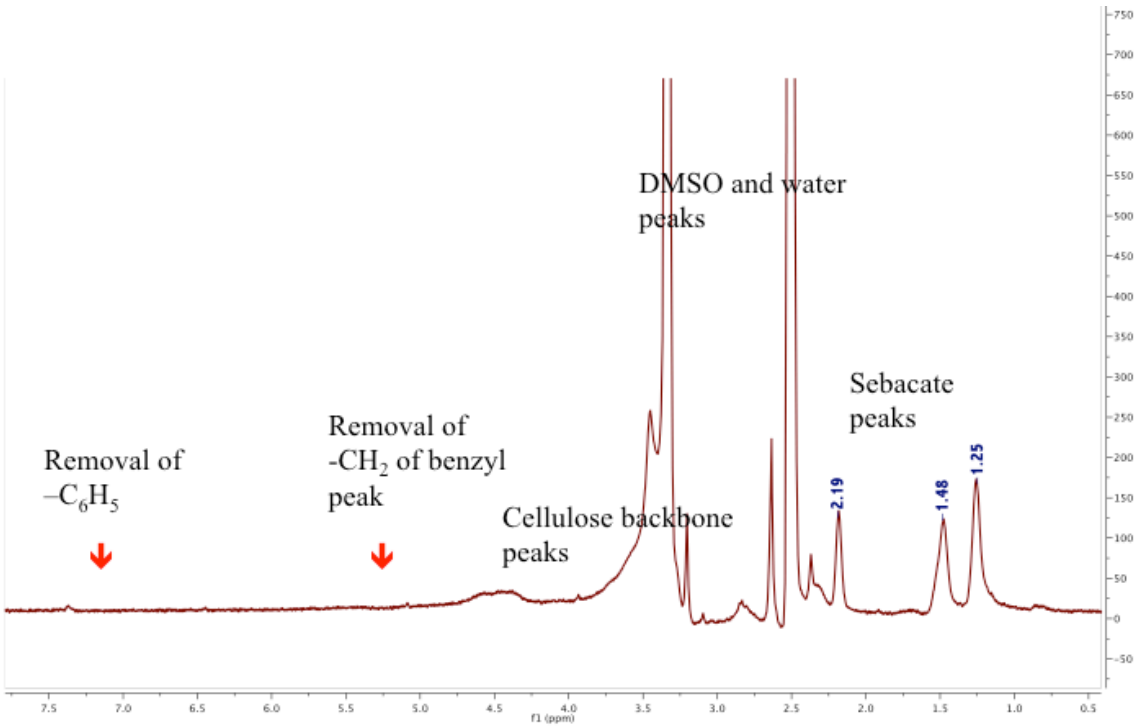

Figure 6.6: ^{1}H NMR spectrum of MCSeb (DMSO-d_6).

Hydrogenolysis was smooth and easy for the EC esters but more problematic for the less soluble MC esters. The hydrogenolysis protocol in THF, that was successful for all benzyl EC esters as well as benzyl MC adipate, achieved only partial hydrogenolysis of the benzyl esters of MC suberate and sebacate. We hypothesize that THF is not as good a solvent for these esters, resulting in more folding of the long side chains and decreased accessibility to the heterogeneous catalyst. We therefore switched to the more polar DMI solvent for hydrogenolysis of benzyl MC suberate and sebacate; the hydrogenation was also carried out at higher temperature (55°C vs. room temperature for the other esters in THF). Both changes were designed to promote side chain unfolding, and the result was successful, quantitative removal of the protective benzyl groups by hydrogenolysis (**Figure 6.6**).

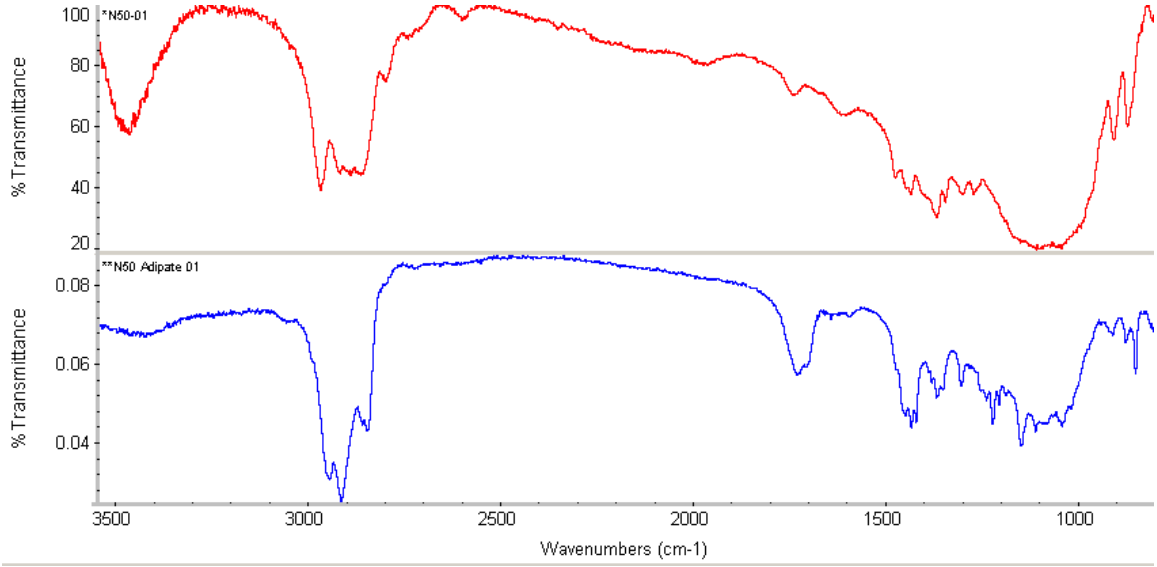

Figure 6.7: FTIR spectra of EC (red, upper) and ECAd (blue, lower).

The exemplary FTIR spectrum of ECAd (**Figure 6.7**), compared with that of starting EC, also provides evidence of successful esterification and deprotection. The new carbonyl absorbance (ECAd, lower (blue) trace) at 1700 cm^{-1} clearly shows the formation of adipate ester bonds. In addition, the added hydrocarbon chain enhances the C-H stretch at 1290 cm^{-1} in the cellulose ether ester spectra. The strong decrease in hydroxyl stretch at 3500 cm^{-1} of ECAd reflects the expected decrease in free hydroxyl groups as a result of esterification.

Table 6.2: Cellulose ether ester properties (polymer: catalyst: acid chloride ratio (1:8:10)

Ref. No.	Ether type	Ester type	DS(ester)	Total DS	DP	T_g (°C)	Solubility Parameter ($MPa^{1/2}$)
1	EC	Adipate	0.54	2.8	31*	144	20.84
2	EC	Suberate	0.53	2.79	29*	104	20.63
3	EC	Sebacate	0.54	2.8	34*	100	20.44
4	MC	Adipate	1.1	2.96	213**	105	22.14
5	MC	Suberate	1.06	2.92	167**	98	21.66
6	MC	Sebacate	0.99	2.85	288**	97	21.43

*SEC in THF, detailed information can be found in the supplementary data.

**SEC in chloroform (benzyl derivative), detailed information can be found in the supplementary data.

Thermal properties of the cellulose ether ω-carboxyalkanoates are of particular interest, since high T_g is an especially desirable characteristic for ASD polymers. Polymer T_g values that are well above any possible ambient temperature that would be experienced during storage or transport help to maintain the drug/polymer formulation T_g at a value higher than ambient temperature, realizing that the drug may act as a plasticizer, and water from ambient humidity is highly likely to plasticize a polysaccharide derivative. The rule of thumb that is often used is that polymer T_g should be at least 50ºC above any possible ambient temperature, in order to compensate for these plasticizing effects in the formulation. T_g values of the obtained cellulose ether esters were obtained by modulated DSC (**Figure 6.8** and **Table 6.2**). Glass transitions were rather sharp and easily observed in the DSC thermograms of all of these derivatives. All T_g values for the ether esters are 100°C or higher, even for the EC esters and even for the longer chain w-carboxyalkanoate groups (e.g. ECSeb). As the added hydrocarbon chain length increases,

the polymer T_g decreases as expected, but the inherently high T_g of the cellulose ethers keeps the final product T_g values at levels that are promising for use in ASD as shown in **Figure 6.8**.

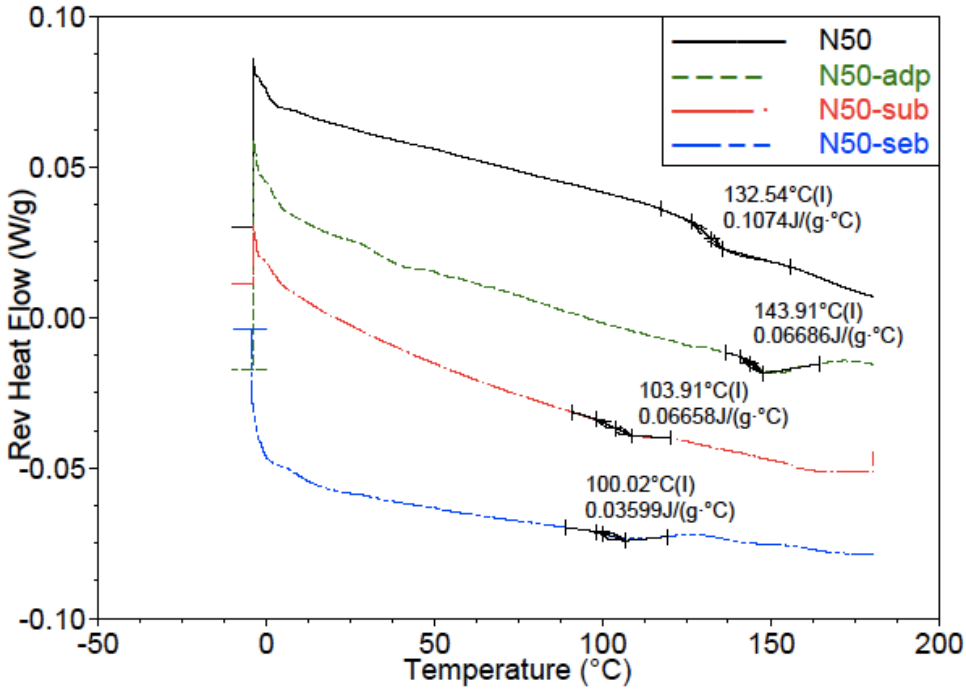

Figure 6.8: DSC thermograms of untreated EC and EC esters (N50 refers to EC).

Table 6.3: Solubility of Cellulose Ether ω-Carboxyalkanoates

Ref. No.	Ether type	Ester type	THF	$CHCl_3$	DMSO	EtOH	MeOH	i-PrOH	DMAc	Water
1	EC	-	S	S	S	S	S	S	S	x
2	EC	Adipate	S	S	S	S	S	S	S	x
3	EC	Suberate	S	S	S	S	S	S	S	x
4	EC	Sebacate	S	S	S	S	≈	≈	S	x
5	MC	-	x	x	S	x	x	x	S	S
6	MC	Adipate	S	≈	S	x	x	x	S	x
7	MC	Suberate	S	≈	S	x	x	x	S	x
8	MC	Sebacate	S	≈	S	x	x	x	S	x

(S = Soluble; ≈ = Partly Soluble; x = Insoluble; MeOH = methanol; EtOH = ethanol; i-PrOH = isopropanol)

Cellulose ether ester solubility properties are summarized in **Table 6.3**, and compared with those of the starting cellulose ethers. While the starting EC is soluble in all the common solvents tested, as the ester product hydrocarbon chain length increases, solubility of the polymer in alcohol solvents is lost; this is to be expected given the loss of free hydroxyl groups in the product EC ω-carboxyalkanoates. The alcohol solubility (ethanol, methanol, isopropanol) of the EC adipate and suberate is unusual for a cellulose derivative and is remarkable. Starting MC on the other hand is a water-soluble polymer, with limited organic solubility. As it is substituted with relatively hydrophobic w-carboxyalkanoate groups, solubility in solvents like THF, DMAc, and DMSO is

enhanced. This enhanced solubility (and, likely, compatibility) is useful for ASD formulation from drug/polymer solutions, as well as for ASD performance.

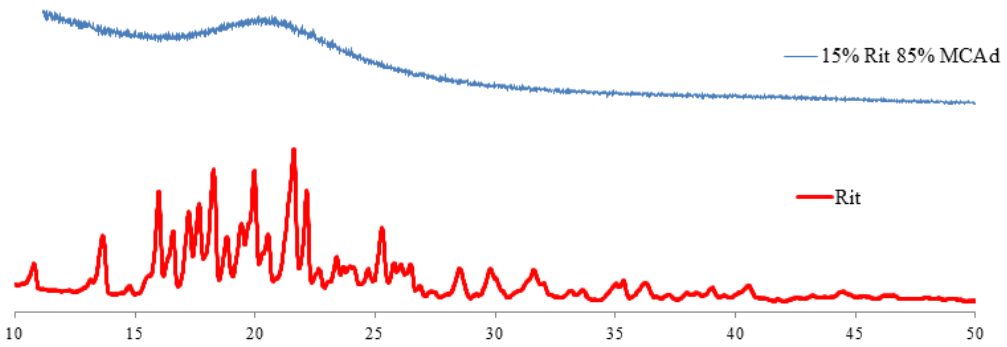

Figure 6.9: XRD spectra of ritonavir solid dispersion (15% Rit, 85% MCAd) vs. crystalline ritonavir.

Solid dispersions of the model drug ritonavir in a MCAd matrix were prepared by solvent casting clear films after dissolving in the common solvent THF. We chose to carry out this initial exploratory *in vitro* study with MCAd in part because it was the most hydrophilic of the alkyl cellulose ω-carboxyalkanoates prepared (solubility parameter, 22.14); the solubility parameter matches up well with those of many poorly soluble drugs, and as it is the highest among these derivatives, may predict faster drug release from the matrix. The dispersion containing 15% ritonavir (w/w) in MCAd was analyzed by XRD and DSC to determine whether ritonavir in the dispersion was amorphous. The XRD diffraction patterns of crystalline ritonavir and 15% ritonavir MCAd ASD are shown in **Figure 6.9**. Crystalline ritonavir shows sharp characteristic diffraction peaks (especially between 15 and 25 2θ), while the 15% ritonavir MCAd dispersion lacks any sharp peaks, but instead shows an amorphous halo, indicating that the ritonavir in the MCAd dispersion is amorphous.

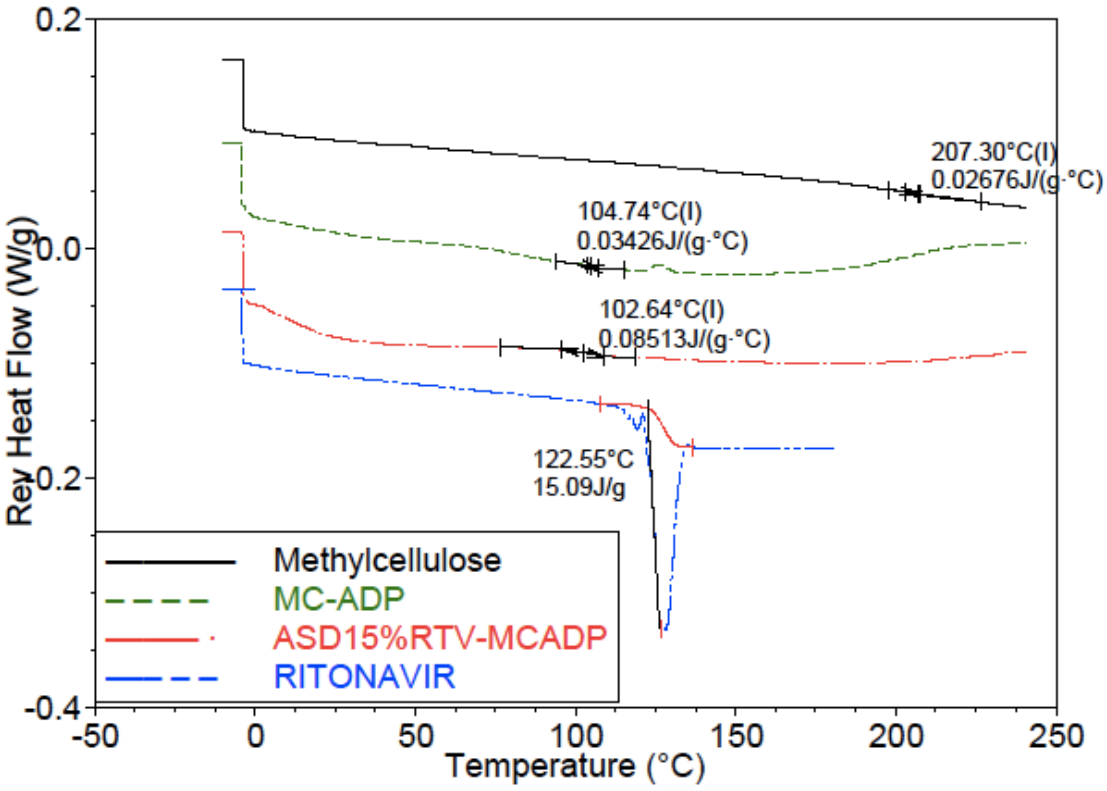

Figure 6.10: DSC thermograms of MC (untreated pure polymer), MCAd (cellulose ether ester), Rit (pure drug), and 15% Rit dispersion in MCAd.

To confirm the XRD results, we analyzed the ritonavir/MCAd dispersion by DSC (**Figure 6.10**). The T_g of the starting MC is 207°C and, as expected esterification decreased the T_g of the MCAd product, to 105°C. Pure ritonavir displays a strong melting endotherm at 122.55ºC, very close to the literature melting point (122.7ºC) for ritonavir [26]. The dispersion has only one glass transition, at approximately 103ºC, between the polymer and drug T_g values (ritonavir T_g has been reported as 50ºC (Zhou, Zhang, Law, Grant, Schmitt (2002)), supporting the hypothesis that the ritonavir in the dispersion is amorphous. It should be noted that the Flory equation predicts a T_g of 90º for a miscible dispersion (ASD), thus the dispersion does not perfectly obey the Flory equation. In addition, the complete absence of a ritonavir melting peak (123°C) on the ASD provides further strong support for elimination of ritonavir crystallinity.

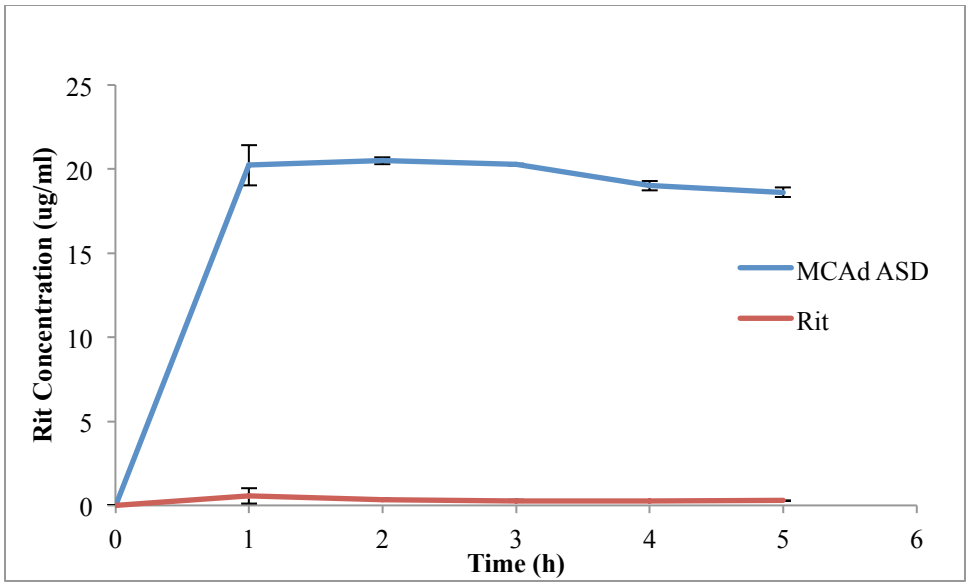

Figure 6.11: Dissolution results of the ASD and crystalline drug Rit at pH 6.8 (n=3).

Having confirmed the ability of the new MCAd polymer to form ASDs at least up to 15% ritonavir (we have not yet explored the loading limits for ritonavir in these dispersions), we wished to carry out a brief exploratory dissolution study to see whether this polymer would show relatively fast release, as expected, and whether it would effectively prevent ritonavir recrystallization from solution. We carried out the brief dissolution study using the 15% ritonavir ASD in MCAd, under supersaturating conditions (appropriate for evaluating ASD performance). Dissolution was carried out at pH 6.8 (mimicking small intestine pH (phosphate buffer)) and 37°C, while monitoring ritonavir concentration in the liquid phase by HPLC. The dissolution profile is presented as the concentration of ritonavir in solution vs. time in **Figure 6.11**. The results from the dissolution study showed polymer-dependent solution concentration enhancement of ritonavir from MCAd ASD. Release was complete within 1h, and once released, ritonavir concentration was essentially stable for the rest of the 5h experiment. The measured solubility of crystalline ritonavir was calculated to be 1.3-1.5 mg/mL, as shown in literature[26]. The maximum concentration from the ASD was approximately 20 µg/mL; thus the supersaturation achieved is the maximum possible for ritonavir[26], and the MCAd ASD was able to maintain this ritonavir concentration for at least a time roughly equal to the normal transit time through the absorptive zone of the gastrointestinal tract.

6.5 Conclusions

Cellulose alkyl ethers can be successfully esterified by reaction with monobenzyl adipoyl, suberoyl, and sebacoyl chlorides. Nearly complete substitution can be achieved, but requires significant excesses of reagent due to the low reactivity of residual hydroxyl groups on conventionally prepared alkyl cellulose ethers. These cellulose ether ester products are more hydrophobic than the starting ethers, and thus have good solubility in medium polarity solvents, and in polar aprotic solvents; the ethyl cellulose esters have broader organic solubility, due both to their higher DS(alkyl) as well as the more hydrophobic nature of the ethyl group than methyl. This organic solubility will be helpful for formation of ASDs from common solutions of drug and polymer, and is also predictive of broad miscibility with drug structures. The alkyl cellulose w-carboxyalkanoates are promising for ASDs with regard to drug release and stabilization of amorphous drug against recrystallization after release. This chemistry promises to make available a very broad range of alkyl cellulose w-carboxyalkanoates. The promise of these renewable-based amphiphiles for solubility and bioavailability enhancement of otherwise poorly soluble drugs is underlined by successful formation of an ASD of ritonavir at 15% drug in methyl cellulose adipate. Release of ritonavir from this ASD was rapid, as desired and expected; these ether esters are likely to have faster release properties than some of the cellulose alkanoate ω-carboxyalkanoates we have previously investigated. Initial release studies from the MCAd ASD also show maximum supersaturation, and stability of the supersaturated dispersion in the presence of MCAd against recrystallization for a time period equivalent to the probable duration of passage through the absorptive zone of the GI tract. From a synthetic perspective, these polymers are readily synthesized by a process that lends itself to adjustments in substituent DS and thereby to property adjustments. The requirement for an excess of acyl chloride reagent does mean that this process is not as efficient as would ideally be desired. On the other hand, the process eliminates crosslinking issues experienced with previous cellulose ether ester processes. The structures produced are relatively simple, and the process should lend itself to repeatable control to desired substituent proportions and DS; product analysis is also straightforward. We will build upon this initial study to further investigate

the drug release and recrystallization prevention properties of these promising new ASD polymers.

6.6 Acknowledgments

We thank Ashland Inc. for their kind donation of EC used in this work. We thank the NSF for funding this work through award 1312157-IIP. We are grateful to the Macromolecules and Interfaces Institute (MII), and the Institute for Critical Technologies and Applied Science (ICTAS) at Virginia Tech for their financial, facility, and educational support. We thank to Dr. Ann Norris for assistance with XRD experiments, and Mr. Scott Radzinski and Mr. Kevin Drummey for assistance with SEC experiments.

6.7 References

Albertsson, A.C.; Lundmark, S. (1990). Melt polymerization of adipic anhydride (oxepane-2,7-dione). *J. Macromol. Sci.*, *27*, 397-412.

(1) Kawabata, Y.; Wada, K.; Nakatani, M.; Yamada, S.; Onoue, S. Formulation Design for Poorly Water-Soluble Drugs Based on Biopharmaceutics Classification System: Basic Approaches and Practical Applications. *Int. J. Pharm.* **2011**, *420*, 1–10.

(2) Van den Mooter, G. The Use of Amorphous Solid Dispersions: A Formulation Strategy to Overcome Poor Solubility and Dissolution Rate. *Drug Discov. Today. Technol.* **2012**, *9*, e71–e174.

(3) Miller, J. M.; Beig, A.; Carr, R. A.; Spence, J. K.; Dahan, A. A Win–Win Solution in Oral Delivery of Lipophilic Drugs: Supersaturation via Amorphous Solid Dispersions Increases Apparent Solubility without Sacrifice of Intestinal Membrane Permeability. *Mol. Pharm.* **2012**, *9*, 2009–2016.

(4) Vasconcelos, T.; Sarmento, B.; Costa, P. Solid Dispersions as Strategy to Improve Oral Bioavailability of Poor Water Soluble Drugs. *Drug Discov Today* **2007**, *12*, 1068–1075.

(5) Khougaz, K.; Clas, S. D. Crystallization Inhibition in Solid Dispersions of MK-0591 and Poly(vinylpyrrolidone) Polymers. *J Pharm Sci* **2000**, *89*, 1325–1334.

(6) Qian, F.; Huang, J.; Hussain, M. A. Drug-Polymer Solubility and Miscibility: Stability Consideration and Practical Challenges in Amorphous Solid Dispersion Development. *J. Pharm. Sci.* **2010**, *99*, 2941–2947.

(7) Pereira, J. M.; Mejia-Ariza, R.; Ilevbare, G. A.; McGettigan, H. E.; Sriranganathan, N.; Taylor, L. S.; Davis, R. M.; Edgar, K. J. Interplay of Degradation, Dissolution and Stabilization of Clarithromycin and Its Amorphous Solid Dispersions. *Mol Pharm* **2013**, *10*, 4640–4653.

(8) Li, B.; Harich, K.; Wegiel, L.; Taylor, L. S.; Edgar, K. J. Stability and Solubility Enhancement of Ellagic Acid in Cellulose Ester Solid Dispersions. *Carbohydr Polym* **2013**, *92*, 1443–1450.

(9) Li, B.; Konecke, S.; Harich, K.; Wegiel, L.; Taylor, L. S.; Edgar, K. J. Solid Dispersion of Quercetin in Cellulose Derivative Matrices Influences Both Solubility and stabilityLi B, Konecke S, Harich K, et Al (2013) Solid Dispersion of Quercetin in Cellulose Derivative Matrices Influences Both Solubility and Stability. Carbohy. *Carbohydr Polym* **2013**, *92*, 2033–2040.

(10) B. Li; S. Konecke; L.A. Wegielb; L.S. Taylor; K.J. Edgar. Both Solubility and Chemical Stability of Curcumin Are Enhanced by Solid Dispersion in Cellulose Derivative Matrices. *Carbohydr Polym* **2013**, *98*, 1108–1116.

(11) Shelton, M. C. .; Posey-Dowty, J. D. .; Lingerfelt, L. R. .; Kirk, S. K. .; Klein, S. .; Edgar, K. J. *Enhanced Dissolution of Poorly Soluble Drugs from Solid Dispersions in Carboxymethylcellulose Acetate Butyrate Matrices*; American Chemical Society, 2009; Vol. 1017.

(12) Arca, H. C.; Mosquera-Giraldo, L. I.; Pereira, J. M.; Sriranganathan, N.; Taylor, L. S.; Edgar, K. J. Rifampin Stability and Solution Concentration Enhancement through Amorphous Solid Dispersion in Cellulose ω-Carboxyalkanoate Matrices. *J Pharm Sci* **2016**.

(13) Posey-Dowty, J. D.; Watterson, T. L.; Wilson, A. K.; Edgar, K. J.; Shelton, M. C.;

Jr., L. R. L. Zero-Order Release Formulations Using a Novel Cellulose Ester. *Cellulose* **2007**, *14*, 73–83.

(14) Sarode, A. L.; Sandhu, H.; Shah, N.; Malick, W.; Zia, H. Hot Melt Extrusion (HME) for Amorphous Solid Dispersions: Predictive Tools for Processing and Impact of Drug-Polymer Interactions on Supersaturation. *Eur J Pharm Sci* **2013**, *48*, 371–384.

(15) Rumondor, A. C.; Stanford, L. A.; Taylor, L. S. Effects of Polymer Type and Storage Relative Humidity on the Kinetics of Felodipine Crystallization from Amorphous Solid Dispersions. *Pharm Res* **2009**, *26*, 2599–2606.

(16) Tanno, F.; Nishiyama, Y.; Kokubo, H.; Obara, S. Evaluation of Hypromellose Acetate Succinate (HPMCAS) as a Carrier in Solid Dispersions. *Drug Dev Ind Pharm* **2004**, *30*, 9–17.

(17) Al-Obaidi, H.; Buckton, G. Evaluation of Griseofulvin Binary and Ternary Solid Dispersions with HPMCAS. *AAPS PharmSciTech* **2009**, *10*, 1172–1177.

(18) Krayz, G. T.; Averbuch, M.; Zelkind, I.; Gitis, L. Compositions Comprising Lipophilic Active Compounds and Method for Their Preparation. US 20090098200 A1, April 16, 2009.

(19) Chow, S.-L.; Wong, D. Controlled Release Hydrogel Formulation. US 20110165236 A1, July 7, 2011.

(20) Bittorf, K. J.; Kastra, J. P.; Gaspar, F. Pharmaceutical Compositions. US 20120083441 A1, April 5, 2012.

(21) Assessment Report Duloxetine Zentiva EMA/CHMP/373461/2015 http://www.ema.europa.eu/docs/en_GB/document_library/EPAR_-_Public_assessment_report/human/003935/WC500192516.pdf (accessed Apr 10, 2016).

(22) Lauer, M. E.; Grassmann, O.; Siam, M.; Tardio, J.; Jacob, L.; Page, S.; Kindt, J. H.; Engel, A.; Alsenz, J. Atomic Force Microscopy-Based Screening of Drug-Excipient Miscibility and Stability of Solid Dispersions. *Pharm. Res.* **2011**, *28*, 572–584.

(23) Kar, N.; Liu, H.; Edgar, K. J. Synthesis of Cellulose Adipate Derivatives. *Biomacromolecules* **2011**, *12*, 1106–1115.

(24) Liu, H.; Ilevbare, G. A.; Cherniawski, B. P.; Ritchie, E. T.; Taylor, L. S.; Edgar, K. J. Synthesis and Structure-Property Evaluation of Cellulose ω-Carboxyesters for Amorphous Solid Dispersions. *Carbohydr. Polym.* **2014**, *100*, 116–125.

(25) Ilevbare, G. A.; Liu, H.; Edgar, K. J. Understanding Polymer Properties Important for Crystal Growth Inhibition – Impact of Chemically Diverse Polymers on Solution Crystal Growth of Ritonavir. *Cryst. Growth Des.* **2012**, *12*, 3133–3143.

(26) Ilevbare, G. A. .; Liu, H. .; Edgar, K. J. .; Taylor, L. S. Maintaining Supersaturation in Aqueous Drug Solutions: Impact of Different Polymers on Induction Times. *Cryst. Growth Des.* **2013**, *13*, 740–751.

(27) Ilevbare, G. A.; Liu, H.; Edgar, K. J.; Taylor, L. S. Inhibition of Solution Crystal Growth of Ritonavir by Cellulose Polymers – Factors Influencing Polymer Effectiveness. *CrystEngComm* **2012**, *14*, 6503–6514.

(28) Wegiel, L. A.; Zhao, Y.; Mauer, L. J.; Edgar, K. J.; Taylor, L. S. Curcumin Amorphous Solid Dispersions: The Influence of Intra and Intermolecular Bonding on Physical Stability. *Pharm. Dev. Technol.* **2014**, *19*, 976–986.

(29) Li, B.; Konecke, S.; Harich, K.; Wegiel, L.; Taylor, L. S.; Edgar, K. J. Solid Dispersion of Quercetin in Cellulose Derivative Matrices Influences Both Solubility and Stability. *Carbohydr Polym* **2013**, *92*, 2033–2040.

(30) Casterlow, S. A. Characterization and Pharmacokinetics of Rifampicin Laden Carboxymethylcellulose Acetate Butyrate Particles, Virginia Tech, 2012.

(31) Zheng, X.; Gandour, R. D.; Edgar, K. J. TBAF-Catalyzed Deacylation of Cellulose Esters: Reaction Scope and Influence of Reaction Parameters. *Carbohydr. Polym.* **2013**, *98*, 692–698.

(32) Malm, C. J.; Emerson, J.; Hiait, G. D. Cellulose Acetate Phthalate as an Enteric Coating Material. *J. Am. Pharm. Assoc. (Scientific ed.)* **1951**, *40*, 520–525.

(33) Malm, C. J.; Laird, B. C.; Smith, G. D.; Tanghe, L. J. Determination of Total and Primary Hydroxyl in Cellulose Esters by Ultraviolet Absorption Methods. *Anal.*

Chem. **1954**, *26*, 188–190.

(34) Fedors, R. F. A Method for Estimating Both the Solubility Parameters and Molar Volumes of Liquids. *Polym. Eng. Sci.* **1974**, *14*, 147–154.

(35) Babcock, W. C.; Friesen, D. T.; Lyon, D. K.; Miller, W. K.; Smithey, D. T. Pharmaceutical Compositions with Enhanced Performance. WO 2005115330 A2, December 8, 2005.

(36) Terbojevich, M.; Cosani, A.; Camilot, M.; Focher, B. Solution Studies of Cellulose Tricarbanilates Obtained in Homogeneous Phase. *J. Appl. Polym. Sci.* **1995**, *55*, 1663–1671.

(37) Heinze, T.; Liebert, T. Unconventional Methods in Cellulose Functionalization. *Prog. Polym. Sci.* **2001**, *26*, 1689–1762.

(38) Erler, U.; Mischnick, P.; Stein, A.; Klemm, D. Determination of the Substitution Patterns of Cellulose Methyl Ethers by HPLC and GLC-Comparison of Methods. *Polym. Bull.* **1992**, *29*, 349–356.

(39) Nasatto, P.; Pignon, F.; Silveira, J.; Duarte, M.; Noseda, M.; Rinaudo, M. Methylcellulose, a Cellulose Derivative with Original Physical Properties and Extended Applications. *Polymers (Basel).* **2015**, *7*, 777–803.

Chapter 7. Novel Cellulose-Based Amorphous Solid Dispersions Enhance Quercetin Solution Concentrations *In Vitro*

Adapted from "Gilley A.; Arca, H. C.; Nichols B.; Edgar K. J.; Neilson A. P. *Carbohydrate Polymers* 2016 Submitted."

7.1 Abstract

Quercetin (Q) is a bioactive flavonol with potential to benefit human health. However, Q bioavailability is relatively low, due to its poor aqueous solubility and extensive phase-II metabolism (conjugation reaction to increase solubility of the drugs). Strategies to increase solution concentrations in the small intestinal lumen have the potential to substantially increase Q bioavailability, and by extension, efficacy. We aimed to achieve this by incorporating Q into amorphous solid dispersions (ASDs) with cellulose derivatives. Q was dispersed in matrices of cellulose esters including 6-carboxycellulose acetate butyrate (CCAB), hydroxypropylmethylcellulose acetate succinate (HPMCAS) and cellulose acetate suberate (CASub) to afford ASDs that provided stability against crystallization, and pH-triggered release. Blends of CASub and CCAB with the hydrophilic polyvinylpyrrolidone (PVP) further enhanced dissolution. The ASD 10% Q:20% PVP:70% CASub most significantly enhanced Q solution concentration under intestinal pH conditions, increasing area under the concentration/time curve (AUC) 18-fold compared to Q alone. This novel ASD method promises to enhance Q bioavailability *in vivo*.

7.2 Introduction

Q (**Figure 7.1**) is a dietary flavonol (a subclass of flavonoids) present at high levels in foods including apples, onions, and broccoli [1, 2]. Q intake has been associated with many potential health benefits, including reduced risk of cardiovascular disease [3, 4], cancer [5-7], and diabetes and obesity [8-10].

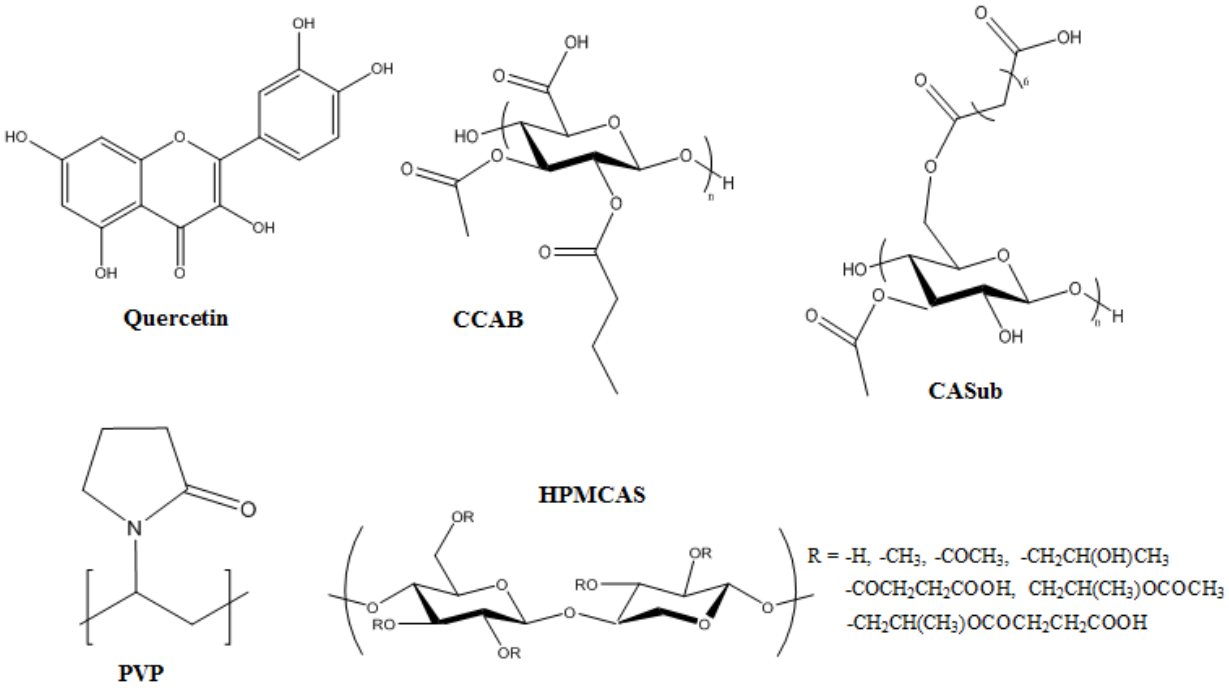

Figure 7.1 Chemical structures of Q, CCAB, CASub, PVP, and HPMCAS. The cellulosic structures are not meant to convey regioselective substitution; depictions of substituent location are merely for convenience and clarity of depiction.

Poor Q oral bioavailability severely limits its potential to benefit health. This low bioavailability is largely due to its crystallinity, and hence poor solubility (ranging from 2.15-7.7 μg/mL at 25°C [11, 12]) in the aqueous milieu of gut lumen, as well as extensive metabolism and subsequent luminal efflux by gut epithelial cells (Phase-II and Phase-III xenobiotic metabolism, respectively). Improved Q solubility may increase bioavailability by increasing the amount

available for absorption, and by saturating Phase-II and Phase-III metabolic enzymes; both effects are likely to result in increased net flux into circulation.

Many techniques have been employed to improve Q oral bioavailability, such as protein- or cellulose-based nanoparticles [13-15], encapsulation [16], nanoemulsifying drug delivery systems [17], and ASD [18-20]. ASD preparation with polymer dispersants is an attractive way to stabilize the high energy, amorphous drug in a glassy polymeric matrix. Exposure of the ASD to the GI lumen not only provides supersaturated drug solutions, but also enhances permeation by increasing the drug concentration gradient across the enterocytes. Polymer selection is key for ASD performance because the dispersion must be miscible, with strong polymer-drug interactions (e.g. hydrogen bonding) for stability against crystallization [20, 21]. Amphiphilic polymers possessing carboxylic acid functionality perform well in ASD due to strong polymer-drug interactions; their pH responsiveness is also valuable. At gastric pH, the protonated form protects the drug and minimizes release, while deprotonation at near-neutral intestinal pH swells the polymer and triggers drug release [19, 20]. Cellulose derivatives are popular ASD polymers due to their generally benign nature and high T_g values. CASub and cellulose acetate adipate propionate (CAAdP) were synthesized in the Edgar lab and show high promise for ASD [19, 22].

ASD has been only lightly explored for Q dissolution enhancement. Lauro *et al.* achieved slight dissolution enhancement using ASDs prepared with cross-linked sodium carboxymethylcellulose and sodium starch glycolate [12]. Similarly, Lauro *et al.* used spray dried dispersions with cellulose acetate trimellitate and cellulose acetate phthalate to improve Q release at pH 6.8 [23]. Recently, several polymers were evaluated for their ability to improve Q dissolution *in vitro* [19]. HPMCAS afforded ASDs containing up to 50% Q content; optimal dissolution was obtained from 10% Q ASDs, optimally in polymer blends containing 10% of the water-soluble (PVP) [24-26]. Employing PVP in blends with other cellulosic polymers may generally enhance drug release, while retaining the excellent stabilization against crystallization from the cellulosic polymer [27] as a result of the interactions (hydrogen bonding) between polymer carboxyl groups of the cellulose derivatives and drug functional groups such as amines and amides. PVP was added to the formulations since it has amorphous and hydrophilic nature and, it is miscible with the cellulose derivatives to promote the release from the ASDs without phase separation.

The objective of this study was to assess the performance of the novel polymer CASub for making Q ASDs and creating supersaturated Q solutions at physiological pH, vs. crystalline Q as negative control and HPMCAS/Q ASD as positive control. We hypothesized that 1) CASub would provide enhanced solution concentration and preferable dissolution kinetics compared to HPMCAS, and 2) that blending CASub with PVP would further enhance Q dissolution.

7.3 Experimental

7.3.1 Materials

Q (≥ 95% by HPLC), epicatechin (EC) (≥ 90% by HPLC), and KCl (solid, anhydrous, ≥ 99%) were purchased from Sigma-Aldrich. Cellulose acetate propionate (CAP-504-0.2; degree of substitution (DS) (acetate) = 0.04, DS (propionate) = 2.09; M_n = 15,000); CCAB; DS (butyrate) = 1.62, DS (acetate) = 0.06, DS (carboxylic acid) = 0.28); Mw = 252,000) and cellulose acetate (CA 320S, DS (acetate) = 1.82) M_n = 50,000) were from Eastman Chemical Company. HPMCAS (wt %: methoxyl 20-24%, hydroxypropyl 5-9%, acetyl 5-9%, succinoyl 14-18%; Mw = 18,000) was from Shin-Etsu Chemical Co., Ltd. Chemical structures of ASD polymers used (HPMCAS, PVP, CCAB, and CASub) are provided in **Figure 7.1**. Acetonitrile (ACN, HPLC-grade), methylene chloride (HPLC-grade), tetrahydrofuran (THF), reagent ethanol, sodium phosphate monobasic, and sodium hydroxide (NaOH) were purchased from Fisher Scientific and used as received. HCl (12.1 M) was obtained from Macron Chemicals. Suberic acid, adipic acid, methyl ethyl ketone (MEK), *p*-toluenesulfonic acid (PTSA), triethylamine (Et_3N), and oxalyl chloride were purchased from ACROS Organics. 1,3-Dimethyl-2-imidazolidinone (DMI) was purchased from ACROS Organics and dried over 4 Å molecular sieves. Water was purified by reverse osmosis and ion exchange using a Barnstead RO pure ST (Barnstead/Thermolyne) purification system. LCMS grade ACN, water and formic acid were obtained from VWR.

7.3.2 Synthesis of CASub

CASub was synthesized as previously reported [22]. See Sup Data for full details.

7.3.3 Preparation of ASDs via spray drying

Sup Data contains full description of preparation of ASDs containing Q. Our convention for naming treatments is to list the % polymer(s), with the remainder being Q. For example, 10%

Q/90% CCAB is referred to as 90 CCAB in the text, figures and tables. ASDs prepared were: 90 CCAB, 75 CCAB, 50 CCAB, 10 PVP:80 CCAB, 20 PVP:70 CCAB, 90 HPMCAS, 90 CASub, 10 PVP:80 CASub, 20 PVP:70 CASub. ASDs Q content was confirmed by UPLC to be within 4% of targeted value in every case (Sup Data Table S7.1).

7.3.4 XRD, DSC and FT-IR

X-ray powder diffraction, DSC and FTIR were performed as described in Sup Data.

7.3.5 Determination of crystalline and amorphous Q solubility

Crystalline solubility: An excess of crystalline Q was added to 15 mL pH 6.8 buffer solution, or pH 2.5 solution. Solutions were equilibrated at 37 ˚C/48 h with constant agitation, protecting them from light.

Amorphous solubility: Supersaturated Q solutions were prepared by adding a specific amount of Q stock solution (4 mg/mL in MeOH) to 15 mL buffer at 37 ˚C. Potassium phosphate buffer (100 mM, pH 6.8) with 100 μg/mL PVP (Kollidon® 12 PF); or acidified distilled water (pH 2.5) with 100 μg/mL PVP was used. The polymer was added to inhibit drug crystallization during the experiment and accurately determine the "amorphous solubility" of Q. Total Q concentration of was 80 μg/ml.

Crystalline and supersaturated solutions were centrifuged at 35,000 rpm (274,356 *x* g) for 30 minutes to separate the precipitated drug phase using an Optima L-100 XP ultracentrifuge equipped with Swinging-Bucket Rotor SW 41 Ti (Beckman Coulter, Inc., Brea, CA). Following centrifugation, the supernatant was collected, diluted (1:1) with methanol, and the final concentrations were measured by HPLC using an Agilent HPLC 1260 Infinity system (Agilent Technologies, CA, USA) with an Agilent Eclipse plus C18, 4.6 x 250 mm, 5 μm analytical column (Agilent technologies, CA, USA). Full HPLC methodological details are presented in Sup Data.

7.3.6 *In vitro* dissolution

In vitro dissolution was performed under non-sink conditions to evaluate Q dissolution concentrations and kinetics achieved via ASD delivery, compared to crystalline Q alone, under conditions similar to normal human gastrointestinal conditions. Full details in Sup Data.

7.3.7 UPLC-MS/MS

Internal standard solution (50 µL, 0.8 mg/mL EC in ethanol), 50 µL diluted dissolution supernatant, and 900 µL of 0.1% formic acid in 80% water/20% 80:20 ACN/THF were added to Waters UPLC vials (Milford, MA) and mixed. Analysis of Q content within ASDs and subsequent *in vitro* dissolution solution concentrations were by UPLC-MS/MS (method details in Sup Data)**.**

7.3.8 Data Analysis and Statistics

Dissolution results are reported as soluble Q vs. time. Dissolution kinetics were determined from this data. Pseudo-pharmacokinetic parameters (area under the concentration-time curve: AUC; maximal observed solution concentration: C_{MAX}; time at which maximal solution concentration was observed: T_{MAX}) were computed from Q concentration/time data using standard plugins for Microsoft Excel (Redmond, WA). Prism v. 6.0d (GraphPad, la Jolla, CA) was used to perform statistical comparisons. Dixon's Q-test ($\alpha = 0.05$) was utilized to identify and exclude any outliers as necessary. Significant differences in dissolution parameters between treatments were determined using one-way ANOVA with Tukey's HSD *post hoc* test performed on treatment means. Significance was defined as $P < 0.05$.

7.4 Results And Discussion

Three promising carboxylated cellulose derivatives were selected for ASD preparation in order to increase Q solubility. CCAB is a new commercial carboxylated cellulose ester [28], and HPMCAS is a cellulose ether-ester that is in commercial use as an efficient ASD polymer [19]. CASub was recently designed by the Edgar and Taylor groups as a promising ASD polymer and crystal growth inhibitor [22]. The above-mentioned polymers may not only stabilize amorphous Q in the solid state and prevent recrystallization after release, but also provide targeted pH-controlled release to the small intestine where Q absorption occurs. We also investigated blends of CASub and CCAB with PVP to promote enhanced Q dissolution, since Q and thus its ASDs with polymers like CASub and CCAB (δ = 22.66 and 24.44, respectively) are rather

hydrophobic. ASD drug concentration influences both the practicality of the method and ASD performance, so to explore this influence, Q concentration in the ASD was varied (10%, 25% and 50% Q (w/w)), using readily available commercial CCAB (90 CCAB, 75 CCAB, 50 CCAB) as the test system. To compare effectiveness of novel polymers and polymer blends, dissolution profiles were compared against commercial polymers HPMCAS and CCAB.

7.4.1 Solid State Characterization of Q loaded ASDs

Morphology was examined by SEM (**Figure 7.2**; other SEM images see Sup Data Figure S1-4). All ASD particles exhibited a smooth surface, indicating absence of evident crystals, except for

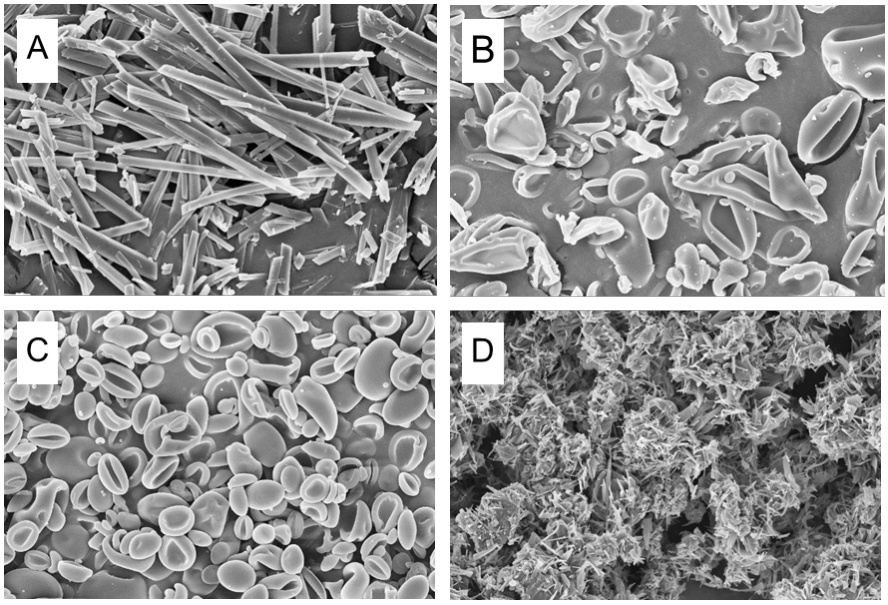

Figure 7.2 SEM images (mag. 10X) for crystalline Q (A), 90 CCAB (B), 75 CCAB (C), and 50 CCAB (D) are shown to illustrate particle size range (1-3 μm) and morphology.

XRD was used to determine whether dispersions were amorphous. All XRD spectra showed only amorphous haloes (**Figure 7.3**), except those of crystalline Q and 50% Q in CCAB (**Fig. 3A**). XRD data strongly support the amorphous nature of these dispersions except for 50 CCAB, which was therefore excluded from further testing. XRD spectra for 90 HPMCAS and 90 CASub are presented in Sup Data Figure S7.5.

DSC was used to further examine dispersion morphology of Q and polymers; data from CASub and CCAB is presented in **Figure 7.4**. Although crystalline Q melts at 326 °C, DSC scans were

kept ≤ 185°C, due to concerns about potential crosslinking of these polymers (containing both OH and CO_2H groups) above that temperature [29, 30]. For ASDs a glass transition (T_g) temperature lower than that of the pure polymer is expected. Polymer T_g values are 175°C (PVP), 144°C (CASub) and 134°C (CCAB). ASDs (10% Q) all had lower T_g values than the corresponding pure polymer, indicating that Q acted as a plasticizer. Since Q melts higher than the decomposition temperatures of several of our polymers, absence of Q T_m and T_c in the ASDs could not be confirmed. DSC T_g values along with the XRD data were sufficient to confirm the amorphous character of Q in these dispersions. DSC heating curves for all other dispersions are presented in Sup Data Figure S7.6.

FT-IR spectra are presented and discussed in the Sup Data.

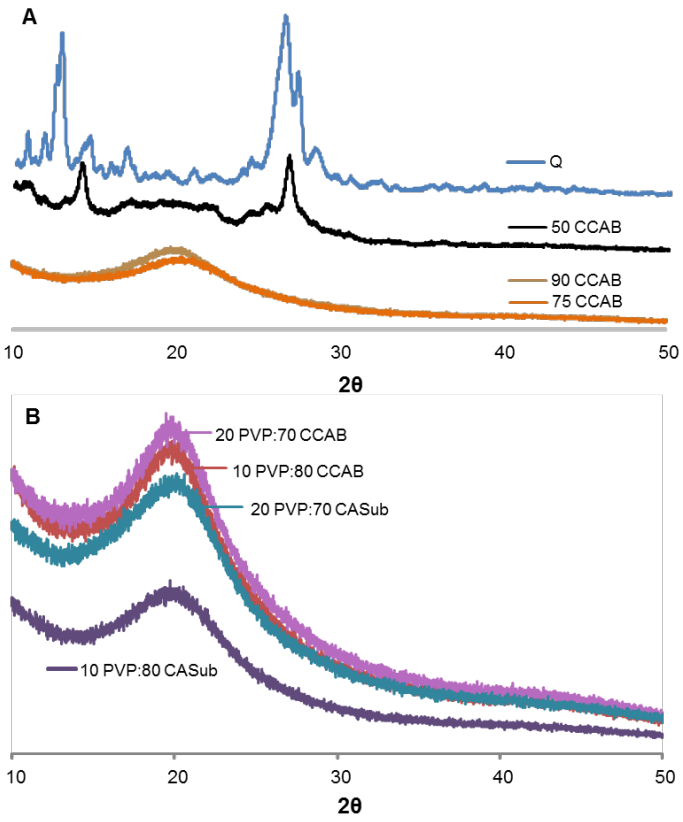

Figure 7.3. XRD spectra of Q, 50 CCAB, 75 CCAB, and 90 CCAB (A) as well as the PVP blends with both CCAB and CASub (B).

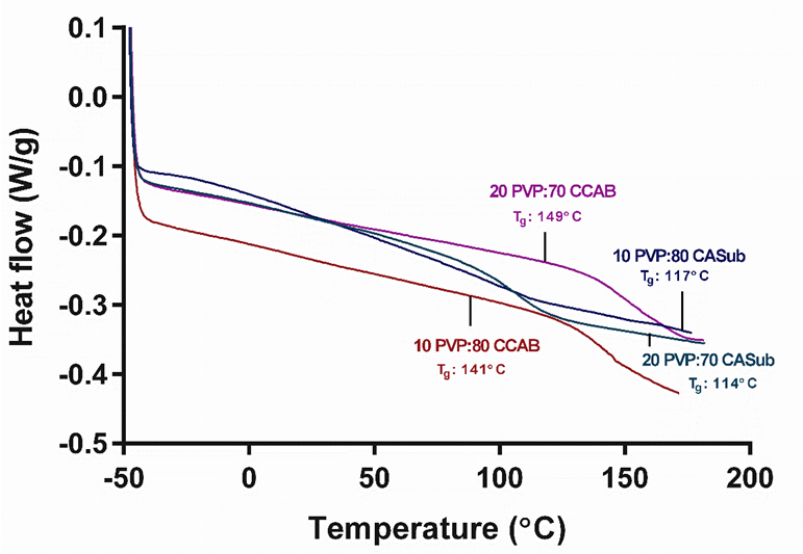

Figure 7.4. DSC second heating curves of Q-loaded ASDs of CASub, CCAB, and their respective blends containing 20% PVP.

7.4.2 Determination of crystalline and amorphous Q solubility

We attempted to confirm the crystalline solubility and measure Q amorphous solubility. Amorphous forms of compounds have a maximum apparent solubility, which represents the maximum amount of free drug achievable in solution, termed amorphous solubility [31]. The experimental amorphous solubility can be measured by creating supersaturated solutions by a solvent-shift method, and then measuring the concentration of drug in the supernatant. However, for compounds that are fast crystallizers (like Q), it is necessary to add a small amount of polymer (in this case PVP) to stabilize the supersaturated solution, inhibiting crystallization, and permitting accurate measurement of amorphous solubility. It was impossible to measure Q amorphous solubility in the absence of polymer, because the drug crystallized upon contact with the aqueous solution. We measured Q crystalline solubility at low (2.5) pH, where Q is un-ionized, and at pH 6.8 where it is partially ionized. Q amorphous solubility was also measured at both pH values. Crystalline solubility values were determined in the absence and presence of PVP, while amorphous solubility was determined only in the presence of PVP. Amorphous solubility was significantly higher than its crystalline counterpart at both pH values. Q crystalline solubility was similar to literature reports, and amorphous solubility appears to be at least 31 mg/mL at small intestine pH.

Table 7.1 Crystalline and amorphous solubility of Q in varying dissolution medium.

Medium	Crystalline solubility (µg/ml)	Amorphous solubility (µg/ml)
Acidified water (pH 2.5)[a]	0.64 ± 0.11	N/A[b]
Acidified water (pH 2.5)[a] + 100 µg/ml PVP	1.03 ± 0.20	23.48 ± 0.06
100 mM potassium phosphate buffer (pH 6.8)	1.03 ± 0.08	N/A[b]
100 mM potassium phosphate buffer (pH 6.8) + 100 µg/ml PVP	N/A[b]	31.29 ± 1.80

[a] Acidified with phosphoric acid

[b] Measurement not performed in absence of polymer due to fast Q crystallization upon contact with the solution

[c] Measurement not performed

7.4.3 In vitro dissolution.

7.4.3.1 Impact of Q content upon release

ASDs containing 10 and 25 wt% in CCAB were evaluated with regard to Q release. As presented in **Figure 7.5A**, both 10% and 25% Q loaded CCAB ASDs (90 CCAB, 25 CCAB) effectively protected Q from release at acidic pH; indeed, solution concentrations were significantly lower than that from crystalline Q alone. At the neutral pH that mimics the small intestine, release from the 10 % Q dispersion (90 CCAB, **Figure 7.5B**) reached much higher solution concentrations than from the 25% Q ASD (75 CCAB) or from crystalline Q alone. This is predictable given the quite hydrophobic nature of Q (more Q in the ASD makes it more hydrophobic, slowing drug release), and is consistent with our results with CAAdP and other polymers [19]. As a result we chose to compare subsequent ASD formulations with different polymers using 10% Q in each ASD.

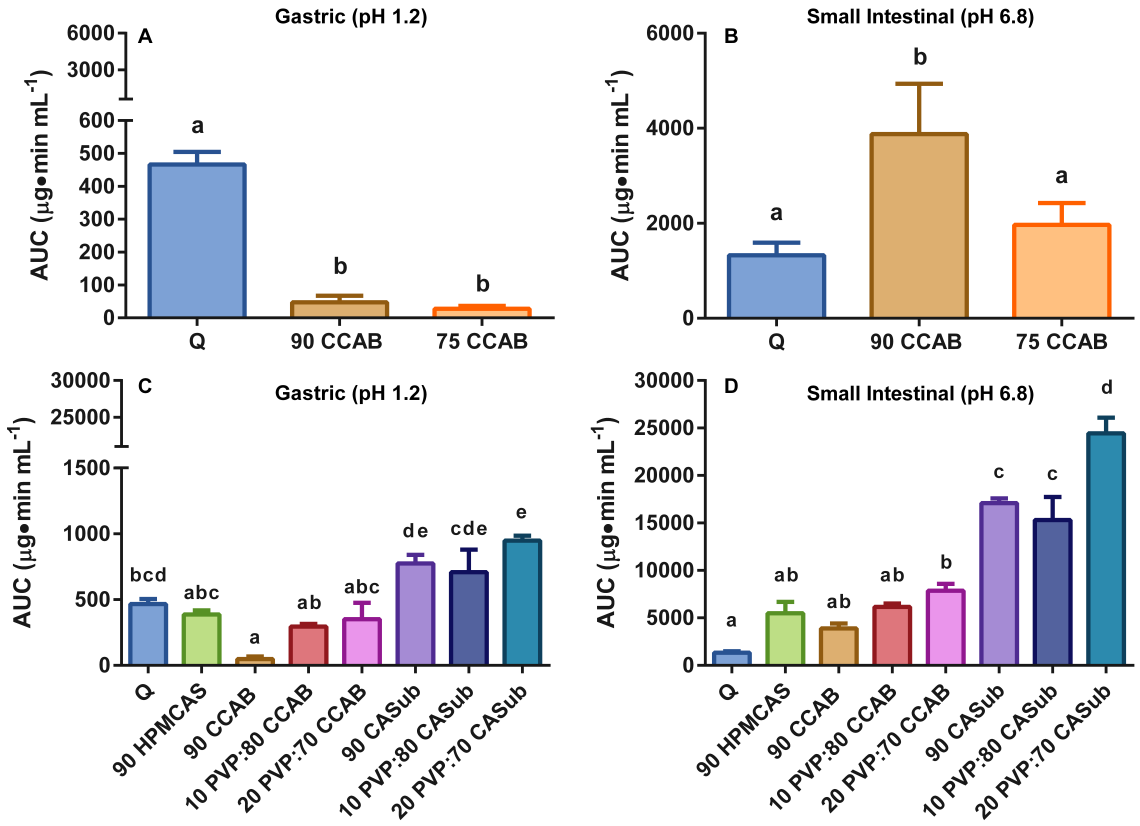

Figure 7.5 Dissolution area under the curve (AUC) values for all treatments. Q compared to 90 CCAB and 75:25 CCAB is given for both gastric pH (A) and intestinal pH (B). Q compared to all treatments that employed 10% Q loads are shown for both gastric pH (C) and intestinal pH (D). Different letters above each bar represent statistically significant differences in AUC between treatments ($p<0.05$) by 1-way ANOVA with Tukey's post hoc test.

7.4.3.2 Simulated gastric conditions (pH = 1.2)

Crystalline Q and all Q ASDs had extremely low dissolution in the gastric environment (**Figure 5C,** Sup Data Table S7.2). This was expected due to the inherent properties of crystalline Q, and of carboxylated cellulose derivatives (protonated, thus neutral/poorly soluble at acidic pH). Maximum low pH Q release was from 10% Q dispersed in 20% PVP:70% CASub, reaching only a mean C_{MAX} of 13.4 µg/mL and AUC of 972 µg·min/mL. All other polymers were relatively successful in preventing Q release at gastric pH. Even the AUC from 20%PVP:70% CASub at pH 1.2 was quite low compared to observed AUC values for any treatment at pH 6.8.

7.4.3.3 Simulated small intestinal conditions (pH = 6.8)

Dissolution experiments were performed at pH 6.8 to mimic the small intestine, and under non-sink conditions where ≥ 31-fold supersaturation would be achieved if all drug dissolved, in order to permit observation and quantification of the supersaturation expected from ASDs. AUC measurements for all formulations are presented in **Figure 7.5D;** AUC, C_{MAX}, and T_{MAX} values are summarized in **Table 7.2**. All ASDs examined provided some degree of supersaturation vs. Q alone. ASDs prepared with only HPMCAS or CCAB provided only modest improvements in Q solution concentrations; this is particularly interesting for HPMCAS, which has some solubility in water (ca. 23 mg/mL) [19]. In contrast, CCAB blended with PVP, and CASub either by itself or blended with PVP all give very significantly supersaturated Q solutions. Optimum Q dissolution was observed with CASub and PVP:CASub blends. Overall, 10% Q dispersed in 20 PVP:70 CASub provided the most significant enhancement ($p < 0.05$) in Q apparent solution concentration, with an 18-fold increase in AUC compared to crystalline Q (~ 24,400 vs. 1,330 μg·min/mL, respectively). This ASD was also able to produce the highest maximum solution concentration (C_{MAX} = 78.3 μg/mL) over the course of 8 hours at pH 6.8. This average C_{MAX} value is 12.7-fold higher than the average C_{MAX} value attained by crystalline Q (6.16 μg/mL). The degrees of enhancement of Q solution concentrations achieved are comparable to those achieved from different amorphous matrices by others [32] and in our previous work [19].

Table 7.2 Pseudo-pharmacokinetic parameters of Q at intestinal pH (6.8).

ASD Formulation	AUC[a] (μg min/mL)	C_{MAX}[a] (μg/mL)	T_{MAX}[a] (min)
Q	1330 ± 133	6.16 ± 0.141	120
90 CCAB	3880 ± 529	18.4 ± 2.15	60
75 CCAB	1940 ± 254	7.16 ± 1.49	60
50 CCAB	2550 ± 137	8.21 ± 0.760	N/A[b]
10 PVP:80 CCAB	6210 ± 382	20.0 ± 1.33	480
20 PVP:70 CCAB	7850 ± 733	27.4 ± 3.03	420
90 HPMCAS[c]	5480 ± 1210	64.1 ± 19.7	30
90 CASub[c]	17100 ± 485	48.7 ± 1.74	N/A[b]
10 PVP:80 CASub[c]	15300 ± 2434	50.4 ± 4.58	90
20 PVP:70 CASub[c]	24400 ± 1640	78.3 ± 7.12	N/A[b]

[a]Data are mean ± SEM AUC, average C_{MAX} and T_{MAX} (n = 4 except where indicated)

[b]T_{MAX} values listed as "N/A" had 4 separate times where C_{MAX} occurred

[c]n = 3

Blending with the miscible and hydrophilic PVP enhanced Q release from both CCAB and CASub as anticipated. The concern was whether the lower concentration of the effective crystallization inhibitor (CCAB (Marks, J.A., Nichols, B.L.B., Edgar, K.J. manuscript in preparation) or CASub [33]) would lead to loss of Q solution concentration due to crystallization. This does not appear to have been the case, and the blending approach was effective at synergistically combining PVP release properties with CASub/CCAB crystallization inhibition properties. Our data suggest that combination of hydrophobic (CCAB and CASub) and hydrophilic (PVP) polymers appears to provide relative protection from gastric conditions, enhanced release profile, and prevent Q recrystallization once in solution.

Polymer solubility parameters, presented in **Table 7.3**, are important, albeit imperfect, predictors of whether the polymer has the right hydrophobic/hydrophilic balance (they do not have the ability to discriminate between ionized and un-ionized carboxyl, which for this purpose is an important flaw). Solubility parameter calculations were performed as previously reported [22, 34] and can be found in Sup Data. Dissolution curves obtained with different ASDs are shown in **Figure 7.6** (pH 6.8) and Sup Data Figure S7.8 (pH 1.2). Higher solubility parameters indicate greater polymer hydrophilicity, therefore the polymers arranged by decreasing hydrophobicity are PVP < CCAB < CASub < HPMCAS. The correlation between Q release and polymer solubility parameter is rather weak; this has been observed also in other polymer-drug systems (Mosquera-Giraldo, L.I., Meng, X., Edgar, K.J., Slipchenko, L.V., Taylor, L.S., manuscript under review). Within more confined data sets, solubility parameters can have predictive value; thus addition of the quite hydrophilic PVP enhances release from the more hydrophobic CCAB and CASub matrices in predictable fashion. Based on solubility parameters alone, for example, the low Q solution concentration obtained from the 10% Q ASD in CCAB ASD was unexpected; a maximum Q solution concentration of only 18.4 µg/mL (**Figure 7.6B**) was attained. Lower concentration with CCAB than with CASub was surprising since CCAB has higher calculated solubility parameter than CASub. CASub was especially effective at enhancing Q solution concentration, reaching a maximum of 48.7 µg/mL within the first hour of dissolution (**Figure 7.6B**). This is fully consistent with the known excellence of CASub as a crystallization inhibitor [33]. When blended with 10% PVP, release and thus solution concentration did not improve noticeably (50.4 µg/mL), but with 20% PVP in the ASD (20 PVP:70 CASub), solution concentration improved markedly to 78.3 µg/mL (**Figure 7.6D**). HPMCAS, the most hydrophobic polymer in the set of polymers investigated, provided interesting Q ASD behavior. Release from the HPMCAS ASD was very rapid, reaching an average solution concentration of 64.1 µg/mL (**Figure 7.6B**) within 30 min. This solution was clear, but quickly became cloudy, and measured solution concentration quickly dropped off, indicating that HPMCAS was ineffective at preventing Q crystallization from supersaturated solution.

Table 7.3 Hildebrand solubility parameters of polymers used to prepare Q ASDs.

Polymer	Solubility parameter, δ ($MPa^{1/2}$)
PVP	28.39
CCAB	24.44
CASub (DS 0.9)	22.66
HPMCAS	22.42

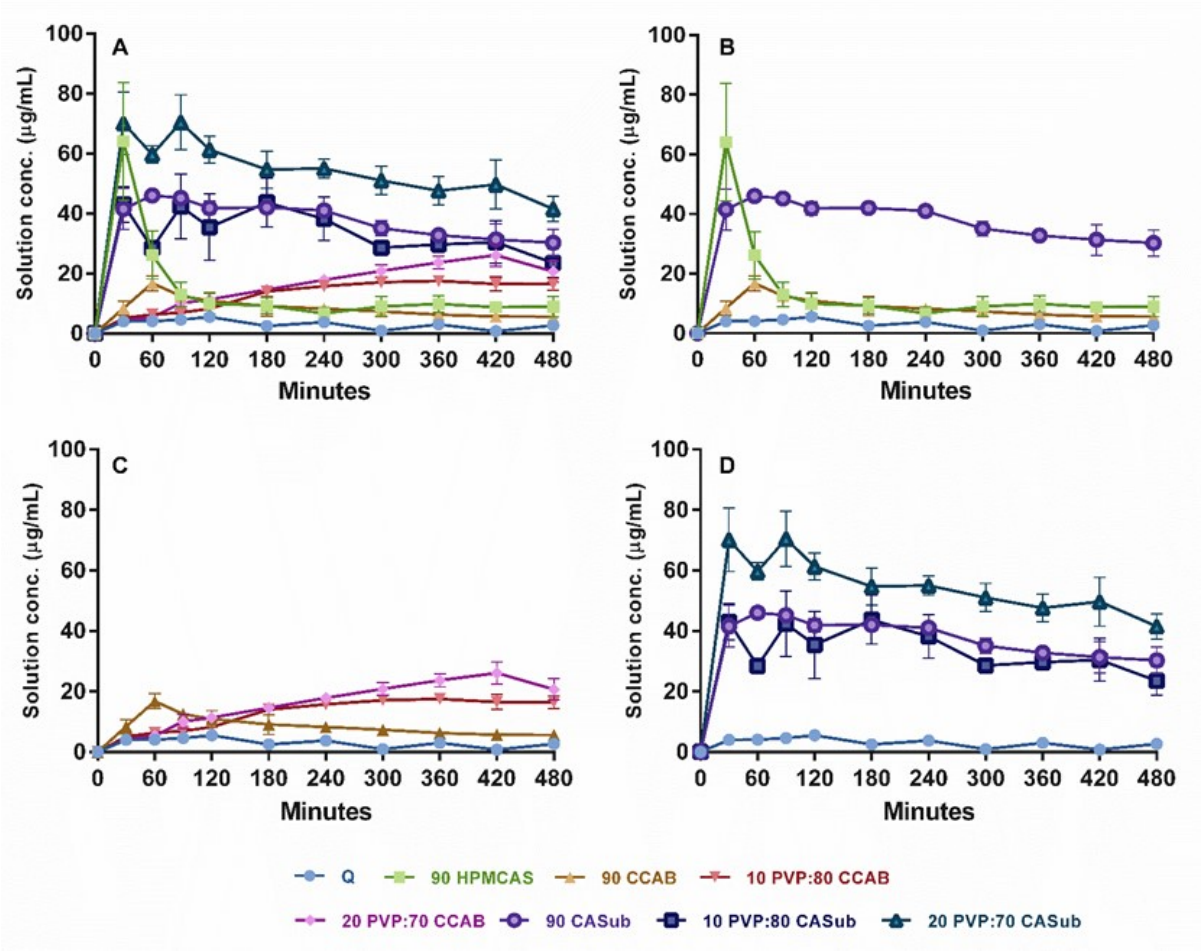

Figure 7.6 Average solution concentrations of Q (mean ± SEM, n = 3-4) plotted over time at pH 6.8 for all treatments (A), 10% Q loaded ASDs only shown for comparison of dissolution properties for each polymer utilized (B), the impact of PVP blending with CCAB (C) and CASub (D). All graphs contain crystalline Q as a control for comparison.

7.5 Conclusions

Amorphous solid dispersions at 10 wt% Q were prepared using the cellulose esters CCAB, HPMCAS, and CASub. Q was also amorphous at 25% in CCAB, but was not fully amorphous at 50% Q in CCAB. All ASDs of Q in these carboxyl-containing cellulose esters protect effectively against Q release at fasting gastric pH, giving substantially lower Q concentrations than from Q without polymer. In contrast, all three cellulose esters provide supersaturated solutions of Q at small intestinal pH, at which pH most of the carboxylic acids are ionized. The degree of supersaturation from CCAB-only dispersions was slight, due in part to ineffective drug release, while release from HPMCAS ASD was rapid, achieving substantial supersaturation. However HPMCAS proved to be a poor inhibitor of Q crystallization from supersaturated solutions, resulting in rapid de-supersaturation. CASub on the other hand provided both substantial Q release at pH 6.8, and stable, high supersaturation. Furthermore, incorporation of the more hydrophilic and water-soluble 10% PVP into ASD blends was effective, enhancing release from CCAB at 10% PVP, and significantly enhancing release and supersaturation from CASub ASDs at 20% PVP. Thus CASub and its blends with PVP are highly effective polymers for enhancing Q solution concentration *in vitro*, and provide a promising opportunity for increasing Q bioaccessibility and bioavailability *in vivo*.

Overall these results confirm our hypotheses, and significantly illuminate structure-property relationships of ASD polymers. We can term polymer properties like sufficiently high T_g (50°C or more above the highest likely ambient temperature) and solubility parameters within an effective range (hydrophobic enough to interact with hydrophobic drugs, hydrophilic enough to release them) as *necessary* but clearly not *sufficient* polymer properties for effectiveness in ASD. This work further confirms the value of the pH-responsive carboxylic acid functional group in providing neutral pH release as well as desirable specific polymer-drug interactions, but this parameter alone is also *insufficient* to fully predict success or failure. This work also provides a further example of the value of polymer blends for achieving performance levels (in this case both release and crystallization inhibition) that would be difficult to achieve by ASD of drug, in this case Q, with a single polymer. More detailed study of expanded sets of polymers is necessary to further sort out the structural features required for effective ASD.

The results of this study, particularly with CASub, warrant *in vivo* investigation of Q ASDs as method for increasing Q bioavailability upon oral administration. They predict that significant supersaturation should be achievable *in vivo*; it will be of great interest to see whether this results in higher permeation *in vivo*, and in saturation of metabolic enzymes, thereby providing enhanced bioavailability, particularly of the unmetabolized native Q. If successful, such an ASD approach should enable animal and human *in vivo* bioavailability enhancement studies, and provide predictable absorbed doses that will enable informative dose-response studies, thus leading to exploration of whether the potential health benefits of Q can be realized in humans.

7.6 Acknowledgements

Funding for this research was provided by the Institute for Critical Technologies and Applied Sciences (ICTAS) at Virginia Tech (VT), via a Junior Faculty Collaborative grant to Drs. Neilson and Edgar. We thank Eastman Chemical Company for their kind donation of CA, CAP, and CCAB. We thank Shin-Etsu Chemical Co., Ltd. for their kind donation of HPMCAS. We are grateful to the VT Macromolecules Innovation Institute for their support, and to VT ICTAS for their material and facilities support. BLBN thanks the National Science Foundation for financial support through grant number DMR-130827. We also wish to thank Steve McCartney (Nanoscale Characterization and Fabrication Laboratory, Virginia Tech) for his help in taking SEM images, and Ann Norris (Department of Sustainable Biomaterials, Virginia Tech) for XRD analyses.

7.7 References

1. Caridi, D.; Trenerry, V. C.; Rochfort, S.; Duong, S.; Laugher, D.; Jones, R. Profiling and quantifying quercetin glucosides in onion (Allium cepa L.) varieties using capillary zone electrophoresis and high performance liquid chromatography. *Food Chem.* **2007,** *105*, (2), 691-699.

2. Price, K. R.; Casuscelli, F.; Colquhoun, I. J.; Rhodes, M. J. C. Composition and content of flavonol glycosides in broccoli florets (Brassica olearacea) and their fate during cooking. *J. Sci. Food Agric.* **1998,** *77*, (4), 468-472.

3. Gabler, N. K.; Ostrowska, E.; Jones, R. B.; Imsic, M.; Jois, M.; Tatham, B. G.; Eagling, D. R.; Dunshea, F. R., Consumption of brown onion (Allium cepa) cultivars reduce the risk factors of cardiovascular disease. Queensland Government, Department of Primary Industries: Brisbane, 2003; pp 178-179.

4. Russo, M.; Spagnuolo, C.; Tedesco, I.; Bilotto, S.; Russo, G. L. The flavonoid quercetin in disease prevention and therapy: Facts and fancies. *Biochem. Pharmacol.* **2012,** *83*, (1), 6-15.

5. Firdous, A. B.; Sharmila, G.; Balakrishnan, S.; RajaSingh, P.; Suganya, S.; Srinivasan, N.; Arunakaran, J. Quercetin, a natural dietary flavonoid, acts as a chemopreventive agent against prostate cancer in an in vivo model by inhibiting the EGFR signaling pathway. *Food & Function* **2014,** *5*, (10), 2632-2645.

6. Jaganathan, S. K. Can flavonoids from honey alter multidrug resistance? *Medical Hypotheses* **2011,** *76*, (4), 535-537.

7. Zhou, W.; Kallifatidis, G.; Baumann, B.; Rausch, V.; Mattern, J.; Gladkich, J.; Giese, N.; Moldenhauer, G.; Wirth, T.; Buchler, M. W.; Salnikov, A. V.; Herr, I. Dietary polyphenol quercetin targets pancreatic cancer stem cells. *Int. J. Oncol.* **2010,** *37*, (3).

8. Song. Associations of dietary flavonoids with risk of type 2 diabetes, and markers of insulin resistance and systemic inflammation in women: a prospective study and cross-sectional analysis. *Journal of the American College of Nutrition* **2005,** *24*, (5), 376-384.

9. Chiş, I. C.; Baltaru, D.; Maier, M.; Mureşan, A.; Clichici, S. Effects of quercetin and chronic (training) exercise on oxidative stress status in animals with streptozotocin-induced diabetes. *Bulletin of University of Agricultural Sciences and Veterinary Medicine Cluj-Napoca. Veterinary Medicine* **2013,** *70*, (1), 31-39.

10. Gutierrez, J. C.; Prater, M. R.; Holladay, S. D. Quercetin supplementation reduces maternal hyperglycemia in a type 2 diabetes mellitus mouse model. *Annual Research & Review in Biology* **2014,** *4*, (1), 306-311.

11. Srinivas, K.; King, J. W.; Howard, L. R.; Monrad, J. K. Solubility and solution thermodynamic properties of quercetin and quercetin dihydrate in subcritical water. *J. Food Eng.* **2010,** *100*, (2), 208-218.

12. Lauro, M. R.; Torre, M. L.; Maggi, L.; De Simone, F.; Conte, U.; Aquino, R. P. Fast- and Slow-Release Tablets for Oral Administration of Flavonoids: Rutin and Quercetin. *Drug Dev. Ind. Pharm.* **2002,** *28*, (4), 371-379.

13. Fang, R.; Jing, H.; Chai, Z.; Zhao, G.; Stoll, S.; Ren, F.; Liu, F.; Leng, X. Design and characterization of protein-quercetin bioactive nanoparticles. *Journal of Nanobiotechnology* **2011,** *9*, (1), 19.

14. Kakran, M.; Sahoo, N. G.; Li, L.; Judeh, Z. Fabrication of quercetin nanoparticles by anti-solvent precipitation method for enhanced dissolution. *Powder Technology* **2012,** *223*, (0), 59-64.

15. Sahu, S.; Saraf, S.; Kaur, C. D.; Saraf, S. Biocompatible Nanoparticles for Sustained Topical Delivery of Anticancer Phytoconstituent Quercetin. *Pakistan Journal of Biological Sciences* **2013,** *16*, (13), 601-9.

16. Dian, L.; Yu, E.; Chen, X.; Wen, X.; Zhang, Z.; Qin, L.; Wang, Q.; Li, G.; Wu, C. Enhancing oral bioavailability of quercetin using novel soluplus polymeric micelles. *Nanoscale Res Lett* **2014,** *9*, (1), 1-11.

17. Tran, T. H.; Guo, Y.; Song, D.; Bruno, R. S. Quercetin-Containing Self-Nanoemulsifying Drug Delivery System for Improving Oral Bioavailability. *J. Pharm. Sci. 103*, (3), 840-852.

18. Ilevbare, G. A.; Liu, H.; Edgar, K. J.; Taylor, L. S. Understanding Polymer Properties Important for Crystal Growth Inhibition—Impact of Chemically Diverse Polymers on Solution Crystal Growth of Ritonavir. *Crystal Growth & Design* **2012,** *12*, (6), 3133-3143.

19. Li, B.; Konecke, S.; Harich, K.; Wegiel, L.; Taylor, L. S.; Edgar, K. J. Solid dispersion of quercetin in cellulose derivative matrices influences both solubility and stability. *Carbohydrate Polymers* **2013,** *92*, (2), 2033-2040.

20. Pereira, J. M.; Mejia-Ariza, R.; Ilevbare, G. A.; McGettigan, H. E.; Sriranganathan, N.; Taylor, L. S.; Davis, R. M.; Edgar, K. J. Interplay of Degradation, Dissolution and Stabilization of Clarithromycin and Its Amorphous Solid Dispersions. *Mol. Pharm.* **2013,** *10*, (12), 4640-4653.

21. Vasconcelos, T.; Sarmento, B.; Costa, P. Solid dispersions as strategy to improve oral bioavailability of poor water soluble drugs. *Drug Discov. Today* **2007,** *12*, (23–24), 1068-1075.

22. Liu, H.; Ilevbare, G. A.; Cherniawski, B. P.; Ritchie, E. T.; Taylor, L. S.; Edgar, K. J. Synthesis and structure–property evaluation of cellulose ω-carboxyesters for amorphous solid dispersions. *Carbohydrate Polymers* **2014,** *100*, 116-125.

23. Lauro, M. R.; Maggi, L.; Conte, U.; De Simone, F.; Aquino, R. P. Rutin and quercetin gastro-resistant microparticles obtained by spray-drying technique. *J. Drug Deliv. Sci. Technol.* **2005,** *15*, (5), 363-369.

24. Van den Mooter, G.; Wuyts, M.; Blaton, N.; Busson, R.; Grobet, P.; Augustijns, P.; Kinget, R. Physical stabilisation of amorphous ketoconazole in solid dispersions with polyvinylpyrrolidone K25. *Eur. J. Pharm. Sci.* **2001,** *12*, (3), 261-269.

25. Konno, H.; Handa, T.; Alonzo, D. E.; Taylor, L. S. Effect of polymer type on the dissolution profile of amorphous solid dispersions containing felodipine. *European Journal of Pharmaceutics and Biopharmaceutics* **2008,** *70*, (2), 493-499.

26. Gupta, P.; Kakumanu, V. K.; Bansal, A. K. Stability and Solubility of Celecoxib-PVP Amorphous Dispersions: A Molecular Perspective. *Pharm Res* **2004,** *21*, (10), 1762-1769.

27. Marks, J. A.; Wegiel, L. A.; Taylor, L. S.; Edgar, K. J. Pairwise Polymer Blends for Oral Drug Delivery. *J. Pharm. Sci.* **2014,** *103*, (9), 2871-2883.

28. Buchanan, C. M.; Buchanan, N. L.; Carty, S. N.; Kuo, C. M.; Lambert, J. L.; Posey-Dowty, J. D.; Watterson, T. L.; Wood, M. D.; Malcolm, M. O.; Lindblad, M. S., Cellulose interpolymers and methods of oxidation. 2014.

29. Shelton, M. C.; Posey-Dowty, J. D.; Lingerfelt, L.; Kirk, S. K.; Klein, S.; Edgar, K. J., Enhanced dissolution of poorly soluble drugs from solid dispersions in carboxymethylcellulose acetate butyrate matrices. In *Polysaccharide Materials: Performance by Design*, American Chemical Society: 2009; Vol. 1017, pp 93-113.

30. Posey-Dowty, J. D.; Watterson, T. L.; Wilson, A. K.; Edgar, K. J.; Shelton, M. C.; Lingerfelt, L. R. Zero-order release formulations using a novel cellulose ester. *Cellulose* **2007,** *14*, (1), 73-83.

31. Ilevbare, G. A.; Taylor, L. S. Liquid–Liquid Phase Separation in Highly Supersaturated Aqueous Solutions of Poorly Water-Soluble Drugs: Implications for Solubility Enhancing Formulations. *Crystal Growth & Design* **2013,** *13*, (4), 1497-1509.

32. Fujimori, M.; Kadota, K.; Shimono, K.; Shirakawa, Y.; Sato, H.; Tozuka, Y. Enhanced solubility of quercetin by forming composite particles with transglycosylated materials. *J. Food Eng.* **2015,** *149*, 248-254.

33. Ilevbare, G. A.; Liu, H.; Edgar, K. J.; Taylor, L. S. Impact of Polymers on Crystal Growth Rate of Structurally Diverse Compounds from Aqueous Solution. *Mol. Pharm.* **2013,** *10*, (6), 2381-2393.

34. Fedors, R. F. A method for estimating both the solubility parameters and molar volumes of liquids. *Polymer Engineering & Science* **1974,** *14*, (2), 147-154.

Chapter 8. Summary and Future Work

Cellulose esters have been used for drug delivery formulations and tested for ASD studies before since they are natural-based, non-toxic, and generally biocompatible polymers with a wide range of molecular weights, and have potential for various applications. However the specific design of cellulose derivatives for oral drug delivery purposes has great importance and is a new field of study.

My doctoral research has focused on the investigation of carboxylated cellulose esters and cellulose ether esters for oral delivery using ASDs to increase solution concentrations of crystalline and poorly water-soluble drugs, and development of a carboxylated cellulose ether ester derivative family for the same purpose, including methyl and ethyl cellulose adipates, suberates and sebacates.

8.1 Rif solubility enhancement and bioavailability increase

Rif is a vital first line drug for TB treatment that is given to patients at a very high dose (600 mg/day) to achieve a moderate and variable bioavailability as a result of its instability at acidic pH and moderate solubility at neutral pH. To overcome these problems, we prepared ASDs with cellulose ω-carboxyalkanoates (CASub, CAAdP, and CABSeb) and with CMCAB as a positive control and Rif itself as negative control.

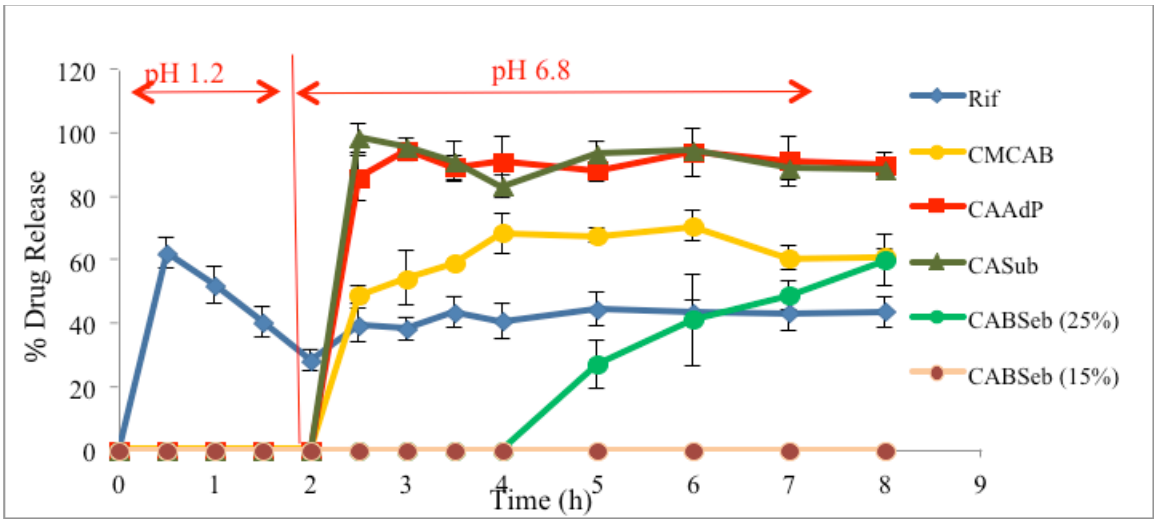

Figure 8.1: Rif dissolution from pH switch experiment under sink conditions; pH 1.2 for 2 h, then pH 6.8 for 6h. Error bars indicate one standard deviation (n = 3).

As shown in Figure 8.1, CAAdP and CASub reached almost 100% release; on the other hand only 40% of the crystalline drug stayed intact till the end of the experiment. CABSeb release profile is very similar to first order release and both CMCAB and CABSeb released 70% of the drug. All the ASD formulations effectively prevented Rif release at gastric pH; we expect that such ASDs would prevent acid-catalyzed Rif degradation.

8.2 Cellulose ether ester synthesis and their application to ASDs

A cellulose carboxy ether ester derivative family was synthesized by the reaction of cellulose alkyl ethers with monoprotected (benzyl ester), monofunctional long chain acid chlorides, followed by protecting group removal to form the target alkyl cellulose ω-carboxyalkanoates as shown in **Figure 8.2**.

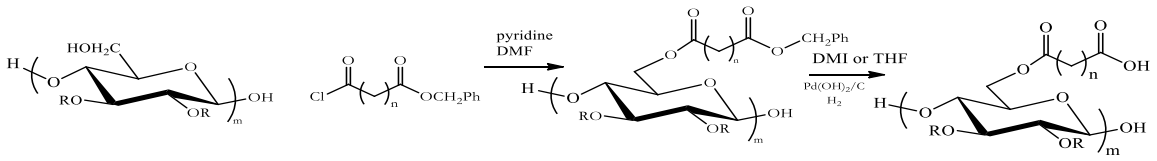

Figure 8.2: Synthesis scheme of ethyl ether cellulose derivatives.

8.3 Cellulose ester ASDs to increase solubility of anti-HIV drugs and Que

We prepared 3 drug anti-HIV ASD formulations with cellulose esters (CAAdP, CASub, CCAB and CMCAB) and tested the release for one drug, two drugs and three drug formulations to investigate the effect of multiple drug application on amorphous solubility and recognized that Etra solubility increases when applied with Rit and Efa; on the other hand the solution concentrations of Efa and Rit decrease. Mechanistic studies showed that this was primarily a result of each dissolved drug influencing dissolution of the others, rather than an influence on release behavior, for example as a result of drug hydrophobicity. The behavior of Etra (increase of solution concentration when dissolved with Efa and Rit) was unexpected and its solubility was increased 8 fold more than the crystalline drug. There is little literature precedent for observing these kinds of drug interactions in multidrug formulations, and we believe that this work will have powerful impact on design of these important formulations.

Que ASDs were prepared with CCAB, CASub, and HPMCAS. PVP/CASub blends and PVP/CCAB blends were also investigated for expected higher Que release in the presence of water-soluble PVP. These studies showed that as the PVP content of the formulation increases, drug release increases as expected. However Que is a highly crystalline drug and its stabilization after release was a challenge. The ASD polymer designed by our group and successful in many ASD systems, CASub (DS 0.9), had the highest efficiency in preventing recrystallization of the amorphous drug after the release. As a result, 20% PVP 70% CASub was the most successful formulation that could maintain Que supersaturation for at least 8h. Follow-up *in vivo* Que ASD studies with our best polymers in rats have been completed and data analysis is under way, for future publication.

8.4 Proposed future work

The valuable properties of the novel polymers and their potential in application have been shown in the thesis, however there are still issues to be addressed. It is required to carry out an acute toxicology study to show the safety of the best polymers, to realize their potential in human use. In addition, a histopathology study can address the lower damage

of the reduced dose drug in ASDs than the crystalline drug, especially in the Rif studies. In addition, completion of the *in vivo* study of CAAdP Rif and CMCAB Rif in rats, that have a more human-like GI tract than mice, will be important confirmation of the value of these polymers for ASD of drugs in marketed formulations.

I would also suggest to develop a mathematical model to predict the release properties of the drug delivery system according to the polymer hydrophobicity, polymer structure, drug hydrophobicity and drug structure (functional groups hydrogen bonding accepting and donation) since the polymer to drug and polymer to polymer interactions in a range of pH (6.8-7.2) will have a great impact on the release.

Electrospinning of these cellulose derivatives is another valuable research approach for tissue engineering and stem cell engineering studies since cellulose esters we prepared in our lab are hydrophobic materials, therefore they will have only limited interaction and solubility with the water systems and as a result they have great potential to maintain the structure of the scaffold for a weeks and support the cell lines mechanically. It is a common problem that the polymeric scaffolds (especially made with hydrogels) cannot maintain morphology for a long time at 37°C in cell culture media and there are investigations in that field[1] but more research is essential. Moreover, ASDs can be prepared by this method if the scaffold would like to be used as a medical device for drug delivery or growth factors can be loaded to the scaffolds for growth factor delivery to promote the cell line phenotype maintenance. In literature, cellulose acetate (CA)[2,3] or cellulose nanocrystal[4] based electrospin scaffolds have been prepared before, but the investigation can be extended and with the addition of the hydrocarbon chains the polymer will become more hydrophobic than CA, therefore has definitely more potential.

CAAdP has been prepared by direct synthesis with adipic anhydrides published by Edgar lab before[5] that was a much easier protocol than the method required cellulose esterification and protective group removal by hydrogenolysis[6,7]. The study can be extended with the direct synthesis of CASub with 2,9-oxonanedione (commercially

available) that should eliminate the use of expensive hydrogenolysis catalyst and reduce the steps of the process.

The HIV multidrug study can be extended with other FDA approved crystalline HIV drugs such as dolutegravir (class II drug, 0.0922 mg/ml[8]), to investigate whether we can identify other drugs that will behave like Etra, either with higher solubility when applied with other drugs or able to promote Etra solubility when applied together. In addition, multidrug formulations can be investigated with other cellulose esters that are powerful in recrystallization prevention such as ethyl cellulose adipate or suberate.

8.5 References

(1) Eyrich, D.; Brandl, F.; Appel, B.; Wiese, H.; Maier, G.; Wenzel, M.; Staudenmaier, R.; Goepferich, A.; Blunk, T. Long-Term Stable Fibrin Gels for Cartilage Engineering. *Biomaterials* **2007**, *28*, 55–65.

(2) Liu, H.; Hsieh, Y. Lo. Ultrafine Fibrous Cellulose Membranes from Electrospinning of Cellulose Acetate. *J. Polym. Sci. Part B Polym. Phys.* **2002**, *40*, 2119–2129.

(3) Son, W. K.; Youk, J. H.; Lee, T. S.; Park, W. H. Electrospinning of Ultrafine Cellulose Acetate Fibers: Studies of a New Solvent System and Deacetylation of Ultrafine Cellulose Acetate Fibers. *J. Polym. Sci. Part B Polym. Phys.* **2004**, *42*, 5–11.

(4) Zhou, C.; Shi, Q.; Guo, W.; Terrell, L.; Qureshi, A. T.; Hayes, D. J.; Wu, Q. Electrospun Bio-Nanocomposite Scaffolds for Bone Tissue Engineering by Cellulose Nanocrystals Reinforcing Maleic Anhydride Grafted PLA. *ACS Appl. Mater. Interfaces* **2013**, *5*, 3847–3854.

(5) Liu, H. Y.; Kar, N.; Edgar, K. J. Direct Synthesis of Cellulose Adipate Derivatives Using Adipic Anhydride. *Cellulose* **2012**, *19*, 1279–1293.

(6) Kar, N.; Liu, H.; Edgar, K. J. Synthesis of Cellulose Adipate Derivatives. *Biomacromolecules* **2011**, *12*, 1106–1115.

(7) Liu, H.; Ilevbare, G. A.; Cherniawski, B. P.; Ritchie, E. T.; Taylor, L. S.; Edgar, K.

J. Synthesis and Structure-Property Evaluation of Cellulose ω-Carboxyesters for Amorphous Solid Dispersions. *Carbohydr. Polym.* **2014**, *100*, 116–125.

(8) Dolutegravir http://www.drugbank.ca/drugs/DB08930.

Appendix

Chapter 3. Rifampin Stability and Solution Concentration Enhancement through Amorphous Solid Dispersion in Cellulose ω-Carboxyalkanoate Matrices

Table S3.1: Drug loading of spray-dried Rif/polymer dispersions

	CAAdP	CABSeb (15%)	CABSeb (25%)	CMCAB	CASub
Drug load Target (%)	15.0	15.0	25.0	15.0	15.0
Drug load measured (%)	14.8	14.4	23.6	13.5	14.8
Drug load Efficiency (%)	98.8	96.3	94.5	90.0	98.9

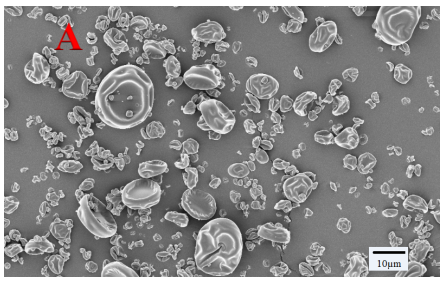

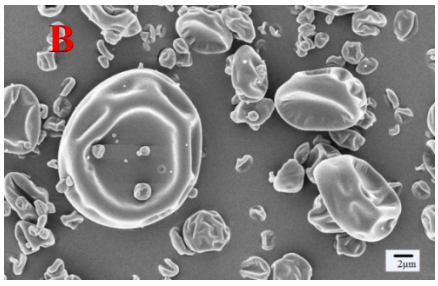

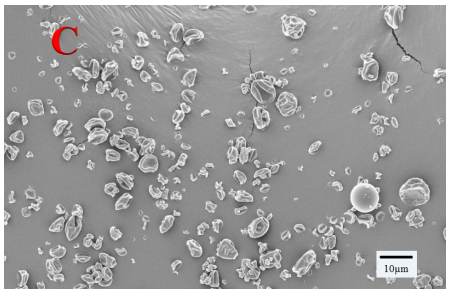

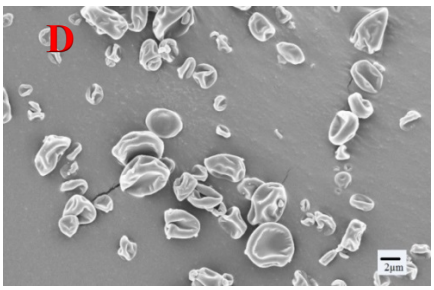

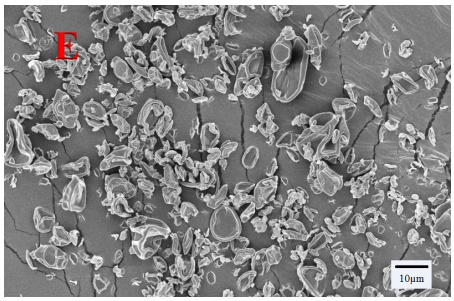

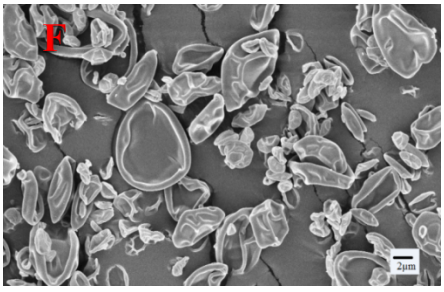

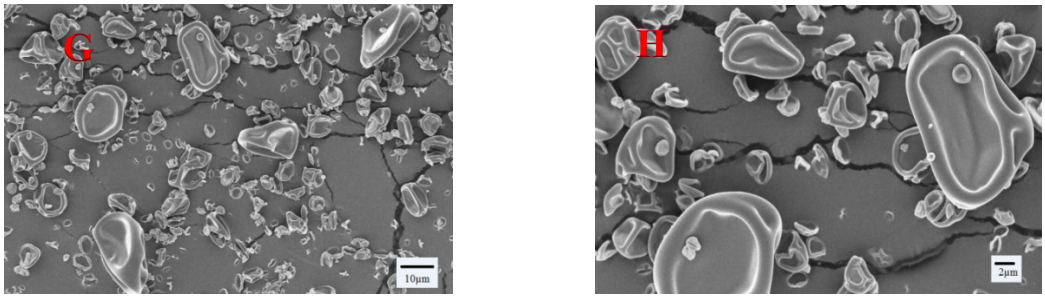

Figure S3.1: SEM images of Rif/polymer spray-dried dispersions at 2Kx (A, C, D and G) and 5Kx magnification (B, D, F and H): CABSeb (A, B), CAAdP (C, D), CASub (E, F) and CMCAB (G, H)

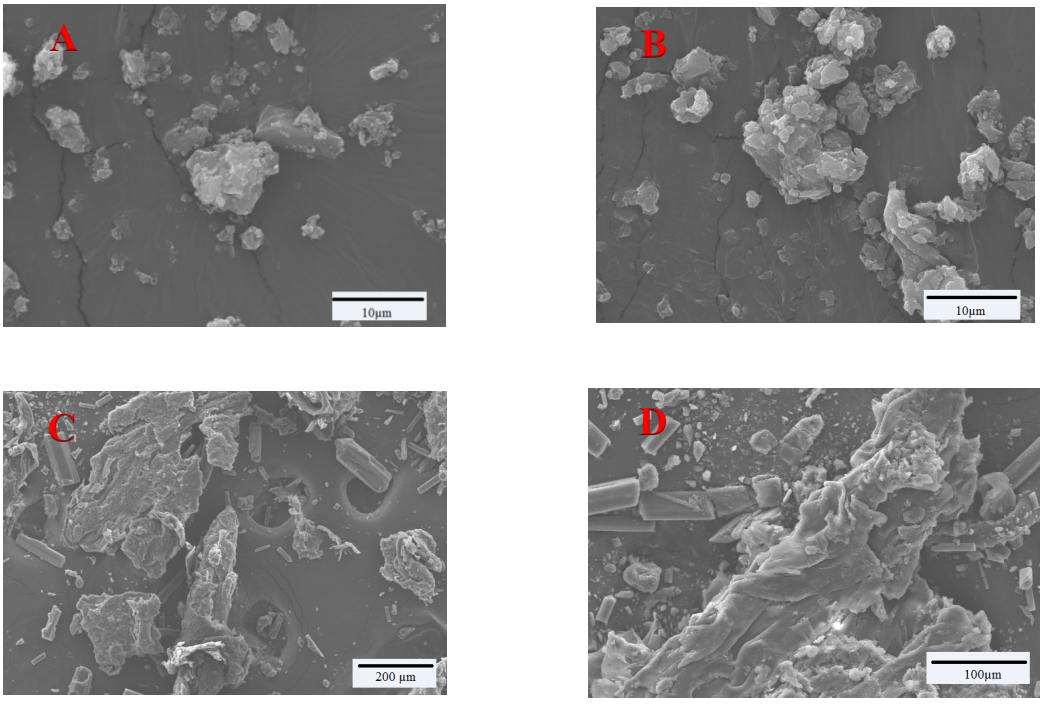

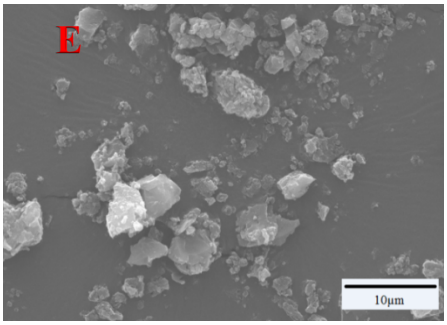

Figure S3.2: SEM images of physical mixtures prepared with Rif and A)CAAdP B)CASub C)25% CABSeb D)CABSeb 15% and E)CMCAB.

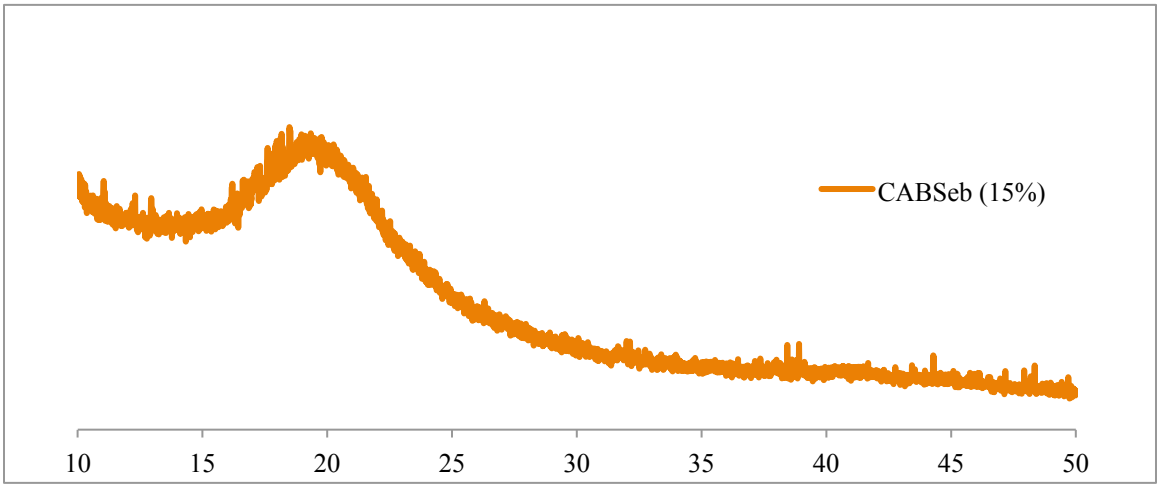

Figure S3.3: XRD spectra of spray-dried CABSeb (15%) Rif Formulation.

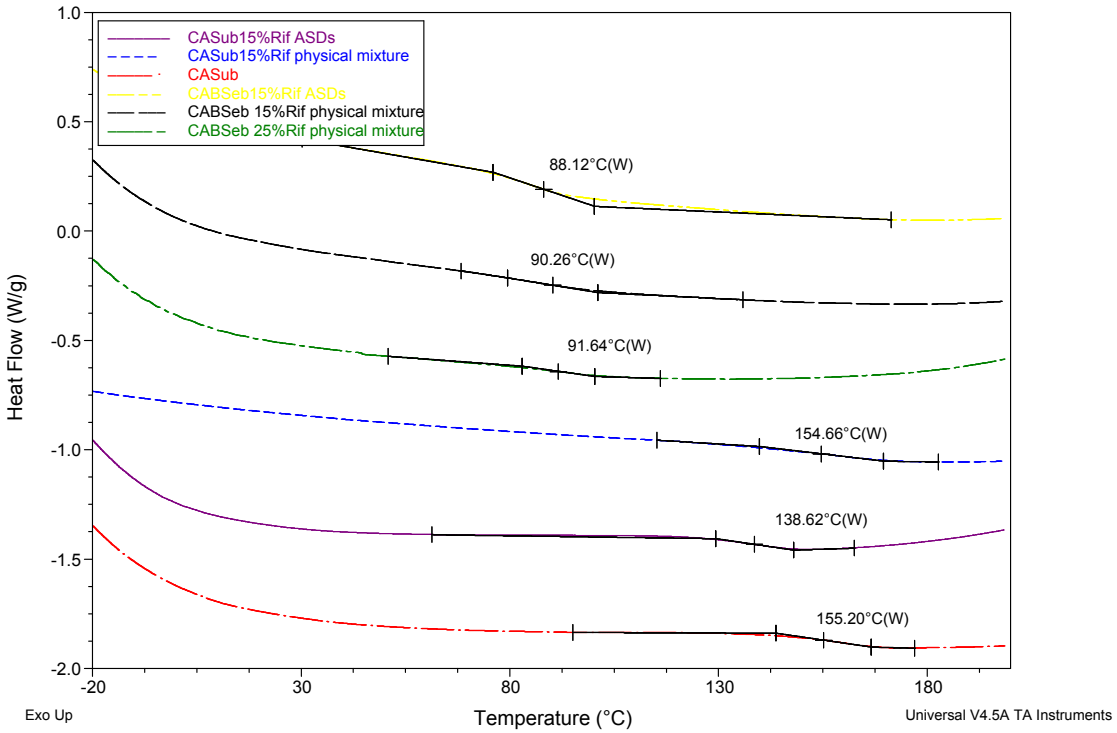

Figure S3.4: DSC thermograms of polymers, polymer/Rif amorphous dispersions and polymer/Rif physical mixtures.

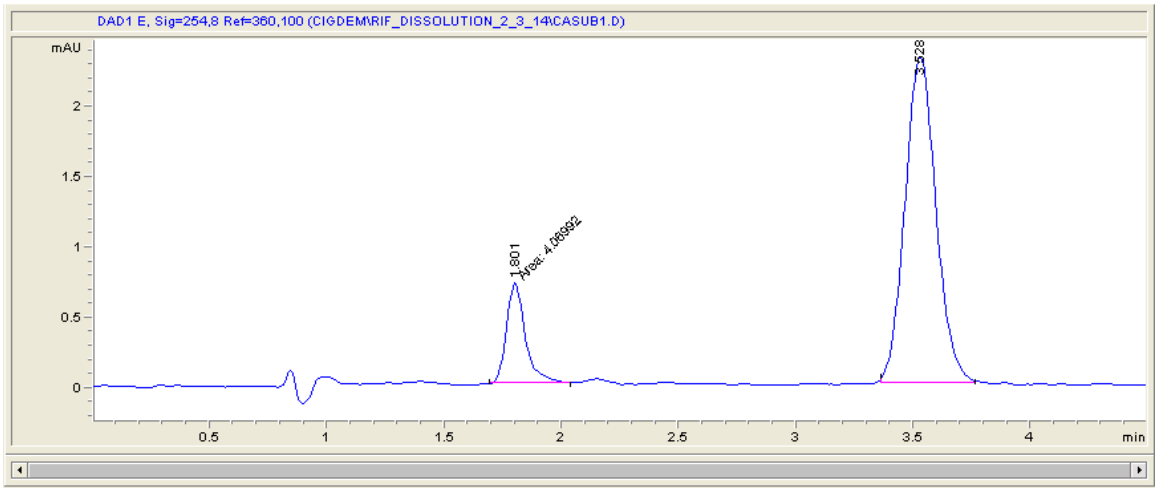

Figure S3.5: CASub dissolution study result at pH 6.8, HPLC spectra after 30 min. Degradation peak : 1.801, Rif peak 3.528

#	Time	Area	Height	Width	Area%	Symmetry
1	1.801	4.1	7.2E-1	0.0948	15.968	0.765
2	3.528	21.4	2.3	0.1416	84.032	0.901

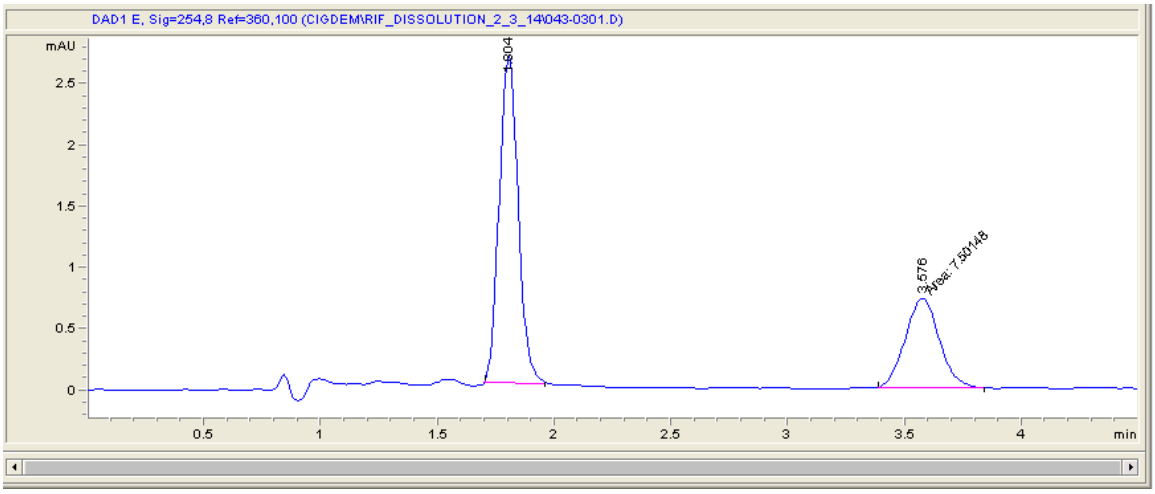

Figure S3.6: CASub dissolution study result at pH 6.8, HPLC spectra after 8 h. Degradation peak: 1.801, Rif peak 3.528

#	Time	Area	Height	Width	Area%	Symmetry
1	1.804	15.2	2.7	0.0881	66.940	0.94
2	3.576	7.5	7.4E-1	0.1699	33.060	1.006

Chapter 5. Amorphous solid dispersions of multiple anti-HIV drugs: impacts of drugs on each other's solution concentrations, and mechanisms thereof

Preparation of monobenzyl adipate: Adipic acid (73 g, 0.5 mol), benzyl alcohol (81 g, 0.75 mol), PTSA (0.95 g, 5 mmol), and toluene (200 mL) were stirred in a flask equipped with Dean-Stark trap and heated at reflux for 3 hours. Water (200 mL) water was added to the cooled reaction medium and pH was adjusted to 8 with 6M NaOH. Then the aqueous layer was separated and mixed with 200 mL ether. The pH was adjusted to 2.00 with 6M HCl, then the mixture was shaken and the ether layer separated, then dried by under reduced pressure at 40°C. The product monobenzyl adipate was a colorless oil. Yield: 90%. ^{1}H NMR ($CDCl_3$); 1.68 (m, 4H), 2.36 (m, 4H), 5.09 (s, 2H), and 7.32 (m, 5H).

Preparation of monobenzyl adipoyl chloride: Monobenzyl adipate (20 g, 0.08 mol) and DMF (3 drops) in 200 mL dichloromethane were combined in a flask and cooled to 0°C. Then oxalyl chloride (57.15 g, 0.2 mol) was slowly added and then the solution stirred for 2 h at room temperature. The solvent was removed under reduced pressure, then 20 mL toluene was added and the solvent was again evaporated under reduced pressure. The product monobenzyl adipoyl chloride was a yellow oil. ^{1}H NMR ($CDCl_3$): 1.73 (m, 4 H), 2.39 (t, 2 H), 2.90 (t, 2 H), 5.12 (s, 2 H), 7.32 (m, 5 H).

Similar procedures were followed to synthesize monobenzyl suberoyl chloride (^{1}H NMR ($CDCl_3$): 1.34 (m, 4H), 1.66 (m, 4H), 2.36 (t, 2H), 2.86 (t, 2H), 5.12 (s, 2H), 7.35 (m, 5H)).

CAAdP monobenzyl ester synthesis: CAP (1 g, 3.52 mmol) was dissolved in MEK (10 mL), and then Et_3N (1.6 mL, 11.6 mmol, 3.3 equiv) was added all at once. Then monobenzyl adipoyl chloride (2.67 g, 10.56 mmol, 3 equiv) was added. After stirring 20 h at 60°C under nitrogen, the product was precipitated by adding the reaction mixture slowly to 300 mL ethanol. The product was isolated by filtration, washed with 500 mL water, re-dissolved in THF and then re-precipitated in 300 mL hexane. After collecting the polymer by vacuum filtration, it was dried in vacuum oven at 40°C

overnight (yield 88%) and the white powder product was characterized by ^{1}H NMR ($CDCl_3$): δ 1.02_1.20 (m, $COCH_2\underline{CH_3}$ of propionate), 1.66 (broad s, $COCH_2\underline{CH_2}\underline{CH_2}CH_2CO$ of adipate), 2.16-2.35 (m, $CO\underline{CH_2}CH_3$ of propionate, $COCH_3$ of acetate and $CO\underline{CH_2}CH_2CH_2\underline{CH_2}CO$ of adipate), 3.25-5.24 (cellulose backbone), 5.10 ($\underline{CH_2}C_6H_5$), 7.33 ($CH_2\underline{C_6H_5}$). DS by ^{1}H NMR ($CDCl_3$): adipate 0.9, propionate 2.09, acetate 0.04.

Monobenzyl CASub was synthesized by a procedure similar to that previously reported[26], as summarized here. CA 320S (1.00 g, 4.19 mmol) was dissolved in 20 mL DMI, and triethylamine (1.94 mL, 13.8 mmol, 3.3 equiv) was added to the reaction mixture at 90°C under nitrogen. Monobenzyl suberoyl chloride (3.92 g, 12.57 mmol, 3 equiv.) was added and the resulting solution was stirred at 90 °C for 20 h. Then the product was precipitated by adding the cooled reaction mixture to ethanol. The precipitate was isolated by vacuum filtration, then washed with water, re-dissolved in a minimum amount of THF, then re-precipitated into hexane, isolated by vacuum filtration, and dried in vacuum oven at 50°C overnight (yield 78%) and the white powder product was characterized by ^{1}H NMR.

Hydrogenation of cellulose ω-carboxyalkanoate benzyl esters: The hydrogenation of CAAdP benzyl ester will serve to exemplify the methods used. CAAdP benzyl ester (500 mg) was dissolved in 100 ml THF and to this solution palladium hydroxide on carbon (250 mg) was added. The solution was stirred at high speed under a hydrogen atmosphere in a high-pressure reactor (Parr reactor Model 4848) at 120-psi bar pressure for 24 h at room temperature. Then the solution was filtered through Celite® (filter aid, Celite AW Standard Supercel®, Alfa Aesar) in order to remove the catalyst, concentrated under reduced pressure and then precipitated into hexane (50 mL) and isolated by filtration.

^{1}H NMR CAAdP (DMSO): 1.02-1.20 (m, $COCH_2\underline{CH_3}$ of propionate), 1.66 (broad s, $COCH_2$-$\underline{CH_2}\underline{CH_2}CH_2CO$ of adipate), 2.16-2.35 (m, $CO\underline{CH_2}CH_3$ of propionate, $COCH_3$ of acetate and $CO\underline{CH_2}CH_2CH_2\underline{CH_2}CO$ of adipate), 3.25-5.24 (cellulose backbone). DS by ^{1}H NMR: adipate 0.9, propionate 2.09, acetate 0.04.

^{1}H NMR CASub (DMSO): 1.2 ($COCH_2CH_2\underline{CH_2}\underline{CH_2}CH_2CH_2CO$ of suberate), 1.4-1.6 ($COCH_2\underline{CH_2}CH_2CH_2\underline{CH_2}CH_2CO$ of suberate), 2.10–2.46 ($CO\underline{CH_2}CH_2CH_2CH_2CH_2\underline{CH_2}CO$ of suberate, and $COCH_3$ of acetate), and 3.00–5.20 (cellulose backbone).

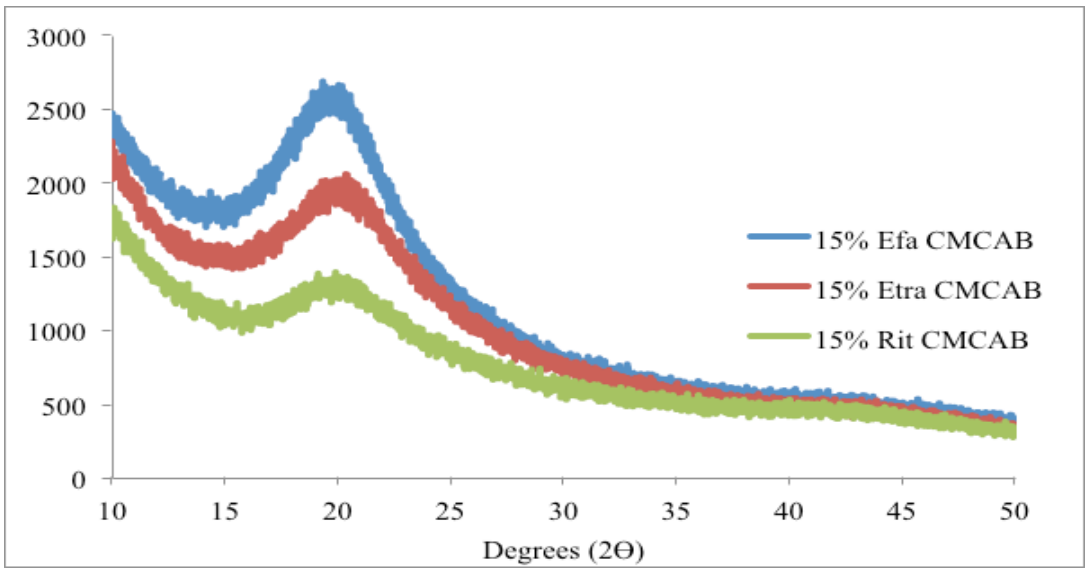

Figure S5.1: XRD spectra of single drug formulations prepared with CMCAB

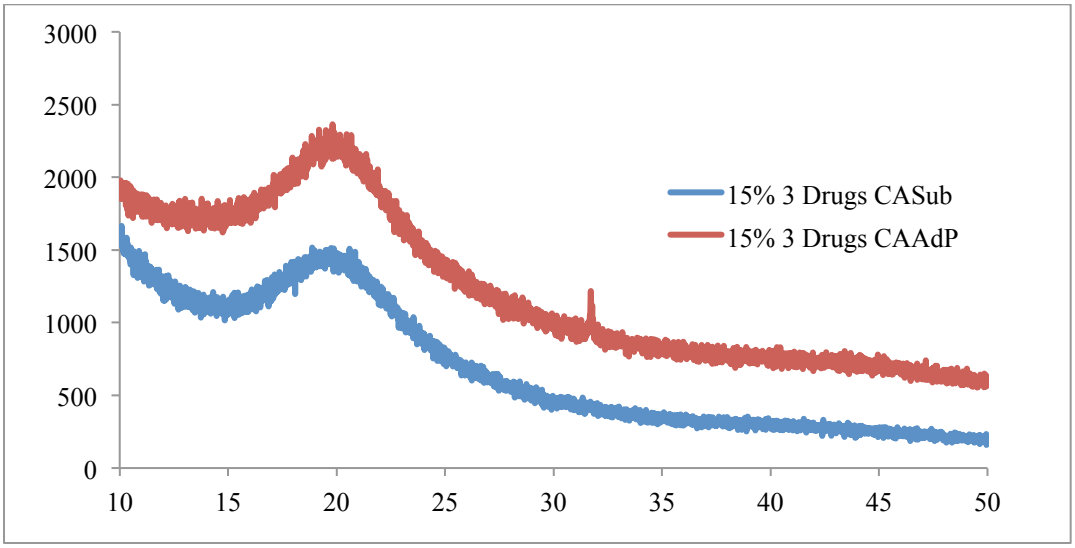

Figure S5.2: XRD spectra of CASub and CAADP 3 drug formulations

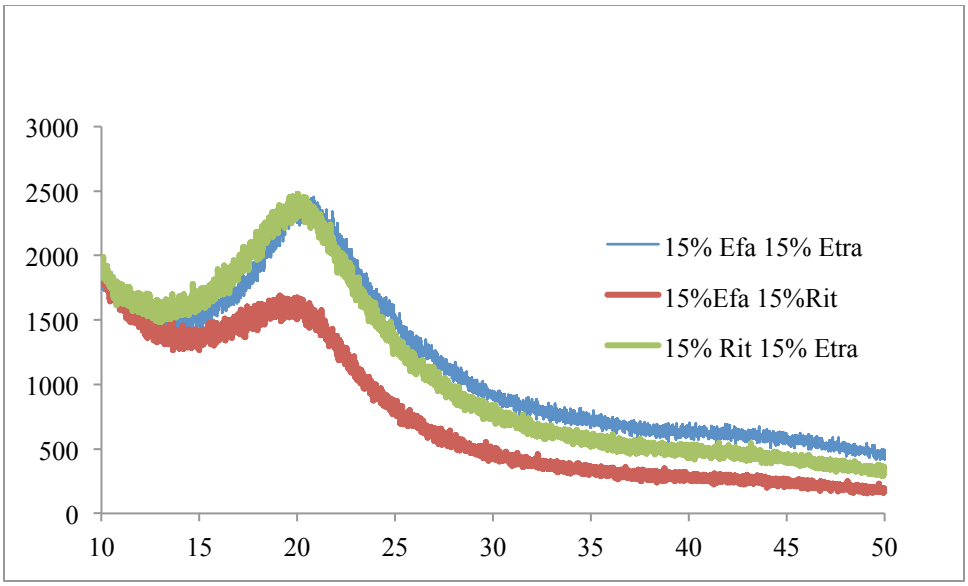

Figure S5.3: XRD spectra of 2 drug formulations with CMCAB.

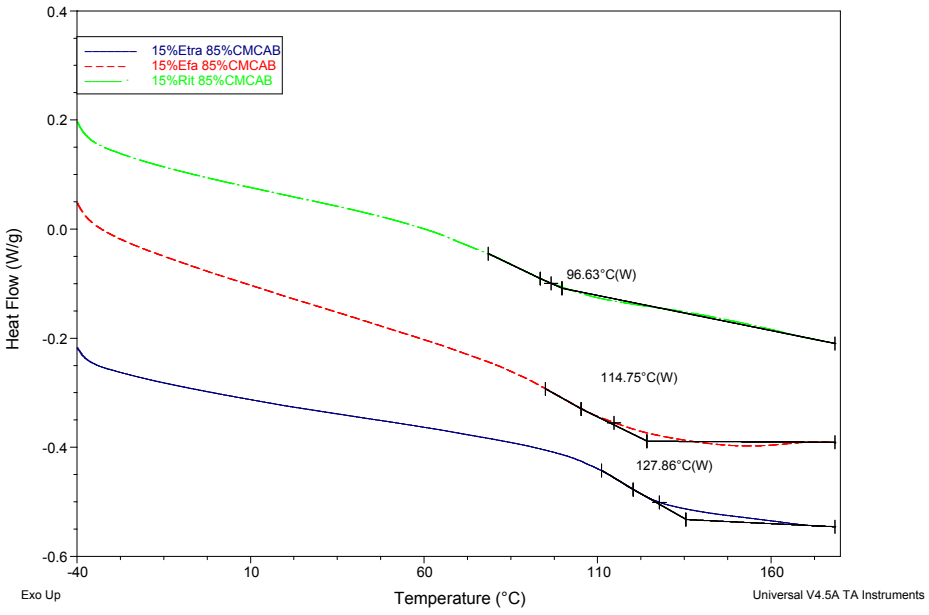

Figure S5.4: DSC thermograms of single drug formulations prepared with CMCAB.

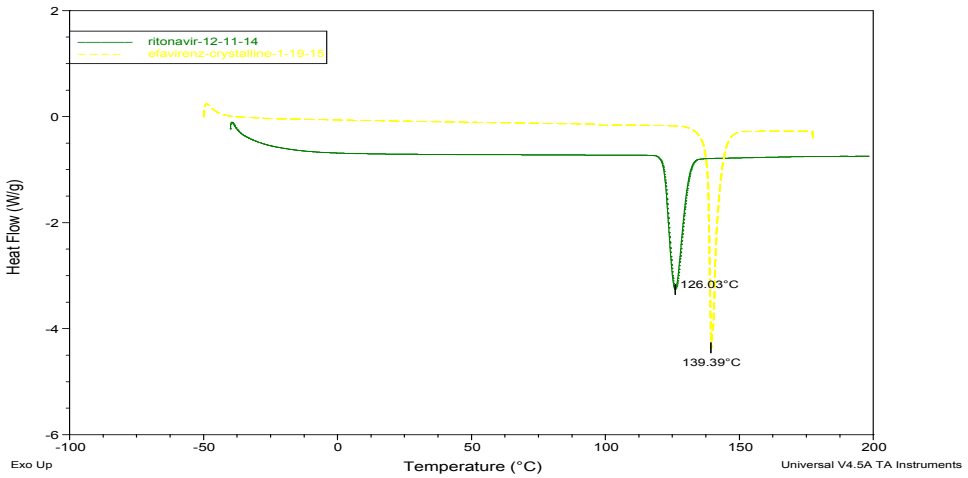

Figure S5.5: The melting peaks of the crystalline drugs on the second heating curve.

Table S5.1: Theoretical T_g and Calculated T_g values of ASDs.

Formulations	Measured T_g	Calculated T_g
15% 3 Drug CMCAB	77 °C	119.7
15% 3 Drug CCAB	74°C	101
15% 3 Drugs CAAdP	58 °C	106
15% 3 Drugs CASub	58 °C	98
15% Etra 15% Efa CMCAB	55 °C	88.5
15% Etra 15% Rit CMCAB	86 °C	76.2
15% Efa 15% Rit CMCAB	66 °C	66.3

15% Rit CMCAB	97 °C	127 °C
15% Etra CMCAB	128 °C	134 °C
15% Efa CMCAB	115 °C	127 °C

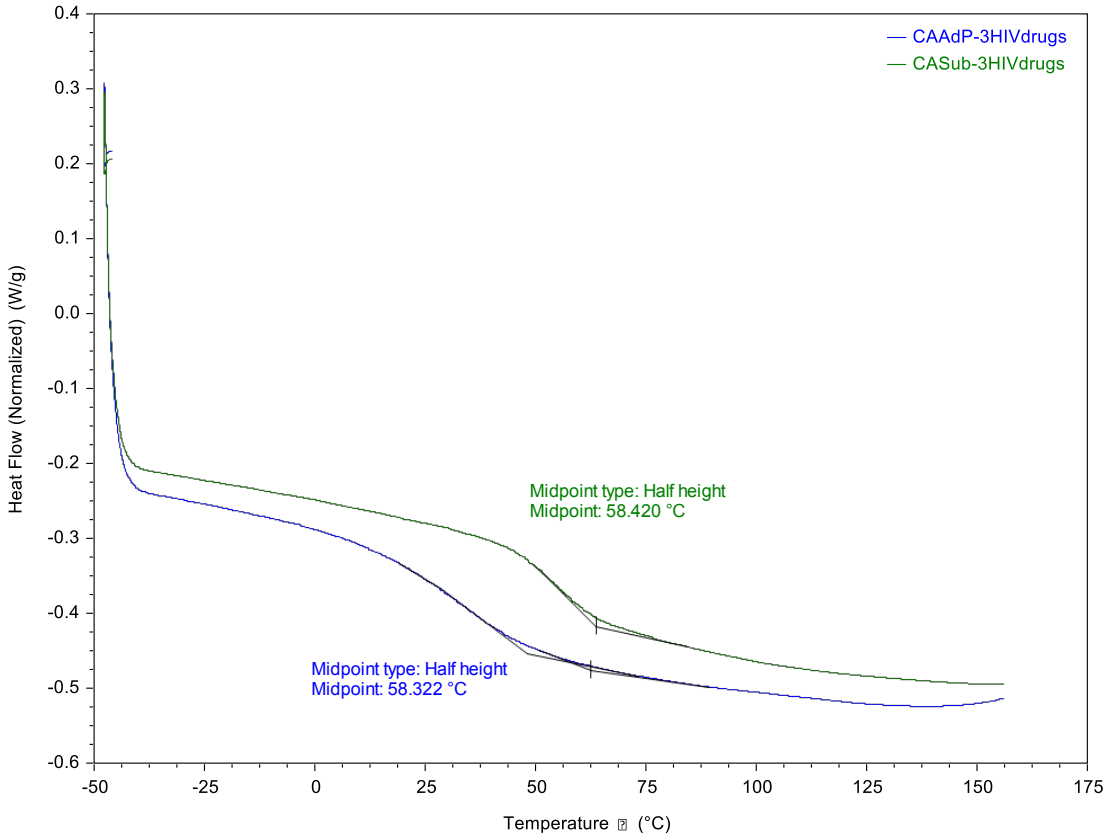

Figure S5.6: DSC thermograms of CAPAd and CASub three drug formulations.

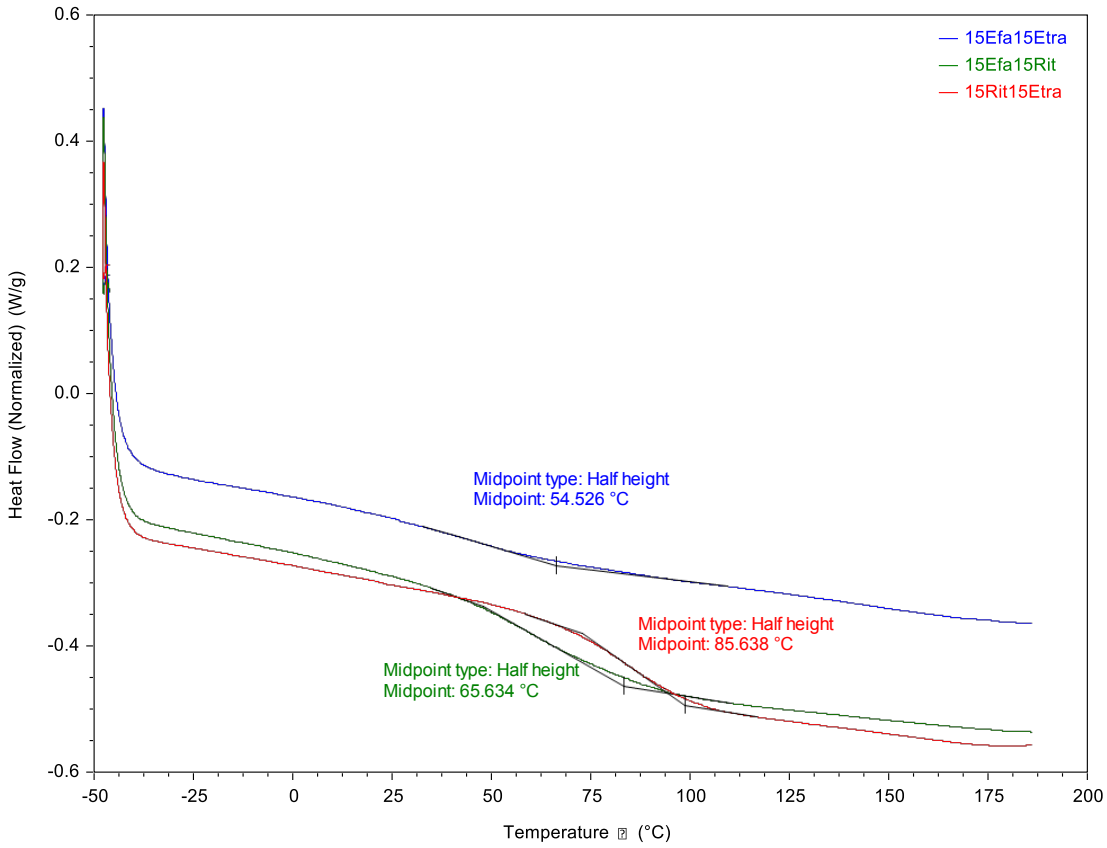

Figure S5.7: DSC thermograms of double drug formulations prepared with CMCAB.

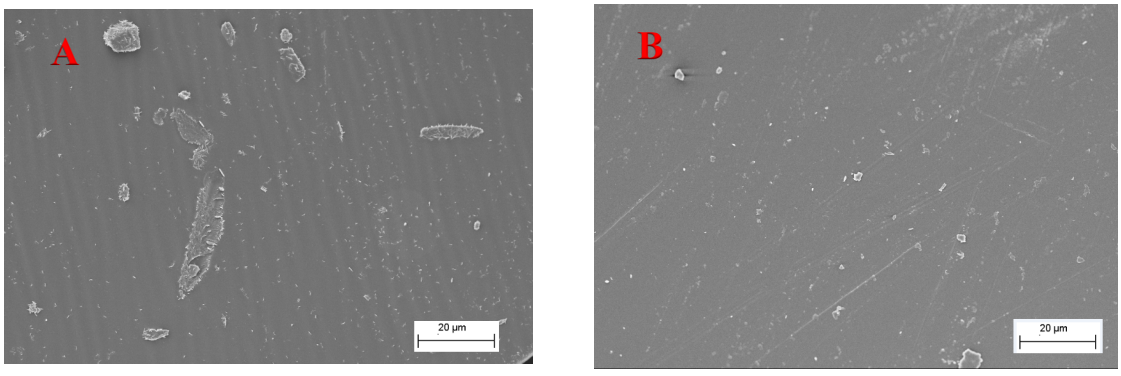

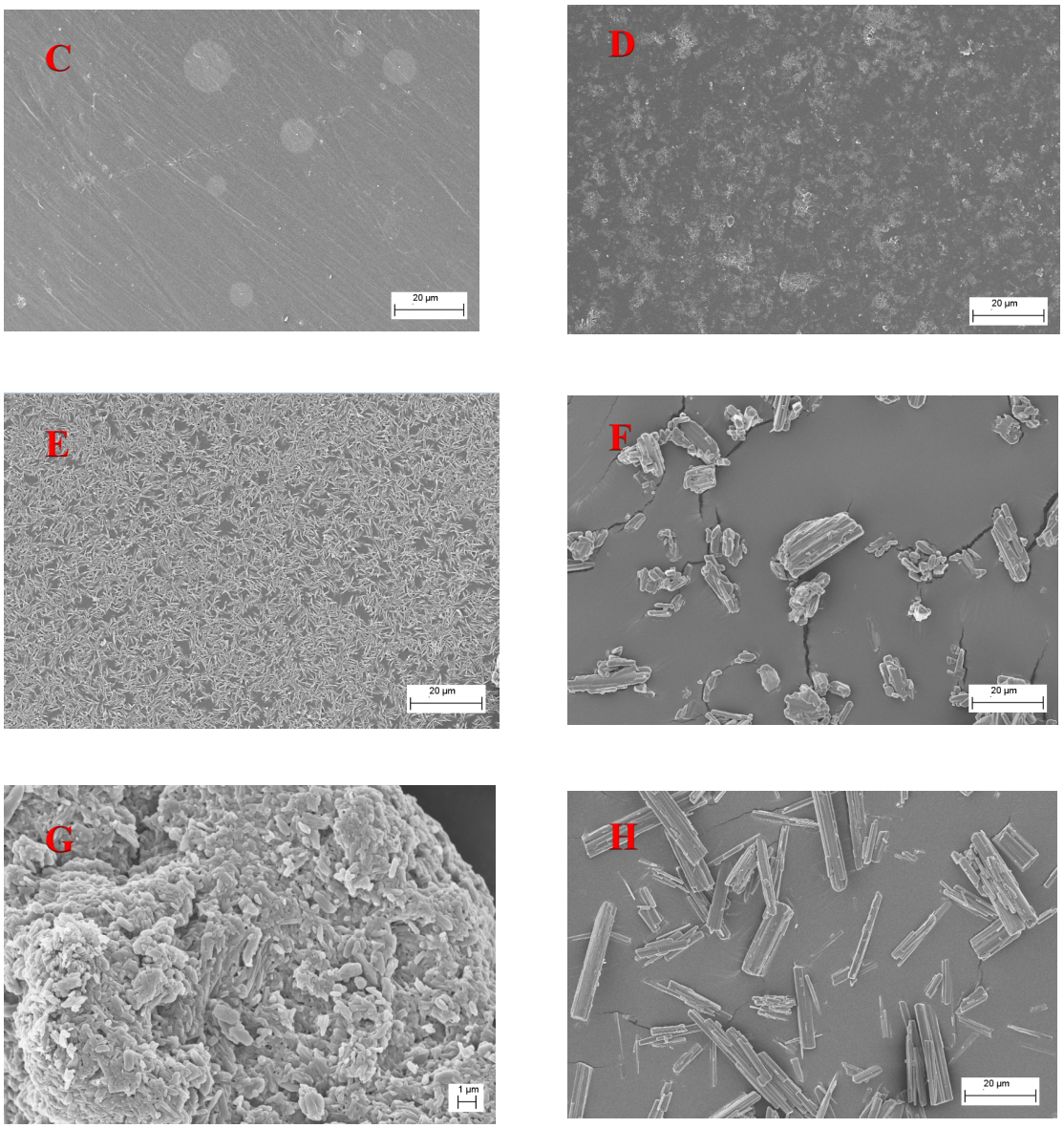

Figure S5.8: SEM images of (A) 15% 3 Drugs CMCAB, (B) 15% Efa CMCAB, (C) 15% Etra CMCAB, (D) 15% Rit CMCAB, (E) 15% TPGS 15% 3 Drugs CMCAB, (F) Efa (only drug), (G) Etra (only drug) and (H) Rit (only drug) at 10Kx magnification.

Chapter 6. Synthesis and characterization of alkyl cellulose ω-carboxyesters for amorphous solid dispersion

Table S6.1 shows how the solubility parameter was calculated for the methyl cellulose adipate polymer, and Figure 1 is a schematic of the groups that are affected by DS and the ones that are not.

Table S6.1: Solubility parameter calculation for methyl cellulose adipate

Group	Number of groups			E (cal*mol^{-1})	$\sum$ E (cal $*$ mol^{-1})	V (cm^3*mol^{-1})	$\sum$ V (cm^3 $*$ m^{-1})
	a	b	Total				
-CH_3	0	1.86	1.86	1125	2092	33.5	62.3
-CH_2	1	4.40	5.40	1180	6372	16.1	86.9
-CH	5	0	5.00	820	4100	-1	-5
Ring closure[c]	1	0	1	250	250	16	16
-OH	0	0.04	0.04	7120	285	10	0.4
-O-	2	1.86	3.86	800	3088	3.8	14.7
-COOH	0	1.10	1.10	6600	7260	28.5	31.4
-CO_2	0	1.10	1.10	4300	4730	18	19.8
Correction[d]	-	-	-	-	-	-	14.0
Total	-	-	-	-	28177		240.5
Solubility Parameter ($MPa^{1/2}$)	22.14						

[a]Constant number of groups for all cellulose based polymers

[b]It will change depending on DS for different substituents

[c]Ring closure (5 or more atoms)

[d]Correction when T_g > 25°C

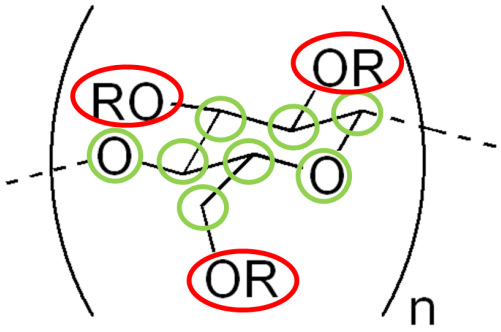

Figure S6.1: Schematic for SP calculation. The groups in green are not affected by the DS and are constant for diverse cellulose based polymers: 1 ring closure, 5 -CH, 1 -CH_2 and 2 –O–. The groups in red will change depending on the DS for each polymer: OR.

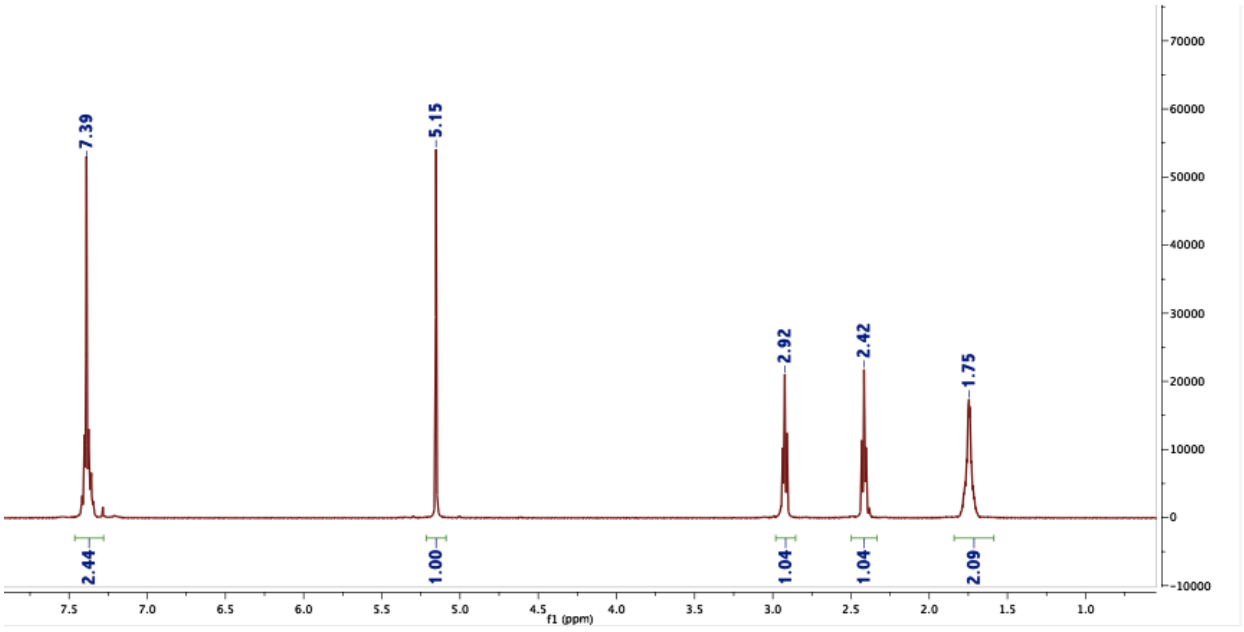

Figure S6.2: ^{1}H-NMR of monobenzyl adipoyl chloride

Table S6.2: Detailed information of SEC results.

Ref. No.	Ether type	Ester type	Mn	Poly dispersity	*Calculated Mw	DP
1	EC	Adipate	10000	1.45	296.6	34
2	EC	Suberate	9000	1.50	310.1	29
3	EC	Sebacate	10000	1.48	326.8	31
4	MC	Benzyl Adipate	82600	4.23	386.0	213
5	MC	Benzyl Suberate	69596	3.62	416.9	167
6	MC	Benzyl Sebacate	122319	4.9	424.1	288

- Molecular weight is calculated according to the degree of substitution.

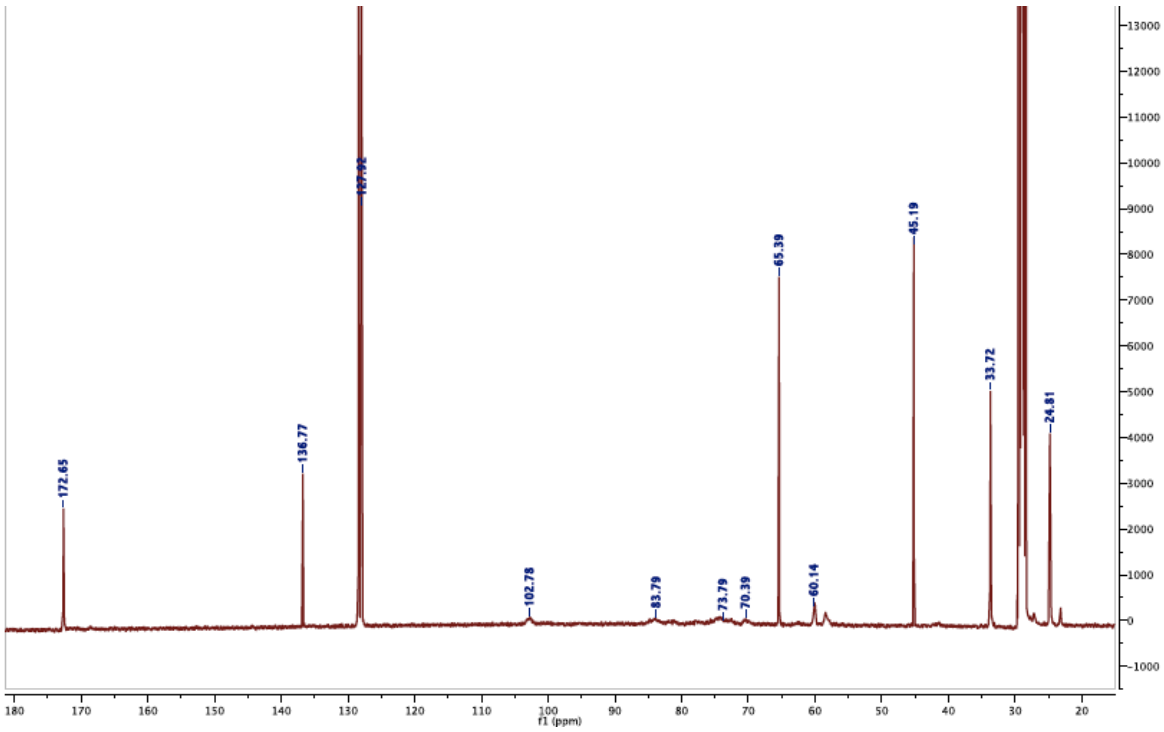

Figure S6.3: ^{13}C NMR of benzyl MCSeb in d_6-acetone.

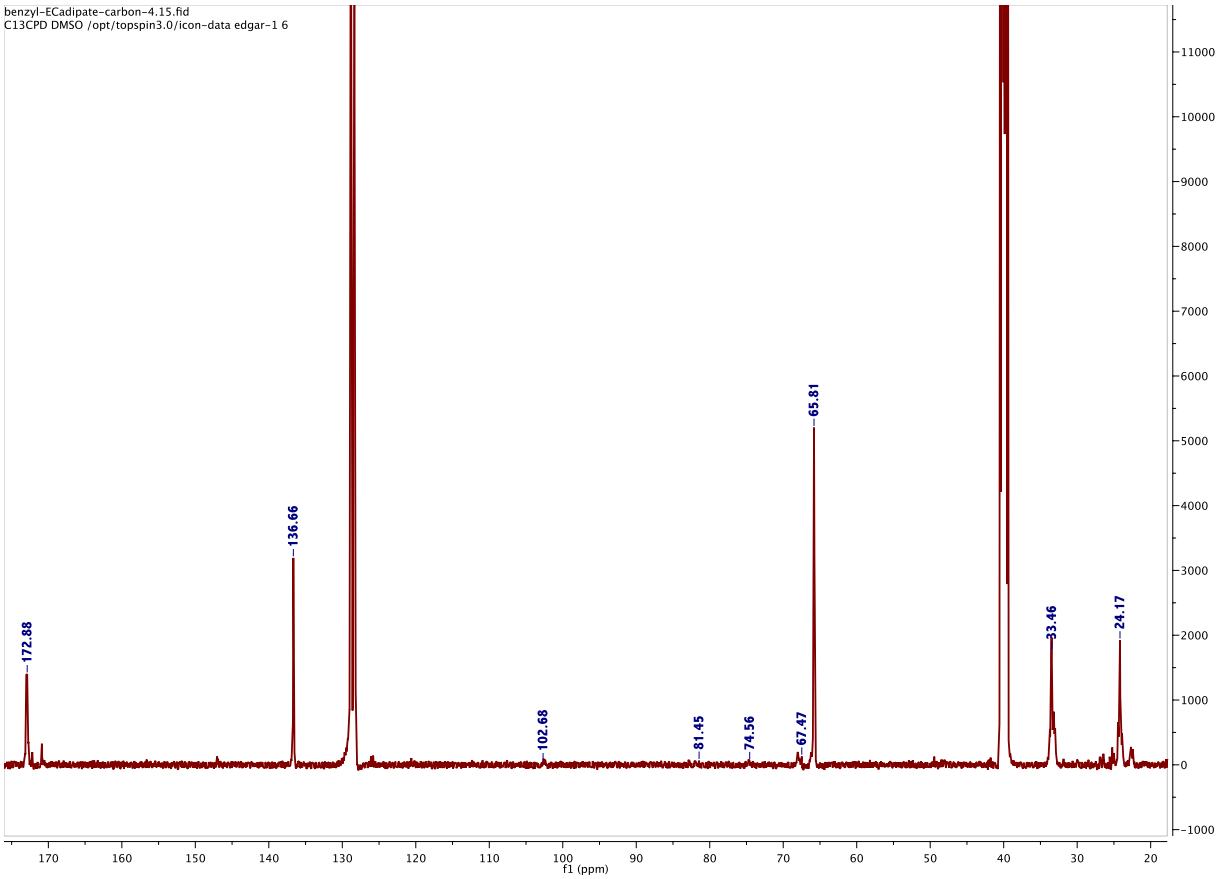

Figure S6.4:^{13}C-NMR of benzyl ECAd in d_6-DMSO.

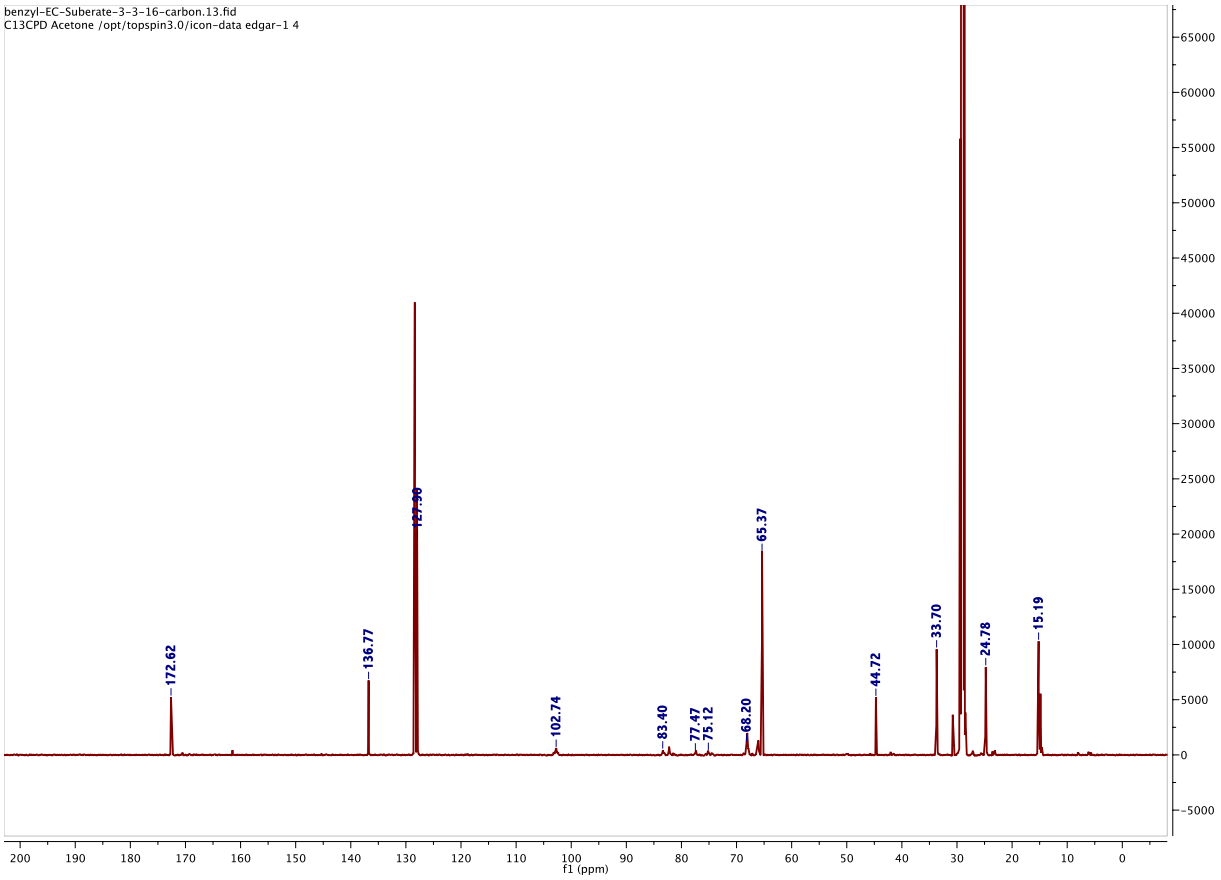

Figure S6.5: ^{13}C-NMR of benzyl ECSub in d_6-acetone.

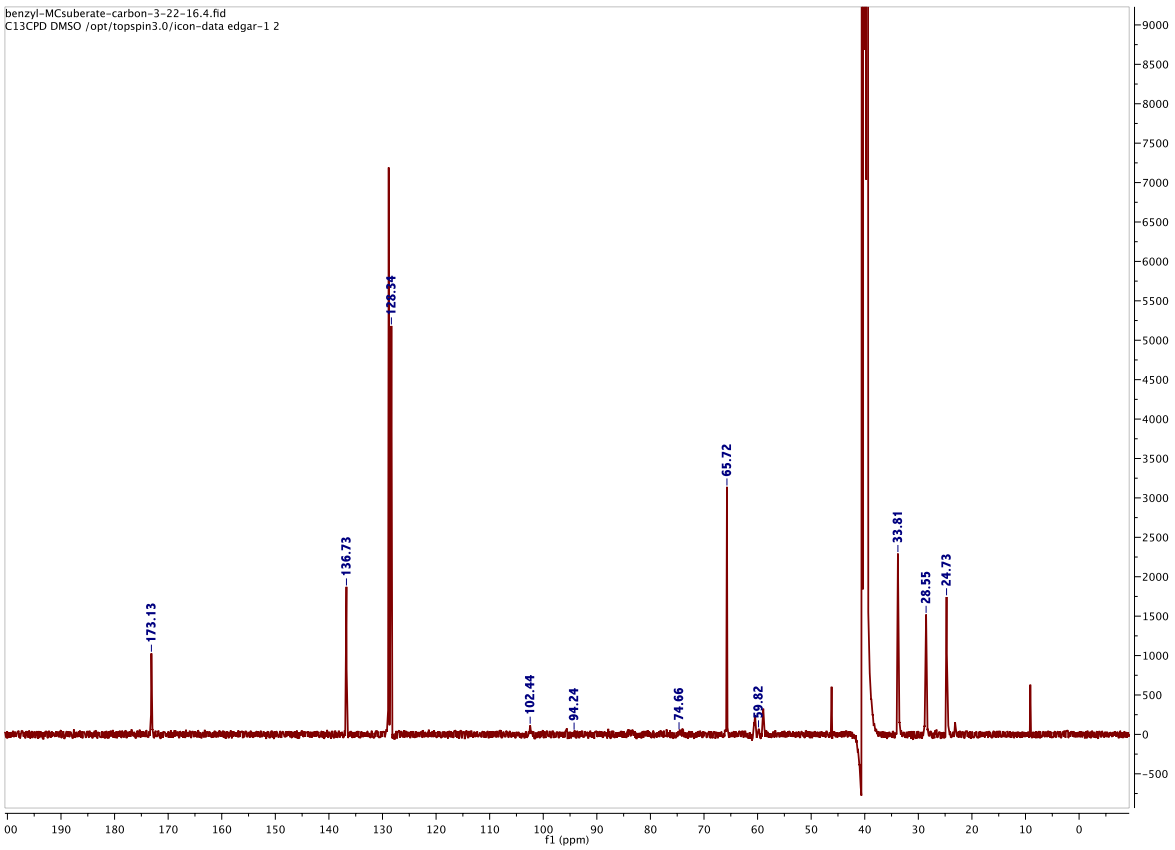

Figure S6.6: ^{13}C-NMR of benzyl MCSub in d_6-DMSO.

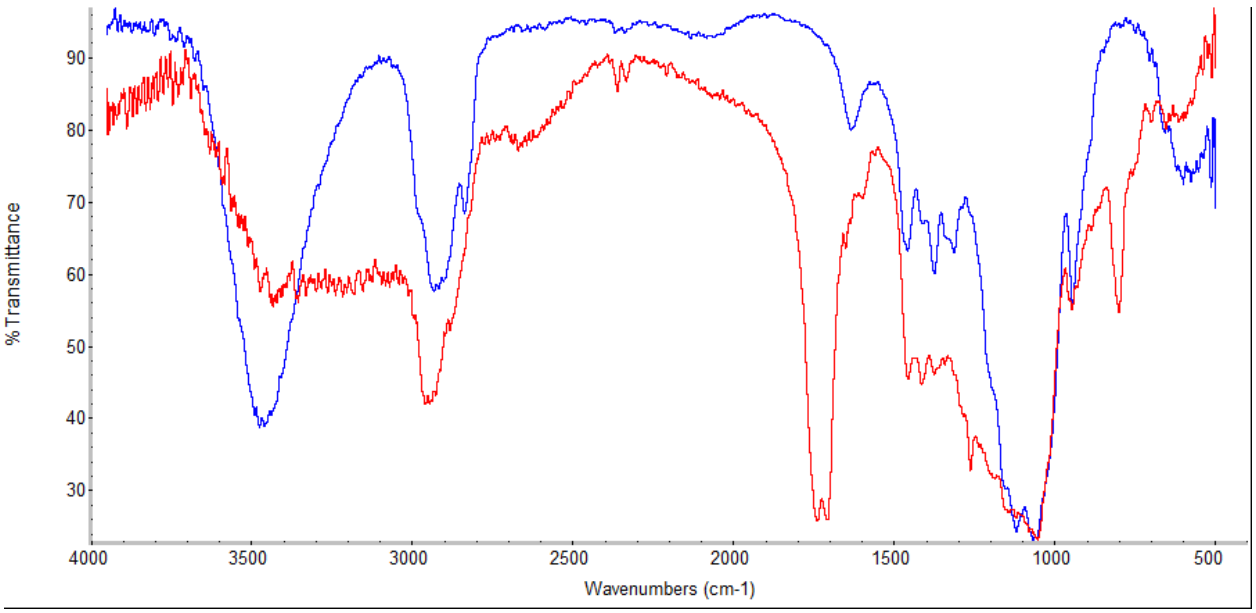

Figure S6.7: FTIR spectra of MC (blue) and MCAd (Red).

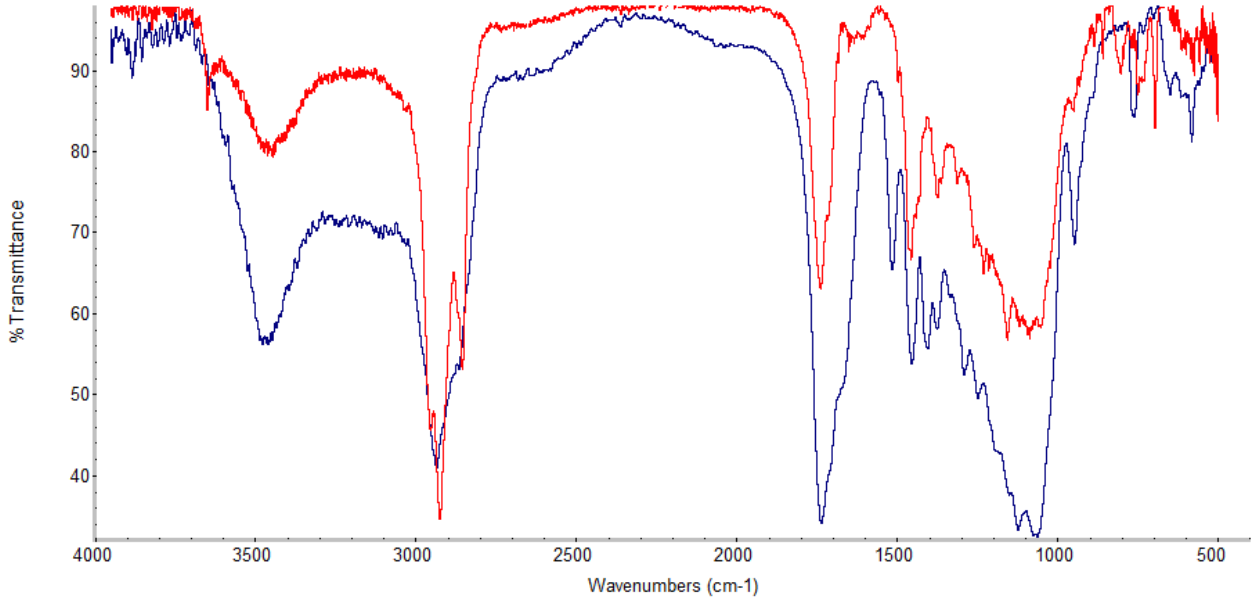

Figure S6.8: FTIR spectra of MCSub (blue) and MCSeb (Red).

Chapter 7. Quercetin solution concentration enhancement through amorphous solid dispersions of cellulose esters

Synthesis of CASub

Preparation of monobenzyl suberate: suberic acid (87 g, 0.5 mol), benzyl alcohol (81 g, 0.75 mol), PTSA (0.95 g, 5 mmol), and toluene (200 mL) were stirred in a flask equipped with Dean-Stark trap and heated at reflux for 3 h until the theoretical amount of water was collected. The resulting mixture was cooled to room temperature, water (200 mL) was added, and the pH adjusted to 9 with 6M NaOH. The aqueous layer was separated by centrifuge, mixed with ethyl ether (150 mL), and the pH adjusted to 2 with 6M HCl. The ether layer was separated and concentrated under reduced pressure to afford a colorless oil. ^{1}H NMR ($CDCl_3$): δ 1.33 (m, 4H), 1.68 (m, 4H), 2.36 (m, 4H), 5.09 (s, 2H), and 7.32 (m, 5H).

Synthesis of monobenzyl suberoyl chloride: Monobenzyl suberate (30 g, 113 mmol), DMF (3 drops), and 200 mL dichloromethane were cooled in a round bottomed flask to 0°C. Oxalyl chloride (25.4 g, 200 mmol) was added drop by drop under vigorous magnetic stirring, then stirred 2 h at room temperature till gas formation ceased. Solvent was removed under reduced pressure, 10 mL toluene was added, and then it was concentrated again under reduced pressure. The product was a yellow oil. ^{1}H NMR ($CDCl_3$): δ 1.34 (m, 4H), 1.66 (m, 4H), 2.36 (t, 2H), 2.86 (t, 2H), 5.12 (s, 2H), 7.35 (m, 5H).

Benzyl CASub synthesis: CA 320S (1.00 g, 4.19 mmol) was dissolved in DMI (20 mL), Et_3N (1.95 mL, 13.83 mmol, 3.3 eq) was added all at once, then monobenzyl suberoyl chloride (3.7 g, 12.57 mmol, 3 eq) was added. After 20 hours at 90°C under nitrogen, the reaction mixture was cooled, then added to ethanol (250 mL) dropwise to precipitate the product, which was isolated by vacuum filtration, then washed with 200 mL water and re-dissolved with 25 mL THF and re-precipitated in 200 mL hexane. The product was characterized by ^{1}H NMR. δ 1.3 ($COCH_2CH_2CH_2CH_2CH_2CH_2CO$ of suberate), 1.6 ($COCH_2CH_2CH_2CH_2CH_2CH_2CO$ of suberate), 2.10–2.46 ($COCH_2CH_2CH_2CH_2CH_2CH_2CO$ of suberate and $COCH_3$ of acetate), 3.00–5.20 (cellulose backbone), 5.10 (s, $CH_2C_6H_5$), 7.35 (CH_2C_6H5).

Hydrogenolysis of benzyl CASub: Benzyl CASub (1 g) was dissolved in 100 mL THF, then $Pd(OH)_2$/C (500 mg) was added. The mixture was stirred, after removal of the air by vacuum, at a high speed under H_2 (balloon) for 24 h at room temperature. Products were isolated by filtering through Celite, then the same protocol was repeated one more time and, the solvent was removed under reduced pressure, and the product precipitated in ethanol (100 mL). ^{1}H NMR CASub (DMSO): δ 1.2 ($COCH_2CH_2CH_2CH_2CH_2CH_2CO$ of suberate), 1.4-1.6 ($COCH_2CH_2CH_2CH_2CH_2CH_2CO$ of suberate), 2.10–2.46 ($COCH_2CH_2CH_2CH_2CH_2CH_2CO$ of suberate, and $COCH_3$ of acetate), 3.00-5.20 (cellulose backbone).

Preparation of ASDs via spray drying

CCAB (0.9 g) was dissolved in 120 mL THF at room temperature for 15 h. Q (0.1 g) was dissolved in 20 mL acetone separately and stirred for 20 min. THF (20 mL) was added, then this Q/acetone/THF solution was added to the polymer/THF solution dropwise. All CCAB/Q solutions were prepared similarly. ASDs were prepared by spray drying the polymer/Q solutions using a nitrogen-blanketed spay dryer (Buchi B-290). Instrument parameters were as follows: inlet temperature 90°C, outlet temperature 75°C, aspirator rate 80%, 40% pump rate, compressed nitrogen height 30 mm and nozzle cleaner 2. HPMCAS (1.8 g) was dissolved in 15 mL THF and 15 mL acetone, stirred overnight, then Q (0.2 g) was added to the solution and stirred for 15 min before spray drying. A similar procedure was followed to prepare CASub spray dried particles, except that acetone was used as solvent. PVP (0.4 g or 0.2 g) was dissolved in 10 mL ethanol and CCAB (1.4 g)/ Q (0.2 g) was dissolved in 80 mL acetone. A similar protocol was followed for PVP/CASub blends with ethanol/THF. Our convention for naming treatments is to list the % polymer(s), with the remainder being Q. For example, 10% Q/90% CCAB is referred to as 90 CCAB in the text, figures and tables.

ASD Characterization

X-ray powder diffraction (XRD) patterns were measured with a Bruker D8 Discover X-ray Defractometer (Billerica, MA) with a Lynxeye detector and a KFL CU 2K X-ray source. Samples were run with a 1 mm slit window between a scan range of 10˚ to 50˚ 2θ. DSC analyses were performed on a Trios TA Instrument (New Castle, DE) with dry samples (5 mg) loaded into TzeroTM aluminum pans. Each sample was equilibrated at 20˚C and then heated to 200˚C at 20˚C/min. Then samples were quench-cooled to −50˚C and reheated to 200˚C at 20˚C/min. Tg values were recorded as the step-change inflection point from second heat scans. FTIR spectra were recorded between 4000 and 500 cm−1, using a resolution of 4 cm−1 and 40 accumulations, on a Nicolet 8700 FT-IR Spectrometer (Thermo Fisher). Pellets were prepared from sample/KBr mixtures (1:100 weight ratio).

UPLC verification of ASD Q content

Incorporation of Q into the ASD was quantified by extraction and UPLC-MS/MS. Each batch of ASD particles was evaluated for Q content (wt %, $n = 4$). Q-containing ASDs were dissolved in ethanol (~ 0.26 mg/mL), and 50 µL of this solution was combined with 50 µL internal standard solution (epicatechin (EC), 0.8 mg/mL in ethanol) and 50 µL 0.1% formic acid in 80% water/20% 80:20 ACN/THF. Solid Q [i.e. 100% Q, ≥ 95% purity) was used as control and analyzed similarly.

***In vitro* Dissolution**

Fasted gastric conditions were simulated using pH 1.2 buffer (500 mL of 0.2 M KCl was combined with 850 mL of 0.2 M HCl, and then diluted to 2 L with MilliQ water). Small intestinal

conditions were simulated using pH 6.8 buffer (6.8 g/L sodium phosphate monobasic in MilliQ Water, adjusted with 0.2 M NaOH to pH 6.8). Dissolution was performed as described previously with modifications (Pereira et al., 2013). Jacketed flasks (250 mL, 37°C) were employed. Dissolution medium consisted of 100 mL gastric or small intestinal buffer. All treatments contained a fixed Q amount (7 mg) to ensure supersaturation if all dissolved, and were continuously stirred with a magnetic stir bar at 400 rpm for 2 h (gastric) or 8 h (intestinal). Sample aliquots (1 mL) were taken at 30, 60, 90, 120 min (gastric) or 30, 60, 90, 120, 180, 240, 300, 360, 420, and 480 min (small intestinal) and each aliquot was replaced with 1 mL buffer to maintain constant volume. Aliquots were centrifuged (10 min, 37°C, 47,000 x *g*) on a Beckman Coulter Avanti JE high-speed centrifuge (Sunnyvale, CA). Following centrifugation, the supernatant (i.e. soluble fraction) was collected, diluted (1:1) with ethanol, and stored at −80°C for further analysis.

HPLC Analysis

Analyses were measured by HPLC using an Agilent HPLC 1260 Infinity system (Agilent Technologies, CA, USA) with an Agilent Eclipse plus C18, 4.6 x 250 mm, 5 µm analytical column (Agilent technologies, CA, USA). The mobile phase was 40 % acetonitrile: 60 % DI water acidified with phosphoric acid at pH 2.5. The experimental conditions were: 1.3 mL/ min flow rate, 370 nm wavelength and 20 µL injection volume, and controlling the column temperature at 35 ˚C. The retention time was 3.6 minutes.

UPLC-MS/MS Analysis

Analyses were performed on a Waters Acquity H-class UPLC separation model (milford, MA) equipped with a Waters Acquity UPLC BEH C18 column (2.1 mm x 50 mm, 1.7 µm particle size). Column and sample temperatures were maintained at 40˚C and room temperature (24 ± 1˚C), respectively. The binary mobile phase consisted of 0.1% (v/v) aqueous formic acid (phase A) and 0.1% formic acid in 80% ACN/20% THF (phase B) (all solvents LC-MS grade except THF). System flow rate was 0.6 mL/min . A linear elution gradient was employed as follows: 80% A at 0 min, 10% A at 2.20 min, 100% A at 2.25 min. An injection volume of 2 µL was employed. A second injection of 100 µL DMSO was used in between sample injections to remove any carryover quercetin, with isocratic mobile phase (100% B for 2 min), and subsequent reconditioning for 2.25 min to initial gradient conditions. Electrospray (ESI)-MS/MS analysis was performed in negative mode on a Waters Acquity TQD (triple quadrupole) mass spectrometer equipped with a Z-spray electrospray interface as described in Goodrich & Neilson with modifications (Goodrich & Neilson, 2014). Capillary voltage was −1.5 kV, cone voltage 56 V for quercetin and 34 V for EC, source temperature 150˚C, and desolvation temperature 500˚C. Desolvation and cone gasses were N_2 at flow rates of 1,000 and 50 L/hr, respectively. Detection was performed by multi-reaction monitoring (MRM) of parent psuedomolecular ($[M-H^-]$) ion to daughter (fragment) ion transitions during collision-induced dissociation (CID, Ar gas: 0.25 mL/min). The MRM transitions for quercetin and EC were 300.77 m/z → 150.88 m/z and 288.79 m/z → 245.02 m/z, respectively, with collision energies of 20.0 eV for quercetin and 10 eV for

EC. Quantification was based on an internal standard curve prepared using varying levels of quercetin with the fixed internal standard, EC.

Solubility Parameter Evaluation

The following equation can be used to evaluate solubility parameters for a polymer of interest:

$\delta = \sqrt{\frac{\sum_i \Delta e_i}{\sum_i \Delta v_i}} = \sqrt{\frac{\Delta E_v}{V}}$; where Δe_i = the additive atomic and group contribution for the energy of vaporization and Δv_i = the additive atomic and group contribution for the molar volume. Polymers with high molecular weights and $T_g > 25^{\circ}C$, a discrepancy between experimentally measured ΔE_v and V is seen. For these differences, a correction factor was introduced: $\Delta v_i = 4n, n < 3$ and $\Delta v_i = 2n, n \geq 3$; where n is the number of main chain skeletal atoms in the smallest repeating unit of the polymer.

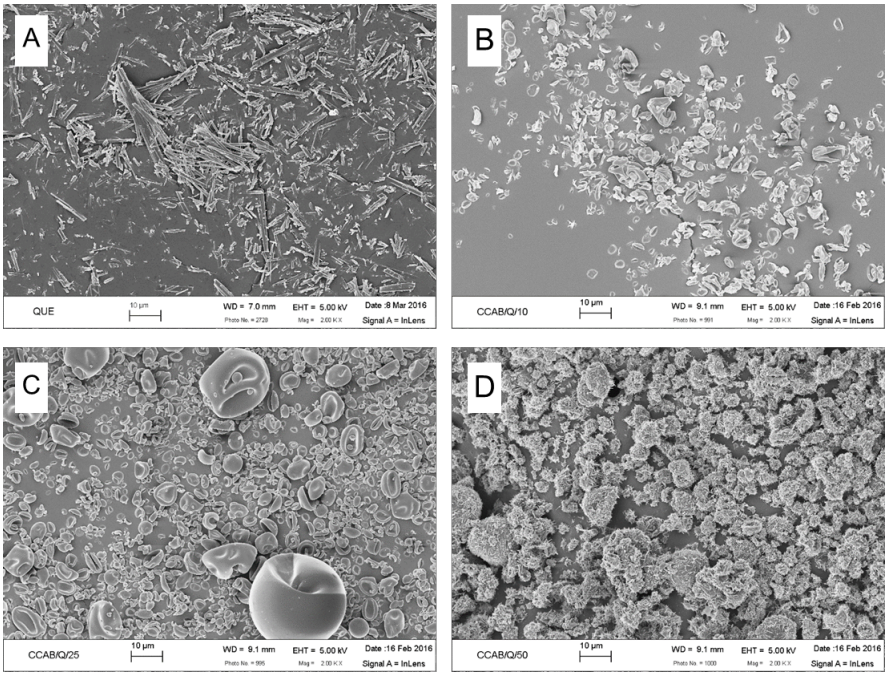

Figure S7.1 SEM images for Q (A), 90 CCAB (B), 75 CCAB (C), and 50 CCAB (D) are shown at 2X magnification.

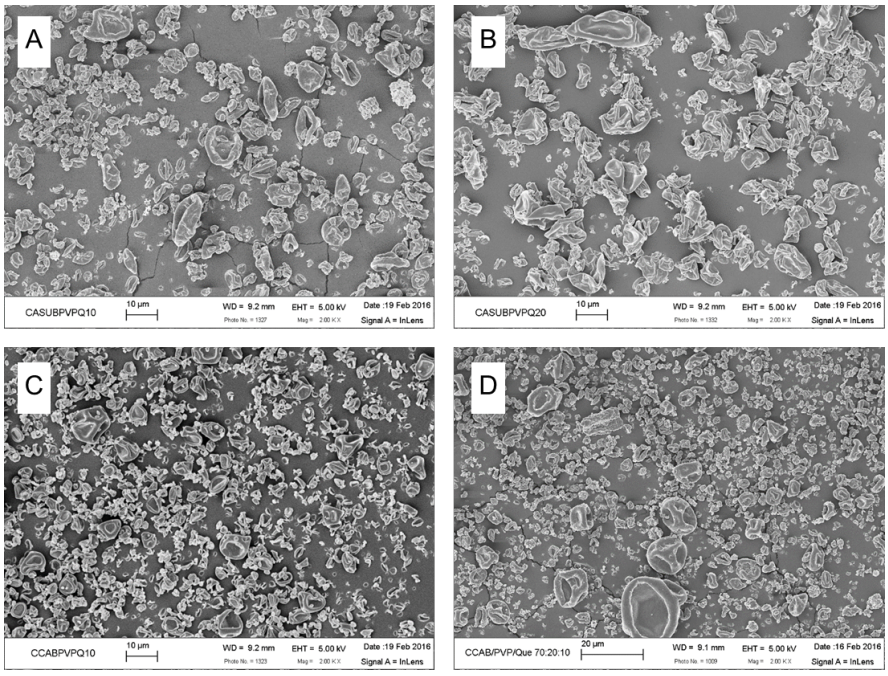

Figure S7.2 SEM images for 10 PVP:80 CASub (A), 20 PVP:70 CASub (B), 10 PVP:80 CCAB (C), and 20 PVP:70 CCAB (D) are shown at 2X magnification.

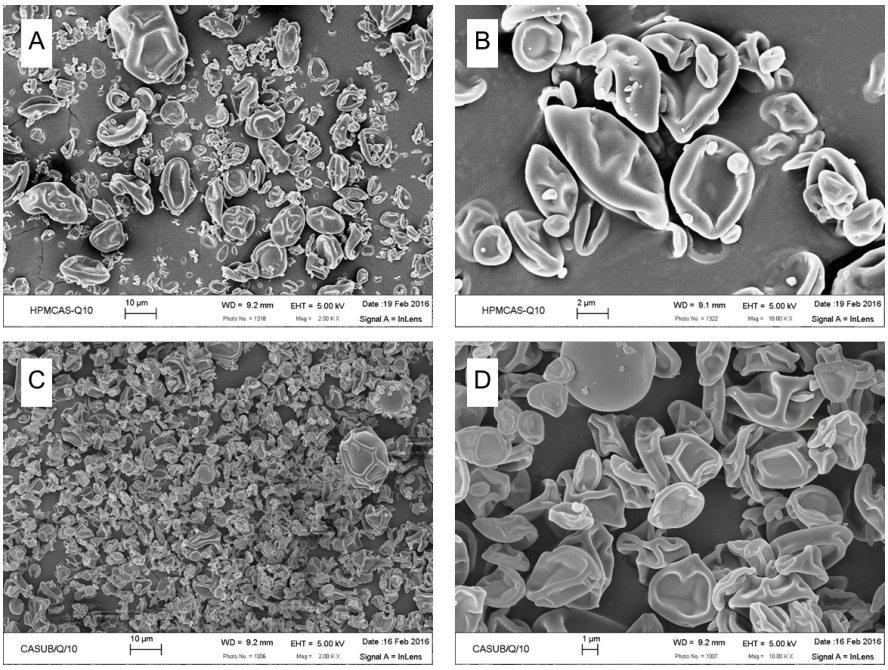

Figure S7.3 SEM images for 90 HPMCAS (A, B) and 90 CASub (C, D) are shown at both 2X and 10X magnification.

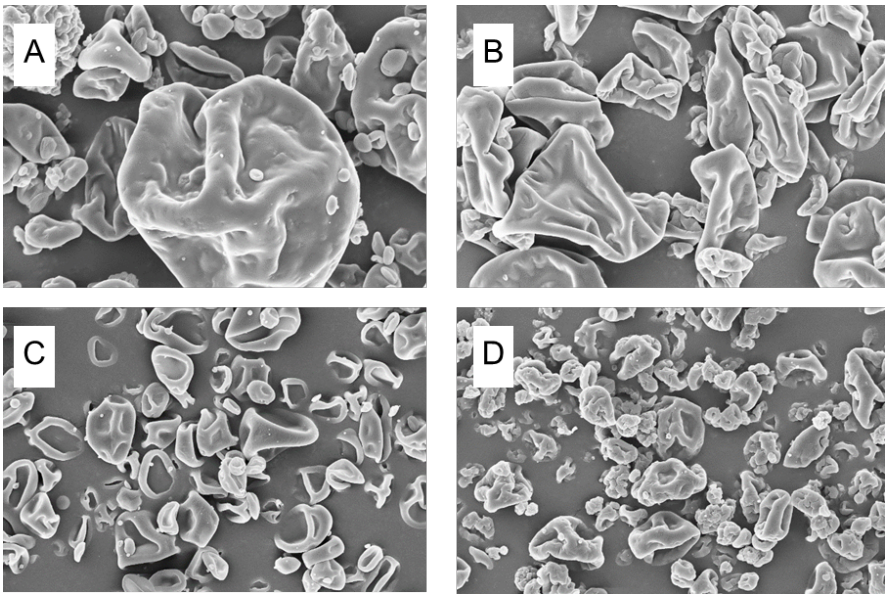

Figure S7.4 SEM images (mag. 10X) for 10 PVP:80 CASub (A), 20 PVP:70 CASub (B), 10 PVP:80 CCAB (C), and 20 PVP:70 CCAB (D) are shown to illustrate particle size range (1-3 µm) and morphology

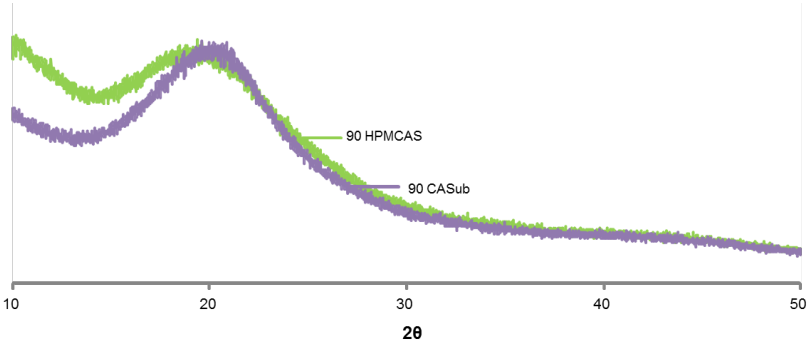

Figure 7.5. XRD spectra of 90 HPMCAS and 90 CASub.

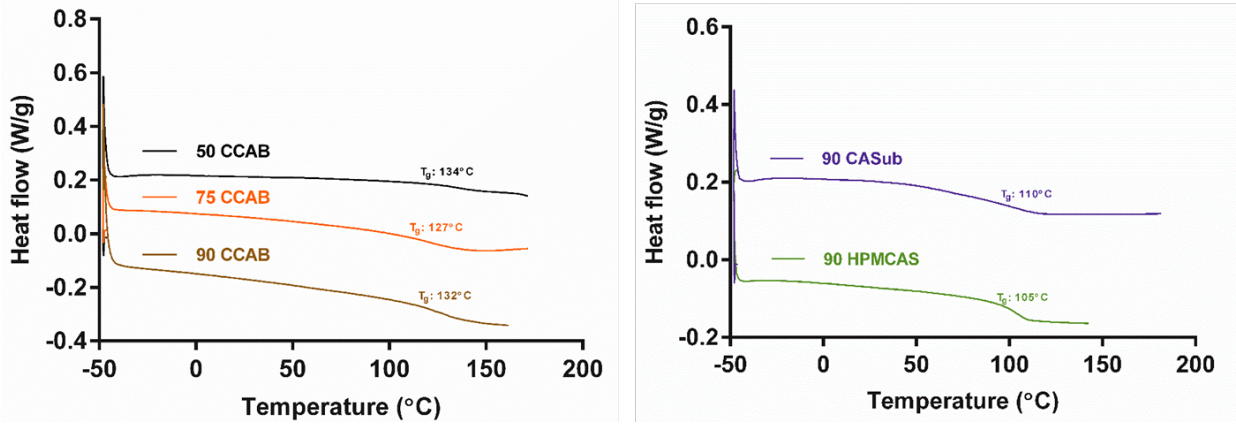

Figure S7.6 DSC second heating curves of Q-loaded ASDs of CCAB, CASub, PVP blends of CCAB and CASub, and HPMCAS.

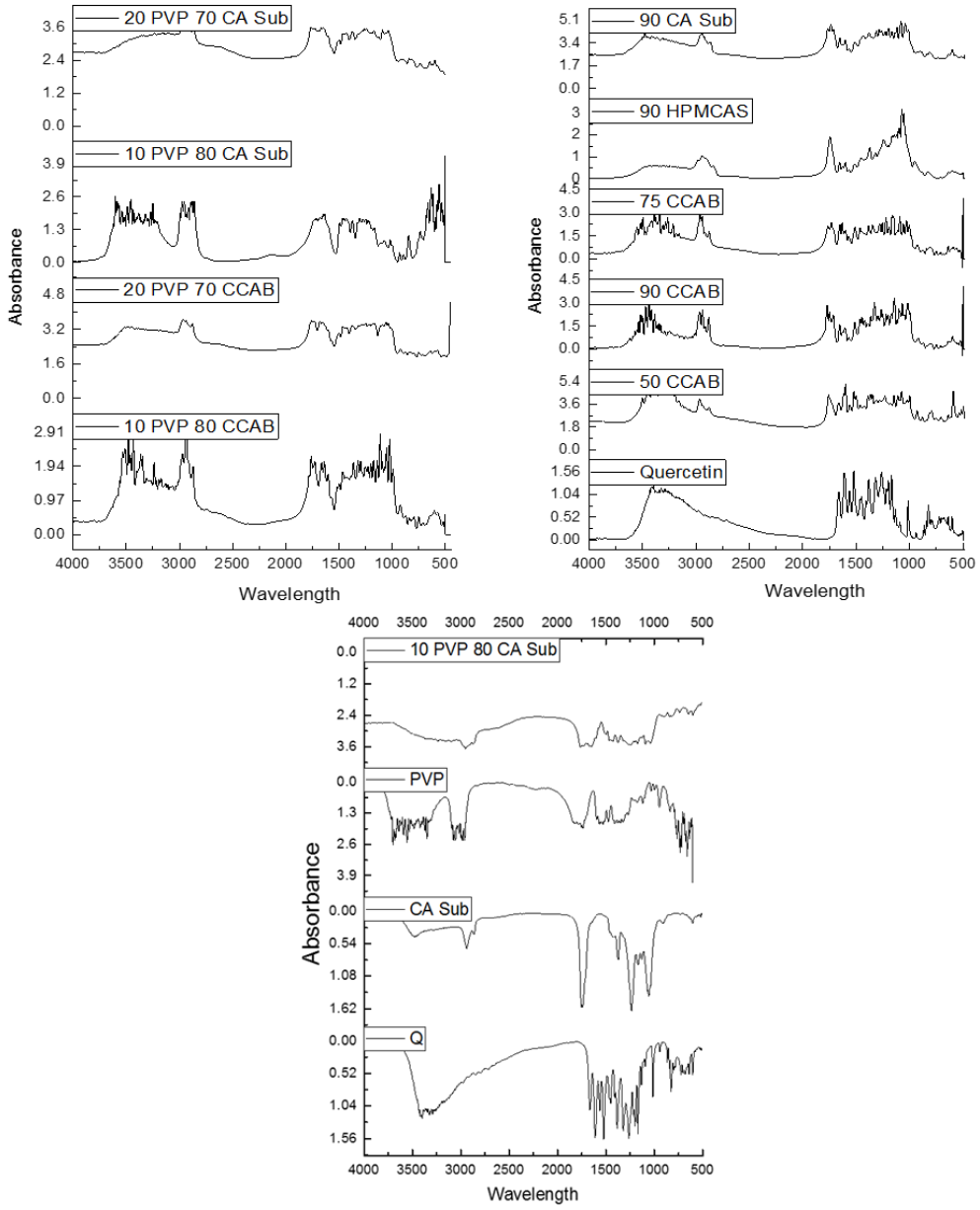

Figure S7.7. FT-IR spectra for all treatments, crystalline Q, and two polymers used in the study (CASub and PVP).

FT-IR was used to observe interactions between Q and the polymers in ASDs. Q has five phenolic hydroxyl groups (hydrogen bond donors, **Fig. S7.1** in main manuscript) that can interact with the carbonyl groups of the cellulose esters (hydrogen bond acceptors). The polymers contain a large number of these carbonyl groups, as seen in the sharp carbonyl peak in the FT-IR spectra of CASub, for example. Compared to the spectra of pure Q (hydroxyl stretch 3300–3500 cm^{-1}), the polymer blends show a broadening of the hydroxyl stretch, indicating hydrogen bonding and a disruption of crystallinity of the pure Q.

UPLC determination of ASD Q loading

In order to characterize ASD formulations and standardize Q levels (7 mg/flask) for *in vitro* dissolution experiments, Q purity was measured, and Q-containing ASDs were analyzed, by UPLC-MS/MS. ASD Q contents conformed closely to targeted levels, though greater variability was seen at higher Q contents.

Table S7.1. Actual (Q) content of prepared ASD formulations

ASD Formulation[a]	Q (wt %)[b]
Q	91.9 ± 4.63[c]
90 CCAB	10.4 ± 1.68
75 CCAB	28.2 ± 4.29
50 CCAB	45.4 ± 4.95
10 PVP:80 CCAB	9.44 ± 0.128
20 PVP:70 CCAB	9.13 ± 0.258
90 HPMCAS	12.5 ± 0.279[d]
90 CASub[e]	12.0 ± 0.585[d]
10 PVP:80 CASub[e]	10.6 ± 0.718[d]
20 PVP:70 CASub[e]	9.92 ± 0.287[d]

[a]Values in this column refer to formulation targets (wt %); convention for naming treatments is to list the % polymer(s), with the remainder being Q
[b]Data shown are mean ± SEM (n = 4, unless otherwise specified)
[c]Supplier specification indicates Q purity ≥ 95% (wt %)
[d]n = 3 due to limited quantities of ASDs available
[e] DS(0.9), M_w = 20,000-25,000 g/mol

Table S7.2 Pseudo-pharmacokinetic parameters of Q at gastric pH (1.2).

ASD Formulation	AUC[a] (μg min/mL)	C_{MAX}[a] (μg/mL)	T_{MAX}[a] (min)
Q	164 ± 76.0	4.61 ± 1.76	30
90 CCAB	47.1 ± 20.6	1.21 ± 0.493	120
75 CCAB	27.7 ± 8.68	0.582 ± 0.225	90
50 CCAB	181 ± 35.7	2.92 ± 0.462	30, 60[b]
10 PVP:80 CCAB	295 ± 20.1	4.33 ± 0.206	120
20 PVP:70 CCAB	350 ± 124	5.27 ± 1.92	120
90 HPMCAS[c]	387 ± 30.3	5.55 ± 0.833	90
90 CASub[c]	774 ± 64.4	11.5 ± 1.78	30
10 PVP:80 CASub[c]	707 ± 172	12.3 ± 0.298	90
20 PVP:70 CASub[c]	972 ± 58.0	13.4 ± 0.707	90

[a]Data are mean ± SEM AUC, average C_{MAX} and T_{MAX} (n = 4 except where indicated)
[b]C_{MAX} occurred twice at 2 separate time points
[c]n = 3

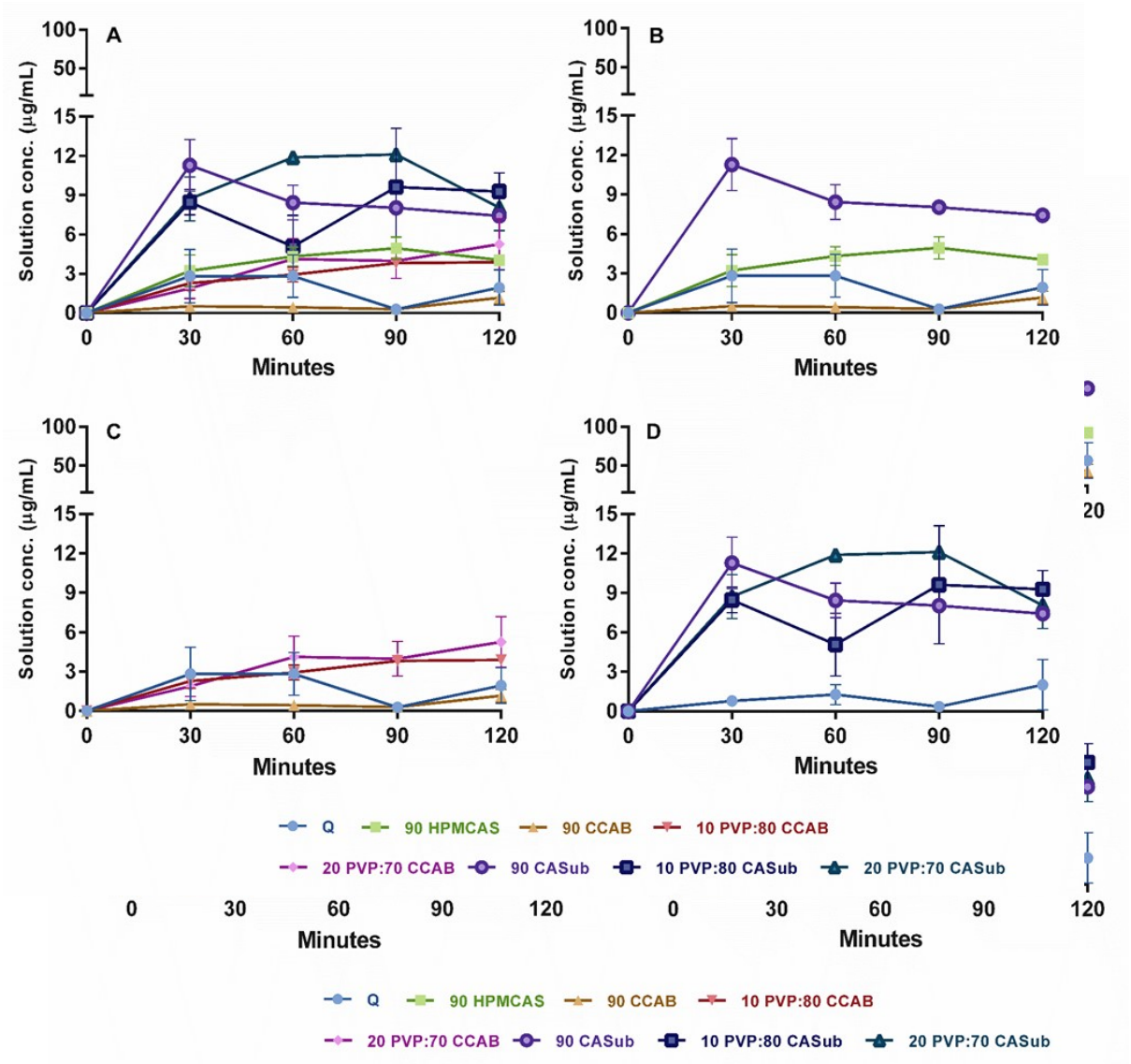

Figure S7.8. Average solution concentrations of Q (mean ± SEM, n = 3-4) plotted over time at pH 1.2 for all treatments (A), 10% Q loaded ASDs only shown for comparison of dissolution properties for each polymer utilized (B), the impact of PVP blending with CCAB (C) and CASub (D). All graphs contain crystalline Q as a control for comparison.